DITION REPORTS
9115
.N
1.2

V.2

NAGA REPORT

Volume 2

LIBRARY
APR 27 1962
FISH & WILDLIFE

Scientific Results
of Marine Investigations of the South China Sea
and the Gulf of Thailand
1959-1961

Sponsored by

South Viet Nam, Thailand
and the
United States of America

Physical Oceanography of the Southeast Asian Waters

by

KLAUS WYRTKI

The University of California
Scripps Institution of Oceanography
La Jolla, California

1961

NMFS Honolulu Library
00000000005353

NAGA REPORT

Volume 2

Scientific Results

of Marine Investigations of the South China Sea

and the Gulf of Thailand

1959-1961

Sponsored by

South Viet Nam, Thailand

and the

United States of America

Physical Oceanography of the Southeast Asian Waters

by

KLAUS WYRTKI

The University of California
Scripps Institution of Oceanography
La Jolla, California
1961

90° E
100°
110°
20°
10° N
0°
10° S
20°
CHINA
HONGKONG
Irawadi R
Saluen R
Mekong R
BURMA
HANOI
GULF OF TONKING
HAINAN
GULF OF BENGAL
RANGOON
THAILAND
PARACEL IS.
PREPARIS CHANNEL
Menam R
BANGKOK
CAMBODIA
VIET NAM
CHINA SEA
ANDAMAN IS.
ANDAMAN
SAIGON
TEN DEGREE CHANNEL
SEA
GULF OF THAILAND
NICOBAR IS.
STRAIT OF MALACCA
MALAYA
SINGAPORE
NATUNA IS.
ANAMBAS
SUMATRA
PONTIANAK
Kapuas River
PADANG
MENTAWAI
BANKA
GASPER STRAIT
BILITON
KARIMATA STRAIT
BORNEO
JAVA SEA
BAWEAN
SUNDA STRAIT
DJAKARTA
JAVA
MADURA
SURABAYA
INDIAN OCEAN
BALI
LOMBO
CHRISTMAS I
COCOS I

120°
130°
140° E
20°
10° N
0°
10° S
20°
FORMOSA STRAIT
FORMOSA
KOTO SYO IS.
BASHI CHANNEL
PACIFIC
OCEAN
LUZON
MANILA
PHILIPPINES
MINDORO
PANAY
NEGROS
SAMAR
PALAWAN I.
SULU
SEA
MINDANAO
SULU ARCHIPELAGO
JOLO
YAPA
PALAU
CELEBES
SEA
TALAUT
SANGI
MOROTAI
HALMAHERA
MOLUCCA SEA
MENADO
MANGOLE
LIFAMATOLA STRAITS
OBI
TALIABU
CERAM
AMBON
BURU
CELEBES
MACASSAR
STRAIT OF MACASSAR
BANDA
SEA
BANDA
KAI IS.
MANUK
ARU IS.
NEW GUINEA
FLORES SEA
DAMAR
WETA
TANIMBAR
BABAR
ARAFURA
SEA
LESSER SUNDA IS.
FLORES
ALOR
TIMOR I.
SAPE STR.
SUMBA
SAWU SEA
SAWU
ROTI
TIMOR SEA
TORRES STRAIT
DARWIN
GULF OF CARPENTARIA
AUSTRALIA

NEYENESCH PRINTERS, SAN DIEGO, CALIFORNIA

PREFACE

In 1954, when I left Germany for a three year stay in Indonesia, I suddenly found myself in an area of seas and islands of particular interest to the oceanographer. Indonesia lies in the region which forms the connection between the Pacific and Indian Oceans, and in which the monsoons cause strong seasonal variations of climate and ocean circulation.

The scientific publications dealing with this region show not so much a lack of observations as a lack of an adequate attempt to synthesize these results to give a comprehensive description of the region. Even Sverdrup *et al.* in "The Oceans" and Dietrich in "Allgemeine Meereskunde" treat this region superficially except in their discussion of the deep sea basins, whose peculiarities are striking.

Therefore I soon decided to devote most of my time during my three years' stay in Indonesia to the preparation of a general description of the oceanography of these waters. It quickly became apparent, that such an analysis could not be limited to Indonesian waters, but would have to cover the whole of the Southeast Asian Waters. In addition to the published data for the region, the Indonesian research vessel "Samudera," although she had limited facilities, was able to add some observations.

This book is the outcome of my analysis of all available knowledge of the Southeast Asian Waters. It is hoped that workers in the region, whether in oceanography or other branches of science may find it a source of information and a stimulus to undertake further research in these waters.

Some chapters in this book are summaries and condensations of already known facts, but others offer new ideas and interpretations, particularly those chapters on monsoon circulations and their dynamics, on deep circulation and its relation to surface circulation, on the energy exchange between sea and atmosphere, and on the quantitative description of the exchange of water in the deep sea basins.

For the reader not familiar with oceanographical terms, it is suggested that reference be made to Sverdrup *et al.* "The Oceans" for definitions of terms, descriptions of methods, and discussion of the physical principles governing the interaction of various factors, because such matters cannot be included in a regional description.

I would like to thank the staff of the Institute of Marine Research in Djakarta for carrying out many of the calculations and for drawing most of the charts. Sincere thanks go to Mrs. L. M. Willings of the Division of Fisheries and Oceanography in Cronulla for her helpful assistance in correcting my English. I am also much indebted to the Scripps Institution of Oceanography for publishing the book.*

Klaus Wyrtki

Cronulla, Sydney, November 1960

*Publication of this work was done under International Cooperation Administration Contract ICAc—1085.

PHYSICAL OCEANOGRAPHY OF THE SOUTHEAST ASIAN WATERS

by Klaus Wyrtki

1. Introduction.
2. Configuration of seas and basins.
3. The wind systems and the circulation at the surface.
   - 3.1 The monsoons.
   - 3.2 The construction of the surface current charts.
   - 3.3 The surface currents of the northeastern Indian Ocean.
   - 3.4 The surface currents of the western North Pacific Ocean.
   - 3.5 Surface currents in the Southeast Asian Waters.
4. The properties of the water in the surface layer.
   - 4.1 The homogeneous layer.
   - 4.2 The discontinuity layer.
   - 4.3 The temperature of the surface layer.
   - 4.4 The salinity of the surface layer.
   - 4.5 The distribution of nutrients, productivity and transparency.
5. Precipitation, evaporation and energy exchange at the surface of the Southeast Asian Waters.
   - 5.1 The distribution of rainfall.
   - 5.2 The calculation of the evaporation.
   - 5.3 The calculation of the energy exchange.
   - 5.4 The annual variation of the climatic factors.
6. The water masses in the depth.
   - 6.1 The water masses in the depth of the northeastern Indian Ocean.
   - 6.2 The water masses in the depth of the western North Pacific Ocean.
   - 6.3 The water masses in the depth of the China and Sulu Seas.
   - 6.4 The Subtropical Lower Water in the Eastern Archipelago.
   - 6.5 The salinity and oxygen minima in the Eastern Archipelago.
   - 6.6 The water masses in the deep layer.
   - 6.7 The water masses in the deep sea basins.
   - 6.8 Summary: the water masses and their movements in the Eastern Archipelago.
7. The dynamics of the circulation.
   - 7.1 Relations between winds, sea level and currents.
   - 7.2 The topography of the sea surface relative to 800 decibars.
   - 7.3 The vertical distribution of the velocities and the transports.
   - 7.4 Charts of the mass transports.
   - 7.5 Regions of upwelling and sinking.
   - 7.6 The sea level in the Southeast Asian Waters.
   - 7.7 The dynamics of the water movements in the China Sea.
8. Tides and tidal currents.
   - 8.1 The semidiurnal tide.
   - 8.2 The diurnal tide.
   - 8.3 The geographical distribution of tidal types.
   - 8.4 Tidal currents and internal waves.

CHAPTER I

INTRODUCTION

The waters and islands between Asia and Australia and between the Pacific and the Indian Oceans form a geographical and oceanographical unit because of their special structure and position. Geographically the whole region is a part of Asia and is denoted as Southeast Asia; oceanographically, the waters are part of the Pacific Ocean. This is justified not only by the position of the most obvious boundary between the Pacific and the Indian Oceans formed by Malaya, Sumatra, Java, and the Lesser Sunda Islands, but also by the fact that these seas are filled with water from the Pacific, to which they have the readier access.

In scientific literature, the name Austral-Asiatic Mediterranean has been used, but this name is probably too artificial ever to come into common use. The names Indo-Malayan Archipelago and East Indian Archipelago also appear, but either these are no longer in use or are applied only to parts of the region. Therefore the more commonly known terms, Southeast Asia, already introduced into geography by Dobby (1956), and Southeast Asian Waters, are used here.

The Southeast Asian Waters consist of the China Sea, the Java Sea, the Sulu Sea, the Philippine Waters, the Celebes Sea, the Banda Sea, the Flores Sea, the Arafura Sea, the Timor Sea, and the Andaman Sea. The whole region comprises an area of 8.94 million square kilometres, which is 2.5 per cent. of the surface of all oceans. Together they form a real geographic unit, even if the region does not belong as a whole to one or other of the two oceans. The boundary between them runs through the region. The Andaman Sea is undoubtedly part of the Indian Ocean, but must be included in the Southeast Asian Waters as defined here. The Timor and Arafura Seas and the Gulf of Carpentaria are often regarded as part of the Pacific Ocean, but, as pointed out by Schott (1935), it would be very hard to explain to a sailor navigating from Timor to the Torres Strait that he is sailing on the Pacific Ocean. However, an analysis of the water masses demonstrates that these seas derive their water from the Pacific (see Section 6.5), so for geographical convenience this division may be accepted to fix the standard boundaries between the oceans.

As in most parts of the world, exploration in marine sciences started with biological investigations. All the earlier expeditions, beginning with the Portuguese, are carefully summarized by Naber in the historical review appearing in van der Stok (1922). The first information concerning weather at sea, currents and tides was collected by captains who navigated in these seas for the large shipping companies. Actual oceanographic investigations, including deep sea soundings, bottom sampling, determinations of temperature and salinity were first carried out by the CHALLENGER in 1874, by the GAZELLE in 1875, by the VALDIVIA in 1899 and by the SIBOGA in 1899-1900, to mention only the more important expeditions. On the basis of these results, the first bathymetric chart of the region was drawn up by Tydeman (1903). Investigations of the PLANET in 1906-7 supplied further information, especially on the structure of the water masses. With these expeditions the first period of exploration of these waters ended, and the period of more systematic oceanographic approach could start.

The SNELLIUS Expedition in 1929-30 investigated comprehensively the oceanography of the deep sea basins of the Eastern Archipelago between the Sunda and Sahul Shelves (van Riehl, 1932). This expedition was planned using as a model the METEOR Expedition in the Atlantic Ocean, and its leader, P. M. van Riehl, accepted many suggestions from members of the METEOR Expedition. The fundamental plan was to obtain a three-dimensional picture of the structure and movements of the water masses in an enclosed part of the ocean. Now, looking back after thirty years, it is clear that, in planning the SNELLIUS

Expedition, certain fundamental differences between the Atlantic Ocean and the Southeast Asian Waters were disregarded, though some of these omissions were probably unavoidable at that stage of oceanographic research. The size and topography of the regions investigated by the two expeditions are so different that it is improbable that the same methods could be used successfully in each region. In the Atlantic Ocean a large-scale circulation was investigated, whereas in the Southeast Asian Waters a considerable number of local effects and features had to be expected. The METEOR Expedition, working in a large ocean, had to investigate quasi-stationary conditions whereas the SNELLIUS Expedition, working in a monsoon region, could expect a strong annual variation of oceanographic conditions. Consequently, not one but at least two surveys during different seasons would have been necessary in Southeast Asian Waters. Thus, the data from the upper layers above about 600 m, cannot give a conclusive picture of the circulation unless observations made during other seasons are available. The influence of internal waves and tides on the observations is of such an order that in some cases it prevents the obtaining of reliable results. These difficulties are, however, not yet overcome in present research.

Although these critical remarks are necessary to understand the factors limiting the evaluation of the observations of the SNELLIUS Expedition, the success of the Expedition consists of a complete presentation of the complicated topography of the region, an explanation of the flow of bottom water based on very careful observations, and investigations of the occurrence and the effects of the internal waves and tides in these waters. In addition important geological, meteorological, and biological results were obtained. Thus, the SNELLIUS Expedition gives a comprehensive picture of the oceanography of this most interesting part of the Southeast Asian Waters, which, after thirty years, still provides the most dependable information for any part of the region. An appreciation of the results of this expedition is given by Dietrich (1939).

In 1929 the DANA crossed these waters and occupied a considerable number of oceanographic stations. In some areas, notably the China Sea, in waters north of New Guinea and southwest of Sumatra, her stations supply the only available observations.

Between 1928 and 1941 Japanese research ships made numerous observations in the western Pacific Ocean as far south as the coast of New Guinea, and some in the China Sea. No oxygen determinations were made and most of the stations lie outside the region of the present study.

The ALBATROSS in 1948, and the GALATHEA in 1951 also passed through these waters, but they occupied only a few oceanographic stations in the region, as the interest of both expeditions was directed more to biological and geological problems.

From 1947 to 1950 the United States Fish and Wildlife Service made comprehensive investigations of the waters round the Philippines with the ships SPENCER F. BAIRD and ALOR STAR. Although the station data have not yet been published, they were placed at my disposal through the courtesy of the Scripps Institution of Oceanography. Data from all of the oceanographic stations of the expeditions discussed above and listed in table 3 were used in compiling Chapters 6 and 7.

Compared with the wealth of observations made by these expeditions the data available from the local oceanographic institutes are rather meagre. The Institut Oceanographique d'Indochine at Nhatrang has been chiefly interested in biological problems and has carried out little oceanographic work. Its annual reports give information on the activities of the Institute. Information on tides and tidal currents for that area were obtained from French hydrographic surveys. In the Philippines the Bureau of Fisheries made some oceanographic observations around 1930; these and other later activities have been summarized in a handbook on Philip-

pine fisheries prepared by the Technical staff of the Bureau of Fisheries for the Indo-Pacific Fisheries Council meeting in Quezon City in 1952 (I.P.F.C. 1952). In recent years the Royal Thai Navy has started oceanographic work in the Gulf of Thailand and some results are reported by Penyapol (1957).

Hardenberg (1950, 1952) has reported on the activities and history of the Dutch Laboratorium for Zeeondersoek located in Djakarta. This institute was chiefly interested in fisheries but has made fairly comprehensive investigations of the waters of the Sunda Shelf. Oceanographical investigations were also carried out, especially during the periods 1914-19 in the Java Sea, the southern parts of the China Sea and the Straits of Malacca, and from 1939-1941 in the Java Sea. The results of the latter have not been published but they have been used in part in Section 4.4. In 1949 the institute investigated the upper layers of the Celebes Sea from the vessel SIBOELA. From 1949 onwards an extensive programme of surface sampling from merchant ships was carried out in Indonesian waters, and was later extended over the whole Southeast Asian Waters. The Indonesian research vessel SAMUDERA occupied in 1956-57 about 100 oceanographic stations in the Eastern Archipelago, to the south of Java and on the Sunda Shelf.

The remaining institutes working in the area are concerned almost exclusively with problems in biology and fisheries. The Indo-Pacific Fisheries Council (1957) has prepared a Directory of Fisheries Institutions which gives details of the work done by all institutes in this area.

In addition to these scientific investigations, information on oceanographic conditions has been increased considerably by merchant ships, which navigate in these waters and take observations of currents, winds and temperatures. Hydrographic offices of the countries interested in the region have analysed and published these observations in many atlases, describing the currents, as well as meteorological and climatological conditions. These atlases are used as the basic material for Chapters 3 and 5 and they are listed there. Data on tides along the coasts are chiefly taken from surveys of hydrographic offices, and the tidal constants published by them are used to compile the charts in Chapter 8. The information on mean sea level and its annual variations, used in Chapter 7, is based on the operation of more or less permanent tide gauges. Another valuable source of information on weather, climate, local effects of currents and tidal streams are the sailing directions issued by the different hydrographic offices.

A bibliography, including all the literature cited and various additional papers not mentioned in the text, is given at the end of each chapter. Since "References on the Physical oceanography of the western Pacific Ocean" published by the US Navy Hydrographic Office (1946) lists all publications on this subject prior to 1945, early publications and those of minor importance are not listed here. Three works discussing general aspects of the region are: "Southeast Asia" by Dobby (1956) dealing with the geography of the region, "Het Klimaat van Nederlandsch Indie" by Braak (1921) containing a considerable amount of detailed statistical material, and "De Zeeen van Nederlandsch Oost Indie" edited by van der Stok (1922), summarizing all investigations of the early exploration period immediately prior to that of systematic research started by the SNELLIUS Expedition.

LITERATURE

Braak, C.
1921. Het Klimaat van Nederlandsch Indie. Verh. Magn. Met. Obs. Batavia. 8.

Dietrich, G.
1939. Die bisherigen Ergebnisse der Niederländischen Snellius Expedition für die Ozeanographie des Australasiatischen Mittelmeeres.
Ann. Hydrogr. Berl. 67 : 475-487.

Dobby, E. H. G.
1956. Southeast Asia. 5th. ed. London.

Hardenberg, J. D. F.
1950. Zee Ondersoek in de Indonesische Wateren.
Chron. Nat. 106 : 187-192.

Hardenberg, J. D. F.
1952. Report of work carried out since 1939 in the Java Sea by the Laboratory for Investigations of the Sea, Batavia.
Proc. 7 Pacif. Sci. Congr. 3 : 190-2.

Indo Pacific Fisheries Council.
1952. Philippine fisheries, a handbook prepared by the technical staff of the Bureau of Fisheries.
pp 185. Manila 1952.

Indo Pacific Fisheries Council.
1957. Directory of Fisheries Institutions. Asia and the Far East. Bangkok.

Penyapol, A.
1957. Report on oceanographic surveys carried out in the Gulf of Thailand during the years 1956-7.
Hydrogr. Dept. Bangkok.

van Riehl, P. M.
1932. The Snellius Expedition.
J. Cons. Int. Explor. Mer. 7 : 212-217.

Schott, G.
1935. Geographie des Indischen und Stillen Ozeans.
pp. 413, Hamburg.

van der Stok, J. P.
1922. De Zeeen van Nederlandsch Oost Indie. pp. 506, Leiden.

Tydeman, G. F.
1903. Hydrographic results of the Siboga Expedition.
Siboga Exped. 3. pp. 93.

United States Navy Hydrographic Office.
1946. References on the physical oceanography of the western Pacific Ocean.
Publ. n. 238, pp. 168 Washington.

CHAPTER 2

CONFIGURATION OF SEAS AND BASINS

The distribution of water and land alone characterizes the Southeast Asian Waters as one of the regions with the most complex structure on the earth. Numerous large and small islands subdivide the region into different seas, which are connected with each other by many passages and channels. When considering in addition the structure of the bottom of the seas, and that of the surface of the land, this unusual character appears still more pronounced. Deep trenches, high mountain chains, rows of volcanoes, deep sea basins and innumerable coral islands form a complexity of phenomena which are not found over such an extended area in any other part of the world. Therefore it is not surprising that this region has attracted the interest of research workers, and that we have a quite advanced knowledge of its topography, geology and tectonics as well as of its geophysical conditions.

In this book, the study of the topography of the different seas, and of the passages connecting them, has been confined to those aspects basic to the examination of the exchange of water. Particular attention is given to the topography of the sills, which are so important in the study of the replenishment of the bottom water and the ventilation of the deep sea basins. The information given here is based on the soundings of the SNELLIUS Expedition (van Riehl, 1934). In regions outside the area covered by this expedition data from Dutch, British and United States nautical charts are used. The General Bathymetric Chart of the Oceans is on too small a scale to show the details in this region. The SNELLIUS Expedition charts give an excellent presentation of the topography, but since there are relatively few deep sea soundings in the other regions, no new bathymetric chart is presented here. The preparation of a new more detailed chart of the Southeast Asian Waters is a task for the future, when additional soundings have been made.

An analysis of the origin of these seas has already been given by a competent author, Kuenen (1935, 1950), who fully supports the ideas of Molengraaff (1922) on the formation of the Indonesian depressions. Geophysical investigations, especially gravity measurements by Vening Meinesz (1934), confirm these results. However, Kuenen's investigations are restricted to the region of the Indonesian deep sea depressions and do not include the Philippines and the Sulu Sea, in spite of the fact that their formations are closely related to those of the Indonesian depressions. A description of the distribution and origin of coral reefs in the Indonesian Archipelago is given by Molengraaff (1929), by Kuenen (1933, 1950) and by Umbgrove (1947).

In Southeast Asian Waters, practically all types of topographical features are to be found: shelves, deep sea basins, troughs, trenches, continental slopes of various shapes, and volcanic and coral islands. Sills are formed between the islands by submarine ridges which divide the deep sea basins and govern the exchange of their bottom water, making them of special interest for the oceanographer. In this book the depressions of the bottom relief are classified as basins, troughs and trenches, terms used by Sverdrup *et al.* (1946). In the new nomenclature proposed by Wiseman and Ovey (1955), the term trough no longer appears but this term seems desirable to define weaker depressions, which can be classified neither as trenches nor as basins. But all these terms give no account of the origin of the different depressions, in contrast with the terminology used by Kuenen (1950) who differentiates between basins, U-troughs and V-troughs. His V-troughs usually correspond to trenches, while structural U-troughs are often denoted as basins.

The whole of the Southeast Asian waters are considered principally as part of the Pacific Ocean and their southern boundary is placed at the southern entrances of the Savu and Timor Seas. This is discussed in detail in Section 6·5

where an analysis of the water masses supports this position of the boundary. The subdivision of the surface of the oceans adopted by the International Hydrographic Bureau (1953) is in agreement with this analysis. Such subdivisions, depending on surface features, are not always satisfactory; for example the China Sea would unquestionably be classed as a geographical unit from an examination of surface features, but further examination of deeper features shows that its southern part belongs to the Sunda Shelf and its northern part is a deep sea basin.

Any subdivision of a region must necessarily separate correlated and neighbouring features, because the limits can be drawn only from one particular point of view at a time, and will not be conclusive from another. Where it is necessary to define sharp limits, such as for the determination of the area and volume of a sea, these limits must be more or less arbitrary lines. For oceanographical or geological study the areas can be separated by boundary zones rather than by lines. Consequently, in this work, the Southeast Asian Waters have been subdivided into the following areas: the Sunda Shelf, the China Sea, the Philippine Waters, the Eastern Archipelago, the Arafura Shelf, the Sahul Shelf, and the Andaman Sea, but no precise boundaries are given.

The SUNDA SHELF connects the three large islands Sumatra, Borneo and Java with the mainland of Asia and includes the southern parts of the China Sea, the Gulf of Thailand and the Java Sea, as well as the shallow parts of the Straits of Malacca. The southern part of the China Sea is a very flat trough, being about 40 m deep at its periphery and up to 100 m in its central part, so that a stratification of the water can

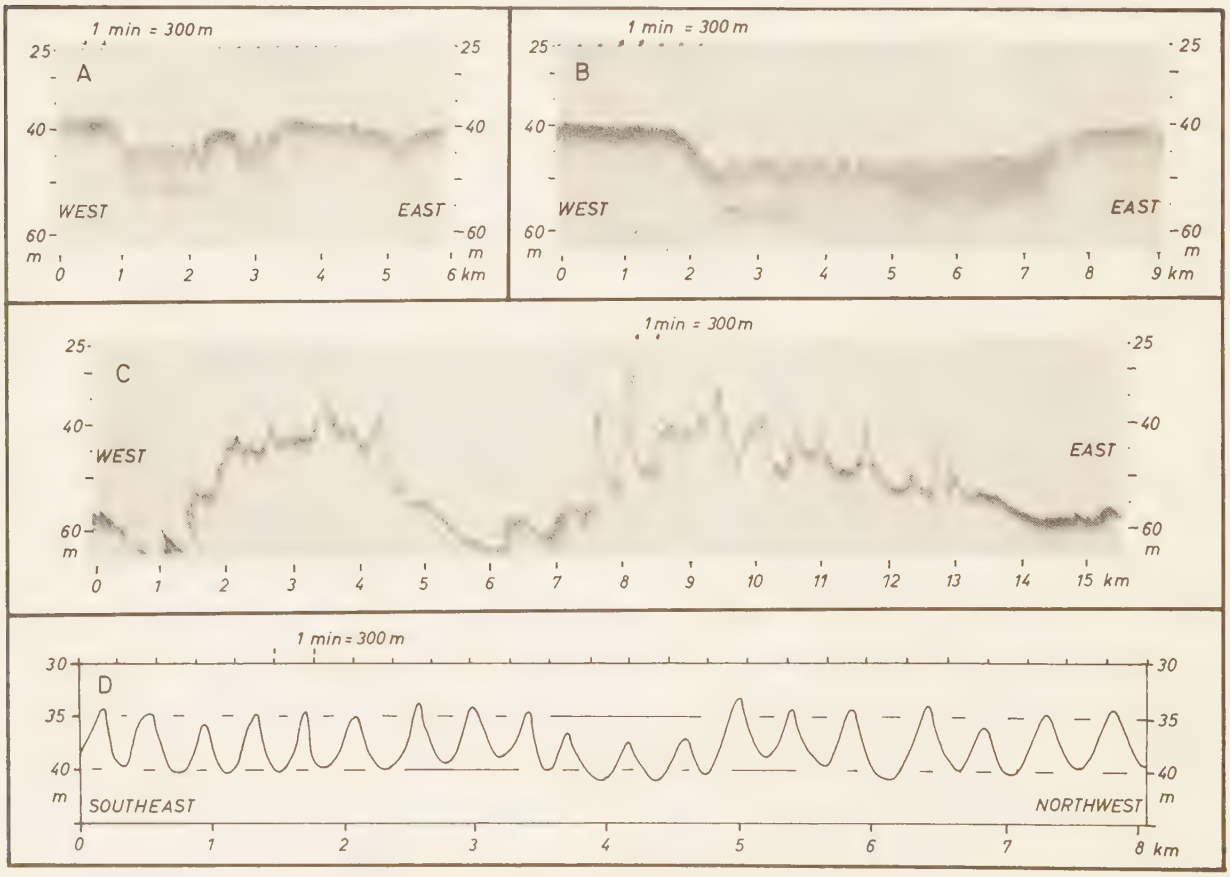

Fig. 2·1. Echo profiles across conspicuous structures on the bottom of the Sunda Shelf.
A and B, submerged river valleys south of Borneo.
C submerged coral island.
D sand waves in the Malacca Strait near One Fathom Bank.
For positions see fig. 2·2.

develop seasonally. The adjoining Gulf of Thailand is about 70 m deep in its central part. To the south, between Sumatra and Borneo, the shelf becomes shallower and the depths decrease south of the equator to less than 40 m.

The connection with the Java Sea is by the Karimata, Gaspar and Banka Straits; the first two, through which almost the whole water exchange occurs, are of the same depth as the surrounding areas. The Banka Strait is narrow and is closed at its southern end by a bank with a threshold of only 13 m. The depths in the Java Sea increase from about 20 m off the coast of south Sumatra to more than 60 m in its eastern part. Although the Sunda and Malacca Straits form the only connections with the Indian Ocean, the water exchange through them is comparatively weak. The Sunda Strait, in its narrowest part, is only 24 km wide, deeper than the Java Sea and of very irregular bottom topography.

The Malacca Strait, in its narrowest part, is about 30 m deep and 35 km wide, the depth increasing gradually to about 100 m before the continental slope to the Andaman Sea begins. On the bottom of this strait, in which strong tidal currents occur, large sand ripples of considerable uniformity are formed, with crests rectangular to the direction of the tidal currents. These ripples are shown in an echogram (fig. 2 · 1), which demonstrates clearly the regularity of their appearance over a considerable distance. The height of the ripples is between 4 and 7 m and their wave length varies between 250 and 450 m. In addition to these ripples at right angles to the direction of the tidal currents,

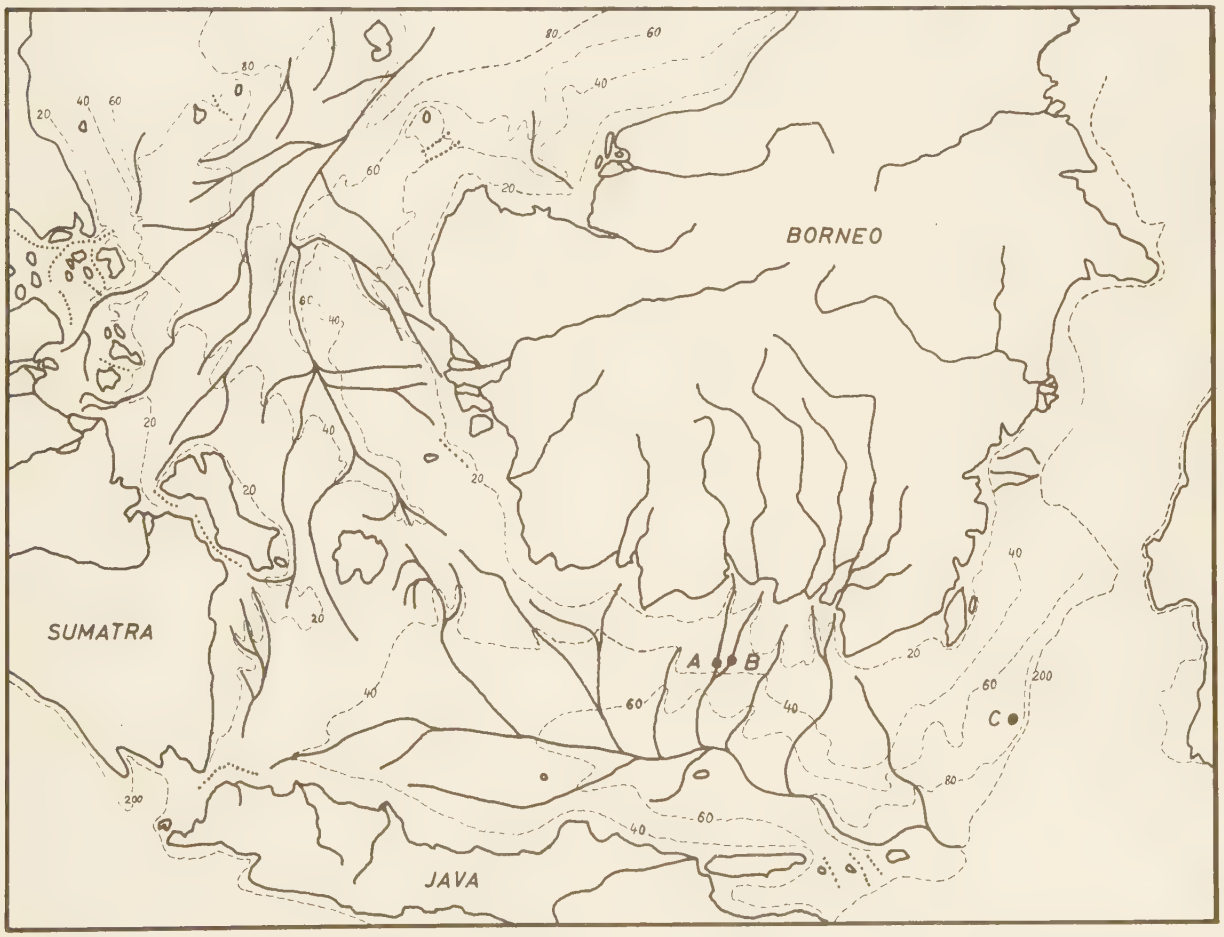

Fig. 2·2. Chart of the submerged river valleys on the Sunda Shelf, chiefly according to Kuenen. Depth contours indicated.
····· deeper channels, probably due to the action of tidal currents. A, B, C, positions of echograms, shown in fig. 2·1.

other forms of long ridges, parallel to the direction of the tidal currents and of larger dimensions appear in the strait. So, the One Fathom Bank rises from a depth of 30 to 40 m to only 2 to 15 m and is about 25 km long and 1500 m wide. These features are in general very similar to those in the Straits of Dover, which were extensively investigated and described by van Veen (1936).

On the bottom of the Sunda Shelf, there are a number of submerged river valleys, which all flow together into two large streams, the Java and Sunda Rivers, flowing into the Bali Trough and the China Basin, respectively. These systems of submerged rivers have already been presented and described by Molengraaff (1922) and Kuenen (1950), but are shown in figure 2 · 2 because of their peculiarity. Although these submerged rivers were discernible on charts based on wire soundings, their full details were only brought out by echo soundings. Echo profiles of two such submerged valleys south of the Sampit River off south Borneo are shown in figure 2·1A and B, and their positions are indicated in figure 2·2. The different tributaries are cut into the bottom of the sea and are 400, 1200 and 5400 m wide. In the river valley itself, a layer of sediment 8 to 15 m thick is found. The echo from the original river bottom, being between 17 and 24 m below the surroundings, can be clearly seen in figure 2 · 1 A, and being 13 m below the bottom in figure 2 · 1 B.

At the edge of the continental slope, near the submerged mouths of the Sunda and Java Rivers, and between the islands of the Natuna and Kangean groups, deep valleys are found. These, however, seem to be more of the nature of tidal inlets deepened by strong tidal currents, than natural river valleys. West of Kangean Island, these tidal inlets have 120 to 150 m maximal depth in contrast to their surroundings, which are only 80 to 90 m deep. They are also shown in figure 2 · 2.

Large bars are formed off the mouths of the various rivers, which drain the rainy land around the Sunda Shelf, transporting enormous masses of deposits. These are often serious obstacles to navigation and some of them rise to about 1 m below low water.

An echo profile across a submerged coral island is shown in figure 2 · 1 C, and its position indicated in figure 2 · 2. Near the edge of the Sunda Shelf the island rises from a depth of about 70 m. It extends about 10 km in a west-east direction and shows a very irregular topography. The highest points, however, reach to about 10 m below the surface, but are not shown in this echogram.

The CHINA SEA is the large sea extending from Formosa to Singapore. This name is a simplification and follows Schott (1935) thus employing the name popularly used by navigators and avoiding confusion with the East China Sea. It is the largest continuous sea in Southeast Asian Waters; its southern part belongs to the Sunda Shelf and has already been discussed in that section. Its northern part, on the other hand, is a deep sea basin with a maximal depth of 5016 m. At depths of more than 4000 m the China Basin is divided into three parts; in its central part, an abyssal plain with a depth of about 4300 m is found. The continental slope is rather steep near Palawan and Luzon, and the deepest sounding is to be found off the latter island. Off the coast of China, a shelf extends about 300 km into the sea and includes the Formosa Strait and the Gulf of Tonkin. The islands of Formosa and Hainan are situated on this shelf. The Gulf of Tonkin deepens from the coast gradually to the centre, where the maximal depth is only 70 m. In the Formosa Strait, which is about 150 km wide, a number of reefs and banks are situated. The sill depth of this strait, about 70 m, is only a little below the average depth, which is 60 m in the northern part and 50 m in the southern part.

The main entrance to the China Sea from the Pacific Ocean is the deep Bashi Channel, through which also the replacement of its bottom waters occurs. Although the few soundings in the neighbourhood of the sill indicate a threshold of about 2600 m, temperature observa-

tions suggest a much higher sill (see Section 6·7). Another somewhat higher sill exists between the Koto Syo Islands and Formosa, the sill depth, according to soundings, appearing to be 1800 m.

In the China Sea, there is a large number of peaks, which appear as coral reefs, atolls or banks. The extensive reef area west of Palawan needs special consideration in this connection. In the General Bathymetric Chart of this region, published in 1940, this area appears as a shelf, separated from Palawan, Borneo and the Sunda Shelf by a trough more than 1500 m deep. The soundings of that region entered in the British Admiralty Charts, however, show the whole area as being rather deep with the different reefs rising steeply. Also, Tydemann (1922) and van Riehl (1934) had already realized and clearly indicated this fact in their depth charts of the East Indian Archipelago.

A depth chart of this region based on British Admiralty Charts (fig. 2·3) demonstrates clearly, in spite of the relatively small number of soundings, that the different reefs and islands stand on a comparatively deep and level plateau. This varies between 1700 and 2500 m. Only the Reed Bank in the northeast is shallower, its base appearing to lie in 300 to 500 m depth. The Palawan Trough extends along the steep continental slope between Palawan and Borneo on the one side and these reefs on the other. It has a maximal depth of about 3475 m. Its deepest

Fig. 2·3. Bathymetric chart of the reef region in the China Sea.

connection with the China Basin is a deep channel through the reef region with a sill depth of about 2050 m. The sill to the north between Palawan and the Reed Bank is only 1400 m deep. Further soundings in this region might add interesting details to this picture.

The SULU SEA is outstanding because of the height of its sill, which is only 420 m deep and encloses a large basin of 5580 m maximal depth, in which exceptional biological conditions are found. The Sulu Basin is nearly rectangular in shape, its bottom sloping from about 1500 m in the west to more than 5000 m in the east. Off the Philippines and along the Sulu Archipelago, the continental slope is very steep. The deepest connection with the China Sea is through a channel running along the western side of Mindoro and Panay Islands. The sills in this channel are south of Mindoro and west of Panay, with between them the Panay Trough of 1400 m depth. As the bottom relief in this area is extremely irregular, the density of the soundings is not sufficent to determine the exact depth of the two sills, which are estimated at approximately 450 m. However, the temperature observations in these basins indicate that the western sill is deeper (470 m) because colder water is found in the Panay Trough than in the Sulu Basin. The sill governing the water exchange of the Sulu Basin lies in a depth of about 420 m south of the Panay Trough (see also Section 6·7).

In addition to the replacement of the bottom water of the Sulu Basin across this threshold, there is an exchange of surface water with the China Sea through the Balabac Strait. This Strait is narrowed by extensive coral reefs and contains in its narrowest part a channel 200 m deep, which is probably eroded by strong tidal currents. At its eastern entrance the strait is closed by a sill only 105 m in depth, but in the west the sill is somewhat deeper, being about 135 m. A considerably wider entrance for surface water exists through the Sulu Archipelago; this is very shallow in large areas and consists of numerous coral banks. Two channels, one east of Jolo with a sill of about 200 m depth, and another east of Sibutu, with a sill of about 270 m depth, form slightly deeper, but very narrow thresholds.

Through the PHILIPPINE ISLANDS an exchange of surface water with the Pacific Ocean is possible through the San Bernardino and the Surigao Straits; in these two straits not only strong tidal currents but also residual currents are observed. They transport only water of the surface layer over a sill of 110 m depth in the San Bernardino Strait and of 65 m in the Surigao Strait. Between the islands of the Philippines a number of smaller troughs are situated, the more important of which are listed in table 7. They are connected by several passages, but are of minor importance for water exchange.

The term EASTERN ARCHIPELAGO is used to denote the whole region between the Sunda Shelf in the west, the Arafura Shelf in the east, Mindanao in the north and the Indian Ocean in the south. It is the only deep connection between the Pacific and the Indian Oceans in lower latitudes. It is topographically and oceanographically a homogeneous region, but in the SNELLIUS Expedition reports it was given the rather clumsy title 'Eastern parts of the East Indian Archipelago.' The name Eastern Archipelago is not substantially new, it has been used in British Admiralty Charts to denote the whole Indonesian waters, but here it is given more precise definition. The topography of this region was intensively explored by the SNELLIUS Expedition. The numerous soundings, especially in the neighbourhood of the various sills, are discussed by van Riehl (1934) in connection with the spreading of the bottom water. He gives a large scale map of the whole region and several detailed charts of important sections, which still constitute the best information on this area. The supply of the different basins with bottom water is, oceanographically, an extremely interesting process and is dealt with in Section 6·7. A list of the different basins with their maximal and sill depths is given in table 7, and the general topography can be seen in plate 37. Because of the excellent SNELLIUS description of this region only the general structure is discussed here.

Between Mindanao and Halmahera, the Molucca Basin is closed by a ridge with a sill of 2340 m. Its bottom is divided into five smaller basins, which have maximal depths between 3400 and 4800 m and are connected below the sill of the Molucca Basin. The Sangihe Trough, extending along the ridge which connects North Celebes with Mindanao, has a shallower sill depth of only 2050 m and a maximal depth of 3820 m. This ridge is crowned by a number of islands and has four narrow thresholds, each about 1400 m deep through which the large Celebes Basin is supplied with bottom water. In its central parts a large abyssal plain is situated in a depth of about 5100 m. Directly connected with the Celebes Basin is the Macassar Trough, whose deeper portions are about 2300 m. In the south it is closed by a ridge connecting Celebes with the Sunda Shelf in a depth of less than 800 m.

The Molucca Basin is closed in the south by a ridge running from Celebes to New Guinea, and on which the islands of Taliabu, Mangole and Obi are situated. The deepest threshold through this ridge is the Lifamatola Strait with a sill depth of 1880 m, which governs the replacement of the bottom water of all basins south of it. The 2000 m isobath includes, south of this ridge, the whole Ceram Basin, the Banda Basin with the Weber Deep, the Flores Basin and the Sawu Basin. The different secondary basins of this region have maximal depths between 3350 and 7440 m (table 7), and some are separated from the others only at levels deeper than 4000 m. It is remarkable that the Sawu Basin, although situated south of the Lesser Sunda Islands, still belongs to this large basin.

The Lesser Sunda Islands, situated in the prolongation of Java, continue in a ridge, running in a large arc from Wetar by way of Damar, Manuk and the Banda Islands to Ceram. The thresholds between the different islands of this chain become deeper to the east. Thus, the Bali Strait is only about 60 m deep, Lombok Strait reaches a depth of 300 m, the strait between Alor and Wetar more than 1200 m and the threshold to the Weber Deep as much as 4300 m. Consequently the basins south and east of this island chain, the Weber Deep, the Wetar Basin and the Sawu Basin, still belong to the Banda Sea group of deep sea basins.

The second ridge, which separates the Bali Trench from the Java Trench south of Java, continues through the islands of Sawu, Roti and Timor and from there it runs parallel to the first ridge in a large arc, also ending at Ceram. On this ridge, Babar, the Tanimbar and Kai Islands are situated. The two deepest thresholds in this ridge are between Timor and Babar with sill depths of approximately 1600 m. The island of Sumba, south of Flores, connects these two ridges, and south of it the deepest connection between the Bali and the Java Trenches is found, and here occurs a disturbance of the parallel structure of these two island chains and adjoining trenches. The southern entrances of the Sawu Sea are formed on both sides of Sawu Island by sills about 1150 m deep.

The second ridge is separated from the Sahul and Arafura Shelves again by a depression, which is an extension of the Java Trench in the form of the Timor Trough and the Aru Basin, and which extends further into the Ceram Basin. The Timor Trough is separated from the Indian Ocean by a sill 1940 m deep, and is supplied with Indian Ocean water. From the Timor Trough a long narrow channel of very even bottom depth of about 1600 m leads to the Aru Basin. This basin, with a maximal depth of 3680 m, is connected by a channel, also 1600 m deep with the Ceram Basin, so that replacement of its bottom water takes place from both the Pacific and the Indian Oceans. Three sections through this system of trenches and ridges at 110°E, 126.5°E and 6°S are shown in figure 2 · 4. They demonstrate clearly the sequence of depressions and island chains in this wave-like folding structure.

The Arafura Shelf, connecting New Guinea and Australia, is 30 to 90 m deep and includes the Aru Islands in its northwestern part. A slightly deeper channel leads in a west-east

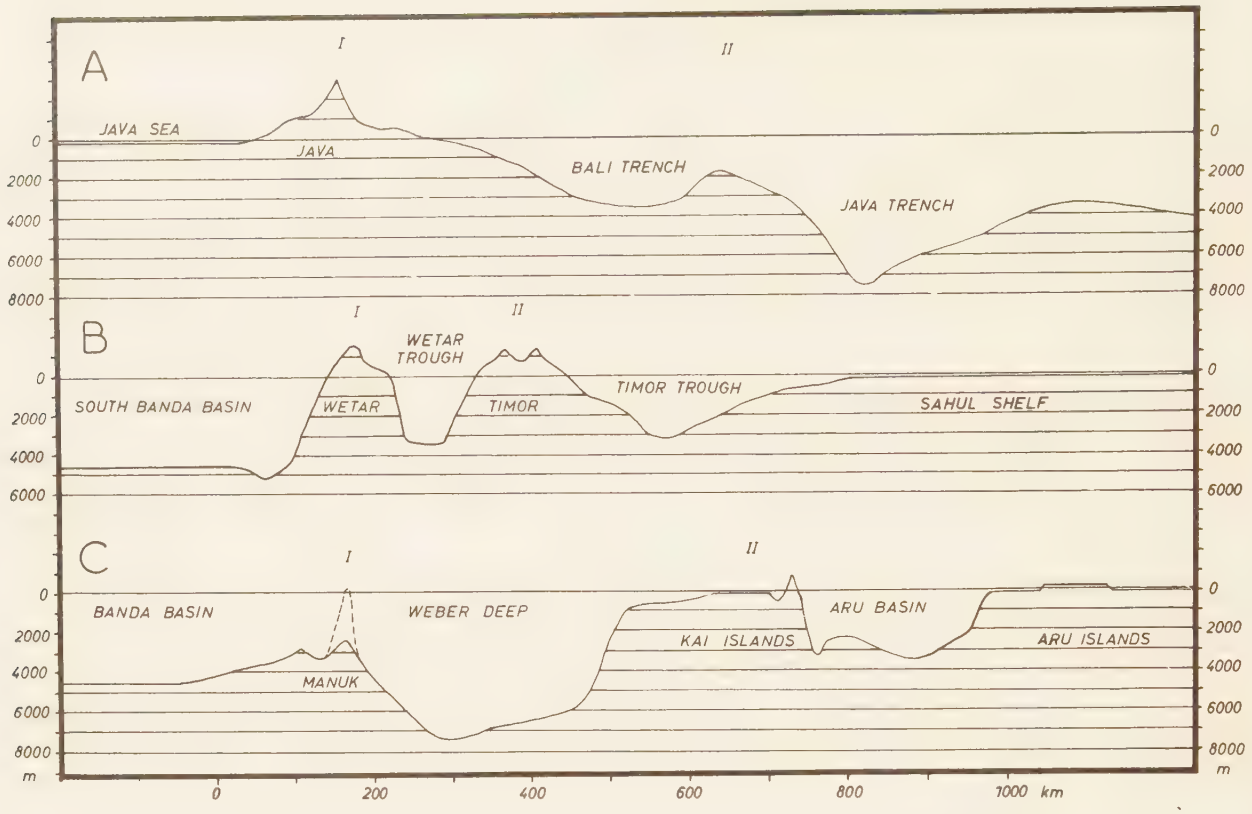

Fig. 2·4. Profiles across the system of trenches and ridges in the Indonesian Archipelago.
I Java and inner Banda arc.
II Outer Banda arc.
Profile A in 110°E, B in 126.5°E, and C in 6°S.
Vertical exaggeration : 25:1.

direction to the Torres Strait, which is blocked by large coral reefs. Some small channels up to 12 m in depth lead through these reefs permitting only a weak water exchange. The tidal currents, on the other hand, are of considerable strength in the strait. The SAHUL SHELF, situated off the northwest coast of Australia, extends about 300 km into the sea with average depths of 80 to 100 m. Near the edge of the shelf, a number of reefs, banks and some islands are situated.

The ANDAMAN SEA contains a relatively extensive basin with a maximal depth of 4360 m, but its bottom is rather uneven. Its western boundary is a ridge on which the Andaman and Nikobar Islands are situated. This must be considered as a prolongation of the mountain chain of Sumatra. Off Burma and the Malayan Peninsula, the shelf is broad and has a rather gradual continental slope. The deepest threshold to the Indian Ocean lies between Sumatra and the Nikobars, near Great Nikobar Island. Its sill depth appears to be between 1800 and 2000 m, but as there are no deep oceanographical stations in the Andaman Sea, it is not possible to confirm this by temperature observations. The Ten Degree Channel between the Nikobar and Andaman Islands has a sill only 900 m deep, and the Andaman Islands themselves are connected with the mainland within the 200 m line, with a sill depth in the Preparis Channel of only 180 m.

In the INDIAN OCEAN, the large India-Australia Basin is situated to the south and west of Java and Sumatra. It can be subdivided into several smaller basins as shown by Stocks

(1960). The Java Trench (max. 7450 m) off the coast of the two islands is its deepest part, and parallel to it, but closer to the coast, runs the Bali Trench (max. 5160 m). The whole system is also often called the Sunda Double Trench. It is, however, not limited to the region south of Java, Bali and Sumbawa, but continues southwest of Sumatra. There a number of islands, some of considerable size, occurs on the ridge separating the two trenches. Both trenches become shallower to the north, the inner, also named the Metawei Trench, reaching depths of less than 200 m south of the equator, but north of the equator it can still be recognized. Schott (1935) noted a gentle rise south of the Java Trench before the abyssal plain of the India-Australia Basin begins. This sequence of rises and depressions gives the whole area between the Sunda Shelf and the India-Australia Basin a wave-like structure. A profile through this structure is shown in figure 2 · 4.

The **Philippine Basin** as part of the Pacific Ocean borders the Southeast Asian Waters in the east, its deepest part being the Philippine Trench (max. 10497 m). It is separated in the southeast from the West Caroline Basin (max. 5798 m), situated north of New Guinea, by a ridge running from Halmahera via the Palau Islands to Yap. A detailed geological description of the region is given by Dietz (1954).

LITERATURE

Bruun, A. F. and A. Kiilerich

1957. Bathymetrical features of the Bali-Lombok Strait.
Mar. Res. Indonesia. 3 : 1-6.

Dietz, R. S.

1954. Marine geology of the northwestern Pacific. Description of Japanese bathymetric chart 6901.
Bull. Geol. Soc. Amer. 65 : 1199-1224.

Fairbridge, R. W.

1954. Report on limits of the Indian Ocean. Pan Indian Ocean Sci. Assoc. Congr. Perth. Sect. F : 18-28.

1955. Some bathymetric and geotectoric features of the eastern part of the Indian Ocean.
Deep-Sea Res. 2 : 161-171.

van Huystee, T.

1944. Soundings and bathymetric charts. III. Echo soundings.
Snellius Expedition 2(2). 134 pp.

International Hydrographic Bureau

1953. Limits of oceans and seas.
3rd ed. spec. Publ. 23. 38 pp.

Kuenen, P. H.

1933. Geology of coral reefs.
Snellius Expedition 5(2). 125 pp.

1935. Geological interpretation of the bathymetrical results.
Snellius Expedition 5(1). 124 pp.

1950. Marine geology.
New York. John Wiley & Sons. 568 pp.

Molengraaff, G. A. F.

1922. De geologie der zeeen van de Nederlandsch Oost-Indie Archipel. pp. 272-357 Chapter g in K. Nederlandsch aardrijkokundig genootschap, Amsterdam, De zeeen van Nederlandsch Oost-Indie.
Leiden, E. J. Brill. 566 pp.

Molengraaf, G. A. F.

1929. The coral reefs in the East Indian Archipelago, their distribution and mode of development.
Proc. 4th. Pacif. Sci. Congr. 11a : 55-88.

van Riehl, P. M.

1934. Soundings and bathymetric charts.
II. The bottom configuration in relation to the flow of bottom water.
Snellius Expedition 2(2). 61 pp.

Schott, G.

1935. Geographie des Indischen und Stillen Ozeans.
Hamburg, C. Boysen. 413 pp.

Stocks, T.

1960. Zur Bedensgestalt des Indischen Ozeans.
Erdkunde 14 : 161-170.

Sverdrup, H. U., M. W. Johnson, and R. H. Fleming.

1942. The oceans, their physics, chemistry and general biology.
New York, Prentice Hall, 1,087 pp.

Tydeman, G. J.

1922. De diepten der zeeen, pp 55-101.
Chapter a in K. Nederlandsch aardrijkokundig genootschap, Amsterdam, De zeeen van Nederlandsch Oost-Indie.
Leiden, E. J. Brill. 556 pp.

Umbgrove, J. H. F.

1947. Coral reefs of the East Indies.
Bull. Geol. Soc. Amer. 58 : 729-778.

van Veen, J.

1936. Onderzoekingen in de Hoofden.
The Hague, Landsdrukkerij. 252 pp.

Vening Meinesz, F. A.

1934. Gravity expeditions at sea, 1923-32.
Publ. Neth. Geod. Comm. 4. 208 pp.

Wiseman, J. D. H., and C. D. Ovey

1955. Proposed names of features on the deep sea floor.
Deep-Sea Res. 2 : 93-106.

CHAPTER 3

THE WIND SYSTEMS AND THE CIRCULATION AT THE SURFACE

Because they are situated between the land masses of Asia and Australia, the Southeast Asian Waters are the ideal monsoon region. The equatorial pressure trough moves according to the position of the sun, crossing the equator twice each year. In the summer hemisphere a low develops over the continent in prolongation of the equatorial pressure trough, while in the winter hemisphere a high is formed over the continent, belonging to the subtropical high. Between the high and the low the monsoons develop. Because the pressure distribution is very stationary, the winds have a high constancy, especially over the sea. The wind forces are generally small; storms and typhoons are observed only over the northern parts of the China Sea and the Philippines, over the Andaman Sea and north of Australia. When the equatorial trough passes the equator the winds are extremely variable, but in the full monsoon they temporarily deviate over land from the direction of the monsoons because of thermal influences. Charts of the wind distribution over the region are not given here; reference may be made to the various meteorological atlases listed in the bibliography. Only small chartlets, which are redrawn from the Atlas of Climate Charts of the Oceans (U.S. Weather Bureau, 1938), are added to the charts of the surface currents (plates 1-6).

3·1 THE MONSOONS

In January the north monsoon is fully developed. Over Asia a high is formed and the equatorial trough lies just north of Australia. Over the whole China Sea and over the Andaman Sea the northeast monsoon blows, and continues towards the Pacific Ocean as the northeast trades. In the China Sea wind force 5 is often exceeded. The monsoon passes the equator as a north wind and south of it turns to the east, where it appears as the northwest monsoon. The equatorial trough lies over the Indian Ocean at about 10°S, south of which the southeast trades are found. Off the northwest coast of Australia the trades are deflected and blow almost parallel to the coast towards the northeast with only a small force. In February the equatorial trough moves northwards and lies over Java and the Lesser Sunda Islands. Over the whole region between Java and Australia southwest winds now prevail, branching off from the southeast trades. North of the equator conditions have not changed; but the strength of the monsoon has decreased. In March the southeast trades of the Indian Ocean extend further northwards and eastwards, while over the Timor and Arafura Seas northwest winds still prevail. Over the China Sea the northeast monsoon has weakened.

In April the equatorial trough moves quickly to the north and lies over the equator. The southeast trades always reach to about 5°S, that is, towards the north of the Lesser Sunda Islands, where it is normally called the southeast monsoon. North of the equator, over the China Sea and over the Philippines weak northeast winds still prevail, while over the Gulf of Bengal southwest winds are blowing, introducing the monsoon for Burma and Thailand.

May brings a complete change of conditions. The system of the northeast winds over the China Sea and the Philippines collapses, and the south monsoon succeeds over the whole of Southeast Asia. South of the equator the southeast monsoon blows, continuing to the Indian Ocean as the southeast trades. At the equator south winds prevail, and north of it the southwest monsoon. In the area of the Philippines and of the Celebes Sea the winds are still weak and unsteady. In June the distribution changes slightly; the winds become stronger, and reach force 4 and more over the Arafura Sea, over the Indian Ocean, and especially over the Gulf of Bengal.

In July and August the south monsoon reaches its full development. In these months the low over Asia and the high over Australia are strongest and the circulation reaches its

greatest strength. Over the open sea wind force 4 is often exceeded, but over the Indonesian Archipelago and over the Philippines the wind remains on the average below force 4.

In September over the waters around Formosa and Hong Kong the first northeast winds occur, indicating a weakening of the Asian low. In the other parts of the region the south monsoon loses only slightly in strength. In October the equatorial trough begins to move rapidly southwards, and by the middle of the month, lies along a line from the centre of the Gulf of Bengal to the north coast of New Guinea. North of this line northeast winds prevail, south of it still the southeast monsoon. In the Indian Ocean between the equator and 10°N the southwest monsoon has turned so far, that it comes almost from the west.

In November the equatorial trough runs clearly south of the equator. The northeast monsoon has intensified especially over the China Sea and normally exceeds wind force 4. Over the Indian Ocean the system of the southeast monsoon has collapsed, and the southeast trades are confined to south of about 5°S. By December the equatorial trough moves further to the south and lies at about 5°S. The northeast monsoon reaches its maximal force over the China Sea, crosses the equator as a north wind and temporarily reaches Java and the Lesser Sunda Islands. Over the Java Sea west winds prevail. The southeast trades of the Indian Ocean have retreated further to the south and reach just up to 10°S, and near the Australian northwest coast, south winds prevail.

This variation of the atmospheric circulation finds its parallel in a corresponding variation of the oceanic circulation. Because of the high constancy of the monsoons and of their regular appearance the ocean currents show the same characteristics. Just as the monsoon changes direction twice a year and the winds are practically reversed at the time of their strongest development, the oceanic circulation is also reversed in large areas. Thus, this complete reversal is really typical of the circulation in these waters.

3·2 THE CONSTRUCTION OF THE SURFACE CURRENT CHARTS

The atlases of the surface currents available for this region, which are listed in the bibliography, normally present for every month the vector average of all observations in every 1° square. In addition the data from 10-25 of these squares, are combined and a current rose is constructed, showing the frequency of the velocities in different directions. Useful as these presentations are for the sailor, they do not give a complete picture of the oceanic circulation, as wanted by the scientist. The observations are too scanty in large areas and the scattering of the vectors, calculated from only a few observations, is too large. Vectors always appear across or reverse to the main direction of the current. This does not mean that these observations are inaccurate, but their number is insufficient to eliminate the effects of eddies and counter currents on the main currents as modern investigations in the Gulf Stream and in the Kuroshio have shown. This fact appears rather clearly, when regions with a large number of observations are compared, for instance along the route Singapore - Hong Kong. There, such a scattering of the vectors is not found, but they result in a quite distinct picture of the average circulation, although in particular cases eddies and counter currents may appear in this area as in others. For the presentation of ocean currents for scientific consideration, a certain smoothing, however, is necessary in order to elaborate the main characteristic of the circulation (Wyrtki, 1960).

The current charts are constructed for every second month, but this is adequate to follow the variations of the circulation in the course of the year (plates 1-6). For the presentation of the currents the approved form of equally long current arrows has been chosen, the velocity being indicated in six steps by feathering. In order to avoid confusion of the charts the constancy of the currents has not been indicated. For this the mentioned atlases must be consulted. But normally a high velocity involves also a high constancy. For obvious reasons the original observa-

tions could not be used for the construction of the charts, rather they were composed from the current vectors of the 1° squares given in the cited atlases. Special consideration was given to the most frequent direction and to the average velocity in this direction as derived from the current roses. The average velocities in the most frequent direction are considered to be the reliable components of the circulation. These normally are much higher than the vector average. but can always be combined into an acceptable current pattern. It might be mentioned here, that the vector velocities given in the atlases of the U.S. Navy Hydrographic Office (1944, 1950) give in nearly all cases higher values than those of the Netherlands Meteorological Institute (1936, 1949, 1952). In the region east of the Philippines and north of New Guinea, where the density of the observations is small in both atlases, the presentations given by Schott (1939) are mainly used. Because of the clear presentation, the current arrows are easily attributed to the different months. Generally when constructing the charts given here, Schott's statement was confirmed that single observations more easily permit the drawing of a current chart than the resultant vectors. Further valuable information on the currents, especially on local effects, are given in the Pilots issued by different hydrographic offices.

Consideration must also be given to current boundaries, divergences, convergences and regions of upwelling. The differences in the density at the surface of tropical oceans are relatively small, so convergences are not pronounced and in no case are they as important as, for instance, the Polar Front. Divergences are also difficult to recognize at the surface, but are indicated at the bottom of the homogeneous layer by an upward curvature of the thermocline. Naturally, current boundaries are recognizable between the different branches of the circulation, but often it is impossible to associate them with convergences or divergences. It even seems likely that the same boundary may appear temporarily as convergence or divergence, especially in regions where currents form or break up, or where large eddies occur. On the other hand very stationary convergences or divergences are developed in connection with the main branches of the circulation, like the divergence of the North Equatorial Current in the Pacific Ocean at about 11°N. Schott (1935, 1939) has also met these difficulties in his presentation of the currents. He gives only current boundaries in the equatorial parts of the oceans, but he marks clearly the Subtropical Convergence and the Antarctic Convergence. So in the current charts of this book the boundaries between the different branches of the circulation are marked, but convergences and divergences are denoted only when a clear distinction was possible.

3·3 THE SURFACE CURRENTS OF THE NORTHEASTERN INDIAN OCEAN

The steady branch of the circulation in the Indian Ocean is the South Equatorial Current. It extends from the northwest corner of Australia between 20°S and 10°S to the other side of the ocean as far as Madagascar. Our presentation shows only its root and its eastern part. It reaches its strongest development in August, when it forms with the Somali Current and the Monsoon Current a large eddy in the equatorial part of the Indian Ocean. Even if this current extends over about 10 degrees of latitude, a careful study of the current observations will always reveal a current axis, clearly distinguishable because of essentially higher velocities. In August the current axis runs close to the coast of Java to the west, but is deflected southwestwards, when joining with the water masses of the monsoon current coming from the north. The South Equatorial Current is supplied chiefly by water masses from the south, partly by water from the Timor Sea and also for a considerable part by water out of the upwelling region to the northwest of Australia. From the Sunda Strait to the southwest the current axis seems to follow the boundary of the tropical and the subtropical water. This deflection to the south is also clearly marked in the current chart for June drawn by

Michaelis (1923). Until October this pattern changes only a little.

By December, when the southeast trades no longer reach the coast of Java, conditions are essentially different. Off the south coast of Java a coastal current develops flowing with relatively high velocities to the east, where it can be followed as far as the Sumba Island. The axis of the South Equatorial Current lies south of 10°S, and west of 100°E it shows a deflection to the south. In February this current rises off the west coast of Australia and one branch turns to the Timor Sea thus causing a divergence between the branches. The current axis runs from the northwest corner of Australia northwestwards and turns to the west where it joins the water masses of the Counter Current at about 9°S, 100°E. The Java Coastal Current is now most strongly developed, but reaches only to the eastern end of the island. With the northward extension of the southeast trades and the beginning of the southeast monsoon over the Timor Sea in April the South Equatorial Current becomes stronger again. Its water sources are chiefly from the south, partly from the upwelling region off northwest Australia and a visible current axis is formed only west of 100°E. The Java Coastal Current has decreased in strength, so with the beginning of the full southeast monsoon in June the current axis shifts closer to the coast of Java, but still the eastgoing current is recognizable off the coast. Water from the Timor and Sawu Seas and from the upwelling region off Australia intensify the South Equatorial Current in this season. The current axis runs south of 10°S, to 100°E, where it joins with the Counter Current, and turns then to the southwest.

Just as the southeast trades, as a permanent feature of the atmospheric circulation, form the permanent South Equatorial Current, so the changing monsoons over the northern part of the Indian Ocean cause an alternating current system. From June to October the southwest monsoon blows with considerable strength towards India and causes the development of a strong drift current north of the equator and of weaker drifts in the Bay of Bengal. These drifts lead to an extremely high piling up of water along the eastern side of the Bay of Bengal. Part of this water flows away through the Andaman Sea and around the west corner of Sumatra to the south, a smaller part flows along the east coast of India. The Monsoon Current flowing south of Ceylon to the east passes partly over into the drift setting against the Andaman Islands, and it is partly deflected to the south, when approaching the west corner of Sumatra.

About 8 degrees to the south the Equatorial Counter Current flows also eastwards. It is separated from the Monsoon Current by a zone of weaker eastward movements, clearly recognizable from the observations. In the zone between 2°N and 5°N the current has not only smaller velocities, but is also more variable in its direction. This phenomenon has not yet been elaborated and always both currents, the Monsoon Current and the Counter Current are shown together as one single branch. The Counter Current lies at or just south of the equator and remains there during the whole year.

The southeast monsoon in October is already so weak, that the Monsoon Current has degenerated into a weak drift and the drift current in the Bay of Bengal has decayed into several eddies; the circulation is generally cyclonic. On the other hand the Counter Current becomes essentially stronger. From June to October the water masses of the Counter Current after joining with the water masses of the Monsoon Current in the region west of Sumatra turn in a broad front to the south and pass over into the South Equatorial Current.

In December with the beginning of the northeast monsoon the circulation in the northern Indian Ocean has changed. From the Bay of Bengal a drift current develops, which gets stronger to the south and passes over into the North Equatorial Current. This current rises about at the northwest corner of Sumatra and is supplied partly by water out of the Malacca Strait, but chiefly by water from the Counter Current, which turns northwards off the west

coast of Sumatra. The axis of the Counter Current lies near the equator, but it reaches with decreasing velocities to about 6°S. In contrast with this the northern boundary is well developed and lies at 2°N. At about 2°S a divergence is developed, dividing the stronger and northwards turning part of the Counter Current from the weaker and southwards turning part. This divergence moves gradually to the south and when the southern branch vanishes in February, forms the boundary against the South Equatorial Current. Later this divergence is replaced by a convergence, when the Counter Current becomes stronger and gives more water off to the south.

A part of the water masses of the Counter Current flows to the southeast always along the west coast of Sumatra. From July to October, when the southeast monsoon touches the south coast of Java in full strength and the South Equatorial Current is pressed far to the north, this branch turns into the South Equatorial Current off the Sunda Strait. But from November the South Equatorial Current deviates from the coast and a small current develops south of Java in continuation of the coastal current off Sumatra. This Java Coastal Current reaches its strongest development in February, when it is reinforced by west winds, (Soeriaatmadja 1957). But it remains until June, after the beginning of the southeast monsoon, which leads to the conclusion, that this current is caused by dynamical conditions rather than by winds. Temporarily also a weak upwelling seems to appear along the boundary between the Java Coastal Current and the South Equatorial Current.

In January and February the northeast monsoon has reached its maximal strength over the Bay of Bengal and also its maximal extension to the south. The North Equatorial Current is strongly developed and in the Bay of Bengal a large anticyclonic eddy is formed. Also south of the axis of the North Equatorial Current a drift to the southwest is found, extending over the equator to the south and being caused by the monsoon. The Counter Current is pressed far to the south and flows between 3°S and 5°S in a small belt. The ALBATROSS Expedition, Jerlov (1953), recorded it in March 1948 even between 6° and 8°S.

The northeast monsoon ends in March and in April the southwest monsoon starts gradually. The anticyclonic eddy in the Bay of Bengal is still present, the North Equatorial Current now very weak, is also present as part of it. On the other hand the Counter Current has increased appreciably and extends from 3°N to 5°S. In broad front it turns at about 7°S into the South Equatorial Current, but parts of it continue in the Java Coastal Current. With the change to the full development of the southeast monsoon the current pattern south of the equator does not change, while north of the equator the drift into the Bay of Bengal becomes stronger and the Monsoon Current is formed. The presentations of the surface currents in the Bay of Bengal given for some months by Ganapati and Murthy (1954) are in full agreement with our current charts.

A schematic presentation of the west-east components of the currents along 90°E between 20°S and 10°N shows the development of the different current branches in the course of the year, figure 3 · 1. The South Equatorial Current

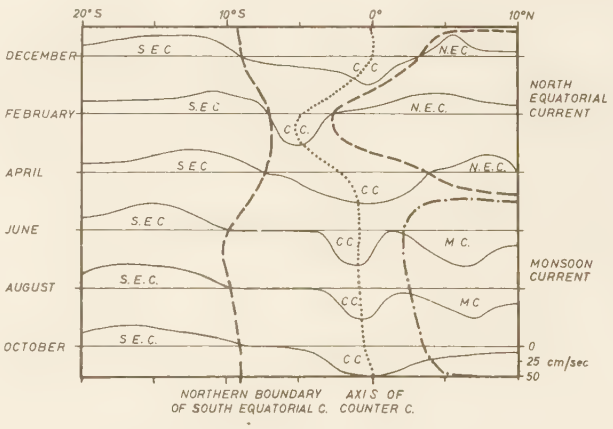

Fig. 3·1. Schematic presentation of the west-east components of the currents in the Indian Ocean along 90°E in different months.

is developed strongly throughout the year and its northern boundary varies only between 7°S and 10°S. On the other hand the current axis shows stronger variations. From June to October it has a southerly position, maximal 16°S in August. In February it lies more to the north at about

11°S, in spite of the fact that the southeast trades reach only to about 10°S.

The Counter Current is developed during the whole year and lies just south of the equator. The only exception is the time from January to March, when it is considerably shifted to the south. This southwards shifting is in close relation to the maximal development of the North Equatorial Current. Probably this might also be the reason for the northward shifting of the South Equatorial Current in these months. It may be assumed, that the whole circulation is compressed into a smaller space, if the South and the North Equatorial Currents are developed simultaneously, which is always the case in the Pacific Ocean.

North of the Counter Current a complete reversal of the circulation takes place during the year according to the monsoons. From December to April the North Equatorial Current flows to the west under the influence of the northeast monsoon, while from June to October the east-going Monsoon Current is developed. Monsoon Current and Counter Current are at least from June to August separate currents, and in October the Monsoon Current is already so weak, that a separation from the strongly developed Counter Current is no longer possible.

In connection with these current systems and the configuration of the coast line, regions of upwelling or sinking develop. The most important seems to be the region off the northwest coast of Australia, which gives a considerable contribution to the supply of the South Equatorial Current from April to September, when the southeast monsoon is blowing as an offshore wind. Another region of upwelling must develop along the west coast of Burma and Thailand from December to February during the northeast monsoon. A description of these regions is given in Section 7 · 5, although practically no oceanographic stations have been worked there.

3 · 4 THE SURFACE CURRENTS OF THE WESTERN NORTH PACIFIC OCEAN

The Southeast Asian Waters are relatively open towards the North Pacific Ocean enabling its water masses a free entrance, while they are closed against the Indian Ocean. The most powerful branch of the circulation in the western Pacific Ocean is the North Equatorial Current flowing steadily during the whole year towards the Philippines. From December to February, that is in the northern winter, it seems to be stronger and from April to June weaker than normal. When approaching the Philippines the current divides, the larger part turns northwards and flows along the east coast of Luzon and Formosa to the north, where it forms the root of the Kuroshio. The annual variation of the current velocity east of Formosa is given in figure 3 · 2 and shows a maximum in May, and in November a minimum which is only about half of the maximum. This does not necessarily mean, that the transports make the same fluctuations, because they depend more on the depth and the width of the current.

The splitting off of the North Equatorial Current occurs along a line of divergence running westwards at about 11°N and bending slightly northwards, when approaching the Philippines.

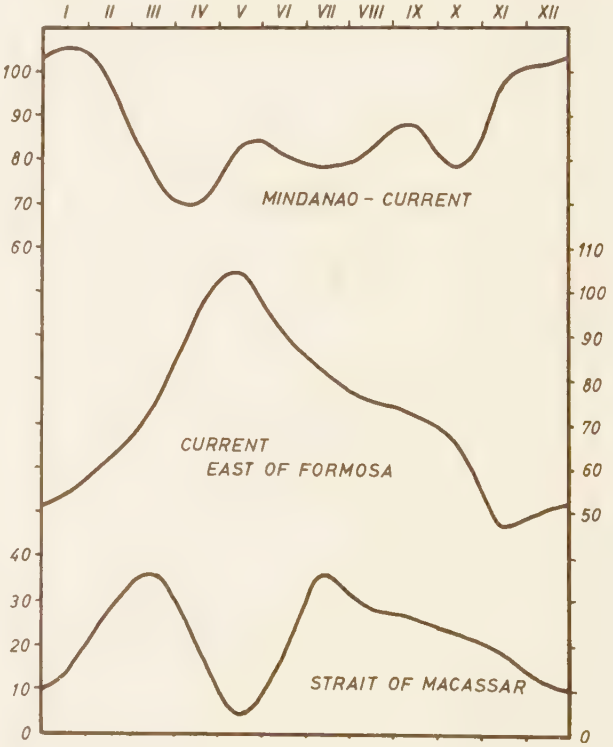

Fig. 3·2. Annual variation of the velocity of the current in cm/sec, off the east coast of Formosa, of the Mindanao Current and of the current through the Macassar Strait.

It ends off the Bernardino Strait north of Samar Island. South of the divergence the direction of the current is southwest, feeding the Mindanao Current, a fact already shown by Schott (1939). The Mindanao Current flows close to the coast of Mindanao to the south and its velocities exceed often 100 cm/sec, figure 3 · 2. About in the latitude of the south point of Mindanao the current splits, one branch continues in the direction of the main current to the south between the islands Sangi and Talaut, the other weaker branch turns to the southwest and enters the Celebes Sea. Within the Celebes Sea a large part of its water is deflected to the south and flows along the north coast of Celebes as a coastal current to the east, where it meets again the branch of the Mindanao Current, which flows directly to the south, and there the root of the Counter Current is formed.

Unlike the currents so far discussed, which are persistent features, those in the region north of New Guinea are marked by strong seasonal fluctuations. This is a region of light winds, from May to October they are southeast trades and from November to April the wind is from the north and west and is a branch of the northeast trades. From June to August the South Equatorial Current is most strongly developed and flows west along the north coast of New Guinea with high velocities as far as Halmahera. Here it is deflected to the north and joins the water masses coming out of the Celebes and Molucca Seas, this causes a further deflection to the right, until the current has reached an easterly direction. There, together with water coming directly from the North Equatorial Current, the Counter Current is formed flowing eastwards with considerable width. In this season the Counter Current reaches its maximal strength and consists chiefly of water masses of the southern hemisphere. Until October the strength of the South Equatorial Current and of the Counter Current decreases without a change of the current pattern.

In November the change over of conditions takes place, because the South Equatorial Current can persist no longer, against the increasing northwest winds. The Counter Current, now carrying exclusively water of the northern hemisphere is still present, but weaker, because it gives off water to the southeast. This water forms under the influence of the wind a coastal current along the north coast of New Guinea setting towards the southeast. This small but powerful coastal current is maintained until February. From November to February, when the Counter Current consists only of water masses from the northern hemisphere and has moreover to give off water towards the southeast, the Mindanao Current reaches its strongest development, figure 3 · 2. By February the South Equatorial Current has come through north of the equator to 140°E. The beginning of the southeast trades in April leads to a simultaneous vanishing of the coastal current and of the Counter Current and in the whole region a weak drift to the west and northwest prevails. The water masses coming out of the Celebes Sea north of Halmahera are deflected to the north and feed again the Mindanao Current, which reaches its lowest velocity in this month.

The change of the currents in the course of the year along 140°E between the north coast of New Guinea and 20°N is presented schematically in figure 3 · 3. The steady North Equatorial Current, which reaches its maximum in winter, gradually extends to the south from June to

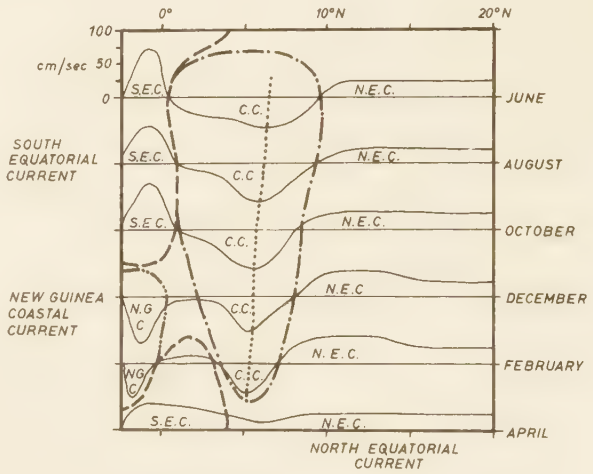

Fig. 3·3. Schematic presentation of the west-east components of the currents in the Pacific Ocean along 140°E in different months.

February. South of it the Counter Current is found. It starts in May, is most strongly developed in August and decreases afterwards gradually until it vanishes in March. The South Equatorial Current appears in February in this region and until April extends so far that it suppresses the Counter Current and joins with the North Equatorial Current. But this situation seems to be stable only for a very short time, and perhaps does not even occur in every year. By May the Counter Current starts with considerable force and presses the South Equatorial Current towards the coast of New Guinea. There it is maintained until the beginning of the northwest winds in November, when it is replaced in December by the coastal current. This coastal current is only of short duration and in March is replaced again by the South Equatorial Current.

In connection with this circulation system two strong eddies are formed, the Mindanao Eddy and the Halmahera Eddy. The Mindanao Eddy is developed during the whole year and in it the water of the North Equatorial Current is turned first into the Mindanao Current and then into the Counter Current. The Halmahera Eddy is developed only from May to October and off the island of Halmahera turns the water masses of the South Equatorial Current into the Counter Current. Further comments on the dynamics of this system are made in Section 7 · 3. From this current system of the Western North Pacific Ocean water masses enter the Southeast Asian Waters through the numerous passages between the Asian mainland and New Guinea, but there is no direct flow of water from the Pacific to the Indian Ocean.

3 · 5 SURFACE CURRENTS IN THE SOUTHEAST ASIAN WATERS

The development of a strong circulation within the Southeast Asian Waters is favoured by their geographical situation. The area formed by the China Sea, the passages between Sumatra and Borneo, the Java Sea, the Flores Sea and the Banda Sea lies with its axis exactly in the main wind direction of both monsoons. The China Sea between Formosa and Singapore extends in a northeast-southwest direction, and the northeast as well as the southwest monsoon blow along its axis. The waters between Sumatra and Borneo situated just below the equator form a north-south connection between the China and Java Seas and the monsoons blow here in a northerly and in a southerly direction. The area formed by the Java, Flores and Banda Seas, extending from west to east lies again in the direction of the monsoons, which blow here from westnorthwest and from eastsoutheast. This situation conditions a strong circulation in this whole region during both monsoons. Moreover this circulation is favoured by the great constancy of the winds, even if they are relatively weak, this is important for the development of a stationary system of currents.

In the other parts of the Southeast Asian Waters the circulation is more irregular and seems to be frequently disturbed; in any case a large scale pattern is lacking. Through the Molucca Sea, the Philippines and the Sulu Sea an exchange of water with the Pacific Ocean takes place. The Celebes Sea is so widely open to the Pacific, that its circulation invades this region. The Macassar Strait, connecting the Celebes Sea and the Java Sea has usually a current to the south which is caused by the slope of the sea surface from the Pacific to the Indian Ocean. The Malacca and the Sunda Straits are relatively narrow and the water exchange, which is normally towards the Indian Ocean, is small, even if the currents are sometimes strong. The same applies for the several straits between the Lesser Sunda Islands. Of greater importance is the flow of water through the Timor Sea into the Indian Ocean. A water exchange with the South Pacific Ocean is possible through the Torres Strait but it is probably small because of the narrowness of the strait.

In the CHINA SEA a wind drift is formed with the beginning of the southwest monsoon in May and June. Off the coast of Vietnam a westward intensification of this current is clearly visible. The wide, uniform drift in the northern China

Sea shows a deflection of the current to the right of the wind. The larger part of the water masses passes over south of Formosa into the root of the Kuroshio; a smaller part flows through the Formosa Strait to the north. Because the supply of water to this current from the Java Sea seems to be insufficient, a current develops off the coast of Borneo towards the southwest, which turns back to the north in the region of the Natuna Islands. The water of this current comes partly out of the Sulu Sea, and partly from a counter current, which is formed in the central parts of the China Sea. This current must develop in close connection with the westward intensification of the main current and be caused dynamically. Along the west coast of Luzon water flows northwards from the Sulu Sea.

At the time of the strongest development of the south monsoon in August the water movements are considerably stronger, the main current shows the same westward intensification and a counter current is developed. From the coast of Vietnam, at about 11°N, the main current flows almost east, later it dissolves and flows again northwards. An addition of water from Sulu Sea no longer takes place, but parts of the counter current are deflected and flow northeastwards as a weak drift along the coast of Borneo and Palawan. A part of this water enters the Sulu Sea north of Palawan together with small parts of the eastgoing main current. In September these movements decrease and in October the northeast monsoon starts blowing with considerable strength. Under the influence of the winds, water masses of the North Equatorial Current are deflected south of Formosa into the China Sea, and other water comes from the north through the Formosa Strait. This water flows along the coast of China to the southwest with a remarkable westward intensification of the current. In the centre of the China Sea a counter current is developed over about 10 degrees of latitude. But not all of this water can flow away into the Java Sea, because there the southeast monsoon is still blowing. Consequently a current arises along the coast of Sarawak flowing northeastwards, continuing as far as Luzon and there turning back into the main current. Small parts of this water also enter the Sulu Sea.

In December the northeast monsoon is fully developed over the China Sea and the currents are strong and off the shore of Vietnam often exceed 100 cm/sec. The westward intensification is stronger than during the southwest monsoon, when a deflection of the current occurs to the east caused by the wind. Again the counter current in the centre of the China Sea is found and lies further to the east because of the strength of the main current. From the Sulu Sea water flows into the China Sea and is mixed into the main current. A very weak flow occurs along the coast of Borneo southwestwards. In February the main current pattern is almost the same as in December. Only in the eastern parts of the China Sea do drift currents to the west occur, they are deflected to the right of the wind. But these are soon turned to the north and mixed with the counter current, which is not pronounced in this month.

By April the whole current system of the northeast monsoon has decayed and the main current has dissolved into two large eddies, one in the northeast, the other in the southeast of Vietnam. In the eastern parts of the China Sea a weak drift to the southwest is present, and in the centre the counter current again occurs. An inflow of water occurs from the Sulu Sea, and an outflow through the Formosa Strait. A weak current also flows into the Java Sea.

Very few observations have been made in the Gulf of Thailand but from available data water movements seem always to be weak. During the south monsoon, from May to September they are anticyclonic and during the northeast monsoon from October to January they are cyclonic. From February to April movements at the surface out of the gulf seem to prevail.

The JAVA SEA is essentially smaller than the China Sea and the currents occupy its full width without the development of larger eddies and counter currents. From May to September the water flows to the west and from November to

March to the east. In April and October the direction of the flow changes and eddies occur. Normally in these months a current towards the east prevails off the coast of Java and a current towards the west off the coast of Borneo. In the small passages between Borneo and Sumatra, in the Karimata and Gaspar Straits, when the winds are fresh the velocities of the currents reach often 100 cm/sec, especially during the full north monsoon.

In the STRAIT OF MACASSAR the flow is directed to the south during the whole year and the velocities are normally small. The annual variation is presented in fig. 3 · 2 and shows minimal velocities in December/January and in May. In these months the currents are very unsteady. The strongest currents occur in February and March and from July to September. The water masses leaving the strait in the south flow during the southeast monsoon into the Java Sea and during the northwest monsoon into the Flores Sea.

Over the FLORES SEA west winds prevail from December to March and southeast winds in all other months. Accordingly, from December to March a uniform current to the east exists, being remarkably intensified along the north coast of the Lesser Sunda Islands. With the disappearance of the west winds in April, a weak westwards current forms under the coast of Celebes, while north of the Lesser Sunda Islands the strong current to the east is still present. Even during the full southeast monsoon in July and August this coastal current remains, but is considerably weakened. During this period the west going drift current in the northern part of the Flores Sea occupies most of its width, and in August has velocities of about 75 cm/sec. With the decrease of the southeast monsoon the coastal current north of the Lesser Sunda Islands is again intensified and in October only a weak drift is to be noted south of Celebes.

In contrast to the channel-like seas, already discussed, in which the direction of the current is given by their configuration, the eastern parts of these waters are connected by various smaller and wider passages, causing sometimes rather complicated current patterns. The number of observations in these waters is very small and the current observations must be used with caution because ships navigating in these areas may pass through several passages within 24 hours and tidal currents, which might seriously influence observations, occur in these passages. Direct current measurements by the SNELLIUS Expedition were made at only a few places.

The BANDA SEA is entered during the northwest monsoon by water masses out of the Flores Sea. A part of this water flows north of Buru into the Ceram Sea and from there through the Halmahera Sea into the Pacific Ocean. Another part moves as a wide drift south of Ceram into the Arafura Sea. At the time of the changing of the monsoon in April the currents are so variable, that a general current pattern cannot be derived. The coastal current north of the Lesser Sunda Islands turns east of Timor sharply to the south. During the southeast monsoon water masses out of the Pacific Ocean flow through the Halmahera and Ceram Seas at both sides of the island Buru into the Banda Sea and pass in a southwest direction into the Flores Sea.

In the ARAFURA SEA and in the eastern parts of the Banda Sea only drift currents with weak velocities are to be observed during the whole year. The Torres Strait is narrow and shallow and the water transport through it is only small, in any case it is of minor importance to the water movements in the Arafura Sea. The direction of the drift current over the shallow parts of the Arafura Sea is everywhere in the direction of the wind. During the southeast monsoon considerable upwelling is observed in this region, see Section 7 · 5.

In the TIMOR SEA a current to the southwest prevails during the whole year, its axis runs close to the coast of Timor. From April to September the current reaches to the Australian coast, although its velocity decreases in that direction. From October to March a weak current towards the northeast is formed off the Australian coast under the influence of winds from the southwest. The Timor Current takes its water from October

to April out of the current flowing along the north coast of the Lesser Sunda Islands to the east, which turns around the eastern end of Timor. Only at the time of the full development of the southeast monsoon is the Timor Current supplied by water out of the upwelling region in the Arafura and eastern Banda Seas.

The **Celebes Sea** is widely open to the Pacific Ocean and its currents enter this region. A branch of the Mindanao Current flows south of Mindanao southwestwards into the Celebes Sea. Its water is deflected to the south and later to the east in the central parts of the sea and flows back to the east along the north coast of Celebes. In the region northwest of Halmahera this coastal current joins again with the branch of the Mindanao Current coming directly from the north between the islands Sangihe and Talaut, and it receives water coming out of the Molucca Sea, all forming the root of the Counter Current. This system of circulation is maintained during the whole year, even though its extension to the west may vary. The current in the Macassar Strait is supported from February to September almost exclusively by water from this current system. But from October to January, when north winds prevail over the Celebes Sea, the eddy, in which the Mindanao Current turns back to the east, is displaced to the east, and water from the Sulu Sea flows through the western part of the Celebes Sea into the Macassar Strait. In the northern part of the Celebes Sea the water movements are normally weak and irregular, but movements into the Sulu Sea prevail from March to July and in the other months movements are towards the southwest.

Through the **Philippines** a continuous transport of water which comes from the North Equatorial Current takes place into the Sulu Sea. From May to September this transport is weak, because the wind opposes it. The maximal inflow occurs in February, when the North Equatorial Current is strongest. In this month the water masses flow away partly to the China Sea, partly to the Celebes Sea. From April to July a weak flow from south to north occurs through the Sulu Sea, from August to October this flow is from north to south, and from December onwards the water entering through the Philippines flows away to both sides.

Through the **Malacca Strait** and through the **Sunda Strait** a small water exchange is possible between the Sunda Shelf and the Indian Ocean. In both straits the water movements are in general directed towards the Indian Ocean and are strongly related to the surface gradient of the sea level through these straits, see figures 7 · 7 and 7 · 8. The flow through the Sunda Strait reaches its maximum in August during the southeast monsoon and a second maximum in December/January at the time of the full development of the north monsoon. In the Malacca Strait the period of strongest flow is from January to April, during the northeast monsoon, but it is chiefly caused by the low sea level in the Andaman Sea in this season.

When comparing the six current charts (plates 1-6) with other publications only small differences are found, while the gross features of the circulation appear the same. For instance the monthly current charts for the South China, Java, Celebes and Sulu Seas, published by the U.S. Navy Hydrographic Office (1945) and the monthly current charts given in the Handbuch für das Südchinesische Meer (1943) show full agreement with these plates. But a detailed comparison with the charts given by Schott (1935) for February and August and that given by Sverdrup (1946) for February shows a completely different current pattern in the Molucca and Halmahera Seas. The current charts presented here for December and February show that movements towards the Pacific Ocean take place through these waters, and that from April to October water of the Pacific Ocean enters the Eastern Archipelago. But Schott gives just the opposite picture, which would mean that during the southeast monsoon in August the upwelling region in the Banda and Arafura Seas had not only to feed the Monsoon Current into the Flores Sea, but also an outflow to the north into the Pacific Ocean. This would require an enormous

upwelling in this region, which has not been observed. In fact considerable water masses flow from the Pacific Ocean in August into the Banda Sea and feed the Monsoon Current, which takes only a small part of its water from the upwelling region.

In February the conditions are quite reversed. The Monsoon Current coming out of the Flores Sea flows mainly through the Molucca Sea into the Pacific Ocean, and only small parts sink down in the Banda Sea. According to the presentations given by Schott and Sverdrup not only the whole Monsoon Current but also water coming from the Pacific Ocean would have to disappear in the Banda Sea. Quantitative values of these transports are given in Section 7 · 4.

LITERATURE

Barlow, E. W.

1935. Currents in the China seas and East Indian Archipelago. I. Meteorological conditions which affect the currents, with summary of current information previous to the present charting.
Mar. Obs. 12 : 69-70. 114-116.

Dale, W. L.

1956. Wind and drift currents in the South China Sea.
Malay. J. Trop. Geogr. 8 : 1-31.

Ganapati, P. N., and V. S. R. Murthy

1954. Salinity and temperature variations of the surface waters of the Visakhapatnan coast.
Andhra Univ. Mem. Oceanogr. 1 : 125-141.

Jerlov, N. G.

1953. The equatorial currents in the Indian Ocean.
Rep. Swed. Deep-Sea Exped. 1947-48. (5) : 115-25.

Michaelis, G.

1923. Die Wasserbewegung an der Oberfläche des Indischen Ozeans im Januar und Juli.
Veroff. Inst. Meeresk. Univ. Berlin N.F.A. 8.32 pp.

Schott, G.

1935. Geographie des Indischen und Stillen Ozeans.
Hamburg, C. Boysen. 413 pp.

1939. Die äquatorialen Strömungen des westlichen Stillen Ozeans.
Ann. Hydrogr. Berl. 67(5) : 247-257.

Soeriaatmadja, R. E.

1957. The coastal current south of Java.
Mar. Res. Indonesia. 3 : 41-55.

Sverdrup, H. U., M. W. Johnson, and R. H. Fleming

1942. The oceans, their physics, chemistry and general biology.
New York, Prentice-Hall. 1,087 pp.

Wyrtki, K.

1957. Die Zirkulation an der Oberfläche der südostasiatischen Gewässer.
Dtsch. Hydrogr. Z. 10(1) : 1-13.

1960. On the presentation of ocean surface currents.
Int. Hydrogr. Rev. 37 : 111-128.

DEUTSCHLAND OBERKOMMANDO DER KREIGSMARINE
1943. Handbuch für das Südchinesische Meer
GREAT BRITAIN, HYDROGRAPHIC DEPARTMENT
1944. Eastern Archipelago : region lat. 10°S - 20°N. long. 94°E - 130°E. Generalised surface currents in January to December. H.D.17799/43.
1945. The surface currents of the South China, Java, Celebes and Sulu Seas. Publ. H.D.709.
KONINKLIJK NEDERLANDS METEOROLOGISCH INSTITUUT
1936. Oceanographic and meteorological observations in the China Seas and in the western part of the North Pacific Ocean. No.115.
1949. Sea areas round Australia. Oceanographic and meteorological data. No. 124.
1952. Indian Ocean, general current circulation. No.125.
UNITED STATES NAVY HYDROGRAPHIC OFFICE
1944. Current charts, Southwestern Pacific Ocean. H.O.No.10058.
1945. Currents in the South China, Java, Celebes and Sulu Seas. H.O.No.236.
1950. Atlas of surface currents, Indian Ocean. H.O.No.566.
1950. Atlas of pilot charts, Pacific and Indian Oceans. H.O.No.577.
UNITED STATES WEATHER BUREAU
1938. Atlas of climatic charts of the oceans. W.B.No.1247.

CHAPTER 4

THE PROPERTIES OF THE WATER IN THE SURFACE LAYER

The water at the surface in the Southeast Asian Waters shows the high temperatures typical of tropical regions. In addition the influence of the low salinity reduces the density. The large excess of rainfall over evaporation causes an average salinity of less than 34‰ within a region enclosed by a line running from Ceylon outside the islands of Sumatra, Java, Celebes, and the Philippines to Formosa. The density of this water remains always below $\sigma_t = 22.0$. This light tropical surface water forms a strong contrast to the cold water masses in the depth with densities of $\sigma_t = 27.7$ to 27.8. The transition between these two water masses takes place in an extremely strong discontinuity layer between 100 and 300 m, and in a depth between 400 and 600 m the density of 27.0 is always exceeded. This stable discontinuity layer practically prevents any vertical exchange of water, and the surface layer may therefore be treated independently. Only in a few places and in certain seasons is the water of the surface driven off so strongly by the wind that the top of the discontinuity layer reaches the surface and upwelling takes place. As a whole the Southeast Asian Waters are a source of warm less-saline surface water, which is given off continuously to both oceans and is replaced by more oceanic water.

The properties of the water at the surface normally extend a certain distance into the depth, before the transition to the colder water takes place. This homogeneous layer is the mixing layer caused by the winds, but can also be deepened by currents and tides. Below this homogeneous layer a change of the properties of the water starts, especially an increase of the density, at first gradually, later rapidly. Finally a maximal density gradient is reached, at the centre of the discontinuity layer. Below this the density increases more gradually, till the cold water of the deep layer is reached. But locally and temporarily there is no homogeneous layer. In these regions an almost continuous change of properties and an increase in density with depth

can be observed, starting from the very surface and leading into the discontinuity layer.

For these reasons it seems necessary to specify more clearly the meaning of the term surface layer. It is not possible to identify the homogeneous layer with the surface layer, because in this case there would be no surface layer at several places. If one chooses to maintain for tropical waters the subdivision of surface layer — discontinuity layer — deep layer, the term surface layer has to be defined in a more precise way. First it might seem a good idea to identify the surface layer with the depth of the surface circulation. But investigations have shown that the discontinuity layer normally takes part in the movements of the surface water and that the boundary of this movement is in the lower part of the discontinuity layer. In other very strong oceanic currents, however, the surface movements reach down several hundred meters and even carry waters below the discontinuity. Consequently the depth of the surface circulation cannot be used as the definition of the surface layer.

Another possible boundary of the surface layer might be the depth of the maximal density gradient within the discontinuity layer, but this means that nearly half of the discontinuity layer would form part of the surface layer. Indeed this determination offers some advantages, because the maximal density gradient is the layer of minimal vertical exchange of properties and therefore forms a real boundary. This definition would be a demarcation from the dynamical point of view.

A third possibility to define the term surface layer is an analysis of the water masses. The variations, especially the annual variations of the properties at the surface influence not only the homogeneous layer, but extend a certain distance into the top of the discontinuity layer. To identify this depth with the surface layer is an advantage especially in regions where sometimes there is no homogeneous layer because of upwelling or of considerable heating and where the stratification already starts from the surface. Thus, the term surface layer is used here to denote all water masses down to a depth to which the variations originating from the surface have an immediate influence, actually this is the depth of penetration of the annual variations of properties. It is not yet possible to present the vertical extent of the surface layer because oceanographic stations in many regions have been worked for only one season and from these it is impossible to follow the penetration into the depths of the annual variations of properties. Therefore the depth of the homogeneous layer, the depth of the maximal density gradient and the average thickness of the discontinuity layer (plates 7-9) are discussed to give an impression of the extent of the surface layer.

4·1 THE HOMOGENEOUS LAYER

The water of the surface is made homogeneous down to a certain depth by the action of the wind and also by currents and tides. The extent of this homogeneous layer is of interest from the dynamical point of view as well as for biological purposes. Its determination from available observations is relatively simple, but certain points need consideration. At the very surface the observations are often disturbed by radiation or heavy rainfall, which makes the values at the surface deviate from those within the homogeneous layer. On the other hand, certain fluctuations with the homogeneous layer are possible without disturbing the general character of this layer. Thus, in working out the material a tolerance of 1°C in the temperature and of 0·2‰ in the salinity has been admitted, corresponding to a fluctuation in the density of 0 · 4. As the average extent of the homogeneous layer is about 50 m, this means only a small density gradient.

The extent of the homogeneous layer is given in plate 7, and it is to be noted that the observations from the China Sea, the Banda Sea and the Indian Ocean are for one season only (August to October). In the other regions approximately the average conditions are given. The deep homogeneous layer in the range of the North and the South Equatorial Current of the Pacific Ocean and off the southwest coast of Sumatra is remarkable. In the latter region the

observations are from September/October, when the Counter Current turns in a broad front to the south to join the South Equatorial Current. In the Pacific Ocean the homogeneous layer is much thinner in the range of the anticyclonic Mindanao Eddy, where the Counter Current is formed. Over the Sunda Shelf and over the Sahul Shelf the homogeneous layer reaches down to the bottom of the shallower parts, but over the deeper parts water of higher density is found below the homogeneous layer, which is about 40 m deep. In the Celebes, Sulu and Flores Seas the homogeneous layer seems to be of about the same extent during the whole year. In the China Sea and in the eastern parts of the Archipelago the annual variation is more important. In the upwelling region of the Banda and Arafura Seas the depth of the homogeneous layer is about 20 to 50 m in October at the end of the upwelling season, and up to 100 m at its beginning in March. A similar variation occurs in the China Sea, especially in its northern and central parts. The homogeneous layer is here only 30 to 40 m deep during the southwest monsoon, but 70 to 90 m during the strong northeast monsoon, an effect which is chiefly due to the vertical circulation discussed in Section 7 · 7.

A comparison of these results with calculations of the depth of the homogeneous layer made by Lumby (1955) by means of theoretical results from Rossby and Montgomery (1935) shows several deviations. Therefore the effect of wind only on the homogeneous layer gives unsatisfactory results and the effects of ocean currents must also be considered. Lumby's charts do not show the deepening of the homogeneous layer in the range of the equatorial currents, nor is his theory applicable in the vicinity of the equator. Thus, at least in these regions, observations seem to give better results than theory can provide. To complete this presentation many bathythermograph records are required.

4 · 2 THE DISCONTINUITY LAYER

There is a close connection between the vertical extent of the surface layer and the position and thickness of the discontinuity layer. From the vertical curves of the density the depth of the maximal density gradient can easily be obtained, this is shown in plate 8. In cases when the discontinuity is split into two parts, the average depth of both maxima has been used The values shown here are naturally subject to relatively large fluctuations, belonging to the annual variations as well as to short period oscillations of the discontinuity layer. The latter based on the anchor stations of the SNELLIUS have been investigated by Lek (1938), and he found at all stations vertical displacements of the discontinuity layer between 25 and 40 m. These very high values indicate a strong activity of internal tides in these waters. The annual variations are related to the fluctuations of the circulation.

The deepest position of the discontinuity layer is found in the range of the two Equatorial Currents in the Pacific Ocean. Between them in the range of the Counter Current the layer is curved upwards and is not deeper than 100 m. On the other hand the topography of the discontinuity layer in the northeastern Indian Ocean is comparatively smooth and it lies in about 120 m depth. Towards the south in the range of the South Equatorial Current it descends to 140 m. These few examples show the close relation between the depth of the discontinuity layer and the circulation in the surface layer. In the China Sea and in the Eastern Archipelago, where no deep going currents develop, the discontinuity is relatively level and lies between 120 and 160 m.

To get an impression of the position and of the thickness of the discontinuity layer, vertical curves of the temperatures from the surface to 600 m depth from different regions are presented in fig. 4.1. These curves in general also show the distribution of the density, because the salinity changes little below the surface layer, and therefore its influence on the density is small. Different types of transition from surface to depth are shown. The station Da 3815 southwest of Sumatra shows a well developed homogeneous layer and below it an extremely sharp discontinuity. On the other hand, the station

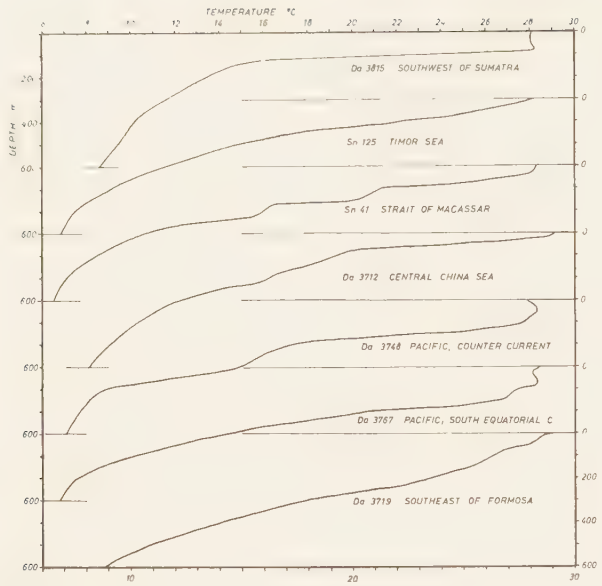
TEMPERATURE °C
DEPTH m
Da 3815 SOUTHWEST OF SUMATRA
Sn 125 TIMOR SEA
Sn 61 STRAIT OF MACASSAR
Da 3712 CENTRAL CHINA SEA
Da 3748 PACIFIC, COUNTER CURRENT
Da 3767 PACIFIC, SOUTH EQUATORIAL C
Da 3719 SOUTHEAST OF FORMOSA

Fig. 4·1. Typical curves of the vertical distribution of temperature between the surface and 600 meters in different regions of the Southeast Asian Waters according to DANA and SNELLIUS stations.

Da 3719 south-east of Formosa like the station Sn 125 in the Timor Sea shows a nearly continuous transition from surface to depth. Below 12°C the decrease of temperature becomes more gradual at most stations, whereas the break in the vertical curves, which really indicates the lower boundary of the discontinuity layer, appears between 8° and 10°C. Considering that the minimal surface temperature in the greatest part of these regions is about 25°C, and this might be approximately the lower boundary of the surface layer, then the discontinuity layer may be said to extend from about 25° to 12°C in these waters.

An analysis of the water masses shows a similar pattern. The surface layer contains water masses exposed to the disturbances coming from the surface, and strong annual variations of its properties result. The discontinuity layer in this region is formed by the Subtropical Lower Water, in which the core layer of the salinity maximum is present. The origin of these waters is in the regions of maximal surface salinity in the subtropics, the water masses are identical with the Central Waters defined by Sverdrup (1946), which practically form the discontinuity layer, but have only a small vertical extent. The lower boundary of the discontinuity layer is given as the boundary between the Subtropical Lower Water and the Intermediate Water. The latter lies with a salinity minimum in its core at temperatures between 9° and 12°C and is the uppermost layer of the cold water sphere.

The thickness of the discontinuity layer is given in plate 9. The water masses belonging to the discontinuity layer in this region have temperatures between 25° and 12°C, being about the upper and lower boundaries. Because these limits naturally have a certain variability, they are not exactly suitable to present the thickness of the discontinuity layer. Therefore a smaller range, 23° to 15°C, has been chosen as a measure for the thickness of the discontinuity. Within this range the maximal density gradient is always found. The depth of the 15° and of the 23° surface has been determined for every station from the vertical curves, and their difference is presented in plate 9 as the thickness of the discontinuity layer. Values between 20 and 200 m indicate its great variability.

The thickness of the discontinuity is, like its depth, mainly affected by dynamical processes. The highest values are found in the region east of Formosa, where the North Equatorial Current turns over into the Kuroshio and, in a large eddy, the warm water masses are presssed into the depth, causing a relatively deep position and a very thick discontinuity. In the range of the Counter Current the discontinuity is very sharp, because movements in opposite directions take place. In the Eastern Archipelago the discontinuity is of relatively uniform thickness of about 100 m. The sharpest discontinuity is found off the coast of Sumatra with only 20 m in October, when the Counter Current turns in broad front to the south.

4·3 THE TEMPERATURE OF THE SURFACE LAYER

The surface layer of the tropical ocean is warm and the annual variation of temperature is normally small. But relatively high daily variations of temperature are very common. Charts of the surface temperatures are not presented be-

cause of the small horizontal gradients and the relatively large fluctuations of the average temperature from year to year in the inner tropical regions. Monthly temperature charts are given in the various climatic atlases, especially in the World Atlas of Sea Surface Temperatures of the U.S. Navy Hydrographic Office (1944). The annual variation of the temperature of the sea surface together with that of the air is given for 15 selected regions in Chapter 5 in the discussion of the energy exchange. The average annual variation of temperature is smaller than 2°C in the equatorial regions, slightly higher values of 3° to 4°C, occur in the Banda, Arafura and Timor Seas as well as south of Java. In the China Sea on the other hand there is a rapid increase of the annual variation towards the north. This is caused by an inflow of cold water through the Formosa Strait during the winter monsoon as well as by the cooling effect due to evaporation and heat exchange with the air. Off the southwest coast of Vietnam the temperature range is 4°C, increasing to 10°C near Hong Kong, and reaching 14°C in the Formosa Strait, fig. 4 · 2. Another region with relatively strong annual variations of temperature is found along the northwest coast of Australia, fig. 4 · 2. Here the temperature is 29°C during the northwest monsoon and decreases to 24°C in July/August at the time of strongest upwelling. A chart of the annual variation of the surface temperature is given by Schott (1935), but his values seem to be slightly high in the southern parts of the China Sea.

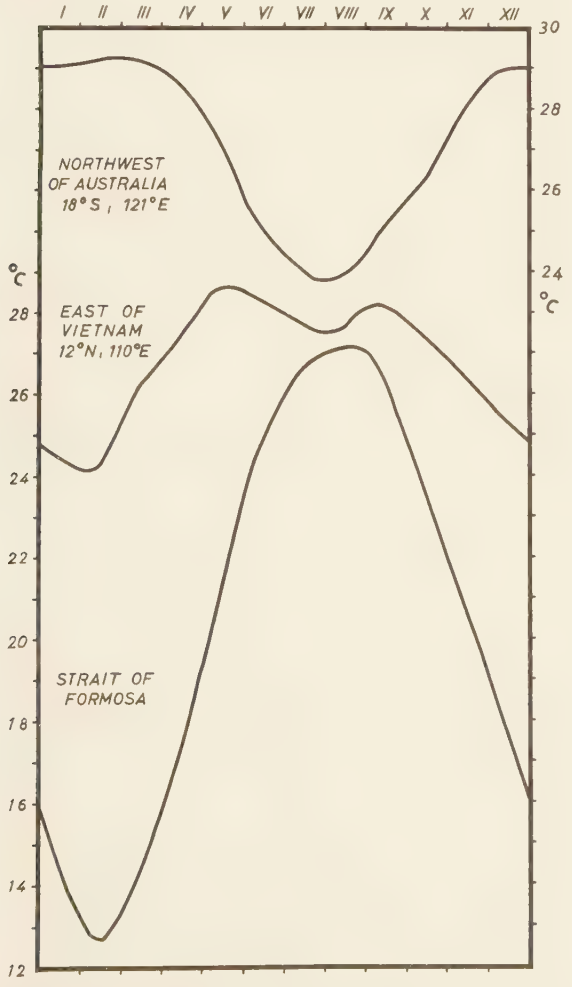

Fig. 4·2. Average annual variaion of sea surface temperature in different regions.

The same temperatures as at the surface are found in the whole homogeneous layer, the extent of which is given in plate 7. Over the shallow parts of the Sunda Shelf, including the Java Sea, the southern China Sea, the Malacca Strait and the Gulf of Thailand as well as over the Sahul Shelf, connecting Australia and New Guinea, the temperatures are constant from the surface to the bottom in large areas.

4 · 4 THE SALINITY OF THE SURFACE LAYER

In contrast to the uniform temperature in this region, the salinity is extremely variable. The high rainfall, the big runoff from the many rivers and the strong geographical subdivisions of the seas are responsible for this. The high rainfall of this tropical region generally causes a low salinity. The distribution of the discharge from land and the presence of large bays and channels with only a small water exchange favour the formation of regions with very low salinity, which serve as sources for a lowering of the salinity in the region. The monsoons cause a rainy and a dry season and consequently a strong annual variation. But with the monsoons also the whole circulation is changed and water masses of low and high salinities are interchanged. These interactions between different factors and influences, the geographical structure, the runoff from the rivers, the rainfall, the evaporation and the circulation result in a highly

complicated distribution of the salinity in these waters and in strong variations.

The presentations of the surface salinity are based on the observations of the five years 1950-1954 and therefore present a really homogeneous material, even though the period is short. Altogether 147,000 observations of the surface salinity are available from these five years, while from all years before 1949 only 9,280 observations are available. It would have been possible to draw charts of the average monthly surface salinity during this period, but such a relatively short period cannot be fully representative. This has already been proved by the charts drawn by Veen (1953) using the whole material up to 1951 (82,665 observations). Actually his charts give the average distribution for the three years 1949 to 1951, because the observations from this period are 85 per cent of all the observations he used and he gave no regard to this fact, when calculating the averages. Especially in the China Sea his charts give completely distorted values, which correspond neither to the charts given by Schott (1935) nor to those presented here.

Because a presentation of average monthly charts does not seem to be advisable with the available material, five charts only have been drawn with the material of the years 1950 to 1954 which can be considered to give an insight into the salinity distribution on the surface. The average annual variation of the surface salinity is given in plate 10. The chart for February shows the situation at the full development of the north monsoon, the chart for August the same for the south monsoon, (plates 11 and 12). Two additional charts (plates 13 and 14) are presented showing the observed maximal and minimal surface salinity, related to monthly averages of 1° squares. These charts may give an indication of the maximal extent of the oceanic and of the coastal waters and of their maximal retreating, and they allow certain conclusions on the upwelling regions.

Information on the actual salinity distribution within the Southeast Asian Waters is given by the monthly salinity charts published by Veen (1951) and by Hardenberg and Soeriaatmadja (1955). From 1955 on, these charts have been published regularly by the Institute of Marine Research in Djakarta, Wyrtki (1956). They give interesting particulars about the movements of certain water bodies and the spreading of disturbances in the surface salinity distribution.

The average annual variation of the surface salinity together with its fluctuations during the five years of observation is given in fig. 4·3 for 14 selected regions the numerical values are given in table 1. The size of the regions has been chosen in such a way that sufficient observations are available for the calculations. They include between 4 and 12 1° squares, situated about in the centre of the region and removed from direct land influences. The presentation gives some interesting particulars about the salinity distribution and its fluctuations. Some regions, such as the Java and the Flores Seas, have a very distinct annual variation, which reproduced every year,

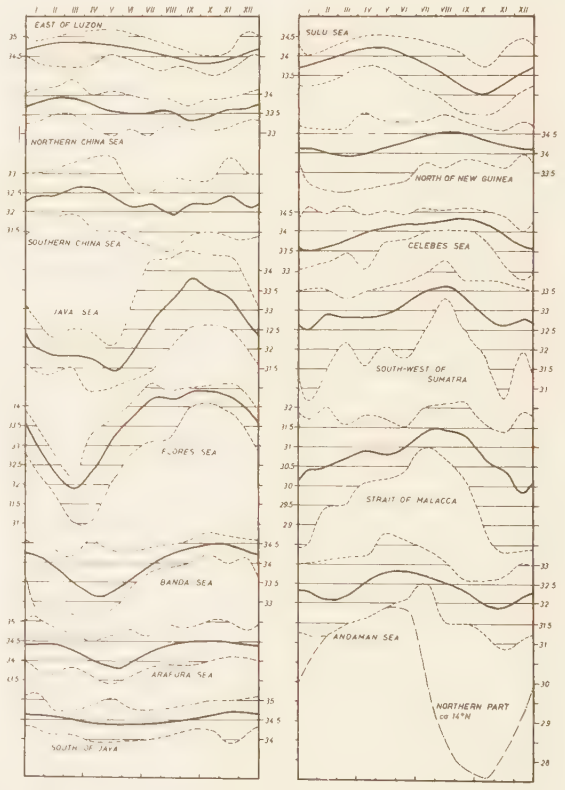

Fig. 4·3. Average annual variation of surface salinity (‰) in different regions, and range of departure of the observed surface salinity during the years 1950-1955. Positions of the regions are given in fig. 5·8.

so that the salinity at the time of its minimum is always lower than the salinity at the time of its maximum. In these regions the annual variation is the dominating process, and it is absolutely regular. On the other hand, there are regions such as that north of New Guinea and the southern China Sea, in which an annual variation can actually be calculated and is real, but it is disturbed so much by unperiodical fluctuations that it is no longer the dominating factor in the salinity distribution. In these regions, at any time of the year, salinities may occur which correspond either to the maximum or to the minimum of the average annual variation. Here the calculation of the annual variation is only of theoretical value, because the real pattern is made by unperiodical processes. Other regions show fluctuations intermediate between both extremes. For instance the Banda Sea and the Malacca Strait have a distinct annual variation, but at any time of the year salinities may occur, which correspond to the maximal values, while the minimal values are limited to a certain season. In the Malacca Strait, salinities below 30‰ are not observed from April to September, but salinities above 31.5‰ may occur during the whole year. This shows that in spite of the strong periodicity and constancy of the monsoons, the salinity is subject to such strong fluctuations that the annual variation is suppressed in some regions by unperiodical effects. The departures of the rainfall and especially the departures of the circulation from the averages seem to be the main reason for these irregularities.

The general distribution of the salinity at the surface is conditioned by the monsoon circulation. In some regions water masses of low salinity are formed by strong rainfall and runoff from rivers, and between these waters of low salinities and the oceanic water masses a larger area of mixed water is formed and transported by the monsoons through the various seas and passages so that the different regions are alternately filled with waters of different origin. It is not easy to estimate the influence of the difference between rainfall and evaporation on the surface salinity, but normally its influence seems to be less than that of the circulation. An approach to this question will be made in Section 5.4, but an estimation of the magnitude of this effect may already be made here. In some regions with a distinct rainy and dry season, the surplus of the rainfall or of the evaporation during one season can reach 800 mm. Such a value leads within a homogeneous layer of 30m depth and 33‰ salinity to an annual variation of 0.9‰. But in large areas this value is much exceeded and the circulation must have more direct influence on the distribution of the salinity. This will be discussed in detail, when dealing with the conditions of the different regions.

The mouths of the big rivers are the regions in which the salinity is continuously lowered. There is the Menam flowing into the Gulf of Thailand and keeping its salinity always below 32.5‰. The Mekong discharges in the south of Vietnam, but its water is rapidly carried away by the strong currents off the coast. The considerable discharge from Sumatra holds the salinity below 32‰ in the inner part of the Malacca Strait and in the Riow Archipelago down to the island of Banka. In extreme cases nearly the whole Gulf of Thailand, the whole Malacca Strait and the region down to the Sunda Strait can be filled with water of less than 30‰, see plate 14. The rivers of Borneo give considerable contribution to the lowering of the salinity too, and off the coasts of this large island the salinity is reduced below 30‰ far out into the sea at the time of the strongest discharge about the end of the rainy season over the different river districts. During the dry season on the other hand, when the discharge is small, water of high salinity always comes up to the shore, plate 13. Another, but perhaps not so important region for the reduction of salinity, seems to be off the southwest coast of New Guinea. Also the big rivers discharging from Burma into the Andaman Sea cause there extremely large annual variations over a wide area, fig. 4 · 3.

The two oceans with their waters of high salinity oppose these sources of low salinity water.

From the Pacific Ocean, surface water continuously penetrates through the Philippines into the Sulu Sea and with the Mindanao Current into the Celebes Sea. From October to March, a branch of the North Equatorial Current turns into the China Sea and brings water of higher salinity. When the South Equatorial Current develops from April to October north of New Guinea, water of high salinity flows through the Halmahera Sea into the Eastern Archipelago. Water of low salinity leaves the China Sea during the southeast monsoon.

The Indian Ocean on the other hand seems to have no influence on the surface water of the Archipelago. The relatively high salinity waters of the South Equatorial Current do not penetrate through the Lesser Sunda Islands to the north, see fig. 4·6. During the southeast monsoon, when such an influence might be expected, the currents in the passages between the Lesser Sunda Islands are directed towards the southwest. Also near Timor the current flows southwestwards all the year. This observation is supported by the existence of a depression of the sea level south of the Lesser Sunda Islands and by the general slope from the Pacific to the Indian Ocean, see Section 7·6. Both prevent the Indian Ocean surface water entering the Archipelago. On the other hand considerable amounts of less saline water flow from the Eastern Archipelago into the Indian Ocean.

Water of high salinity is transported during the southeast monsoon through the Torres Strait into the Arafura Sea, which can be seen from the salinity observations near the strait. But the strait is too shallow and small and there is no big transport of water, which might explain the variation of the surface salinity in the Eastern Archipelago. Therefore this variation has to be ascribed to the effects of evaporation and to upwelling processes.

The salinity distribution in February is determined by the full development of the north monsoon and by the rainy season over the regions south of the equator, plate 11. From the Pacific Ocean water of above 34‰ enters the China Sea and extends with decreasing salinities along the coast of Vietnam to the south. In the central parts of the China Sea the counter current is clearly visible as a tongue of less saline water extending to the northeast. A tongue of high salinity water flows through the southern China Sea into the Java Sea. On both sides of the tongue coastal water of low salinity is found, reducing gradually its salinity by lateral mixing. The Java Sea, the Macassar Strait and the western parts of the Flores Sea are filled with water of low salinity. In the Eastern Archipelago the salinity is normally below 34‰, but the minimum is reached two or three months later. In the Molucca and in the Celebes Seas, the 34‰ isohaline is forced back to the Pacific Ocean. Off the southwest coast of Sumatra a region of reduced salinities is caused by heavy rainfall.

In August the south monsoon is fully developed and brings the rainy season for the area north of the equator, plate 12. In the Eastern Archipelago the salinity is high and exceeds 34‰ nearly everywhere, and the 34‰ isohaline has reached the coast of Borneo and penetrated into the Java Sea. A tongue of high salinity extends through the whole of the Java Sea up to the Karimanta Strait. The salinity in the southern China Sea is considerably reduced, and a tongue with low salinities penetrates to the northeast along the coast of Vietnam. In the opposite direction water of above 33‰ moves to the southwest along the north coast of Borneo. In the Formosa Strait and off the south coast of China, the salinity of the water is reduced by the heavy rainfall of this season. Remnants of water with relatively high salinity are compressed in the northern parts of the China Sea. In the Indian Ocean, the highly saline water of the South Equatorial Current lies closer to the coast of Java.

When comparing these two charts with the charts of the maximal and minimal observed salinity, plate 13 and 14, some remarkable facts are noted. The water entering the China Sea from the Pacific Ocean can fill nearly its whole northern parts with water above 34‰. From the

Sulu Sea a tongue with salinities of above 34‰ can penetrate far to the southwest along the coast of Borneo. Remarkable too, are the high salinities which occur in the South Equatorial Current of the Pacific Ocean and carry water of above 35‰ into the Halmahera Sea. Salinities of above 35‰ are also occasionally observed in the Arafura Sea and are perhaps caused by a relatively strong inflow through the Torres Strait or by high evaporation in this region.* Along the whole south-west coast of Sumatra the salinity can exceed 34‰. On the other hand it is surprising how far waters of low salinity can extend, the 34‰ isohaline can retreat far into both oceans. Off the south-west coast of Sumatra the salinity can decrease below 32‰, and in the Eastern Archipelago the salinity can everywhere fall below 33.5‰. The waters with salinities below 32‰, normally found over the Sunda Shelf, can move considerably, and can cover either the central parts of the China Sea or the Java Sea and the western parts of the Flores Sea. The whole Macassar Strait and the western parts of the Celebes Sea also can be covered with water of below 32‰.

The average annual variation of the surface salinity is shown in plate 10. In both oceans, except in a narrow strip along the coasts, it remains below 0.5‰. Also it is below 1.0‰ in the northern and southern parts of the China Sea, whereas all other parts of the Southeast Asian Waters have a considerably higher annual variation. The highest values of the annual variation with more than 4‰ are found off the mouths of the big rivers of Sumatra and Borneo as well as in the northern parts of the Andaman Sea. But even large areas like the Java Sea, the Flores Sea, the Macassar Strait and the Malacca Strait, have variations of more than 2‰. Also in the Formosa Strait and along the south coast of China a variation of more than 2‰ occurs. Even along an oceanic coast like the southwest coast of Sumatra and the south coast of Java, the annual variation exceeds 1.5‰.

In order to explain the distribution of surface salinity and to estimate numerically its annual variation, it is necessary to compare the distribution of the salinity and its variations with the circulation and with the values of evaporation and rainfall, as well as with the river discharges. The values of rainfall and evaporation as calculated in Chapter 5 are used. Even if a complete solution of the problem cannot be given, an attempt is here made to show for the different regions the factors chiefly responsible for the annual variation of the surface salinity and the size of their influences.

The CHINA SEA as the largest in these waters has a more oceanic character than the other seas, this is indicated by the relatively small annual variations of salinity in its northern and southern parts. The northern part receives water of high salinity from the Pacific Ocean during the northeast monsoon. These waters spread south of Formosa to the west and later along the coast of Vietnam to the south. The salinity gradually decreases in the direction of the flow, which gives the typical picture of a tongue-like spreading. The relatively dry air masses of the strong northeast monsoon also cause a considerable evaporation, which exceeds the rainfall from November to March, so this period has a surplus of evaporation of 620 mm. This would be sufficient to increase the salinity of a 70 m thick homogeneous layer by 0.3‰. But the observed increase during this season is 0.7‰, which shows that influx of water of high salinity also contributes to the increase of salinity. With the beginning of the southwest monsoon and the rainy season in May, the waters of high salinity are pressed back to the north, and their salinity is also decreased by the rain. The excess of the rainfall during this season is about 820 mm, which corresponds to a decrease of almost 0.7‰ in salinity in a homogeneous layer of 40 m during this season.

*Investigations in the Gulf of Carpentaria in August 1960 on Diamantina Cruise Dm 2/60 (CSIRO Aust. 1961) have shown salinities between 35.0 and 35.7‰ in its central part, indicating a source of highly saline waters formed by evaporation during the southeast monsoon season.

Off the south coast of China and along the coast of Vietnam the annual variation is larger, due to river discharge and to the increase of rainfall towards the land. For the Gulf of Tonking no information is available. Generally it can be said that the annual variation of the surface salinity in the northern China Sea is caused by the alternation of a dry and a rainy season, and that water transport by currents is important only during the northeast monsoon.

In the central parts of the China Sea the annual variation of salinity is higher than in the regions north and south of it. Rainfall and evaporation can no longer be regarded as the dominant factors, especially as evaporation decreases rapidly towards the south, while rainfall increases, so currents produce the variation of the salinity. The central parts of the China Sea are alternately filled with waters of higher and lower salinity. With the northeast monsoon, water of high salinity is transported along the coast of Vietnam to the south. In the central parts there is a counter current flowing in the opposite direction and carrying less saline water to the northeast. This effect can clearly be seen in the chart of February, plate 11. During the southwest monsoon the situation is reversed, water of about 32.5‰ is transported along the coast of Vietnam to the north, and in the central parts a counter current carries water of above 33.2‰ to the southwest, plate 12. Because on the average the rainfall exceeds the evaporation in this region, the salinity of the passing water is continuously decreased, though only by a small amount. The relatively big annual variation of about 1.1‰ is caused by currents carrying water of different salinities during the two monsoons.

Off the mouth of the Mekong the annual variation increases to more than 2‰, whereas in the Gulf of Thailand it amounts to about 1.3‰, although this value is still uncertain because of the small number of observations. The salinity in the Gulf of Thailand varies between 30.5‰ in January and 32.0‰ in September. This means that the maximum occurs at the end of the rainy season, after which a decrease of the salinity is observed. But the maximal discharge of the rivers normally occurs at the end of the rainy season, which may explain this variation. On the other hand the waters of low salinity, formed off the mouth of the Mekong, are pressed by the winds into the gulf from October to January and cause a low salinity.

In the southern parts of the China Sea there are two rainy seasons, a weaker one in April/May and a stronger one from October to January. The variation of the salinity also has two maxima, fig. 4.3, but it shows no direct relation to the rainy season. This is why the river discharges from Sumatra and Borneo are more important for the changing of the salinity than the rainfall itself. As the annual excess of rainfall is about 1250 mm and the amount of freshwater discharged from the rivers may be about the same as that from direct rainfall, a continuous lowering of salinity originates from this region. The effect of this large addition of fresh water can be seen from the distribution of the salinity. In February a tongue of high salinity penetrates into the southern China Sea from the north and extends between less saline coastal water on both sides into the Java Sea. On its way the salinity in the core of the tongue is decreased from 33 to 32‰, which is an effect of the rainfall as well as of the lateral mixing with the coastal waters on both sides. With the beginning of the southeast monsoon over the Java Sea its waters of low salinity are pressed to the north, and cause in June, July and August minimal salinities in the southern China Sea. Later in September and October a short increase of salinity occurs, when the waters of high salinity, entering the Java Sea from the east, penetrate as far as the southern China Sea. But their influence is limited to the parts south of the equator. With the beginning of the northeast monsoon over the China Sea, water of high salinity again comes from the north. The weaker secondary minimum of salinity in December seems to be the effect of the maximum of the rainy season in this month. So the southern China Sea is a region in which the excess of rainfall causes a constant

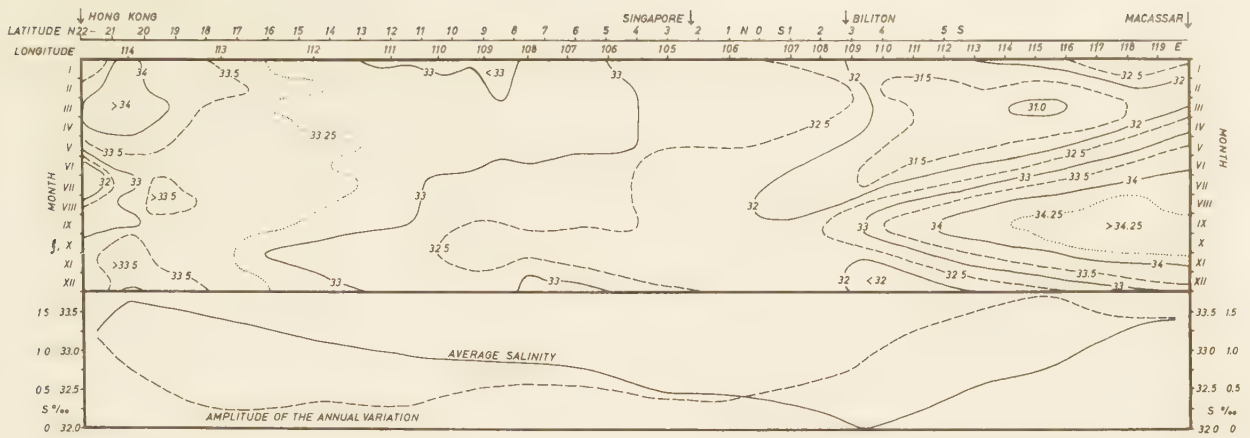

Fig. 4·4. Isopleths of the surface salinity along a section from Hong Kong through the China Sea and Java Sea to Macassar. Lower part gives average salinity and amplitude of the annual variation.

decrease of salinity, and the waters always leave the region with a lower salinity than they had when they entered it. The annual variation of salinity therefore depends more or less on the intensity of the water exchange. The vertical distribution of salinity over the Sunda Shelf is discussed in connection with fig. 4 · 10.

Isopleths of the surface salinity along a line running from Hong Kong through the China Sea and the Java Sea to Macassar on Celebes are shown in fig. 4 ·4. In the lower part of the figure the average annual salinity and the amplitude of the annual variation are given. The boundary between the Java and the China Seas is off the island of Biliton, where the salinities are lowest. All through the China Sea to Hong Kong the salinities increase constantly, but off Hong Kong coastal effects again become important. During the northeast monsoon the isohalines are shifted to the south, during the southeast monsoon to the north. Salinities above 34‰ are observed south of Hong Kong from December to April.

In the region east of Luzon in the Pacific Ocean the variation of the surface salinity is completely smooth, fig. 4 · 3. In this region the rainfall exceeds the evaporation in every month, so that the salinity of the passing water must decrease. But the variations of the surplus of the rainfall are small, and they do not find a reflection in the variation of the surface salinity, because the homogeneous layer is 80 m deep. The annual variation of 0.5‰ therefore may be caused by fluctuations of the salinity of the North Equatorial Current, carrying in winter water of higher salinity and in summer water of lower salinity. These water masses arrive in the region off the Philippines according to the distance from the area of their origin and the velocity of the current.

The SULU SEA has an annual variation of salinity very similar to that east of Luzon, but with a larger amplitude and a lower average salinity. Because there is a continuous inflow of water through the Philippines into the Sulu Sea, this parallelism is not surprising, but the larger amplitude needs explanation. In this region a rainy season from May to September is clearly developed, while during the rest of the year rainfall and evaporation are almost balanced. During the rainy season the excess of the rainfall is about 840 mm, and the drop of salinity is 1.2‰. But with a homogeneous layer of 30 m such an excess of rainfall gives a decrease of only 0.9‰. Therefore the inflow of water from the China Sea must contribute to the drop in salinity, and in fact, from July to October, water with salinities between 33.0 and 33.4‰ enters the Sulu Sea. The increase of the salinity from November to April coincides with the maximum of the inflow of highly saline water from the Pacific.

In the CELEBES SEA the phase of the annual variation of salinity is considerably displaced against the Sulu Sea, but the amplitude is about the same. The maximum of salinity occurs in September, the minimum in January. Almost throughout the year the Celebes Sea is filled with oceanic waters carried by the Mindanao Current.

Only during the north monsoon are water masses from the Sulu Sea transported into the Celebes Sea when they cause a drop in salinity from October to January. Thus, the distribution of salinity is governed by the strength of the Mindanao Current and during the north monsoon by waters from the Sulu Sea. The rainfall over the Celebes Sea is considerable and exceeds the evaporation during all months, causing a continuous decrease of the salinity of the passing water masses. The homogeneous layer is normally smaller than 50 m and the salinity below it increases rapidly to more than 34.5‰.

The region north of New Guinea is alternately occupied by water of the South Equatorial Current and of the Counter Current, this change causes the variation of the salinity. The homogeneous layer in this region extends down to 100 m, so that the considerable rainfall has little effect on salinity. From April to October the region is influenced by the South Equatorial Current, which causes a continuous increase of the salinity. The waters of the Counter Current, dominant from December to March, are of lower salinity.

During the southeast monsoon the region of the Flores, Banda, Arafura and Timor Seas is influenced by its dry air masses and has a considerable excess of evaporation. This amounts in the Flores Sea to 520 mm, in the Banda Sea to 540 mm, over the Arafura Sea to 780 mm and increases over the Timor Sea to 1240 mm, see figs. 5 · 3 and 5 · 4. With a homogeneous layer of only 35 m this would cause an increase of salinity of between 0.5 and 1.2‰ during the dry season. The annual variation, however, does not increase towards the east, but is largest in the west, and is produced by the water exchange.

The ARAFURA SEA and the eastern parts of the Banda Sea are an important region of upwelling, which is discussed in Section 7 · 5. During the northwestern monsoon water masses with salinities of only 33.5 to 34.2‰ are carried into the region by the Monsoon Current and occupy the surface layer to a depth of 100 m, fig. 7 · 14. With the beginning of the southeast monsoon these water masses are again driven back to the west into the Flores Sea and the Java Sea. These horizontal transports are combined with upwelling in the Banda and Arafura Seas, which cause a rise of the discontinuity layer of about 60 m. It is unlikely, but for some local exceptions, that the top of the discontinuity layer ever reaches the very surface. Above the discontinuity layer a layer of higher salinity water usually seems to occur as is shown in fig. 7 · 14. In this 30 to 50 m thick layer only evaporation has an effect on salinity. An estimation of this effect shows, that an excess of the evaporation of 780 mm during the dry season increases the salinity in a 40 m thick layer by 0.7‰ in accordance with the observations. On the other hand, the variations of the salinity below this layer must be entirely attributed to upwelling water of high salinity. During the northwest monsoon the excess of rainfall is not sufficient to account for the reduction in salinity by 0.7‰ in the 80 m thick homogeneous layer so there must be an inflow of water of low salinity during this season. But the decrease of salinity in the Arafura Sea first occurs rather late in February, when the water masses coming from the Java and Flores Seas have reached this region. The minimum of the salinity therefore appears in May at the beginning of the southeast monsoon.

In the BANDA SEA the variation of salinity is about 1.4‰ and much larger than in the Arafura Sea, although the excess of evaporation is smaller, so in this region the currents are responsible for the variations in salinity. During the southeast monsoon the water whose salinity has already been increased by evaporation, is transported westwards by currents. During the northwest monsoon, on the other hand, water masses of low salinity from the Flores Sea cause a considerable decrease of salinity from December to April. In this region the decrease of salinity starts earlier than in the Arafura Sea, and the minimum is reached one month earlier. The difference in depth of penetration of this less saline water into the Banda Sea each year causes the strong variability of the surface salinity in the Banda Sea from January to May, fig. 4 · 3.

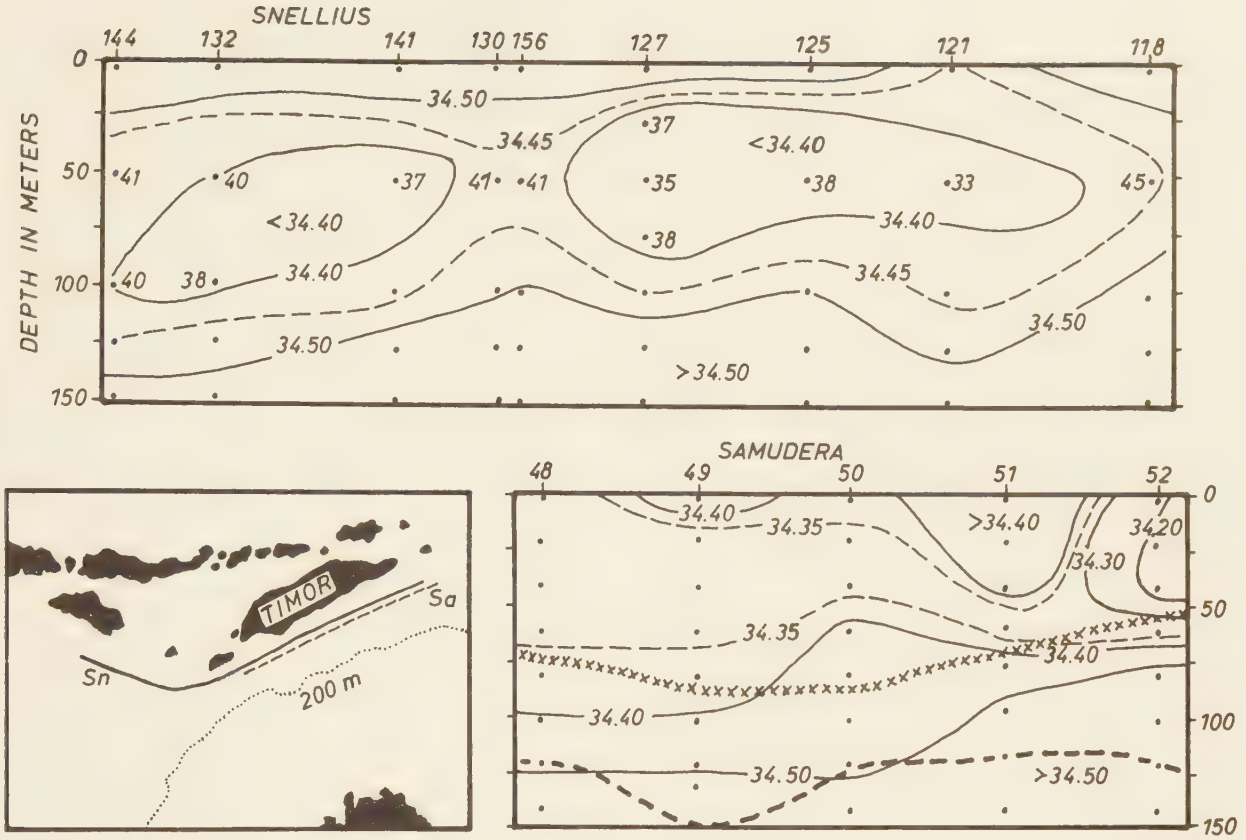

Fig. 4·5. Vertical distribution of salinity between the surface and 150 meters in two sections through the Timor Sea taken by the SNELLIUS in October 1929 and by the SAMUDERA in March 1957. x x x x x top of thermocline. – – – – centre of O_2 minimum.
Inset map shows positions of the sections.

In the **TIMOR SEA** the excess of evaporation is comparatively highest with 1240 mm. The annual variation, however, hardly exceeds 0.5‰, though this value may be uncertain because of the few observations. Off the south coast of Timor the Timor Current flows towards the southwest throughout the year and extends during the southeast monsoon to the Australian coast. This makes the Timor Sea a passage of water masses which are altered in salinity while passing, but this does not necessarily cause strong local variations of salinity.

Two longitudinal sections through the Timor Sea permit an interesting insight into the hydrographic conditions of this region. One was taken by the SNELLIUS in October 1929 and the other by the SAMUDERA in March 1957, fig. 4·5. The section of October at the end of the southeast monsoon shows below a surface layer of only 20 m with salinities between 34.5 and 34.6‰, a layer with a minimum salinity below 34.4‰. This minimum lies between 50 and 100 m, and at 125 m depth the salinity again exceeds 34.5‰. In the whole region the temperature continuously decreases from the surface down. Obviously, the evaporation influences only a relatively thin layer at the surface, while a layer of lower salinity is maintained below it. This intermediate layer also indicates that there is no upwelling in this region.

The section in March at the end of the rainy season surprisingly also shows a minimum of salinity between 30 and 50 m depth, and above it water of slightly higher salinity. But during this month, there exists a nearly isothermal layer which extends to about 75 m and also includes the salinity minimum. Below this layer an oxygen minimum is developed in a depth of about 125 m, which was not observed in October. Based on these observations it must be assumed that the water with salinities between 34.2 and 34.4‰ forming the layer of minimal salinity, is

not formed in this region. It may come from the current flowing eastwards north of the Lesser Sunda Islands and turning into the Timor Current around the east point of Timor. From December to March this current is rather strong and carries the less saline water of the Flores Sea into this region.

Later during the southeast monsoon, which causes only a relatively shallow drift current, the Timor Current is chiefly supplied by water from the Arafura Sea. This water has a higher salinity, which is slightly raised by evaporation, as shown by the section of October at the end of the southeast monsoon period. The oxygen minimum observed at about 125 m depth in March can be explained simply by the movements of water masses. When water masses with a temperature higher than 20°C, that is water from above 150 m, are renewed and water with lower oxygen content moves over water of higher oxygen content, a minimum must be formed. In fact, this seems to happen, but the layer of minimal oxygen content will be later dissolved by mixing. The lower limit of this minimum therefore indicates the depth of the current, amounting for the Timor Current to 150 m. In October the current is deeper and goes down to 250 m, see fig. 7 · 10L.

In the FLORES SEA the annual variation of salinity increases from 1.5‰ in the eastern to 3.0‰ in the western part and currents must be the reason for this considerable variation. Fig. 4 · 3 shows that these variations appear with great regularity, which is a characteristic criterion for the monsoon currents in this region. With the beginning of the west monsoon, water masses of low salinity flowing from the Java Sea into the Flores Sea continuously reduce the salinity from November to March. In addition there is the effect of rainfall, but it could only cause a reduction of the salinity by 0.5‰. With the southeast monsoon, waters of higher salinity from the Banda Sea enter the Flores Sea and the salinity rises. There is no inflow of water of high salinity from the Indian Ocean, as has always been assumed. During this season the charts of the surface currents, plates 2 - 4, show a coastal current flowing eastwards north of the Lesser Sunda Islands. Parts of its water flow between the islands into the Indian Ocean. So the water of high salinity in the Flores Sea can only come from the east or from upwelling processes.

The annual variation of the surface salinity in the Flores Sea together with that in two passages between the Lesser Sunda Islands is shown in fig. 4 · 6. The minimum of the salinity is caused by the flow of water of lower salinity from the Java Sea and occurs in March southwest of Macassar, and one month later in the Lombok, Alas and Sape Straits. With the onset of the southeast monsoon in April the salinity rises in all places. In the following months the salinity north of the Lesser Sunda Islands is always higher than in the Sape Strait. Therefore it is impossible for the water masses raising the salinity in the Flores Sea to enter through the Lesser Sunda Islands from the Indian Ocean. If they did, the higher salinities would first be observed in the passages between the islands. In certain cases, upwelling may contribute to raise the salinity in the Flores Sea from May to August. There were salinities above 34‰ in the region west of Macassar, which have no connection with the waters of similar salinity coming from the Banda Sea. On the other hand, hydrographic stations in this region are so few that available

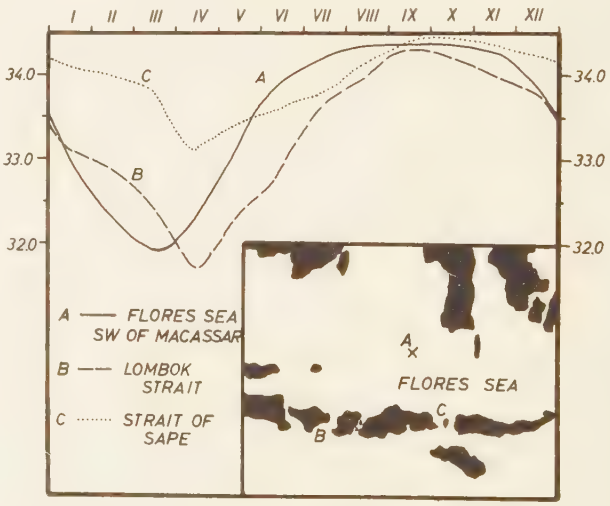

Fig. 4·6. Average annual variation of surface salinity in the Flores Sea, Lombok Strait and Sape Strait. Inset map gives positions of the localities.

data could not prove this assumption, (see Section 7 · 5).

The JAVA SEA together with the southern parts of the China Sea is a source of water masses with low salinities. The runoff from the many rivers of Sumatra, Borneo and Java rather than rainfall over sea reduces considerably the salinity in large regions off the coasts, and the 30‰ isohaline is often pushed far into the open sea, plate 14. In these regions below or just south of the equator the rainy season lasts from about October to March and the maximal discharge of the river occurs with a delay of about one month. Therefore the maximal extent of the water masses of lower salinity occurs in April and May. With the onset of the southeast monsoon these less saline waters are transported by the currents from the Java Sea into the southern China Sea. They are followed by waters of higher salinity from the east, which almost fill the whole Java Sea till September. This change in the salinity distribution is clearly shown in the isopleth diagram, fig. 4 · 4.

The penetration of the water of high salinity into the Java Sea is shown in fig. 4 · 7 by the positions of the 32‰ isohaline from June to September 1950. In June the water of higher salinity entered the Java Sea from the east and as early as August it had reached the island of Biliton. Only in strips along the coast of Borneo and Sumatra was there still water of lower salinity. In September the water of higher salinity penetrated further to the north and joined the water of above 32‰ in the southern China Sea. This connection normally lasts two or three months. In September the water masses of high salinity reach their maximal westward penetration in the Java Sea.

With the onset of the northwest monsoon in October/November these water masses are pushed back again and as the rainy season starts at the same time the salinity is reduced. The Monsoon Current transports water from the China Sea into the Java Sea and further to the east, causing a decrease of salinity even in the Flores Sea. In the Java Sea the salinity is below 32‰ from January to May, but the minimum occurs in May at the time of the maximal extent of the river water from Borneo, fig. 4 · 3. In the Flores Sea this minimum caused by the Monsoon Current occurs in March with salinities of 32‰ and in the Banda Sea in April with 33.2‰. The spreading of this water of low salinity is clearly

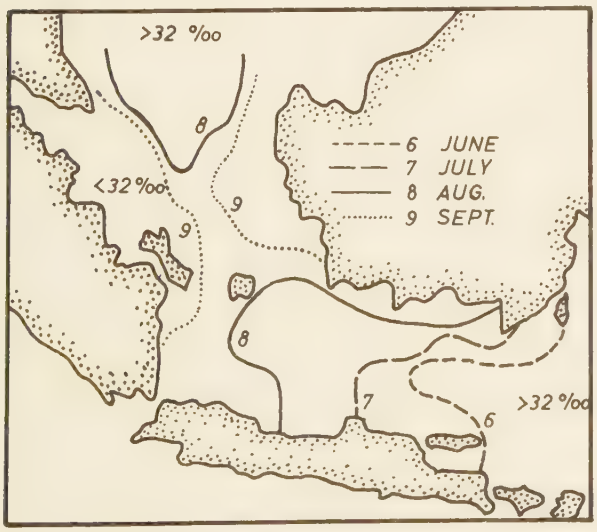

Fig. 4·7. Position of the 32‰ isohaline from June to September 1950 in the Java Sea, demonstrating the advance of the water of high salinity from the east during the southeast monsoon.

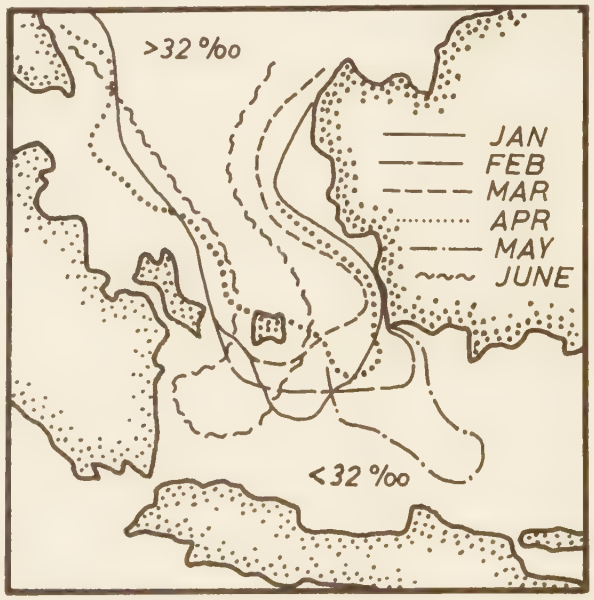

Fig. 4·8. Position of the 32‰ isohaline in the southern China Sea and in the western Java Sea from January to June 1953, showing the position of the tongue of high salinity entering the Java Sea from the north during the north monsoon.

visible in the salinity chart for February, plate 11.

The water masses entering the Java Sea during the north monsoon are soon followed by water of higher salinity from the China Sea. This forms a tongue of water of relatively high salinity in the southern China Sea between the less saline coastal waters off Sumatra and Borneo. The position of this tongue in the first six months of 1953 is shown in fig. 4 · 8. It extends through the Karimanta and Gaspar Straits into the Java Sea. In May the largest extension to the east is reached and in June the tongue is pushed back by the onset of the southeast monsoon against the coast of Sumatra. The fact that both monsoons first carry water of lower and later of higher salinity into the region between Sumatra and Borneo, causes an annual variation of the surface salinity in the southern China Sea and in the western parts of the Java Sea with two maxima and two minima. A detailed description of the salinity distribution along the north coast of Java is given by Soeriaatmadja (1956), who shows that this double salinity maximum is found up to 110°E.

The vertical structure of the water masses in the Java Sea, which is only 30 to 60 m deep, is presented in fig. 4 · 9. During all months the vertical curves of salinity show an almost homogeneous salinity from the surface to the bottom over the more shallow regions. The relatively strong Monsoon Current and the locally rather strong tidal currents may be the reason for this vertical homogenity. Current measurements at various stations in the Java Sea have shown that the velocity remains constant from the surface to the bottom and the decrease occurs only in the last 5 m above the bottom. This is illustrated by the anchor station Sn 312a (Lek, 1938) in the eastern Java Sea and the observations dealt with by Weel (1923). In the region east of Java and along the eastern edge of the Sunda Shelf the variation of salinity is restricted to the upper 40 m. Below this level there is water with salinities always above 34‰. This depth almost corresponds with the depth of the homogeneous layer in the adjoining parts of the Flores Sea.

Off the Sunda Strait the salinity is normally equal from the surface to the bottom in 50 m. Only during the period of strong runoff from the rivers in south Sumatra there develops a surface layer of lower salinities. In February at the

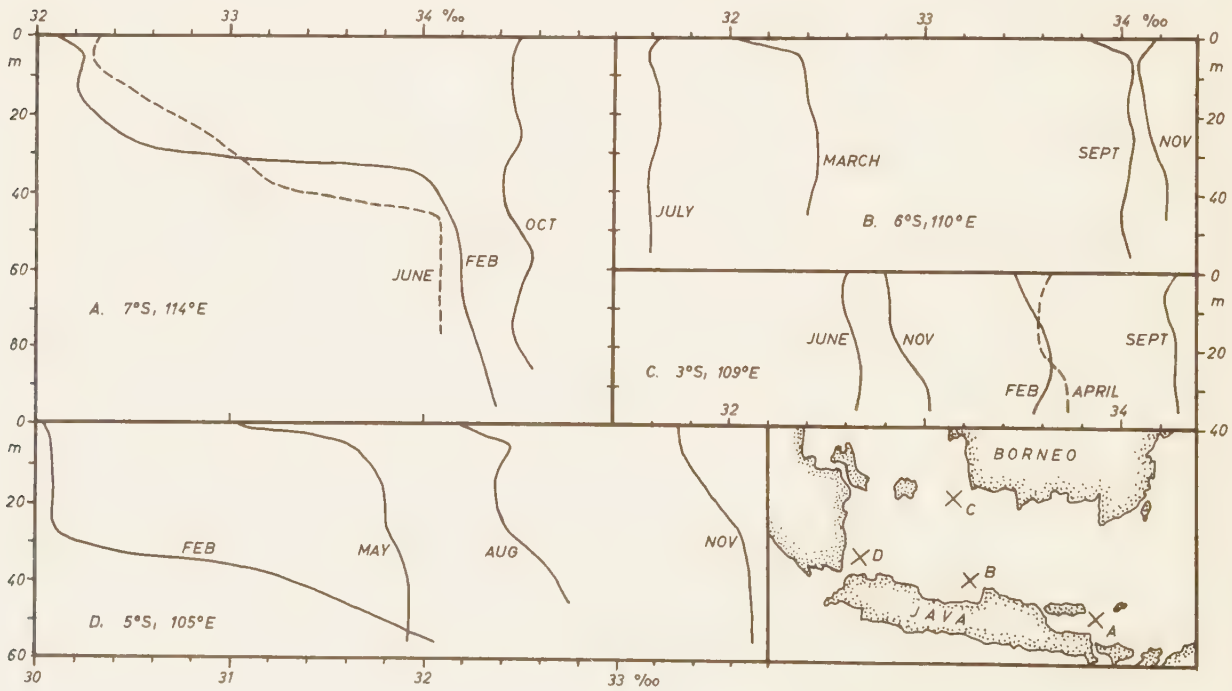

Fig. 4·9. Vertical distribution of the salinity in four localities of the Java Sea during different months. Inset map gives the positions of the observations.

end of the rainy season this layer is about 30 m thick, fig. 4 · 9. It extends from the Banka Strait along the east coast of Sumatra to the south and it is carried southwards by the coastal current developed during this season. Off the Sunda Strait it comes under the influence of westerly winds and forms a tongue of less saline water spreading towards the east and northeast, this has already been described by Berlage (1927). This tongue is in most years recognisable over more than three degrees of longitude, but it was completely absent in February 1918, which may be explained by an unusual advance of water of higher salinity from the China Sea. But the position of this tongue seems to vary widely, because in the chart of the average salinity in February, plate 11, it is indicated only weakly. An influence of the Indian Ocean surface water on the Java Sea as stated by Hardenberg (1956) for individual years, seems not to appear and has not yet been proved.

In the southern parts of the China Sea, over the deeper portions of the Sunda Shelf, stratification is developed temporarily. The distribution of temperature, salinity and oxygen content is shown in a section from Singapore to Pontianak in Borneo, taken by the SAMUDERA in August 1957, fig. 4 · 10. In the upper 40 m, the water is nearly homogeneous, with the exception of a thin surface layer of decreased salinity off the

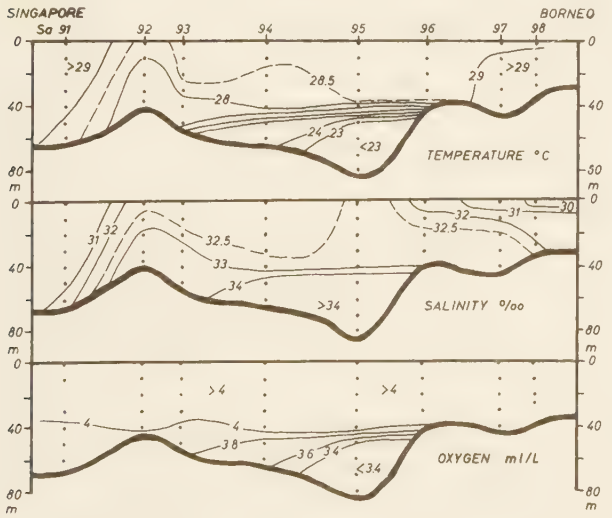

Fig. 4·10. Longitudinal section from Singapore to Pontianac on Borneo, showing the distribution of temperature, salinity and oxygen content in the southern parts of the China Sea.

mouth of the Kapuas River. Between 40 and 50 m depth, a relatively sharp discontinuity is developed, and below it water of lower temperature, higher salinity and lower oxygen content is present, which originates from the China Sea. During August water of about 32.5‰ salinity moves in the surface layer from the Java Sea into the southern parts of the China Sea. Because the passages between these two seas are only 35 to 40 m deep, the moving layer, driven only by weak winds, does not extend deeper, when passing over deeper water. Consequently, water from the China Sea, having a higher density, can penetrate beneath the surface layer and enter the deeper portions of the southern China Sea, as shown in fig. 4 · 10. During the northeast monsoon, on the other hand, such a stratification will probably not develop, because the winds are much stronger and the wind-stirred layer is deeper, but this has not yet been verified by observations.

Through the MALACCA STRAIT there flows a steady current towards the northwest into the Indian Ocean, fig. 7 · 8. During the northeast monsoon the current transports water of the China Sea having a relatively high salinity, and during the southeast monsoon water masses with low salinities formed off the rivers of central Sumatra. This results in a rather regular annual variation of surface salinity in the southern and central parts of the strait. On its way through the strait the salinity of the water is reduced by the discharge of the many rivers and the heavy rainfall. Strong tidal currents cause a complete vertical mixing of the water. In the northern part of the strait, for which the variations of the surface salinity are shown in fig. 4 · 3, the rainfall is of more importance than the currents. During the rainy season from September to January an excess of 720 mm of rain falls on the sea, causing within a homogeneous layer of 30 m depth a drop of 0.7‰ in salinity. In fact the salinity decreases by as much as 1.5‰, which shows that less saline water is also admixed. The deviations of the observed salinities from the averages are exceptionally large in the Malacca Strait. A de-

tailed presentation of the surface salinity in the Malacca Strait is given by Soeriaatmadja (1956), for the Singapore Strait by Tham Ah Kow (1953) Typical series of temperature and salinity and current observations in the strait are dealt with by Weel (1923), but show normally homogeneous conditions.

The adjoining ANDAMAN SEA lies under the influence of the Indian monsoon, which causes a strong and continuous rainy season from May to November, whereas evaporation prevails during the other months. But the discharge from the rivers is of more importance than the rainfall. The minimum of salinity is reached in October/November caused by the currents transporting the less saline waters from the mouth of the Irawadi southeast into the central parts of the Andaman Sea. In October the direction of the circulation changes and oceanic water of higher salinity advances from the south. This change of the water masses due to currents causes an extremely high annual variation of salinity in the northern parts of the Andaman Sea, see plate 10 and fig. 4 · 3. In the southern part of the Andaman Sea, for which the annual variation of salinity is shown in fig. 4 · 3, two minima of salinity are observed. The minimum in October is caused by waters coming from the north, and the minimum in February/March by waters coming out of the Malacca Strait and penetrating northwards. During the northeast monsoon which blows offshore upwelling should be expected along the coast of Burma, but the information on the Andaman Sea is too meagre to confirm this.

In the INDIAN OCEAN, southwest of Sumatra, high rainfall causes a continual decrease of the salinity of the passing water. The excess of rainfall over the evaporation amounts to more than 2000 mm during the year, but the water masses of lower salinity resulting from these rains are carried towards the southeast by the outrunners of the Counter Current. The larger part passes over into the South Equatorial Current at about 10°S, and the smaller part continues in the Java Coastal Current flowing to the east. In the northern part water movements towards the northwest are found from December to February. The lowest values of salinity occur in January at the end of the main rainy season, while the increase falls into the period from May to July, when the rainfall is lowest. The annual variation exceeds

TABLE 1

Average monthly and annual surface salinities in different regions of the Southeast Asian Waters, according to observations from 1950 to 1955. The positions of the regions are indicated in fig. 5 · 8, the values refer to areas of 4 to 12 1° squares, according to the density of observations. For graphical presentations see fig. 4 · 3.

	YEAR	JAN.	FEB.	MAR.	APR.	MAY	JUNE	JULY	AUG.	SEP.	OCT.	NOV.	DEC.
East of Luzon	34.6	34.7	34.8	34.8	34.8	34.7	34.7	34.5	34.5	34.3	34.3	34.4	34.6
N. China Sea	33.6	33.8	33.9	33.9	33.7	33.6	33.5	33.5	33.6	33.3	33.4	33.6	33.6
S. China Sea	32.3	32.4	32.4	32.6	32.6	32.4	32.1	32.2	31.9	32.2	32.2	32.4	32.1
Java Sea	32.5	32.0	31.8	31.8	31.7	31.4	31.9	32.7	33.3	33.8	33.5	33.3	32.6
Flores Sea	33.5	33.0	32.3	31.9	32.4	33.2	33.7	34.2	34.2	34.4	34.4	34.3	33.9
Banda Sea	34.0	34.2	33.9	33.5	33.2	33.3	33.6	34.0	34.3	34.4	34.5	34.5	34.3
Arafura Sea	34.3	34.4	34.4	34.2	34.0	33.8	34.0	34.3	34.4	34.5	34.5	34.5	34.4
South of Java	34.5	34.6	34.6	34.5	34.4	34.4	34.4	34.4	34.5	34.5	34.6	34.7	34.7
Sulu Sea	33.7	33.8	33.9	34.1	34.2	34.2	34.0	33.8	33.5	33.2	33.0	33.3	33.6
N. of N. Guinea	34.2	34.1	34.0	33.9	34.0	34.1	34.3	34.4	34.5	34.5	34.3	34.2	34.1
Celebes Sea	34.0	33.5	33.6	33.8	34.0	34.1	34.2	34.2	34.3	34.3	34.2	33.9	33.6
S.W. of Sumatra	33.0	32.5	32.9	32.8	32.8	32.9	33.2	33.5	33.6	33.3	32.9	32.6	32.8
Malacca Strait	30.9	30.4	30.5	30.7	30.9	30.8	31.0	31.4	31.4	31.3	30.7	30.4	29.8
Andaman Sea	32.4	32.3	32.1	32.2	32.6	32.8	32.8	32.7	32.5	32.3	32.0	31.9	32.2

1.0‰ along the coast and remains below this value outside the coastal islands.

The region south of Java lies under the influence of the southeast trades. The excess of evaporation during the dry season almost equals the excess of rainfall during the rainy season, and amounts to 570 mm. The annual variation of salinity is small and has a value of less than 0.5‰ in the range of the South Equatorial Current. The increase of salinity occurs during the dry southeast monsoon and the decrease during the rainy season. The depth of the homogeneous layer increases from east to west, that is in the direction of the flow. At an average depth of the homogeneous layer of 40 m, the variations of salinity are just compensated by the variations of rainfall and of evaporation. Closer to the coast the annual variation increases to more than 1.0‰ in the range of the Java Coastal Current, and the average salinity decreases.

4·5 THE DISTRIBUTION OF NUTRIENTS, PRODUCTIVITY AND TRANSPARENCY

Our knowledge about the distribution of factors other than temperature and salinity in Southeast Asian Waters is still very meagre. This is firstly due to the fact that their distribution is particularly complex owing to the mixing of coastal and oceanic waters, and the presence of large shelves and land-enclosed deep sea basins. This makes its investigation difficult. Secondly in this region there is no highly developed fishery, which could warrant an investigation of the environmental factors of its fishing grounds. Thus, our knowledge of the distribution of nutrients, productivity and transparency depends on the work of the larger oceanographical expeditions, such as the DANA, ALBATROSS and GALATHEA Expeditions, which have crossed these waters on their voyages, and on a few special studies.

The nutrient content over the deeper portions of the Southeast Asian Waters shows a distribution, which is characteristic of tropical waters. The surface layer is extremely poor in nutrients, the phosphate contents being less than 0.2 μg-atoms/L. Within the discontinuity layer, it rises considerably and normally reaches 1.5 μg-atoms/L at its lower boundary. In the intermediate and deep layers phosphate contents of 2.5 to 3.0 μg-atoms/L are quite normal. The phosphate content in the waters over the shelves is, surprisingly, not much higher, as investigations of Delsman (1939) in the Java Sea have shown. He found phosphate contents of about 0.08 μg-atoms/L with fluctuations between 0.03 and 0.12 μg-atoms/L near the surface, and only slightly higher values near the bottom (0.08 to 0.15 μg-atoms/L, average about 0.12). An increase towards the coast has been observed, but no marked differences between April and October. Delsman mentions that the influence of the discharge of the rivers on the phosphate content in the sea seems to have been overestimated, because the river water is not as rich in phosphate as normally assumed. The distribution of nitrate and silicate generally corresponds to that of the phosphate.

The mechanism of the supply of the surface layer with nutrients is, however, quite different for the shelves and for the deep sea. Over shallow waters, the regeneration of the sinking material occurs at the bottom and the nutrients can easily be brought into the euphotic zone by vertical mixing. Consequently a continuous supply of nutrients to the water masses takes place and enables continuous production. This process makes large parts of the shelves quite fertile and maintains a big stock of fish. The replenishment of the surface layers over the deeper portions of the region with nutrients is, however, completely different, as it is only by upwelling or by divergent movements in the surface layer that more fertile water from the discontinuity layer can ascend and enter the euphotic zone. But these effects occur only locally and consequently the greater part of the water over the deep sea is of very low productivity. An enrichment of the surface layer with nutrients can take place along the coast also by means of currents, which flow from the shelf over deeper water, carrying water of higher nutrient content.

The productivity of these waters has been in-

vestigated by Steeman Nielsen and Jensen (1957) and by Doty (personal communication, 1958). Even if the few observations in this large region give only preliminary information on the organic production, they indicate some interesting details and confirm the above conclusions on the replenishments of the nutrients in the surface layer. A map of the organic production, based on the above mentioned data, is presented in fig. 4 · 11, but shows only the surface values without consideration of the vertical distribution of productivity and of the depth of the photosynthetic layer. In this map, the China Sea, the Philippine Waters and the Celebes Sea have only a small organic production of less than 0.5 g C per m² per day. In contrast to these regions the production is high over the Sunda Shelf: in the Gulf of Thailand, the Malacca Strait, the Java Sea and the waters between Sumatra and Borneo, where values of 1.0 g C per m² per day are often exceeded. The rather high production of 1.2 to 1.8 g C per m² per day in the Banda Sea, observed in September, is remarkable and surprised Steeman Nielsen, when discussing his results. But this high production must be ascribed to upwelling, which occurs in this region from May to September, as explained in Section 7 · 5.

These few data on the productivity of Southeast Asian Waters accord fully with the distribution of nutrients, and support the above remarks on their replenishment. This takes place seasonally and locally by upwelling processes over the deeper parts of the region. Over the shelves, the cycle of nutrient replenishment is short and a high organic production takes place through the year in spite of only a small concentration of nutrients.

Practically no observations are available regarding the transparency of the water and the penetration of light into the sea. According to

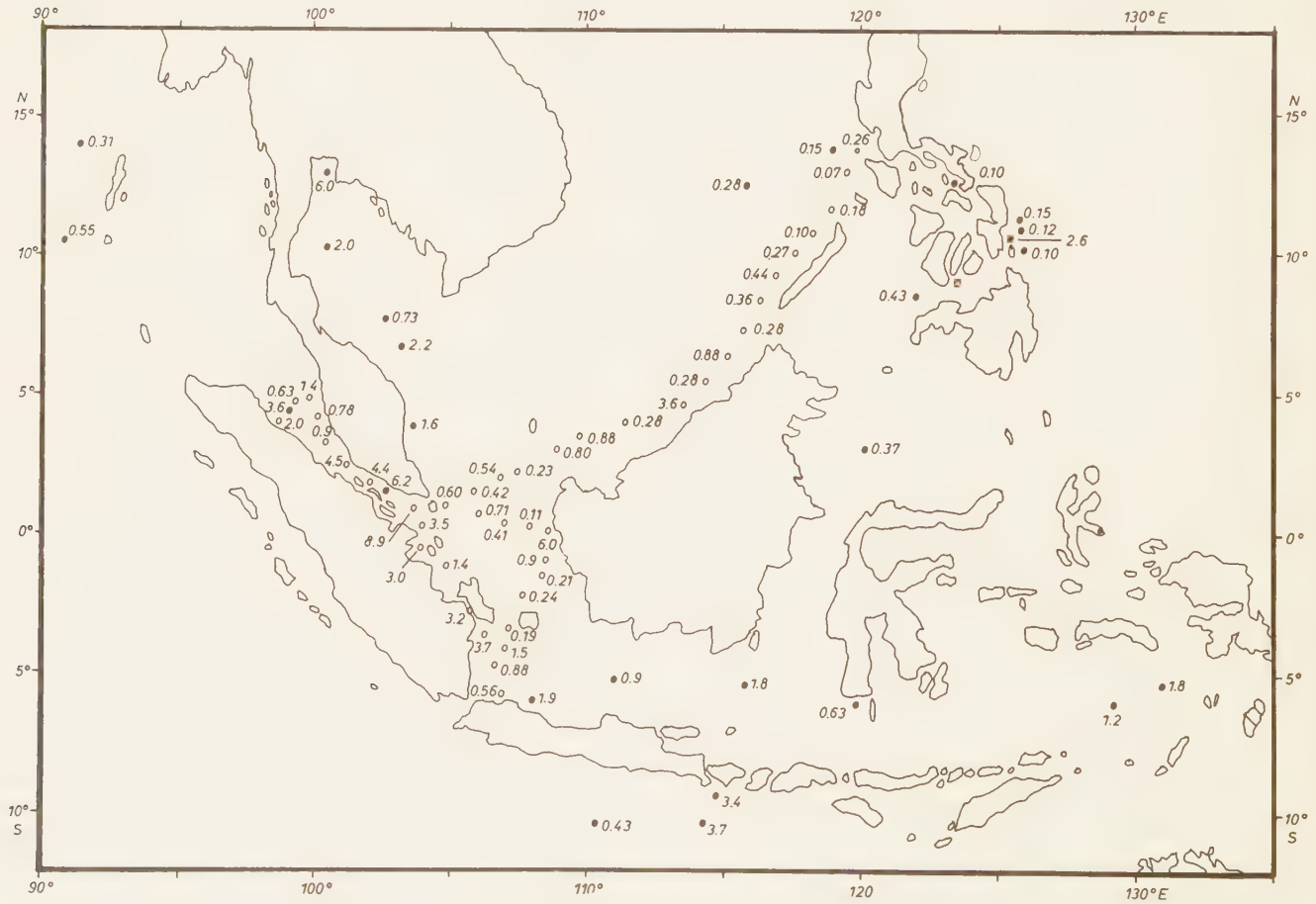

Fig. 4·11. Productivity at the surface in Southeast Asian Waters in g C per m² per day.
- observations from Steemann Nielsen
o observations from Doty

the mixing of various water masses, such as extremely clear ocean water, turbid coastal waters and water of high particle content due to contact with the shelf bottom and to tidal currents, the transparency will show wide variations. Systematic measurements are not available from this region, but reference may be made to some information given by Verwey (1929, 1931) and Motoda (1939), as well as to the reports of the ALBATROSS and the GALATHEA Expeditions, the programmes of which included optical measurements.

LITERATURE

BECKER, R.

1938. Über den jährlichen Temperaturgang auf dem Indischen und Stillen Ozean.
Ann. Hydrogr. Berl. 66 : 336-340.

BERLAGE, H. P.

1927. Monsoon currents in the Java Sea and its entrances.
Verh. Magn. Met. Obs. Batavia. 19. 28 pp.

CAUVET-DUHAMEL, P.

1939. Sur les variations de température des eaux de la Mer de Chine.
Ann. Phys. Fr. outre mer. 6 : 50-54, 59-61.

CHEVEY, P., and P. CARTON

1935. Les courants de la Mer de Chine méridionale et leurs rapports avec le climat de l'Indochine.
Note Inst. Océan. Indochine 26. 13 pp.

CHU TSU YAO

1958. A study on temperature and salinity of the surrounding waters of Taiwan.
Proc. 8th Pacif. Sci. Congr. 3 : 821-5.

DELSMAN, H. C.

1939. Preliminary plankton investigation in the Java Sea.
Treubia 17 : 139-181.

HARDENBERG, J. D. F., and R. E. SOERIAATMADJA

1956. Monthly mean salinities in the Indonesian Archipelago and adjacent waters for the months: March 1950-February 1953.
Bull. Org. Sci. Res. Indonesia No. 21. 68 pp.

KREMPF, A., and P. CHEVEY

1933. The great general currents of the China Sea and hydrological sections of the shores of French Indo China.
Proc. 5th Pacif. Sci. Congr. 1 : 693-696.

LEIPPER, D., and W. WOOD

1947. Temperature and salinity of Philippine waters.
Scripps Inst. Oceanog. Rep. 4.

LEK, L., and G. THIEL

1938. Die Ergebnisse der Strom und Serienmessungen.
Snellius Exped. 1929-30. 2(3). 169 pp.

LUMBY, J. R.

1955. The depth of the wind-produced homogeneous layer in the oceans.
Fish. Invest., Lond. Ser. II. 20(2). 12 pp.

MEGIA, T. G., and A. R. SEBASTIAN

1953. The thermal structure of the surface waters off western Philippines, based on BT observations.
Philipp. J. Fish. 1(2), 1951(1953) : 131-143.

MOTODA, S.

1939. Submarine illumination, silt content, and quantity of food plankton of reef corals in Iwayama Bay, Palao.
Studies Palao Trop Biol. Sta. 1(4) : 637-650.

NIELSEN, E. STEEMANN, and E. A. JENSEN

1957. Primary oceanic production.
Galathea Rep. 1 : 49-125.

ROSSBY, C. G., and R. B. MONTGOMERY

1935. The layer of frictional influence in wind and ocean currents.
Pap. Phys. Oceanogr. 3(3). 101 pp.

SCHOTT, G.

1935. Geographie des Indischen und Stillen Ozeans.
Hamburg, C. Boysen. 413 pp.

SELGA, M.

1931. Observations on the salinity of the sea in the Philippines.
Pub. Manila Obs. 3 : 155-165.

SELGA, M.
1931. Variations of the temperature of the sea with depth in the Philippines.
Pub. Manila Obs. 3 : 141-153.
1932. Sea surface temperatures in the Philippines.
Pub. Manila Obs. 3 : 59-139.

SOERIAATMADJA, R. E.
1956. Seasonal fluctuations in the surface salinity off the north coast of Java.
Mar. Res. Indonesia. 1 : 1-19.
1956. Surface salinity in the Strait of Malacca.
Mar. Res. Indonesia. 2 : 27-48.

SVERDRUP, H. U., M. W. JOHNSON, and R. H. FLEMING
1942. The oceans, their physics, chemistry and general biology.
New York, Prentice Hall, 1,087 pp.

THAM AH KOW
1953. A preliminary study of the physical, chemical and biological characteristics of Singapore Straits.
Gr. Brit. Colonial Off. Fish. Pub. 1(4) 65 pp.

U. S. NAVY HYDROGRAPHIC OFFICE
1944. World Atlas of sea surface temperatures H.O. 225.

VEEN, P. C.
1953. Preliminary charts of the mean surface salinity of the Indonesian Archipelago and adjacent waters.
Bull. Org. Sci. Res. Indonesia. No. 17. 47 pp.
1951. Surface salinities in the Indonesian Archipelago and adjacent waters.
Pub. Org. Sci. Res. Indonesia. No. 33. 20 pp.

VERWEY, J.
1929. Depth of coral reefs and penetration of light with notes on oxygen consumption of corals.
Proc. 4th Pacif. Sci. Congr. 2 : 277-299.
1931. Coral reef studies, the depth of coral reefs in relation to their oxygen consumption and the penetration of light into the water.
Treubia 13 : 169-198.

WEEL, K. M. van
1923. Meteorological and hydrological observations in the western part of the Netherlands East Indian Archipelago.
Treubia 4. 559 pp.
1930. Der Oberflächen-Salzgehalt im Niederländisch-Ostindischen Archipel.
Ann. Hydrogr. Berl. 58 : 196-207.

WYRTKI, K.
1956. Monthly charts of surface salinity in Indonesian and adjacent waters.
J. Cons. Int. Explor. Mer. 21(3) : 268-279.

CHAPTER 5

PRECIPITATION, EVAPORATION AND ENERGY EXCHANGE AT THE SURFACE OF THE SOUTHEAST ASIAN WATERS

The atmosphere affects the ocean by radiation, precipitation and the action of the winds. Radiation is absorbed in the uppermost layers of the sea, except for a small part which is reflected, and causes a heating of these layers. Simultaneously a continuous loss of energy results from the long-wave back radiation from the sea surface which causes cooling. For the ocean, only their difference is effective and that is climatologically always positive in tropical waters. Incoming and outgoing radiation affect directly only the temperature of the ocean.

Rainfall leads to a decrease of the salinity at the surface, and is therefore of importance only for the water balance. The influence of the temperature difference between the rain and the sea water on sea temperature is negligible.

The wind on the other hand is of enormous importance. With the gradients of vapour pressure and temperature over the sea surface, the wind causes the evaporation as well as a pure heat transport, which normally is directed towards the atmosphere. By both these effects the sea surface suffers a loss of energy, causing a cooling. It is to be noted that the energy needed for heat transport is only about 5 to 10% of the energy necessary for evaporation. Evaporation entails an increase of salinity and in this way affects also the water balance. Evaporation as an effect impressed from outside by the meteorological conditions in the lowest layers of the air is therefore not dependent on the amount of the incoming radiation.

The temperature in the upper layers of the ocean therefore will rise if the energy used for evaporation is less than the difference between incoming and outgoing radiation, and it will drop if the energy used for evaporation exceeds the effective available radiation. The heat received or lost in this way by the ocean may cause a local change of temperature, but may also be transferred by advective processes.

A representation of the precipitation, evaporation, and energy exchange, using only average annual values, is inadequate because it misses the variations of the different factors in the course of the year. If an attempt is made to show monthly changes, an endless number of charts would be required, and, in any case, most of the factors have small horizontal gradients in these waters. Therefore a better representation is achieved by using the annual variations of these factors in 15 selected regions (fig. 5 · 8) in the Southeast Asian Waters. The values of the different climatic factors do not relate to a single point, but to areas of about 4 to 12 1° squares, situated in the centre of each selected region, to avoid disturbances from land. The basic values have been estimated from different climatological atlases and are graphically presented in figs. 5 · 1 - 5 · 7. The numerical values of these climatic factors have already been published by Wyrtki (1957), where the methods of their determination are discussed in more detail.

5 · 1 THE DISTRIBUTION OF RAINFALL

The precipitation over the different regions has been taken from graphs and charts given by Wyrtki (1956), where, by evaluation of reports from coastal and island stations within the Indonesian Archipelago, the average annual variation of rainfall over the sea has been estimated. For the regions outside the archipelago the same method has been applied for the determination of the annual variation of rainfall. The average annual rainfall over Southeast Asia is shown in plate 15. Immediately apparent is the strong variation of the rainfall in this region and its close relation to the distribution of land and sea and mountain chains. In addition there is a wide annual variation of rainfall due to the monsoons, which cause a dry and a rainy season in most of the regions. Close to the equator two maxima of the rainfall normally are found without a distinguishable dry season between

them. The departures of rainfall from the averages are very large in this region and reach easily 40% of the average rainfall.

5·2 THE CALCULATION OF THE EVAPORATION

The evaporation of the different regions has been calculated by means of the formula given by Sverdrup (1946). In this formula the evaporation E is proportional to the wind velocity v and to the vapour pressure difference between sea and air $e_w - e_a$.

$$E = k\,(e_w - e_a)\,v$$

This formula has a theoretical basis and has been used successfully for the calculation of evaporation, so that not it, but the data used, need critical consideration. Besides the wind velocity and the water and air temperature, the relative humidity enters the formula. This is difficult to determine, but plays an important role in the calculation. If E_a is the vapour pressure of the saturated air, and q the relative humidity, then the evaporation is given by

$$E = k\,(e_w - E_a + (1 - q)E_a)\,v$$

Because the water and the air temperatures over the sea are nearly equal, the difference $e_w - E_a$ practically vanishes and the evaporation depends effectively on the factor $(1 - q)$, which is the deficit of the saturation. But this value varies considerably in tropical monsoon climates because the humidity is high, between 90 and 70%. This means, that the factor $(1 - q)$ varies as 1 to 3.

The factor k in the evaporation formula, which can be derived from the boundary layer theory, has to be considered carefully, because the formula is valid only for simultaneous values of wind velocity and vapour pressure differences. But because normally the product of averages differs from the average of the single products, this theoretical calculation of k is only of limited value. This means, that the coefficient has to be determined empirically. If the wind velocity v is measured in m/sec, the vapour pressure in millibars and the evaporation in mm/day, the following values of k have been used by the authors named:

Sverdrup	1946	0.103
Jacobs	1951	0.143
Albrecht	1951	0.092
Brogmus	1952	0.104

For these calculations $k = 0.100$ has been taken, giving slightly smaller values than Sverdrup, an effect which could perhaps be balanced because, for the transformation of the wind velocity from Beaufort scale to m/sec, the maritime conversion scale has been used, giving slightly higher values than most other scales in use.

The temperatures of the water and of the air have been taken from the Dutch climatological atlases (1936, 1949). This material is not only very comprehensive, but is based almost throughout upon simultaneous observations of the water and the air temperatures, this is of importance for our investigations. The difference between water and air temperatures varies in the different months and regions between 0.8° and −0.2°C and has an average of 0.31°C. Negative values appear only over the regions of upwelling off the northwest coast of Australia during the southeast monsoon. The results of the Snellius Expedition (Visser 1936), on the other hand, have shown that the temperature of the water is on the average 0.7°C higher than that of the air, indicating a bias in the observations of the merchant ships. Therefore these values cannot be used to calculate the exchange of sensible heat between sea and atmosphere, although the values of the temperature may be considered to be representative for normal climatological conditions.

Relative humidity is necessary for the determination of the vapour pressure of the air, but its determination is difficult and affects considerably the results. The psychometric difference given in the Atlas of Climatic Charts of the Oceans (1938) cannot be used in this case, because only values at Greenwich noon are used, corresponding to 18 to 21 hours local time. This fact has already been criticised by Keyser

(1939). In the beginning of the night, however, the humidity is often high because of rainfall in the afternoon. Therefore the direct climatological observations of the relative humidity at coastal and island stations have been used. The values of the weather side and lee side stations have been compared and it has been accepted that the weather side stations give the real values over the seas. The vapour pressures of the air, obtained in this way, have been compared with those given by Albrecht (1951) and correspond with them with the exception of some explainable cases. Generally the variation of the humidity can be said to run parallel to that of the rainfall, allowing for the selection of suitable values in some doubtful cases.

The wind velocity has been determined in two independent ways. First the ships' observations collected at the Institute of Marine Research in Djakarta for a period of only seven years were examined statistically. Second, the Atlas of Climatic Charts of the Oceans has been used. This gives charts of the wind velocity for every season and in addition charts of the frequency of the wind velocity for every month. In this region the average wind velocity is about Beaufort 3, and, as the atlas gives information on the percentage of winds above and below Beaufort 3, the data of the atlas were very suitable. By means of a statistical analysis of the wind velocities of this region, the average wind velocity corresponding to a certain frequency in the atlas could be determined. These results correspond very closely to the direct ships' observations, so that they were used without further critical consideration.

By means of the temperature of the water and of the air and of the relative humidity, the vapour pressure difference between sea and air can be calculated. Multiplication of these values by the wind velocities v, the factor k and the number of days in the different months gives the evaporation. The annual variations of all these factors are presented in figs. 5 · 1 - 5 · 7 together with the annual variations of the rainfall, of the difference between rainfall and evaporation, and of the surface salinity.

5 · 3 THE CALCULATION OF THE ENERGY EXCHANGE

The energy exchange at the surface of the ocean satisfies the equation

$$Q_r - r\,Q_t - Q_b - Q_e - Q_{conv} \pm Q_{adv} \pm Q_h$$

where the different symbols have the following meanings:

Q_r	total radiation from sun and sky
r	percentage of reflected radiation
Q_b	back radiation from the sea surface
Q_e	energy used for evaporation
Q_{conv}	convection of sensible heat to the atmosphere
Q_{adv}	advection of heat by currents and mixing
Q_h	heat used for heating of the water, cooling negative.

The total incoming radiation is easy to calculate from the values given by Kimball (1928), if the average cloudiness is known. Information on the cloudiness has been taken from the Atlas of Climatic Charts of the Oceans (1938) and from Schott (1935), from which the annual variation of the cloudiness has been interpolated. The values of the incoming radiation at clear sky Q_o according to Kimball have been interpolated for the average latitude of the region and reduced according to the cloudiness C with the formula

$$Q_t = Q_o\,(1 - 0.071\,C).$$

The percentage of reflected radiation has been considered to be 3%. The back radiation is determined by means of the diagram given by Sverdrup (1946) as a function of sea surface temperature and relative humidity. It is reduced according to the cloudiness C with the formula

$$Q_b = Q_{bo}\,(1 - 0.083\,C).$$

From these three values the total effective radiation at the sea surface Q_{eff} is calculated by

$$Q_{eff} = Q_t - r\,Q_r - Q_b$$

These values are given in figs. 5 · 1 - 5 · 7. They show in nearly all regions two maxima during the course of the year, which is due to the position between the two tropics. The influence of the cloudiness modifies this distribution only a little, because in large areas the cloudiness varies

only between 50 and 65%, except during the southeast monsoon when the cloudiness decreases in its range to below 40%.

Opposite to this effective radiation are the energies used for evaporation, heating or cooling, for the exchange with the atmosphere and for advective processes. In tropical regions the evaporation certainly plays the dominant role, and its energy consumption is calculated by multiplying the evaporation by the heat of vapourisation (582 cal/g at 28°C). The exchange of sensible heat amounts in the tropics to about 5 to 10% of the heat used for evaporation and temporarily it may become negative. Its calculation is difficult because of the small temperature difference between sea and air, which is not known exactly. Therefore its calculation has been omitted.

For a presentation of the energy balance of the different regions (figs. 5·1-5·7), the total effective radiation Q_{eff} is shown and the difference $Q_{eff} - Q_e$, being the heat available for heating and cooling of the sea and the atmosphere as well as for advective processes. A comparison between the difference $Q_{eff} - Q_e$ and the annual variations of the water temperature shows in most of the regions a strong correlation between the available heat and the increase or decrease of temperature. Numerically a heat surplus of 100 cal/cm²/day heats by 1°C during one month a water layer of 30 meters. But for an exact comparison of both values a complete knowledge of the thermal structure of the water masses would be necessary, because advective processes might play an important role.

To gain an impression of their magnitude, a short estimation may be valuable. In the discontinuity layer of the Atlantic Ocean, Montgomery (1939) calculates the vertical eddy diffusivity at about 0.4 g cm sec⁻¹. With this value and with a temperature gradient of 10°C within 100 m depth a heat transport of 36 cal/cm²/day results. This rather big amount of heat transported into the depth may be an essential factor in the energy balance of the tropical oceans, but it is difficult to obtain exact values. The horizontal heat transport on the other hand seems to be less important because of the small horizontal temperature gradients in this region, only in special cases will it have some influence and one of them is discussed in connection with the Malacca Strait.

Although this investigation of the energy balance of the Southeast Asian Waters may be pre-

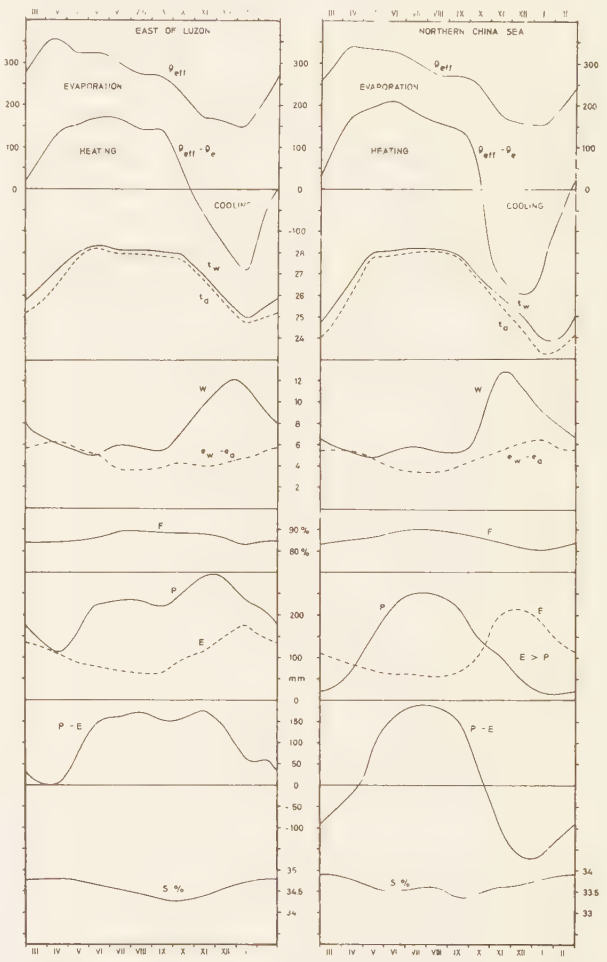

Fig. 5·1. Average annual variation of climatological factors in the region east of Luzon and in the northern China Sea. Symbols used:

Q_{eff} = effective available energy at the sea surface, cal/cm²/day.
Q_e = energy used for evaporation, cal/cm²/day.
t_w = temperature of the sea surface, °C.
t_a = temperature of the air, °C.
w = wind velocity, m/sec.
$e_w - e_a$ = vapour pressure difference between sea surface and air, mb.
F = relative humidity, %
P = precipitation, mm.
E = evaporation, mm.
S = surface salinity, ‰.

liminary, it gives an impression of the combined action of the different factors. This is discussed in some detail, when dealing with the conditions in the different regions in the following section.

5 · 4 THE ANNUAL VARIATION OF THE CLIMATIC FACTORS

Over the northern parts of the CHINA SEA there is a rainy and a dry season; in the latter, evaporation essentially exceeds rainfall (fig. 5 · 1). The high evaporation from November to March is chiefly a result of the strong winds during the northeast monsoon, but is intensified by the lower relative humidity in this season. The maximum of the relative humidity occurs in the rainy season. With the onset of the northeast monsoon the water temperature decreases because more energy is used for evaporation than is available from radiation.

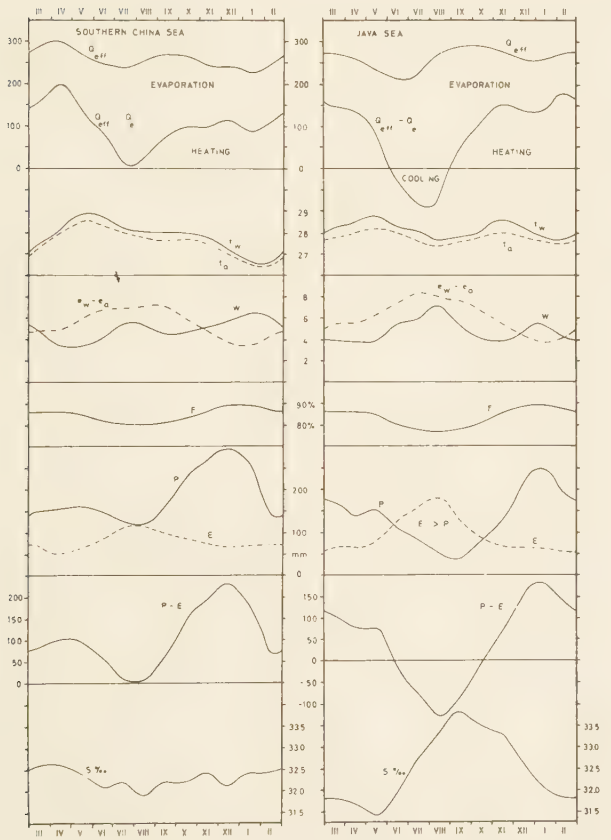

Fig. 5·2. Average annual variation of climatological factors in the southern China Sea and in the Java Sea. For explanation of symbols see figure 5·1.

The region east of Luzon, which is about in the same latitude and has similar wind conditions lacks the dry season, also because during the northeast monsoon wet air masses are dominant and lead to high rainfall through the year (fig. 5 · 1). Rainfall exceeds the evaporation in every month. Also in this region the temperature falls by 4°C during the northeast monsoon.

The energy balance of these two regions shows a similar pattern. The maximal radiation occurs in the months from April to July, that is the season with weak evaporation. During the months of November to February on the other hand the energy consumption by evaporation is larger than the effective radiation causing a cooling of the water. The total energy used for evaporation during these four months in the northern China Sea amounts to 21 000 cal/cm² which is sufficient to cool a layer of 50 meters by 4°C, but the cooled layer is about 70 m thick, consequently advective processes must be effective. This is in agreement with the advance of cool water masses through the Formosa Strait.

Over the southern parts of the China Sea a strong rainy season is developed from October to January, but a real dry season is lacking, so that the rainfall exceeds the evaporation in every month, fig. 5 · 2. Since winds are always weak, the evaporation is low, only in July/August, when the humidity is low, it exceeds 100 mm/month. The energy balance shows that the effective radiation exceeds the energy needed for evaporation in every month. From this a continuous heating of the water results even though a part of the energy is given off to the atmosphere. Because in this region a heat transfer into deeper water is possible only on a very limited scale, horizontal transports must carry the surplus of heat out of the region. From November to February a cooling of 1°C is noted, which must be caused by the advance of cooler water masses from the north. The warmed water moves with the Monsoon Current into the Java Sea, and a warming takes place coinciding with the maximum of the incoming radiation. The stronger evaporation in July/August causes a weak decrease in temperature because, besides the evapo-

ration, heat is given off to the dryer air masses of the southeast monsoon.

Over the **Java Sea** a rainy and a dry season is found, fig. 5 · 2. In the dry season during the southeast monsoon evaporation exceeds rainfall. High wind velocities and a low relative humidity cause an evaporation of more than 100 mm/month. From June to August the energy necessary for evaporation exceeds the available radiation and a cooling takes place. The deficit amounts to 5700 cal/cm² within these three months, corresponding to a cooling of a 40 m deep layer by 1.4°C, this is in accordance with the observations. The cooling in December and January is not in accordance with the energy balance, but during both these months the north monsoon is most strongly developed and with relatively strong winds brings cool and rainy air masses into the region. Perhaps the evaporation may be underestimated in these months. Remarkable in this connection is the variation of the temperature in the Java Sea, showing a semi-annual period well developed. The maxima occur in May and November, during the change of the monsoons when the wind velocities are lowest. The minima of the temperature occur together with the full development of both monsoons in August and February.

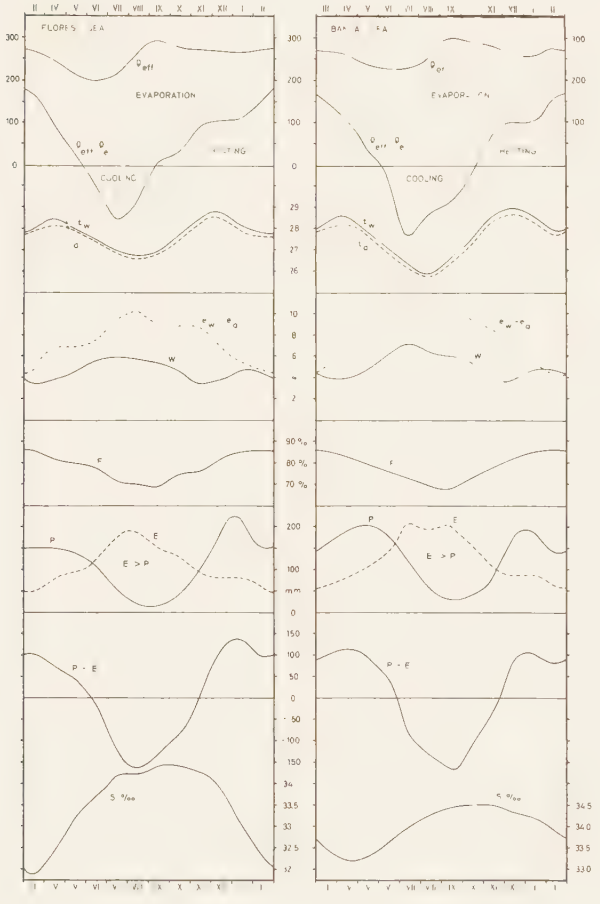

Fig. 5·3. Average annual variation of climatological factors in the Flores Sea and in the Banda Sea. For explanation of symbols see figure 5·1.

In the **Flores Sea** a similar annual variation of temperature exists, but the cooling during the southeast monsoon is stronger, fig. 5 · 3. During four months evaporation exceeds rainfall, and is chiefly caused by the small relative humidity. The energy balance shows from June to August an excess of the energy used for evaporation over the effective radiation. This amounts to 7500 cal/cm² and is sufficient to cool a homogeneous layer of 40 m by 2°C, this is in agreement with the observations. From September the temperature rises again and the maximum is reached in December. At the time of the full development of the west monsoon over the Flores Sea in January the temperature drops again in spite of the positive energy balance during this time.

This cooling effect in the Flores Sea may be interpreted as a vertical extension of the homogeneous layer due to the increase of the wind velocity during the west monsoon. If the homogeneous layer is deepened by mixing, the average temperature must decrease. But to show this requires a detailed knowledge of the variation of the thermal structure of the water masses during the year, which cannot yet be given.

In the Banda Sea the conditions are similar to those in the Flores Sea, but the excess of evaporation and the cooling during the southeast monsoon are stronger. The maxima of the surface temperature occur in April and December about at the time of the change of the monsoons, fig. 5 · 3.

The **Arafura** and the **Timor Seas** are closest to the region of origin of the southeast monsoon, and are most strongly influenced by its dry cool air masses. The wind velocity over these

open seas is high and the humidity of the offshore winds is low, causing extremely high values of evaporation, fig. 5 · 4. But the Atlas of Climatic Charts of the Oceans shows in this region during the whole year depressions of the wet bulb of only 0.5 to 1.0°C, which certainly must be an error during the southeast monsoon season. In the Arafura Sea evaporation exceeds rainfall during five months, in the Timor Sea even during seven months. Maximal values of evaporation of nearly 300 mm/month are reached as a combined effect of strong winds and dry air. In July and August the water temperature is lower than that of the air, which may be due to upwelling. The rainy season in the Timor Sea is short and takes place at the time, when the equatorial trough lies over this region. The Arafura Sea has two rainfall maxima occurring when the equatorial trough passes the region, but the secondary minimum between them is only weakly developed.

The energy balance shows two maxima of radiation, which is an effect of the position inside the tropics. The curves of the effective radiation are strongly modified by the cloudiness, which is very small during the southeast monsoon and above 60% during the rainy season. From May to September, when the energy needed for evaporation exceeds the effective radiation, a strong cooling of the water takes place. The required energy during this time is about 27 000 cal/cm², sufficient to cool a 90 m deep layer by 3°C. Figure 7 · 14, in which vertical curves of the temperature in this region are given, shows an

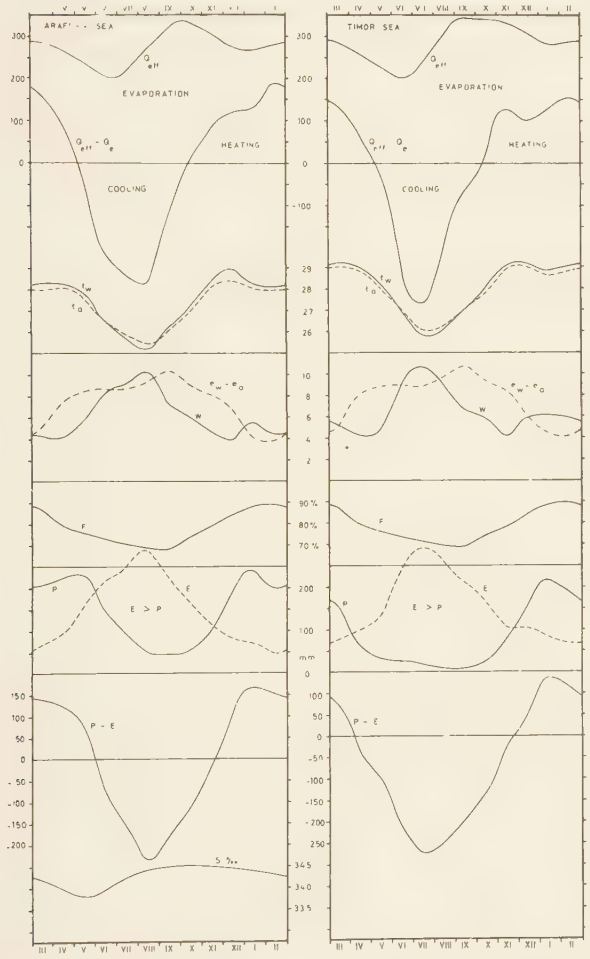

Fig. 5·4. Average annual variation of climatological factors in the Arafura Sea and in the Timor Sea. For explanation of symbols see figure 5·1.

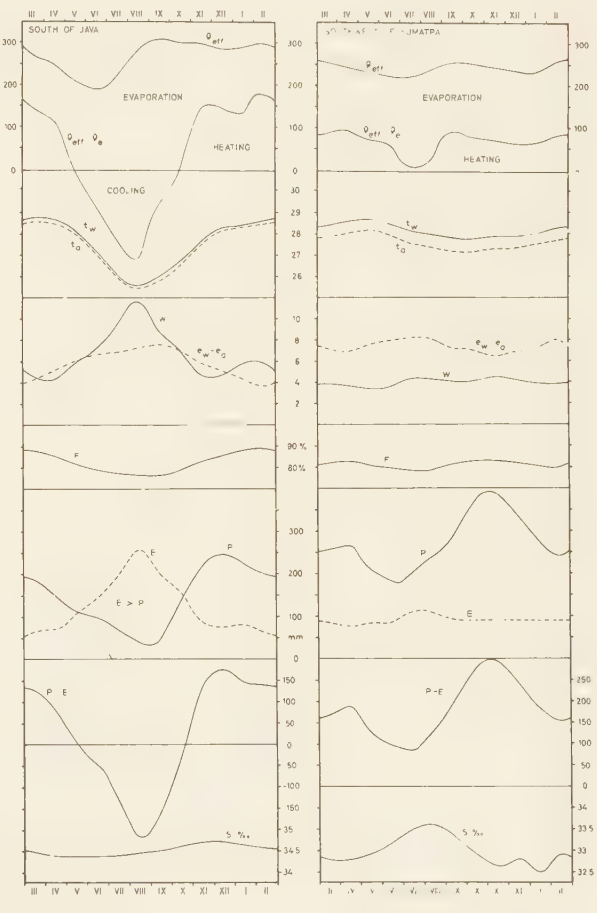

Fig. 5·5. Average annual variation of climatological factors in the regions south of Java and southwest of Sumatra. For explanation of symbols see figure 5·1.

effect of this magnitude. In both regions the energy required for evaporation exceeds the effective radiation in the annual average, this leads to the assumption, that advective processes must be engaged in maintaining the energy balance. This result is to be understood in connection with the upwelling and sinking in this region.

The INDIAN OCEAN south of Java shows qualitatively the same conditions as the other regions in the southeast of the Archipelago, fig. 5 · 5. From May to October it is under the influence of the southeast monsoon, from December to February the equatorial trough lies over the region and brings the rainy season. The highly balanced annual variation of meteorological conditions causes also a smooth run of surface temperature and salinity in this region far from the influence of land. These cycles agree numerically with the calculated values.

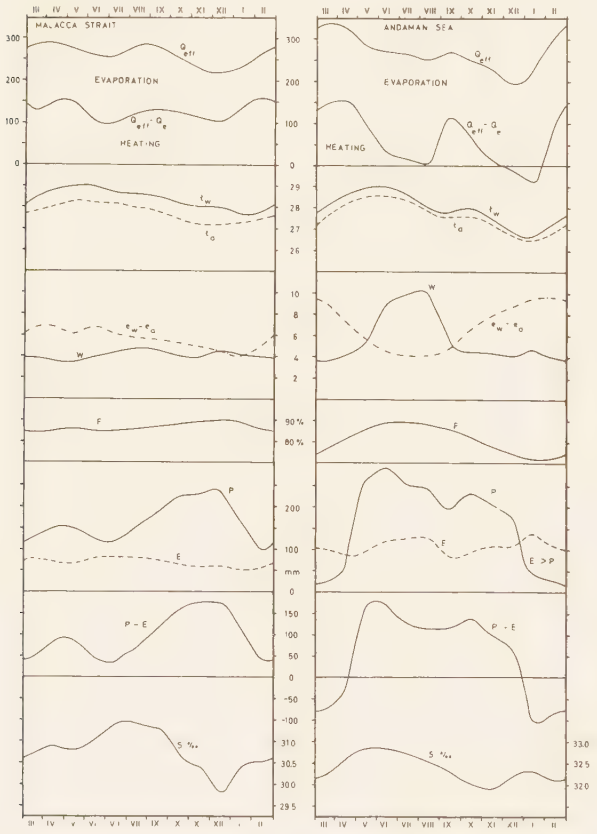

Fig. 5·6. Average annual variation of climatological factors in the Malacca Strait and in the Andaman Sea. For explanation of symbols see figure 5·1.

The region southwest of Sumatra has with 3000 mm/year an extremely high rainfall, which drops in no month below 180 mm, meaning that a really dry season does not exist, fig. 5 · 5. The two periods of especially strong rainfall occur, when the equatorial trough passes the region. During these two periods also the maxima of the relative humidity are found. The curves of wind velocity and of vapour pressure difference show only small variations causing a relatively constant evaporation of about 90 mm/month. An exception is found in July and August, when the southeast monsoon has some influence and the evaporation reaches 110 mm/month.

The energy balance is equalized and throughout the year contributes to the heating of the water. This heat is given off partly to the atmosphere, which follows from the relatively high difference between sea and air temperature. Another part may be transferred by advection horizontally and vertically. The annual variation of the temperature is less than 1°C, an indication of the stability of the conditions.

In the MALACCA STRAIT the conditions are similar, fig. 5 · 6. There also two rainy seasons are found without a really dry season. The relative humidity is extremely high, and because of weak winds the evaporation is small. Only a part of the effective radiation is used for evaporation and so a continuous heating of the water would occur, if advective processes did not transfer the excess heat. It may be useful to estimate the numerical value of this energy transfer. At a horizontal temperature gradient dt/dx of 1°C in 2000 km and a velocity of the current of $v = 25$ cm/sec the heat Q transported in a layer of a depth $D = 40$ m will be $Q = c\,v\,D\,dt/dx$, and numerically 44 cal/cm²/day. Such an amount already has to be considered in the energy balance. Also the difference between sea and air temperatures reaches relatively high values in the Malacca Strait, indicating a large transfer of sensible heat to the atmosphere.

Over the ANDAMAN SEA the regime of the Indian monsoon is first met. It brings from May to November a continuous strong rainy season,

in the other months a nearly rainless dry season, fig. 5 · 6. The evaporation has two weak maxima, one during the dry season, caused by the small relative humidity, the other during the rainy season, when the winds are strongest. Because both factors are counteracting the variation of evaporation is small. In spite of that it exceeds the rainfall considerably during the dry season. The energy balance indicates that the effective radiation normally exceeds the energy used for evaporation. The curve of the surface temperature corresponds to the available energy, during the periods of strongest energy surplus heating takes place, during the periods of maximal evaporation cooling occurs.

Over the SULU SEA an extended rainy season occurs from May to November, but also in the other months the rainfall is high, fig. 5 · 7. The humidity is high and its variation small, while the wind is strongest during the northeast monsoon. In January and February this causes higher values of evaporation, which correspond to low rainfall. The energy balance shows that the effective energy always exceeds the energy required for evaporation, causing a continuous heating of the water and of the atmosphere. In view of the magnitude of the heat surplus horizontal heat transfer must be assumed. The heating of the water occurs from February to May at the time of maximal heat surplus, the cooling from November to January, when the evaporation requires all available energy.

In the CELEBES SEA and in the region north of New Guinea completely equalized conditions are found because of their proximity to the equator, fig. 5 · 7. The rainfall is high and amounts to

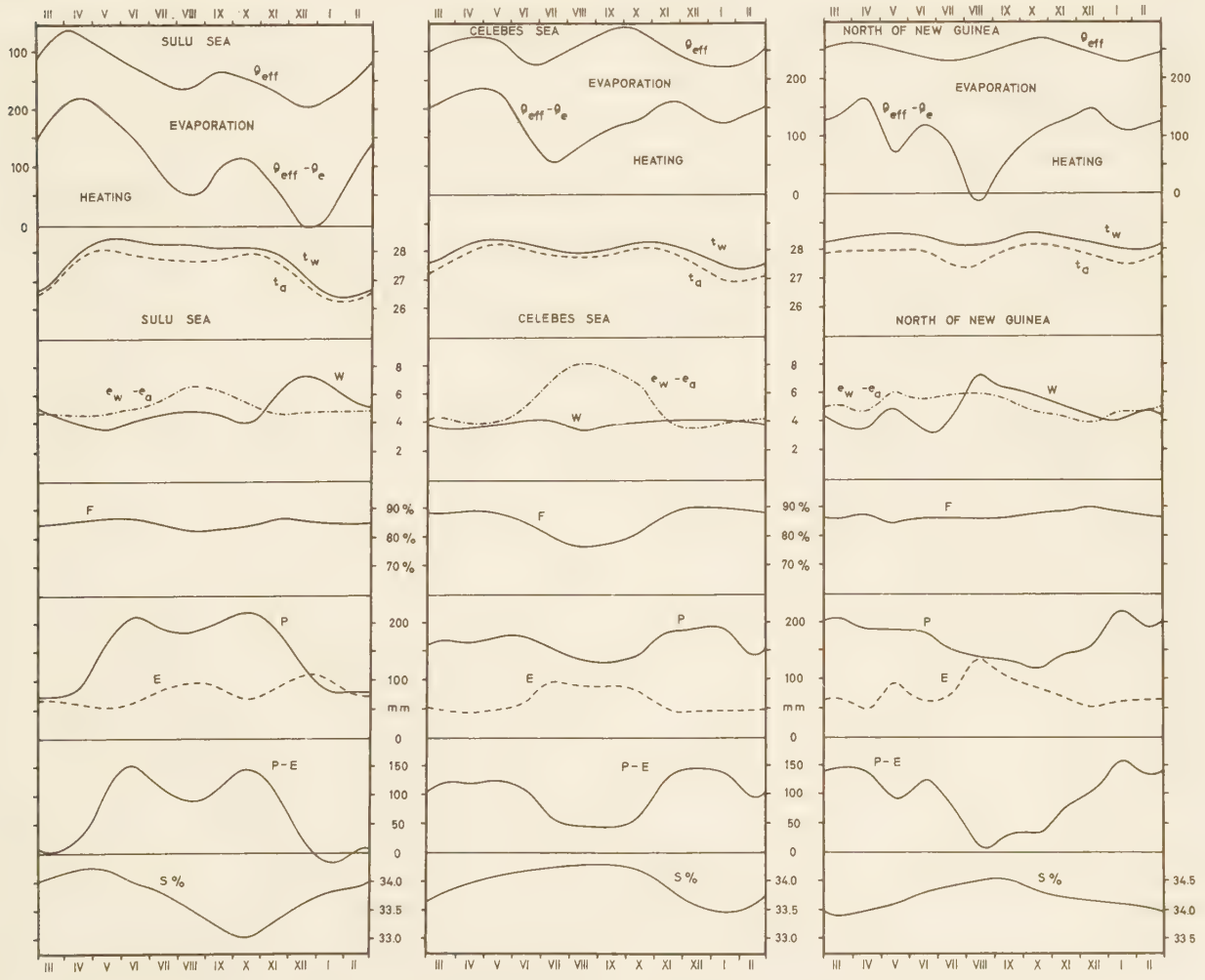

Fig. 5·7. Average annual variation of climatological factors in the Sulu Sea, in the Celebes Sea and in the region north of New Guinea. For explanation of symbols see figure 5·1.

about 150 mm/month throughout the year. Over the Celebes Sea from July to October a branch of the southeast monsoon brings dryer air masses and smaller rainfall and the lower relative humidity causes a higher evaporation. The energy balance indicates, that considerable amounts of heat are available for the heating of the water and of the atmosphere, but the deep homogeneous layer, about 100 m, north of New Guinea, absorbs this energy and the strong currents in this region carry away the heat. The fact that the temperature in this region always exceeds 28°C is indicative of this large heat excess. In the Celebes Sea the temperature drops from January to March below 28°C, indicating a supply of cooler water from the Mindanao Current.

To give an idea of the part played by the different regions of the Southeast Asian Waters in the water and energy balance, the yearly amounts of rainfall, evaporation, of their difference, the total effective radiation, the energy required for evaporation and the energy available for heating processes are given in table 2. The annual amounts of the rainfall, the evaporation and of their difference are repeated in fig. 5·8 at the approximate localities for which the values of the climatic factors were determined. The figure shows clearly the high rainfall and the small evaporation along the equatorial belt and the increase of the evaporation to the north and to the south.

The rainfall differs considerably from region to region and is highest with 300 cm off the coast of Sumatra and lowest with less than 100 cm over the Timor Sea. It is higher in all

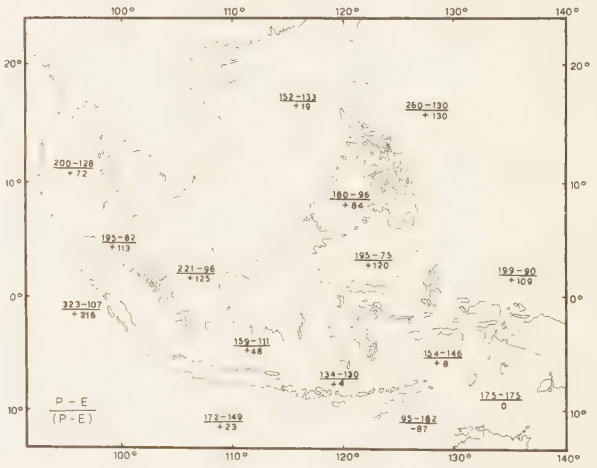

Fig. 5·8. Average annual precipitation P, evaporation E and difference between precipitation and evaporation in different regions of the Southeast Asian Waters.

TABLE 2

Yearly amounts of precipitation P in cm, evaporation E in cm, difference of precipitation and evaporation P - E in cm, average annual total effective radiation Q_{eff} in cal/cm²/day, energy required for evaporation Q_e in cal/cm²/day, energy available for heating processes Q_{eff}-Q_e in cal/cm²/day for different regions of the Southeast Asian Waters.

Region	P	E	P - E	Q_{eff}	Q_e	$Q_{eff} - Q_e$
East of Luzon	260	130	130	259	211	48
Northern China Sea	152	133	19	255	217	38
Southern China Sea	221	96	125	256	156	100
Java Sea	159	111	48	258	181	77
Flores Sea	134	130	4	257	211	46
Banda Sea	154	146	8	264	238	26
Arafura Sea	175	175	0	272	285	—13
Timor Sea	95	182	—87	282	296	—14
South of Java	172	149	23	268	242	26
Southwest of Sumatra	323	107	216	240	174	66
Malacca Strait	195	82	113	261	134	127
Andaman Sea	200	128	72	265	209	56
Sulu Sea	180	96	84	262	155	107
Celebes Sea	195	75	120	251	122	129
North of New Guinea	199	90	109	247	146	101

regions than the zonal averages calculated by Wüst (1954) indicating this monsoon region to be extremely humid. On the other hand the variations of evaporation are smaller; in the equatorial regions evaporation amounts to less than 100 cm, while north and south of this belt higher values are always found. This is why all these regions have a dry season with a high evaporation, see fig. 5·8. With the exception of those over the Arafura and Timor Seas the values of evaporation are between 75 and 150 cm and correspond well to the zonal averages calculated by Wüst (1954), which vary in these latitudes between 113 and 137 cm. Over the Timor Sea even in the annual average an excess of evaporation over rainfall exists. The variation of the effective radiation over this region is very small and not larger than $\pm 8\%$ of the average, but this energy is used quite differently. Table 2 shows that the equatorial regions especially have only a small evaporation and the energy available for heatin processes $(Q_{eff} - Q_e)$ always exceeds 100 cal/cm²/day, and must be transferred by currents, vertical mixing or to the atmosphere. In the other regions this amount of energy is about 50 cal/cm²/day. Over the Timor and the Arafura Seas the energy required for evaporation exceeds even in the annual average the available radiation. These annual values indicate quite clearly, that the Southeast Asian Waters are a source of warm water of low salinity, caused by high rainfall and large amounts of energy available for heating.

LITERATURE

Albrecht, T.

1951. A. Monatskarten des Niederschlages im Indischen und Stillen Ozean.
B. Monatskarten der Verdunstung und des Wasserhaushaltes des Indischen und Stillen Ozeans.
Ber. dtsch. Wetterdienstes. U. S. Zone. No. 29. 39 pp.

Brogmus, W.

1952. Eine Revision des Wasserhaushaltes der Ostsee.
Kieler Meeresforsch. 9(1) : 15-42.

Jacobs, W. C.

1951. The energy exchange between sea and atmosphere and some of its consequences.
Bull. Scripps Instn. Oceanogr. Tech. Ser. 6 (2) : 27-122.

Keyser, H.

1939. Climatologic data on the Pacific.
Proc. 6th. Pacif. Sci. Congr. 3.

Kimball, H.

1928. Amount of solar radiation that reaches the surface of the earth on the land and on the sea.
Mon. Weath. Rev. Wash. 56 : 393-9.

Montgomery, R. B.

1939. Ein Versuch, den vertikalen und seitlichen Austausch in der Tiefe der Sprungschicht im äquatorialen Atlantischen Ozean zu bestimmen.
Ann. Hydrogr. Berl. 67(5) : 244-6.

Schott, G.

1935. Geographie des Indischen und Stillen Ozeans.
Hamburg, C. Boysen. 413 pp.

Sverdrup, H. U., M. W. Johnson, and R. H. Fleming

1942. The oceans, their physics, chemistry and general biology.
New York, Prentice Hall, 1087 pp.

Visser, S. W.

1936. Meteorological observations.
Snellius Exped. 3, 109 pp.

Wüst, G.

1954. Gesetzmässige Wechselbeziehungen zwischen Ozean und Atmosphäre in der zonalen Verteilung von Oberflächensalzgebalt, Verdunstung und Niederschlag.
Arch. Met. Wien. Ser. A 7 : 305-328.

Wyrtki, K.

1956. The rainfall over the Indonesian waters.
Indonesia Lemb. Met. Geofisik Verh. No. 49. 24 pp.

1957. Precipitation, evaporation, and energy exchange on the surface of the Southeast Asian Waters.
Mar. Res. Indonesia No. 3 : 7-40.

ATLASES

U. S. Weather Bureau

1938. Atlas of climatic charts of the oceans.

Netherlands. Meteorologisch Instituut

1936. Oceanographic and meteorological observations in the China Sea.
Publ. 115.

1949. Sea areas round Australia. Oceanographic and meteorological data.
Publ. 124.

U. S. Hydrographic Office

1944. World Atlas of sea surface temperatures.
H. O. No. 225.

CHAPTER 6

THE WATER MASSES IN THE DEPTH

In Southeast Asian Waters light water of low salinity is formed at the surface and the water masses of higher density in and below the discontinuity layer must originate outside the region. Thus, the regions of origin of the Subtropical Lower Water of high salinity, which forms the discontinuity layer, are situated in the trade wind regions, where the highest surface salinities are found. The water masses of lower salinity below them are the last traces of the Intermediate Waters, which sink in the Arctic and Antarctic Polar Fronts, and the water masses in the deep and bottom layers are derived from the Pacific Ocean Deep Water, and are therefore of Antarctic origin. Here again is an example showing that the vertical structure of the ocean near the equator reflects the horizontal distribution of the water masses at the surface in their regions of origin.

The Southeast Asian Waters are moreover so much narrowed by the Sunda and Sahul Shelfs, that only relatively few and narrow passages remain for an exchange of water below the discontinuity layer, and it must be assumed, that this water exchange will be very weak. Extremely slow spreading and lateral mixing processes seem to be the modes of penetration of the different water masses from the adjoining oceans into the Southeast Asian Waters. Below a depth of approximately 1600 m the two oceans are separated and an exchange of waters of the deeper layers is impossible. Consequently the homogeneity of the water masses is the characteristic feature in the numerous large enclosed deep sea basins. These few remarks denote the Southeast Asian Waters as a region in whose depth the last traces of the water masses present in the two adjoining oceans are intermixed. Therefore it is advisable to investigate first the properties of the water masses and their structure in the adjacent parts of the Indian and the Pacific Oceans, and then the conditions in the Southeast Asian Waters.

The observations in this region date from a number of expeditions, which have worked in these waters for rather different purposes, and often hydrographic observations were only of minor importance. This is especially valid for the more biological expeditions at the beginning of the century. In table 3 only those expeditions are listed, whose oceanographic observations have been used for an analysis of the water masses in this region. Stations over the shelf, with observations only above the discontinuity layer, are not included. The observations of the Dana are of special value, because they include complete series of oxygen determinations at all stations, while the bulk of the oxygen data of the Snellius Expedition were only published, after this study had been completed (Postma, 1959). The Japanese research vessels, on the other hand, did not take oxygen samples, so that the Dana observations are the only data on oxygen in large parts of the region. The stations of the Siboela go down only to 250 m depth and also do not include oxygen determinations.

TABLE 3

Oceanographic stations in the Southeast Asian Waters and in the adjoining parts of the Indian and Pacific Oceans used in this chapter.

Vessel and Source	Year	Indian Ocean	Southeast Asian Waters	Pacific Ocean	Sum
		Number of Stations			
PLANET Reichmarineamt, 1909	1906-07	3	1	3	7
DANA Thomsen, 1937	1929	35	56	14	105
SNELLIUS van Riehl, Hamaker, van Eyck, 1950 van Riehl, 1932	1929-30	11	327	12	350
KATURIKI	1936				
KOSYU	1936				
SOYO-MARU	1939				
TAKUNAN-MARU	1939				
KOMAHASI Japanese Hydrographic Bulletin 1950-55	1941	—	36	279	315
ALBATROSS Bruneau, Jerlov, Koczy, 1953	1948	12	2	1	15
SIBOELA Wyrtki, 1956	1949	—	42	15	57
SPENCER F. BAIRD not yet published, received by courtesy of Scripps Institution	1947-50	—	—	44	44
GALATHEA not yet published, received by courtesy of Dr. A. F. Bruun	1951	1	4	—	5
SAMUDERA Wyrtki, 1956, 1957	1956-57	7	46	—	53
	Total	69	514	368	951

The observations of the SPENCER F. BAIRD to the east of the Philippines have been placed at my disposal by the courtesy of the Scripps Institution of Oceanography. The SAMUDERA worked oceanographic stations in 1956/7 in the Eastern Archipelago, especially to complete in other seasons the observations of the SNELLIUS.

This material from approximately 1000 hydrographic stations covers the area under investigation so unequally however, that in many cases it is not even possible to get information about the annual variations of temperature and salinity within the range of the discontinuity layer. Much more scanty are the observations of the oxygen content and a presentation of the distribution of phosphate and other components is practically impossible.

The core layer method as developed by Wüst (1935) when discussing the water masses of the Atlantic Ocean, has been used for the analysis of the observations in this region. This method makes it possible to follow the spreading and mixing of a water type, which is characterized by its temperature, salinity or oxygen content. Normally for such an analysis the maxima and minima of a property are used, these are named

core layers and their spreading can be shown in charts. Core layers, however, are not necessarily identical with the centre of a flowing water mass, as shown by Thorade (1931), because the mixing and the conditions along the boundaries are also of importance. But in the case of pure mixing, the core layer is the central part of the water mass, which is least influenced by mixing, and where the original properties of the water mass are best maintained.

Although the core layer is theoretically a surface only, it is practically the centre of a water mass, having a certain extension upwards and downwards, so that it occupies a certain space on both sides of the core layer. This interpretation of the core layer allows water masses to be followed as extensive bodies from their region of origin until they disappear. It has an advantage over the Central Waters as defined by Sverdrup (1946) because it is also a dynamical unit. Central Waters are from the beginning mixing products and fill the space between two core layers and therefore they participate in the movements of two water bodies, which are normally different.

For the processing of the data the vertical curves of temperature, salinity and oxygen content as well as their TS and TO_2 diagrams have been drawn for each station. These curves allow the interpolation of the values of T, S and O_2 within the S and O_2 maxima and minima, which serve as indications of the different core layers. Then from the vertical curves the depth of the core layer can be taken. The T-S-O_2 values within the different core layers are combined to TS and TO_2 diagrams and are also presented in charts of the properties within the core layers, plates 16-37. In these charts the individual stations are indicated by dots, except in the Eastern Archipelago, in the area worked by the SNELLIUS Expedition, where they were too numerous to be plotted. In the charts of the oxygen content the numerical values at the individual stations are given. In the charts of the depth of the core layers the stations are not entered, because when constructing these charts a smoothing of the highly scattered values was necessary.

It seems appropriate at this point to discuss the normal fluctuations of the properties and the reliability of the charts presented. The standard deviations of the different observed properties have already been discussed in detail by van Riehl (1943), and in the upper layers the main influences result from internal waves and tides as well as from annual variation. But the error due to internal waves is eliminated automatically by the use of the core layer method, because this method is independent of the depth of observation. In a presentation of the depth of the core layer the fluctuations due to vertical movements appear, and must be smoothed out. In the deep layers, on the other hand, the errors due to the inaccuracy of the observations are more important.

The range of fluctuations of properties can be gauged from the repeated series at anchor stations. Thus the observations at anchor stations Sn 135a and Sn 253a when plotted as a TS diagram, where the depth is eliminated, show that the fluctuations of the salinity at all depths between 100 and 800 m are relatively constant at 0.06‰. This value is greater than the error of the salinity determination, so that natural fluctuations of the salinity must be responsible. Consequently, a presentation of the isohalines with an interval of 0.1‰ is in all cases justified and seems to reflect the conditions truly. But also in deeper layers and in the deep sea basins the observations show fluctuations of $\pm$ 0.02 to 0.03‰, which cannot be explained by errors of the salinity determination only.

Faulty determinations of salinity appear at the first SNELLIUS stations in the Macassar Strait and especially at the anchor station 39a, where a number of too low salinities appear in the series, these are often more than 0.2‰ below the average of all other observations in the same depth. It is likely that poorly closing water bottles at the beginning of the expedition are the reason, because such values do not occur later.

6·1 THE WATER MASSES IN THE DEPTH OF THE NORTHEASTERN INDIAN OCEAN

As the Indian Ocean is closed in the north by the land masses of Asia, only water masses of the southern hemisphere and of equatorial regions occur, but it has two adjacent seas, the Red Sea and the Persian Gulf, where water of high salinity is formed; this has considerable influence on the hydrographic conditions in the intermediate layers of the Indian Ocean.

In this book attention has been concentrated on the characteristics of the water masses of only the northeast Indian Ocean, thus restricting discussion to the Andaman Sea and the region off the islands of Sumatra and Java, that is roughly the area northeast of a line running from Australia through the Cocos Islands to Ceylon. In this region a large number of stations of the DANA and of the ALBATROSS are available, as well as some stations of the PLANET, the SNELLIUS and the SAMUDERA. From nearly all of these stations observations of oxygen content are available, so that a detailed study of the oxygen maxima and minima was possible. The deep circulation of the Indian Ocean based on older material has already been discussed by Möller (1929, 1933), Schott (1926, 1935), Thomsen (1933, 1935) and Wüst (1935).

The general vertical structure of the water masses in this region may be seen in the vertical curves (fig. 6·1) for A 205 in 5°S and 88°E where for clearer demonstration a logarithmic scale has been used for the depth. Below the shallow homogeneous layer the temperature and the oxygen content decrease rapidly within the discontinuity layer, while the salinity reaches a maximum at 75m depth, indicating the core layer of the Subtropical Lower Water. Still within the discontinuity layer a salinity minimum and an oxygen minimum follow, below these the decrease of temperature becomes slower, and at about 300 m depth a weak salinity maximum is found together with an oxygen maximum, indicating that this water mass originates from the surface. Below it at about 400 m depth an

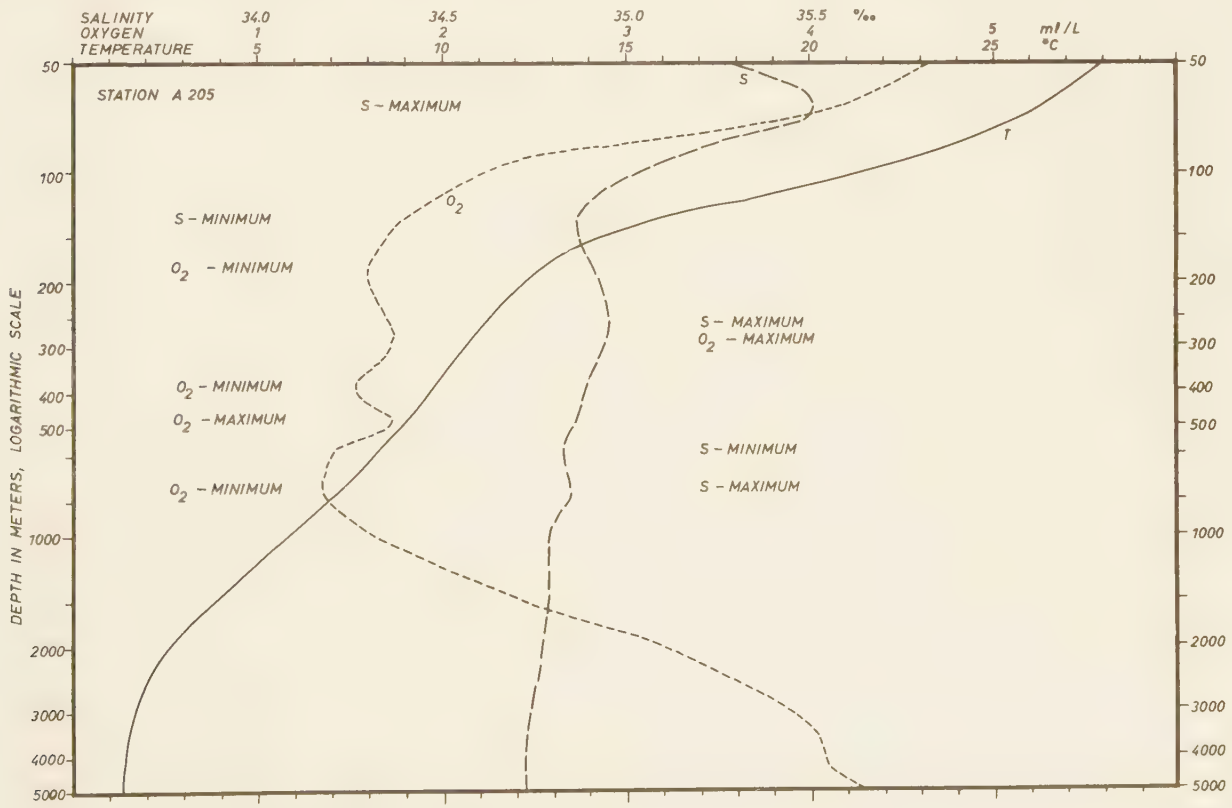

Fig. 6·1. Vertical distribution of temperature, salinity and oxygen content at ALBATROSS station 205, typical for the northeastern Indian Ocean. Depth scale logarithmic.

oxygen minimum is situated, followed by an oxygen maximum and a salinity minimum between 500 and 600 m depth. This salinity minimum is the last trace of the Intermediate Water sinking along the Antarctic Polar Front. At about 800 m depth occurs a salinity maximum with an oxygen minimum, indicating the flow of Red Sea Water of high salinity. From here down, the oxygen content increases continuously from 1000 to 3500 m depth, while the temperature decreases further. The salinity decreases from 34.79‰ in 1500 m gradually to 34.72‰ in 4500 m depth. From 3500 m depth the temperature is practically constant. This vertical structure of the water masses may be taken as typical for the northeastern Indian Ocean, though not all water types will be found everywhere.

An analysis of the water masses is made based on the TS and TO_2 diagrams of the core layers, fig. 6·2. The envelopes of all TS and TO_2 curves are also entered into the figure. They demonstrate that below the discontinuity layer, where the salinity maximum causes large variations of the salinity, the variations are small and decrease with increasing depth. The layer of low oxygen content between 200 and 1000 m depth appears also clearly and in some places the oxygen content becomes almost zero. Below a temperature of 4°C the oxygen content increases again and the variation of the salinity becomes extremely small, indicating the homogeneity of the Deep Water. In order not to overcrowd the presentation the intermediate layer between 14° and 7°C is presented separately in fig. 6·4.

The Subtropical Lower Water with a salinity maximum in its core spreads within the discontinuity layer. As it is immediately below the surface layer, it participates in the surface circulation. These movements may be recognized from the distribution of salinity in the core layer of the Lower Water, plate 16, where two tongues of high salinity spread eastwards. The tongue situated in 5°S seems to correspond with the Counter Current, which occupies this position in

Fig. 6·2. Temperature-salinity and temperature-oxygen diagram of the different core layers of the water masses in the northeastern Indian Ocean together with envelopes of the T-S and T-O_2 curves. For the intermediate layer see figure 6·4.

February, and the northern tongue corresponds to its former position in December, see plates 1 and 6. But during this time the axis of the Counter Current moves quickly to the south, see fig. 3 · 1, and between the two salinity maxima a small strip with lower salinities is found, which seems to indicate a divergence of the currents. The tongue of high salinity reaches Sumatra at about 4°S and is deflected to the south. Along the whole south coast of Java up to the islands of Sumba it appears as a salinity maximum. Only at three stations in the vicinity of the Cocos Islands is the salinity maximum lacking. On the other hand the salinity maximum does not penetrate into the Andaman Sea, as shown also by Rao (1956). Because the layer of maximal salinity is chiefly decomposed from above by mixing during its spreading to the east, the maximum of the salinity comes to lie always at lower temperatures, fig. 6 · 2. In the range of the Counter Current the salinity maximum is found above 25°C, but east of Java it lies at only 15°C. The oxygen content within the core layer of the Lower Water is about 4.0 ml/L in the range of the Counter Current, but decreases in the direction of the spreading. Along the boundary of the South Equatorial Current it is everywhere below 3.0 ml/L, plate 17. Values below 2.5 ml/L are, in fact, nowhere observed.

The chart of the topography of the salinity maximum, plate 18, shows that it lies almost everywhere above the maximal density gradient, plate 8. It reaches its highest position at the southern boundary of the Counter Current in only 50 m. When approaching the coast of Sumatra it falls to about 100 m and along the edge of the South Equatorial Current at about 10° to 12°S it is found in 150 m depth. South of about 6°S an inversion of the oxygen content is found within the lower water with values up to 0.1 ml/L, plate 19. This inversion indicates that the Lower Water in this region consists of relatively old water masses, whose oxygen content is already considerably lowered. Because the spreading of the Lower Water is closely related to the surface circulation it must be assumed that rather strong annual variations in its distribution will take place, however, these could not be investigated because of the few available stations. Such an investigation of the depth of the surface circulation remains a task for the future.

The region of origin of this water mass must be sought in the Arabian Sea. An extrapolation of the envelope of the TS diagram presented in fig. 6 · 2 towards higher temperatures gives a salinity of 36.3‰ at a temperature of 29°C in the region of origin. According to Schott (1935) such values of surface salinity are observed during the whole year in the Arabian Sea. Using data from ALBATROSS stations, the depth of the salinity maximum can be traced to the west, where it reaches the surface at station A 243 off the Red Sea with a temperature of 28.2°C and a salinity of 36.25‰. These observations indicate the region of origin of the Lower Water; further information will be available when the results of the cruises of the MABAHISS are published.

A salinity minimum is situated directly below the Lower Water; it lies at temperatures between 18° and 12°C and belongs therefore to the range of the discontinuity layer. The salinities in it are between 34.5 and 34.9‰ and increase towards the equator, plate 20. This distribution indicates two different regions of origin, a closer analysis is given by means of a TS diagram fig. 6 · 3. In the Gulf of Bengal the salinity increases very gradually from the surface to a maximum in about 300 m depth at a temperature of 12°C, station Da 3893. In this large scale mixing process water masses of low temperature and relatively low salinity are formed below the surface, and the low oxygen content of this water indicates the slowness of the mixing process. This water mass spreads according to its density below the Lower Water, and station Da 3906 shows the TS relation in the area where the northern upper salinity minimum is found. Due to mixing with the Lower Water, the TS values in the northern upper salinity minimum must be displaced from the curve of station Da 3893 towards higher temperatures and salinities, they are indicated by triangles in fig. 6 · 3.

This northern upper salinity minimum, which is also of low oxygen content, spreads with the Monsoon Current in a depth of about 125 m towards the southeast and reaches along the coast of Sumatra to about 5°S, (plates 21, 22), increasing its oxygen content as it spreads. Another branch of the salinity minimum seems to spread south of Ceylon to the west, when the North Equatorial Current is developed. The influence of this water type is not very important because of the small quantities of water formed in vertical mixing processes. But it demonstrates that such processes are possible in principle and that they occur.

For the southern upper salinity minimum another region of origin must be found, and the station Da 3844 at the Cocos Islands gives some indications. At this station, which has no salinity maximum or minimum, the salinity is practically constant from the surface to 400 m depth, so that only a stratification with respect to the temperature exists. These conditions seem to be typical for the whole region between the Cocos Islands and the northwest coast of Australia, where the South Equatorial Current is formed, but there are no oceanographic stations from this region.* This water mass penetrates from

*Oceanographic stations worked in 1959 by HMAS DIAMANTINA on Cruise Dm 2/59 in this region confirm this assumption (CSIRO Aust. 1961).

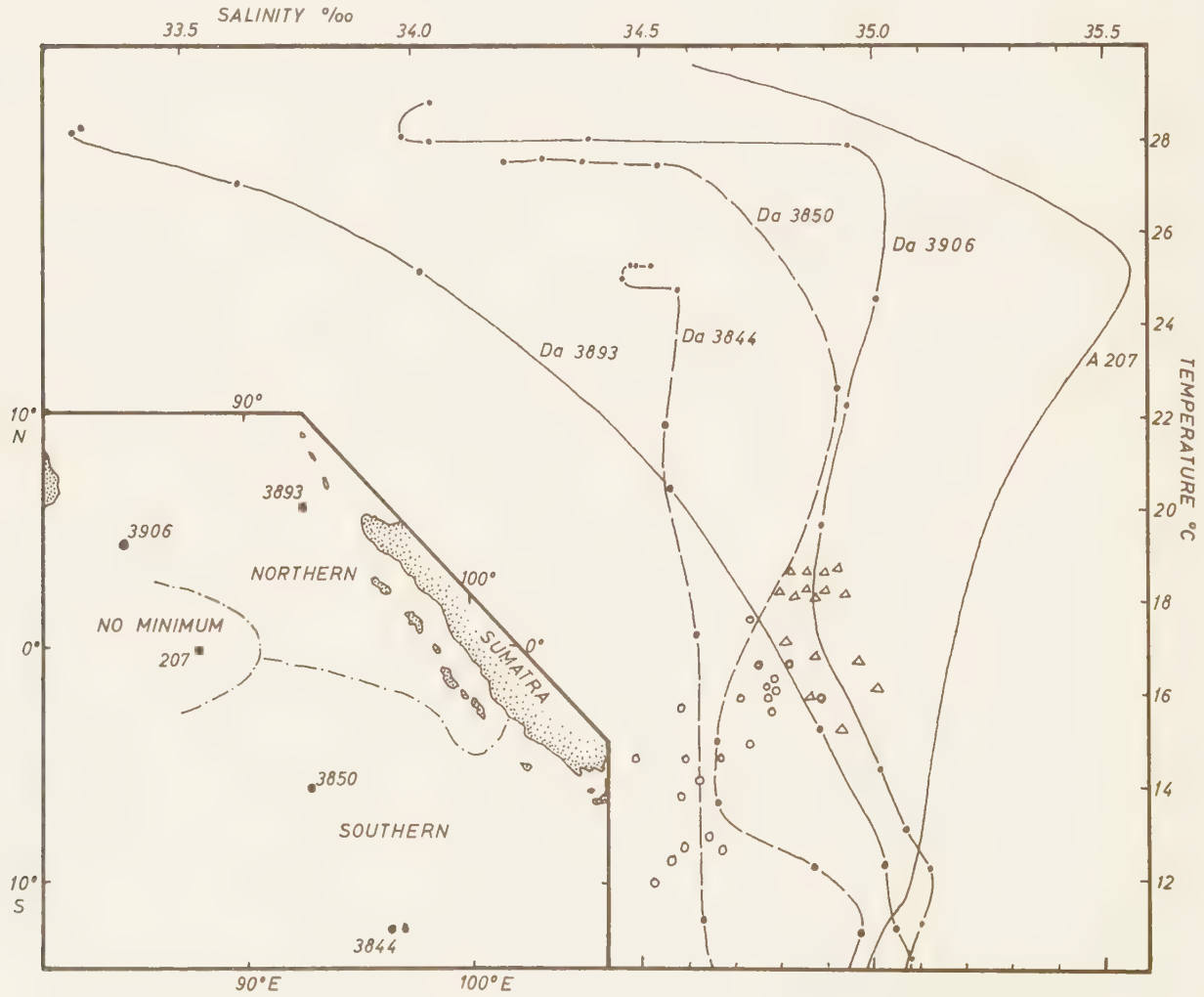

Fig. 6-3. Temperature-salinity diagram of five stations in the northeastern Indian Ocean and T-S values in the northern (Δ) and southern (O) salinity minimum, explaining the origin of the two salinity minima. Inset map shows positions of the stations and distribution of the two salinity minima.

the South Equatorial Current towards the north, but this may occur rather by mixing than by a direct flow. The station Da 3850 demonstrates the hydrographic conditions in the range of the spreading of the southern upper salinity minimum.

Above and below the salinity minimum, water masses of higher salinity are situated and increase the salinity of the minimum by mixing. The oxygen content in the southern upper salinity minimum decreases rapidly in the direction of the spreading; in the range of the South Equatorial Current it is about 2.5 ml/L, plate 21. The core layer of the salinity minimum ascends northwards from 250 to 150 m depth, plate 22, in parallel with the decreasing depth of the South Equatorial Current. But exact conclusions about the origin of this water type can be made only when hydrographic stations are available from the region where the South Equatorial Current is formed.

An oxygen minimum develops in the Gulf of Bengal in depths between 250 and 300 m and reaches, with its last branches, over the equator to about 8°S, plates 23 and 24. The core layer of this upper oxygen minimum rises towards the equator to about 150 m depth, while the oxygen content increases to 1.4 ml/L. South of the equator it descends again to about 200 m depth, but the oxygen content increases further. Clearly visible is a branch of lower oxygen content, which extends along the coast of Sumatra towards the southeast and corresponds to the extension of the northern upper salinity minimum. A strong parallel can be seen between the spreading of the two water masses, but the oxygen minimum lies clearly deeper, at lower temperatures, as shown in fig. 6 · 2, and extends further to the south than the northern upper salinity minimum, as shown in plates 21 and 23. In the range of the South Equatorial Current no oxygen minimum is found in this depth.

The upper salinity maximum spreads tongue-like south of Ceylon eastwards and turns towards southeast, when reaching the coast of Sumatra. The salinity in the centre of the tongue exceeds 35.1‰, plate 25a, but towards the south it decreases gradually to less than 34.8‰. The core layer of the salinity maximum is of relatively high oxygen content, but the highest values are reached along the right flank of the tongue, plate 25b. This distribution is related to the spreading of the upper oxygen maximum, which is discussed later. The TS relations of different stations presented in fig. 6 · 5, show such a maximum at all stations east of Ceylon, while at station Da 3915 the salinity decreases continuously with the depth, but has higher values in all depths than the other stations. The density in the salinity maximum increases from 26.5 at station A 208 to 27.0 in the direction of the spreading to the east. Also the temperature falls in this direction from 14°C to about 8°C. The topography of the core layer of the upper salinity

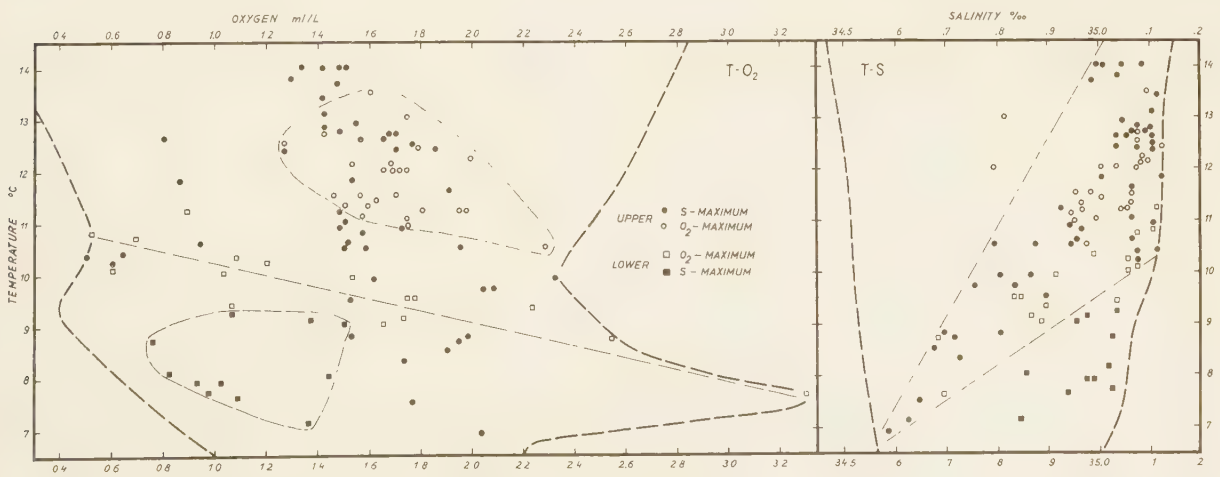

Fig. 6·4. Temperature-salinity and temperature-oxygen diagram of the intermediate layer in the Indian Ocean together with envelopes of the T-S and T-O_2 curves.

maximum, plate 26a, shows its highest position in the vicinity of the equator, where it comes to within less than 200 m of the surface. To the north and to the south the core layer descends to more than 400 m depth.

An oxygen maximum is closely related to the upper salinity maximum and in the TSO_2 diagram the dots of the two water types cannot be separated, fig. 6·4, although the two maxima do not coincide at the individual stations. The tongue of the maximal oxygen content lies south of the tongue of maximal salinity, plate 26b. It spreads from west to east at about 3°S and may be a deep going influence of the Counter Current. Towards the north and the south the oxygen content decreases rapidly until the maximum is no longer distinguishable from the water masses above and below it. Thus, this maximum is restricted to a relatively narrow band along both sides of the equator between 4°N and 5 to 10°S. The core layer of the upper oxygen maximum lies in depths between 200 and 300 m, penetrating the core layer of the upper salinity maximum.

Because of this close relation between the core layers of the upper salinity and the upper oxygen maximum it is necessary to consider the two core layers as only one water type. This water mass of high salinity and high oxygen content must originate at the surface. Because the Subtropical Lower Water is formed in the Arabian Sea, and the water of the Red Sea has a higher density, this water type can originate only from the Persian Gulf and the northern parts of the Arabian Sea. A reliable answer to this question, however, can come only from investigations in that region.

The lower oxygen maximum is situated between 400 and 500 m, but is not noticeable as a maximum over the whole region, plate 27a. Beyond the limits in which it appears as a maximum the oxygen content in 500 m depth is given. The oxygen content decreases rapidly from 3.0 ml/L at about 10°S to less than 2.0 ml/L and then more gradually towards north, till it reaches values of less than 1.0 ml/L in the Gulf of Bengal. This oxygen maximum is related to an intermediate minimum of salinity, but this does not appear clearly from the TS-curves for most stations, fig. 6·5. The combination of low salinity and high oxygen content in these depths is typical of the Antarctic Intermediate Water, which, as shown by a comparison with Schott's (1926) longitudinal section, appears in this region in its last traces. This Antarctic Intermediate Water, which sinks in the Antarctic Polar Front, spreads at a depth of about 1000 m to the north and, when approaching the equator, rises towards 500 m depth. Simultaneously with

Fig. 6·5. Temperature-salinity curves of different stations in the northeastern Indian Ocean demonstrating the positions of the upper salinity maximum (Persian Gulf Water) and the lower salinity maximum (Red Sea Water). Inset map gives the localities of the stations.

the decrease of the oxygen content an increase of its temperature occurs within the oxygen maximum, fig. 6 · 4, both effects are due to mixing. In the TO_2 diagram it is also clear that this water mass is distinguishable from all others.

The lower salinity maximum is not pronounced in the northeastern Indian Ocean, often not even appearing as a maximum. The TS-curves at different stations (fig. 6 · 5) show this; at some stations, Da 3830, A 205, A 200, the maximum is clearly visible, at other stations Da 3915, A 208, the upwards increase of the salinity is so rapid that no maximum appears, but only a break in the curve. These maxima or breaks in the TS-curves are situated at a density between 27 · 2 and 27 · 4 and are clearly distinguished from the upper salinity maximum. The salinity in the core layer of the lower salinity maximum is given in plate 27b and it is indicated whether the values correspond to a real maximum or only to a break in the curves. The spreading of the core layer shows the highest salinities of above 35.0‰ in the north of the region, and a weak tongue of higher salinity extending towards the southeast off the coast of Sumatra. The salinity decreases steadily to the south, values below 34.85‰ appear in no case as a maximum. The core layer of the lower salinity maximum lies between 600 and 800 m depth. As shown in fig. 6 · 4, the lower salinity maximum is distinguished from the upper salinity maximum by its lower temperature as well as by a lower oxygen content.

The low values of the oxygen content within the lower salinity maximum belong to a layer of minimal oxygen content. The TO_2 and the TS values of this lower oxygen minimum are shown in fig. 6 · 2, and are presented again separately in fig. 6 · 6, together with the values of the lower salinity maximum. It is clearly visible that the two groups of values coincide. A decrease of salinity corresponds to an increase of oxygen content and to a decrease of temperature. This means that this water type is at its origin relatively warm, of high salinity and of low oxygen content in contrast to the upper salinity maximum, which is of high oxygen content. It originates in the Red Sea and, after passing the sill it has a temperature of 13°C, a salinity of 36.7‰, and a very low oxygen content (station A 244, 660 m depth). The density of this water is 27 · 3, exactly the same as the values found in the northeastern Indian Ocean. The TS-curve of the station A 240 (fig. 6 · 5) demonstrates clearly the origin of this water mass from the Red Sea.

The oxygen content of the Red Sea Water in the core layer of the oxygen minimum is given in plate 31. The lowest values are found in the north of the region and west of Ceylon. In the other parts the oxygen content shows a distribution similar to that of the salinity. The values of the oxygen content increase towards south, off the coast of Sumatra the isolines are bent

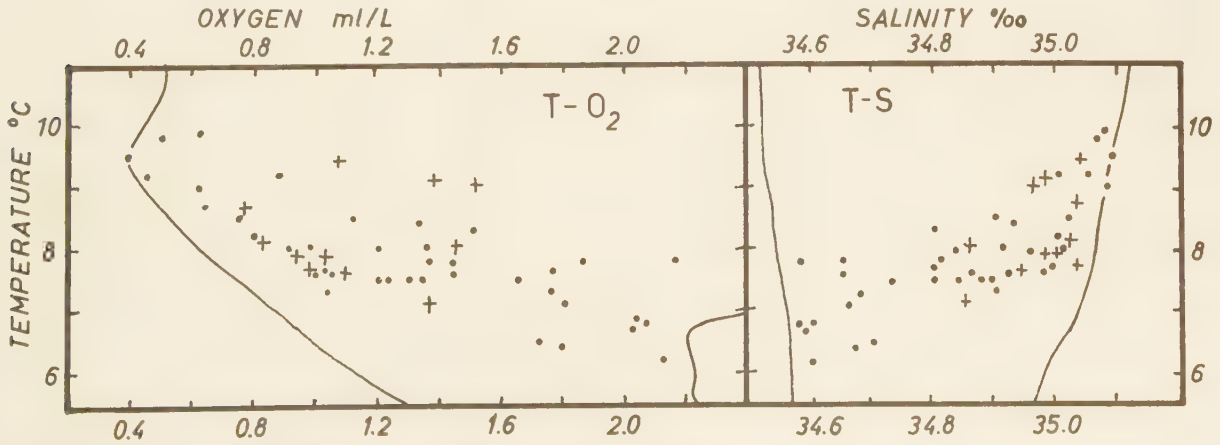

Fig. 6·6. Temperature-salinity and temperature-oxygen diagram of the lower salinity maximum (+) and the lower oxygen minimum (•) in the northeastern Indian Ocean, demonstrating the coincidence of the two core layers, which represent the Red Sea Water.

towards the southeast. The rapid decrease of the oxygen content towards the Gulf of Bengal may be caused by an extremely slow exchange of its water masses in these depths. In the inner parts of the Gulf the water masses seem to be almost stagnant and oxygen may be completely consumed.

The topography of the core layer of the Red Sea Water, plate 32, is, however, in complete contrast to the topographies of the other core layers. The Red Sea Water reaches its deepest position just at the equator with 800 m, while all the higher core layers are curved upwards at the equator. Towards north the core layer ascends to 500 m and towards south more gradually to 600 m.

The lower salinity minimum is found only in the southern part of the region south of 5°S, plate 28. The lowest salinity values of less than 34.6‰ appear south of the Lesser Sunda Islands. Towards the northwest the salinity increases to 34.8°, beyond this value a minimum cannot be recognized. Similarly the oxygen content decreases in this direction, plate 29, probably by mixing with the Red Sea Water. The core of this salinity minimum lies in the whole region at about 1000 m depth. The TS and TO_2 values in the core layer are shown in fig. 6·2, and in more detail together with a SO_2 diagram in fig. 6·7. The minimal values of the salinity and the maximal values of the oxygen content of this water type lie in the region south of the Lesser Sunda Islands and Sverdrup (1946) assumed that this water was of Pacific origin. To demonstate this, some TSO_2 values from stations in the Timor Trench and in the Banda Sea in 1000 m depth are entered in fig. 6·7. It is evident that the TS values are not essentially smaller, but that the oxygen content is higher. Consequently, it is evident that this water mass comes from the Eastern Archipelago and therefore originates from water masses of the Pacific Ocean. Whether however, the whole water mass of the lower salinity minimum is of Pacific origin, remains doubtful, because the last traces of the Antarctic Intermediate Water coming from the south could

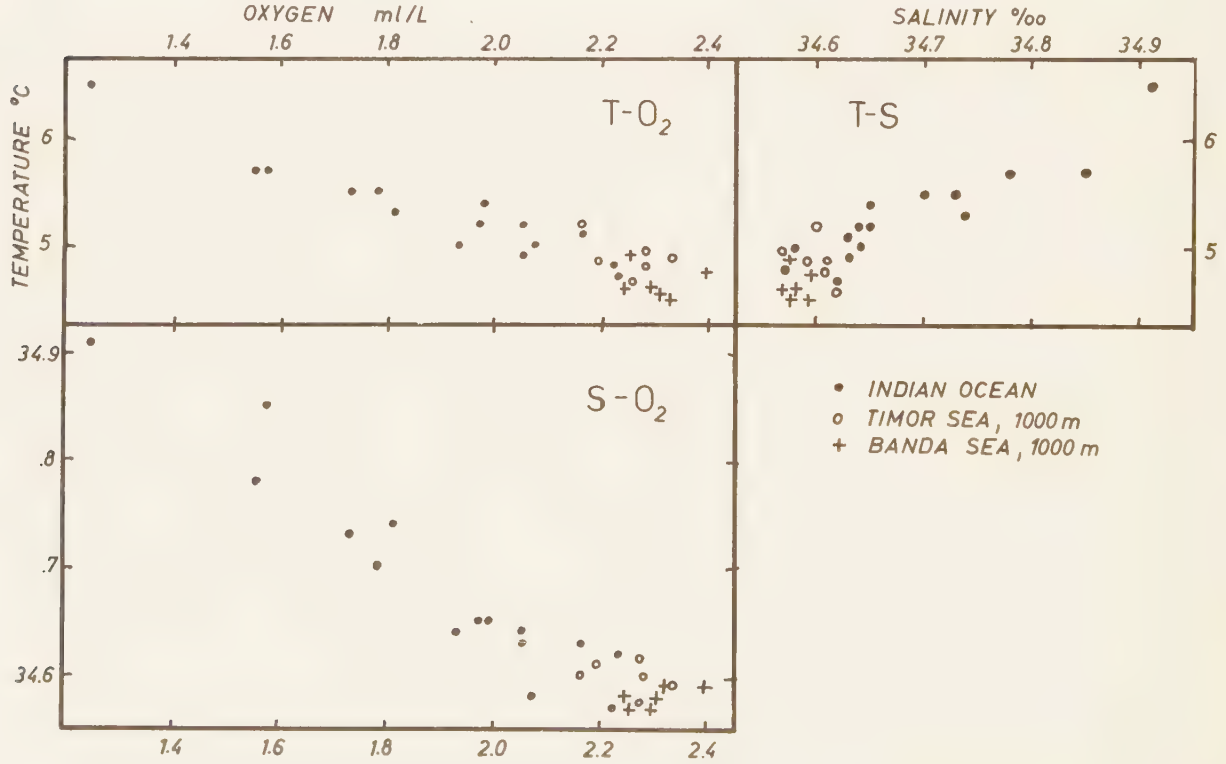

Fig. 6·7. Temperature-salinity, temperature-oxygen and salinity-oxygen diagram of the lower salinity minimum in the northeastern Indian Ocean together with values of temperature, salinity and oxygen content in 1000 meters depth in the Timor Trench and in the Banda Sea.

also contribute to the formation of this salinity minimum. A decision on this question can only come from further hydrographic investigations to the west of Australia. The influence of water from the Eastern Archipelago, however, cannot be denied.

Below a depth of 1000 m the horizontal differences in the salinity of the water become smaller and smaller and converge with decreasing temperature to about 34.72‰ in about 4000 m depth. Fig. 6·8 demonstrates these conditions in a longitudinal section running along the Sunda Trench into the region south of Ceylon. At stations A 190 and A 196 the influence of water of lower salinity with values below 34.7‰ coming from the Eastern Archipelago can be seen. In the western part of the section the Red Sea Water is shown in a depth of 800 m with a salinity above 35.0‰, this decreases only gradually with depth and towards the east. Even in 2000 m depth, salinities above 34.8‰ occur and a tongue with water above 34.75‰ penetrates to the east. Below it is a very homogeneous deep water with salinities of 34.72‰, which extends down to the bottom.

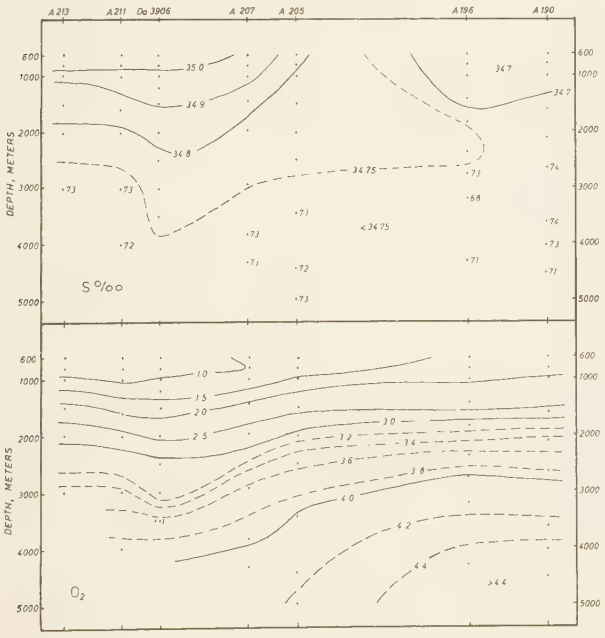

Fig. 6·8. Sections of salinity and oxygen content below 600 meters depth through the deep water of the northeastern Indian Ocean. Position of the section see figure 6·5.

The distribution of the oxygen content in the same section is also shown in fig. 6·8, but the values for the station Da 3906 in 3000 and 3500 m depth seem to be doubtful. In the western part of the section in 800 m depth the layer of minimal oxygen content caused by the Red Sea Water can be seen. Below 1000 m depth the oxygen content increases rapidly, but has always lower values in the west than in the east, especially in the layer between 3000 and 4000 m depth, where water of high oxygen content above 4.0 ml/L penetrates from the east. This deep water has its highest oxygen values of more than 4.6 ml/L just above the bottom. With its northward penetration the oxygen content is reduced considerably, leading to the conclusion that the spreading takes place very slowly.

The temperature decreases from 5° to 6° in 1000 m depth regularly to below 2°C in 2500 m depth. Below this depth only a very small drop to about 1.12°C occurs, corresponding to a potential temperature of 0.75°C, and with this value the temperature minimum is reached in a depth of about 4500 m. The potential temperature of the bottom water, which is between 0.75 and 0.78°C, increases towards the north to about 1.00°C and is an indication of a very slow spreading of the bottom water.

Summarizing, the positions of the core layers of the different water masses in the northeastern Indian Ocean are given in fig. 6·9. The section runs along 88°E from 11°S to 4°N and shows the salinity maximum of the Subtropical Lower Water as the uppermost core layer in depth between 50 and 100 m. Below it in depths of 150 m a salinity minimum is found in the north as well as in the south, which is closely related to the oxygen minimum. This oxygen minimum, however, is everywhere deeper than the salinity minimum and lies between 150 and 200 m. In depths between 200 and 300 m the core layer of the Persian Gulf Water coming from the west is situated. It is of high salinity and high oxygen content. The two core layers do

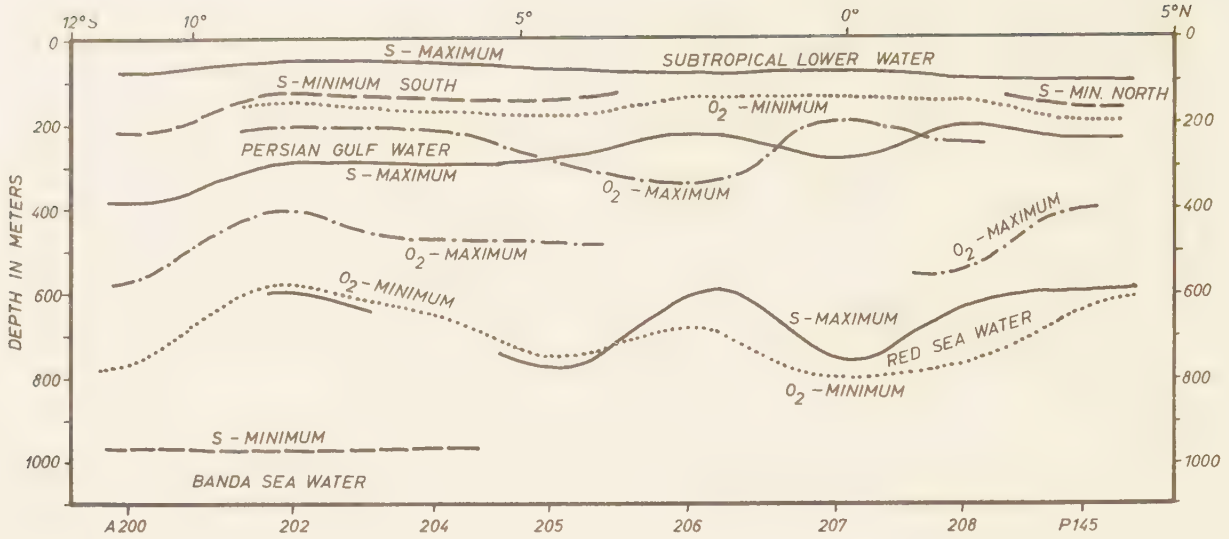

Fig. 6-9. Schematic representation of the position of the core layers of the different water masses in the northeastern Indian Ocean in a section along 88°E between 11°S and 4°N.

not coincide, but intersperse several times. Another oxygen maximum is situated in depths between 400 and 500 m, maximal oxygen values are reached in the south. The core layer of the Red Sea Water is met between 600 and 800 m depth, it is indicated by a salinity maximum and an oxygen minimum, which do not everywhere coincide. The lowest core layer is the salinity minimum, but it is seen in this section only in the southern part. Below this salinity minimum the Deep and Bottom Waters are found, with low temperatures and high oxygen content. Recent cruises of H.M.A.S. DIAMANTINA in the eastern Indian Ocean have confirmed the analysis given here, the data will be published in C.S.I.R.O. Oceanographic Cruise Reports.

These remarks show that in the northeastern Indian Ocean below a highly differentiated layer, only 1000 m thick the almost homogeneous water of the depth begins. It can be assumed, that in this region ascending water movements from the bottom layer to the intermediate layers occur, causing this stratification, which is not so well developed in the other parts of the Indian Ocean. The properties of the different water masses are given in table 4.

TABLE 4

Properties of subsurface water masses in the Northeastern Indian Ocean.

Water Type	Characteristic	T	S	O_2
Subtropical Lower Water	S maximum	16 - 27	34.6-36.0	>2.5
Northern Salinity Minimum	S minimum	16 - 19	34.8-35.0	1.0-2.0
Southern Salinity Minimum	S minimum	12 - 17	34.5-34.8	1.6-2.5
Upper Oxygen Minimum	O_2 minimum	12 - 16	34.8-35.1	<1.6
Persian Gulf Water	S maximum	8 - 14	34.6-35.1	1.0-2.0
$\sigma_t < 27.0$	O_2 maximum	11 - 13	34.9-35.1	1.2-2.2
Lower Oxygen Maximum	O_2 maximum	8 - 11	34.7-35.1	3.2-0.4
Red Sea Water	S maximum	7 - 9	>34.8	0.7-1.4
$\sigma_t = 27.2 - 27.4$	O_2 minimum	6 - 10	34.6-35.0	<2.1
Banda Sea Water	S minimum	4.5 - 6	34.5-34.9	1.3-2.4

6 · 2 THE WATER MASSES IN THE DEPTHS OF THE WESTERN NORTH PACIFIC OCEAN

Unlike the Indian Ocean, where only a small number of oceanographic stations is available, the Pacific Ocean has been extensively explored during the last few years. While the more recent observations are far from being fully evaluated, Sverdrup (1944) has given a picture of the circulation of this ocean based on the work of the CARNEGIE. It shows clearly that, as pointed out by Wüst (1929), the structure of the water masses in the Pacific Ocean compared with that of the other oceans is by far the simplest. There are no seas adjacent to the Pacific with waters of high salinity to influence its deep circulation.

The description of the characteristics of the water masses in the western North Pacific Ocean is confined in this book to the region off New Guinea, the Philippines and Formosa. In this area, a large number of oceanographic stations has been worked by Japanese research ships and the results have been discussed by Koenuma (1937-38-39). Unfortunately no oxygen determinations were made so the analysis of the distribution of oxygen here is based on the stations worked by the DANA in the region north of New Guinea and by the SPENCER F. BAIRD east of the Philippines.

The general vertical structure of the water masses in this region is represented by the station Da 3751, situated to the north of New Guinea at about 4°N and 138°E, at a point where all the different water types appear in the vertical curves, fig. 6 · 10, where for the depth, a logarithmic scale is used. The salinity maximum of the Subtropical Lower Water is situated below the homogeneous layer at the upper boundary of the discontinuity layer. At the lower boundary of this layer of high salinity, a weak oxygen minimum and an oxygen inversion are found. The upper salinity minimum is situated in 300 m depth, accompanied by an oxygen minimum in 400 m. A very pronounced oxygen

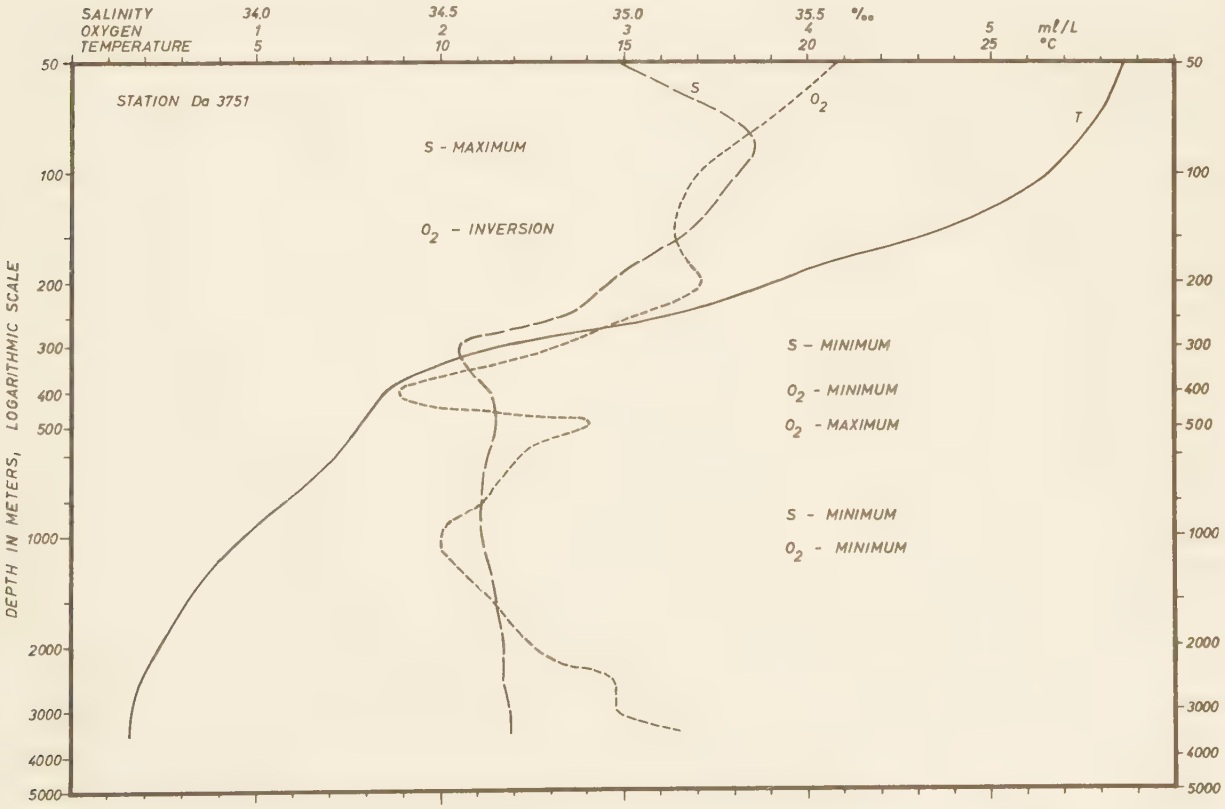

Fig. 6·10. Vertical distribution of temperature, salinity and oxygen content at DANA station 3751, typical for the western equatorial Pacific Ocean. Depth scale logarithmic.

maximum follows in 500 m depth. Considerably deeper, in 900 m, the lower salinity minimum is found, to which the lower oxygen minimum in 1000 m belongs. Below 1200 m depth a gradual increase of salinity and oxygen content takes place and a further decrease of temperature.

The analysis of the water masses by means of the TS and the TO_2 diagram, fig. 6 · 11, is based on the stations of the DANA and the SPENCER F. BAIRD. The envelopes of the TS-curves indicate the presence of less saline surface water, large fluctuations of the salinity in the range of the salinity maximum, the continuous transition to the salinity minima and below them a converging of the salinity towards the values of the bottom water. In the TO_2 diagram, two different series of curves can be seen, indicating the division of the Subtropical Lower Water into a northern and a southern type. The variations of the oxygen content within the range of the salinity and oxygen minima are large. The position of the lower oxygen minimum at about 4°C is clearly indicated even by the envelopes. Below 4°C, the increase of the oxygen content towards the high values of the bottom water takes place.

The Subtropical Lower Water, spreading as a salinity maximum within the discontinuity layer, is the uppermost water type below the homogeneous surface layer. Due to this position, it participates in the movements of the surface layer, which means that it is transported with the South and the North Equatorial Currents. Its regions of origin are situated in the range of the subtropical salinity maxima at the surface, as shown by Wyrtki (1956). The values of the salinity in the core layer of the salinity maximum in plate 16 show water of more than 35.5‰ spreading westwards along the coast of New Guinea with the South Equatorial Current. In about 14°N, another salinity maximum of about 35.2‰ is met, which belongs to the northern Subtropical Lower Water and is carried westwards by the North Equatorial Current. Within the salinity maximum in the range of the Counter Current, much lower values are found, due to a strong mixing and as an indication of the

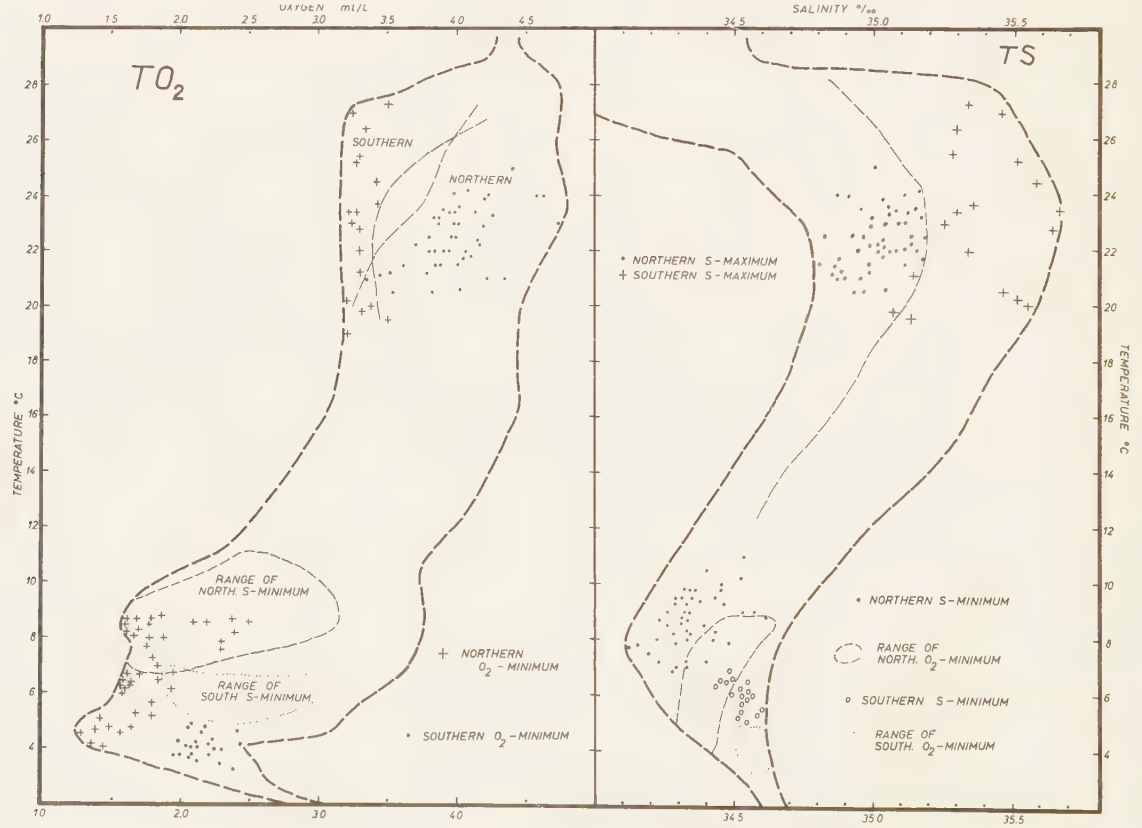

Fig. 6.11. Temperature-salinity and temperature-oxygen diagram of the different core layers of the water masses in the Philippine Sea together with envelopes of the T-S and T-O_2 curves.

position of the boundary between the northern and the southern Subtropical Lower Waters. These findings are in agreement with charts of the salinity maximum drawn by Uda (1957) based on recent Japanese observations.

A simple separation of the two water types is not possible in the TS diagram, but can be effected by means of the oxygen values. The TS, TO_2 and SO_2 diagrams of the core layer of the salinity maximum in fig. 6·12 indicate a clear division into two clouds of dots, when using the oxygen values. The northern Subtropical Lower Water is marked by high oxygen values, combined with relatively low salinities. The southern Subtropical Lower Water, on the other hand, has high salinities at oxygen values of between 3.2 and 3.5 ml/L. This subdivision is also clearly seen in plate 17, which shows the oxygen content in the core layer of the salinity maximum. The boundary between the two water types runs approximately along the axis of the Counter Current in 5°N and turns at 128°E towards the south, where it ends at the island of Halmahera. Naturally the position of this boundary fluctuates in accordance with the rhythm of the annual variation of the circulation.

An indication of such a seasonal effect is given in plate 17, where east of Mindanao the line of 3.8 ml/L oxygen content is curved far to the north. The observations in this region were made in May, and just in the preceding month, the Counter Current is interrupted and an eddy east of Mindanao is developed, formed by the Mindanao Current and a northward flow of water east of it. This surface current pattern is clearly shown in the current chart for April, plate 2, and results in this tongue of lower oxygen content, in which mixing water out of the range of the Counter Current has been transported northwards.

On the basis of the subdivision of the Subtropical Lower Water by means of its oxygen

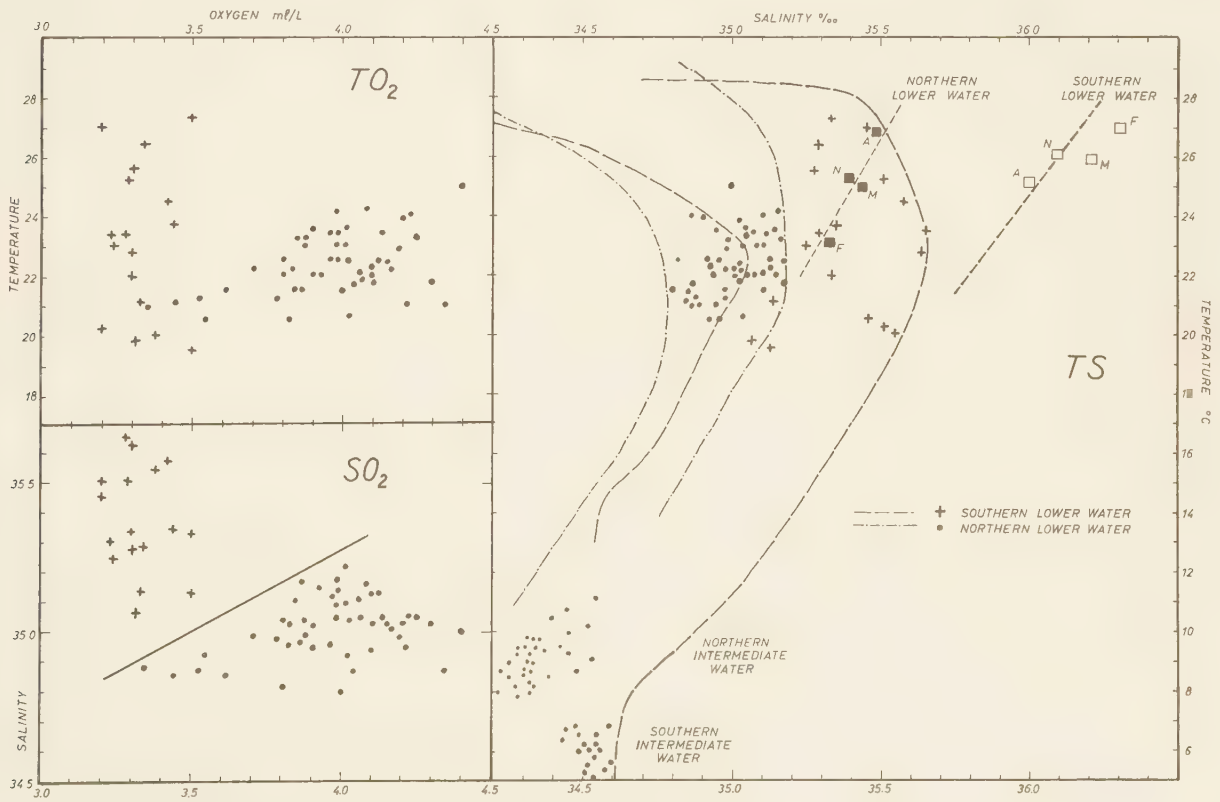

Fig. 6·12. Temperature-salinity, temperature-oxygen and salinity-oxygen diagram of the salinity maximum of the Subtropical Lower Water in the western equatorial Pacific Ocean. The T-S diagram shows envelopes of the T-S curves of the northern —·—·— and of the southern — — — — Subtropical Lower Water and T-S values of the surface water in the regions of origin for the months February, May, August and November (■, □).

content, the dots in the TS diagram can also be split off and the envelopes of the TS-curves of the two Lower Waters can be drawn, fig. 6 · 12. The envelopes of the northern Lower Water, having normally lower salinities, indicate a mixing of three water types: the warm, less saline surface water, the warm, highly saline Subtropical Lower Water, and the cool, less saline Intermediate Water. When extending the branch of the envelopes running from the northern Intermediate Waters to the northern Lower Water, the salinity values in the region of its origin must be found at high temperatures. A comparison of the TS relation at the surface of the North Pacific Ocean shows corresponding TS combinations in the range of the subtropical salinity maximum, as indicated in fig. 6 · 12. Consequently, the region of origin of the northern Subtropical Lower Water must be situated at about 25°N between 165°E and 195°E with salinities of 35.5‰ and temperatures between 24° and 27°C. In the range of the southern Suptropical Lower Water mixing takes place with the southern Intermediate Water. An extension towards high temperatures of the branch of the envelopes connecting the southern Intermediate Water and the southern Lower Water, leads to the TS values in its region of origin. This lies in the South Pacific Ocean between 210°E and 240°E in about 18°S with salinities of about 36.3‰ at temperatures up to 27°C.

The Subtropical Lower Water is always found in the region under consideration in the upper part of the discontinuity layer at temperatures above 20°C, as shown in the TS diagram, and therefore also above the maximal density gradient, plate 8. However, the depth of its core layer fluctuates considerably. The topography of the core layer of the salinity maximum, shown in plate 18, has its deepest positions in the range of the North and South Equatorial Currents, while it rises to less than 100 m in the range of the Counter Current. Its highest position is found in the cyclonic Mindanao Eddy, its lowest in the anticyclonic Halmahera Eddy, in which the South Equatorial Current turns into the Counter Current. Another high position of the core layer of the Lower Water is found at about 20°N and 132°E, where at some stations the salinity maximum is observed even at the surface. In this region the centre of the eddy, in which the North Equatorial Current turns into the Kuroshio, is situated, and also the end of the convergence in which the Subtropical Lower Water is formed, where the salinity maximum must appear at or near the surface.

In the range of the Southern Lower Water, north of New Guinea, and of the northern Lower Water, north of 15°N, an intermediate minimum of oxygen content is found near the maximum of the salinity, causing an oxygen inversion within the Subtropical Lower Water. The magnitude of this inversion and its distribution are shown in plate 19. In some places, it reaches values of more than 0.3 ml/L. it can be assumed that the formation of this inversion is caused more by the annual variation of the circulation, which successively brings water of higher and lower oxygen content into the region, than by consumption of oxygen by biological processes in the vicinity of the maximal density gradient. Processes forming an inversion of properties are discussed in Section 6 · 4 in connection with the explanation of the double salinity maxima. However, a definite decision on this question can only be arrived at by means of investigation of the annual variation of the inversion in relation to that of the water movements.

How important the year to year fluctuations of the salinity in the salinity maximum can be is demonstrated by two charts, based on Japanese observations, fig. 6 · 13. In the chart presenting the conditions during a survey from November 1935 to February 1936, an area with salinities above 35.3‰ is found in the North Equatorial Current, while in April/May 1941 the salinity is just above 35.1‰. Also in the range of the Counter Current, in 1941 the salinity is in large part below 34.8‰, while in 1936 it is above this value. The boundary between the two Lower Waters between 3° and 5°N during the two surveys can be clearly seen. Off the coast of New

Guinea, water above 35.4‰ is always present in the salinity maximum.

The intermediate layer in the Pacific Ocean as a whole normally contains only one salinity and one oxygen minimum. The salinity minimum is formed by the sinking of surface water along the Arctic and Antarctic Polar Fronts, spreading towards the equator according to its density. The oxygen minima originate from consumption processes and are situated below the salinity minima at least in this region. In the equatorial region, the northern and the southern hemispheric salinity and oxygen minima overlap, so that locally two salinity and two oxygen minima are observed. Between them, due to the overlapping, a salinity and an oxygen maximum must be found, as shown in station Da 3751, fig. 6 · 10.

The upper salinity minimum belongs to the North Pacific Ocean, the formation and the spreading of the North Pacific Intermediate Water being described in detail by Sverdrup (1946). A chart of the salinity in the salinity minimum has been drawn by Uda (1958) based on recent Japanese observations. The salinity in the core layer of the salinity minimum shows lowest values in the region east of Formosa, plate 20. Southwards the salinity increases continuously, the southern limit of a recognizable minimum being at about 3°N at values of 34.55‰. A southward curvature of the isohalines is clearly seen off the coast of the Philippines, indicating the flow of the Mindanao Current, which reaches down to these depths. The depth of the core layer of the northern salinity minimum varies considerably, plate 22. It lies off Formosa in more than 600 m depth and rises southwards to less than 300 m along the left flank of the Counter Current. The Intermediate Water is originally of high oxygen content due to its formation at the surface. But owing to its relatively slow spreading and to the high consumption of oxygen below the discontinuity layer, a considerable decrease of the oxygen con-

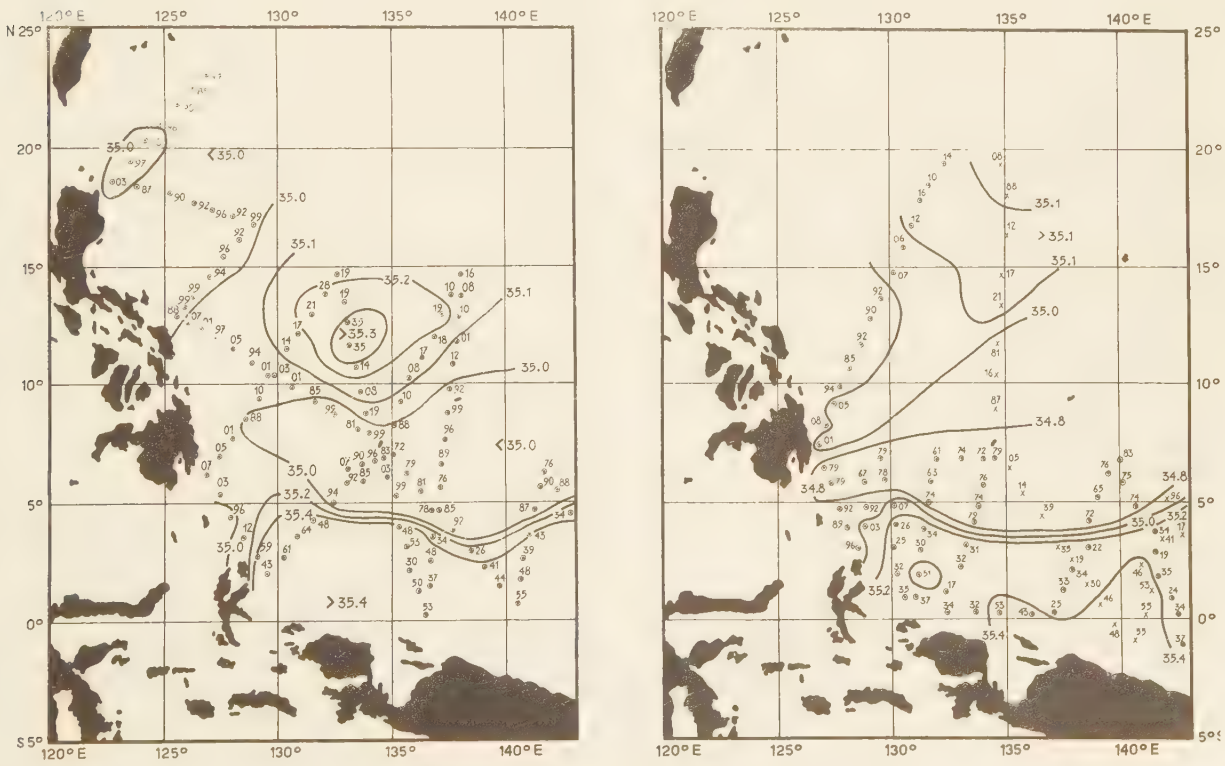

Fig. 6·13. Distribution of salinity in the salinity maximum in the Philippine Sea in different seasons.
Left: November 23, 1935 - February 7, 1936, Japanese survey No. 35.
Right: April 21 - May 11, 1936 (×) and April 22 - May 26, 1941 (O), Japanese surveys Nos. 42 and 68. Figures give 0.01‰.

tent takes place in the direction of its spreading. A chart of the oxygen content in the core layer of the Intermediate Water, plate 21, shows the highest oxygen values off Formosa, together with the lowest salinities, and a general decrease to the south. The variation of the oxygen content in the core layer of the salinity minimum is considerable and very irregular compared with that in the oxygen minimum, situated a little deeper, plate 23. This effect may be partly due to the position of the salinity minimum in the range of decreasing oxygen content, so that slight variations in its depth correspond to large variations in its oxygen content, which is, moreover, not only affected by mixing, but also by consumption.

The variation in the distribution of salinity in the salinity minimum in different years is demonstrated in fig. 6·14, based on Japanese stations. In 1941 the water of less than 34.5‰ reaches further to the south than in the winter of 1935/36. Also the southern limit, to which a minimum can be recognized, fluctuates. In the chart of 1941 a tongue of less saline water may be noted, extending with the Mindanao Current to the south. This tongue explains the temporary observation of extremely low salinities down to 34.2‰ in the salinity minimum below the Counter Current at single stations. These observations seem to be caused by relatively small water bodies with lower salinities, which are transported with the Mindanao Current southwards and pass over into the Counter Current. They are always found in higher levels than normal for the salinity minimum, which explains their rapid movements.

The northern oxygen minimum lies about 100 to 200 m below the salinity minimum, as a comparison of plates 22 and 24 demonstrates. In the TS and TO_2 diagram, fig. 6·11, the clouds of dots representing the two water types overlap partly, indicating a relatively close relation be-

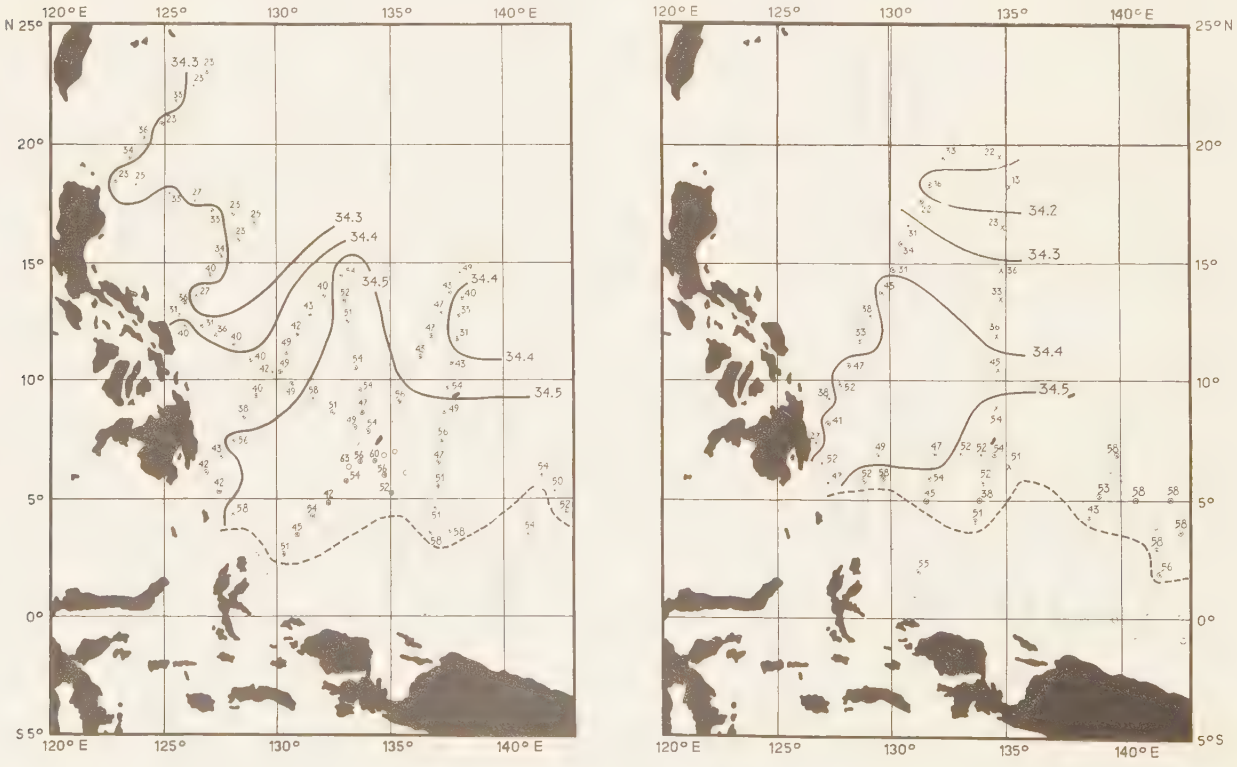

Fig. 6·14. Distribution of salinity in the salinity minimum in the Philippine Sea in different seasons. Left: November 23, 1935 - February 7, 1936, Japanese survey No. 35. Right: April 21 - May 11, 1936 (×) and April 22 - May 26, 1941 (O), Japanese survey Nos. 42 and 68. Figures give 0.01‰. o stations without salinity minimum. — — — — — southern limit of salinity minimum.

tween the salinity and the oxygen minimum. The oxygen values in the oxygen minimum, plate 23, are essentially lower than those in the salinity minimum. The lowest values are found in the north of the region, off the entrance to the China Sea with less than 1.4 ml/L, towards the south they increase to more than 2.4 ml/L. The oxygen minimum reaches southwards nearly to the equator and further to the south than the salinity minimum.

The distribution of properties indicates that the spreading of the oxygen minimum takes place approximately in the same way as that of the salinity minimum, even if essentially slower. So, it can be assumed that the oxygen minimum in this region is associated with the large body of the Intermediate Water with the salinity minimum in its core. The oxygen minimum participates in the movements of the Intermediate Water and forms approximately its lower boundary, although this boundary is not completely motionless. These two water types are clearly differentiated at their formation, low salinity and high oxygen content in the salinity minimum and relatively high salinity and low oxygen content in the oxygen minimum. Later, at this joint spreading, these differences are more and more equalized by mixing and the core layers approach. Near the outer limits of the spreading of these water masses the two core layers often coincide.

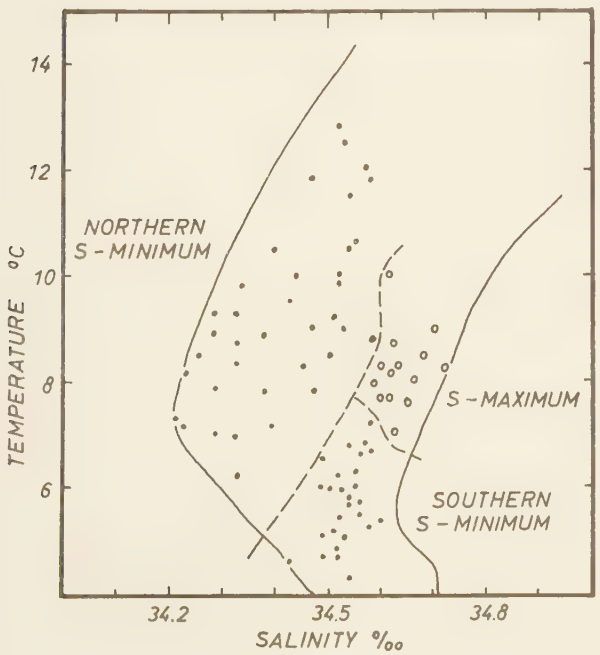

Fig. 6·15. Temperature - salinity diagram for the northern and southern salinity minimum in the Philippine Sea and position of the intermediate salinity maximum.

The lower salinity minimum is the core layer of the Intermediate Water of the South Pacific Ocean. It spreads north of New Guinea towards the northwest in depths between 700 and 900 m, plate 30. The northern limit to which a salinity minimum can be recognized, is in about 10°N, plate 28, the salinities in the minimum are between 34.45 and 34.60‰. But also south of this boundary the salinity minimum is lacking at some stations. Remarkable is the strong decrease of the oxygen content in the core layer in the direction of its spreading, plate 29. North of New Guinea the oxygen content is still 3.0 ml/L and it decreases to less than 2.0 ml/L towards the northwest, this might be due to the very slow spreading of the Intermediate Water. Also here it becomes evident, that the Intermediate Water is at its formation a water mass of high oxygen content.

The lower oxygen minimum is situated between 1000 and 1200 m depth, below the lower salinity minimum, plates 31 and 32. It also seems to extend beyond the limits of the salinity minimum, like the upper oxygen minimum. The oxygen content is very constant between 2.0 and 2.1 ml/L, only north of New Guinea it rises to more than 2.4 ml/L, which might be caused by admixing from the above lying salinity minimum having high oxygen content. Remarks on the origin and formation of these oxygen minima are made in Section 6 · 5.

At the overlapping of the two Intermediate Waters in the range between the equator and 10°N a salinity and an oxygen maximum are formed. The positions of the salinity maximum and of the two salinity minima in the TS diagram are shown in fig. 6 · 15. East of Formosa the northern Intermediate Water has salinities of 34.2‰ at temperatures of about 8°C and by mixing becomes warmer and of higher salinity towards the south. In deeper layers the southern

Intermediate Water is found with temperatures between 4° and 7°C and salinities of 34.45 to 34.55‰. At stations, where the two Intermediate Waters are overlapping, a weak salinity maximum is found at temperatures of about 8°C and salinities above 34.6‰. The formation of this salinity maximum is demonstrated by means of TS-curves of three stations, shown in fig. 6 · 16. At Station Da 3767 off the coast of New Guinea only the southern Intermediate Water appears at a temperature of 7°C, at station SFB 1087 only the northern Intermediate Water at a temperature of 10°C, while at station Da 3751 both salinity minima are present with a weak salinity maximum between them.

In the same way the oxygen maximum is formed between the two Intermediate Waters. The TO_2 curve of station Da 3767 indicates that the southern Intermediate Water is of high oxygen content and the oxygen minimum lies below 4°C. At station SFB 1087, on the other hand the northern Intermediate Water is of lower oxygen content with its corresponding oxygen minimum at 8°C. The station Da 3751, approximately midway between the two preceding stations, shows above 8°C conditions significant for the northern Intermediate Water with low oxygen contents, and below 8°C an oxygen distribution corresponding to that in the southern Intermediate Water with its high oxygen content and its deeper lying oxygen minimum. By this overlapping of the two Intermediate Waters an oxygen maximum appears at 8°C. Remarkable in this connection is the extremely sharp jump

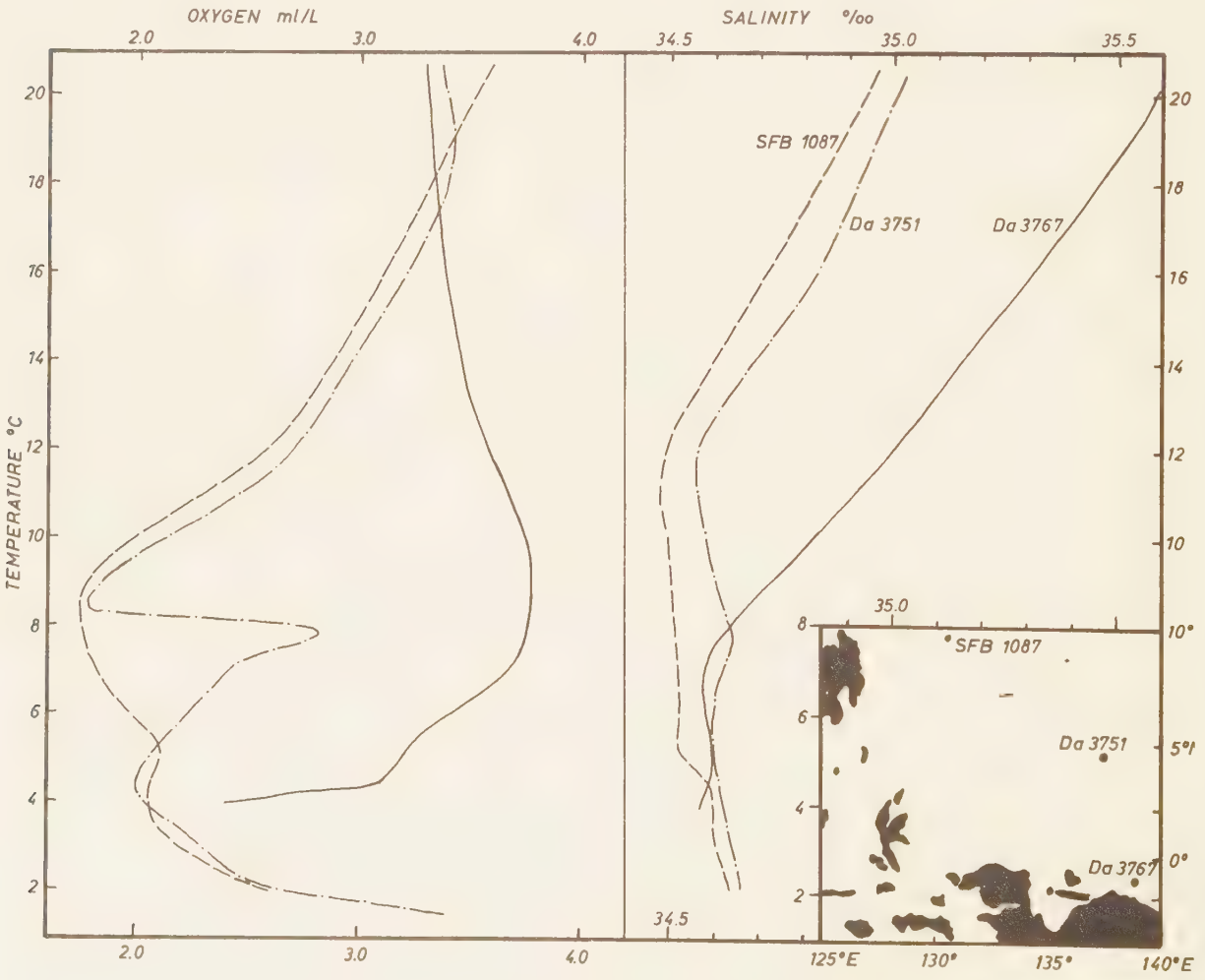

Fig. 6·16. Temperature-salinity and temperature-oxygen diagram of three stations in the western equatorial Pacific Ocean demonstrating the formation of the intermediate salinity and oxygen maximum. Inset map gives positions of stations.

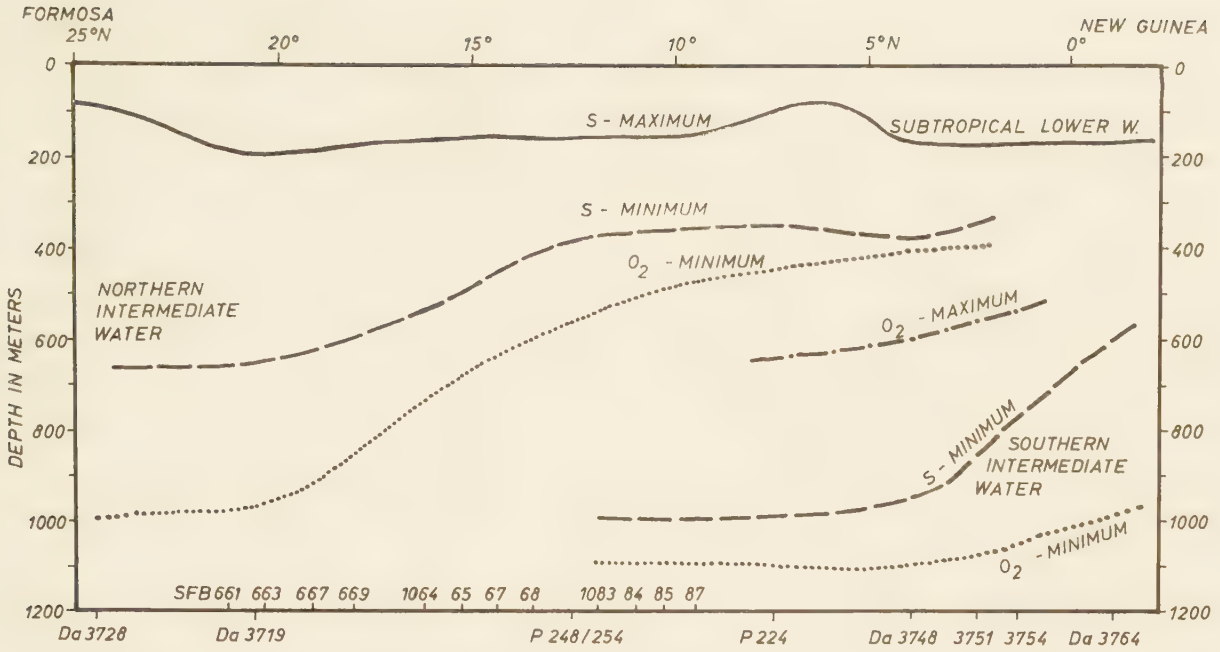

Fig. 6·17. Schematic representation of the position of the core layers of the different water masses in the Philippine Sea in a section from New Guinea to Formosa.

of the oxygen content at 8°C, which amounts to about 1.0 ml/L and occurs within 100 m depth.

Below the Intermediate Waters with their salinity and oxygen minima, generally below about 1200 m, the salinity and the oxygen content increase again. The increase of the oxygen content is considerable, rising from about 2.0 ml/L in the minimum to more than 3.3 ml/L in the bottom water. The increase of the salinity is small, rising from about 34.45‰ in the Intermediate Water to values between 34.65 and 34.70‰ in the bottom water. The temperature decreases from about 4° to 5°C in 1000 m depth very gradually to about 1.60°C in the temperature minimum in a depth of about 3500 m. In still deeper layers an increase is observed due to the adiabatic effect. The potential temperature of the bottom water is about 1.20°C. The water masses in the depth are therefore chiefly denoted by their homogeneity.

Summarizing, the positions of the core layers of the different water masses in the western North Pacific Ocean are presented in a section from New Guinea to Formosa, fig. 6 · 17. This section shows, below the homogeneous surface layer, the Subtropical Lower Water as the upper-

TABLE 5

Properties of subsurface water masses in the Western North Pacific Ocean.

Water Type	Characteristic	T	S	O_2
Northern Subtropical Lower Water	S maximum	20 - 24	34.8-35.2	3.7-4.6
Southern Subtropical Lower Water	S maximum	19 - 27	35.0-35.6	3.2-3.5
Northern Intermediate Water	S minimum	7 - 11	34.1-34.5	1.7-3.0
	O_2 minimum	4 - 9	34.3-34.6	1.2-2.4
Southern Intermediate Water	S minimum	5 - 7	34.45-34.6	1.9-3.0
	O_2 minimum	3.5 - 5	34.5-34.6	2.0-2.4
Deep and Bottom Water	T_p minimum	1.6	34.65-70	3.4

most water mass, appearing as a salinity maximum. It lies in depths between 100 and 200 m. In the north, near Formosa, the salinity minimum of the northern Intermediate Water is situated below it in 600 m depth, accompanied by the northern oxygen minimum in 900 m depth. The two core layers ascend towards the south and are found close together below the Counter Current in 300 and 400 m depth. In the south off New Guinea, the salinity minimum of the southern Intermediate Water is found in depths of about 700 to 900 m, below it the southern oxygen minimum in 1000 to 1200 m. The two core layers decline to the north, underlying the northern Intermediate Water. In this range, between the equator and 10°N, a salinity and an oxygen maximum are formed, indicating the boundary between the two Intermediate Waters in approximately 500 to 600 m depth. Below the Intermediate Waters the large body of the Pacific Deep and Bottom Water is situated. The properties of the different water masses are given in table 5.

6·3 THE WATER MASSES IN THE DEPTH OF THE CHINA AND SULU SEAS

The structure of the water masses off the entrance to the China Sea is typical of the western North Pacific Ocean, with the salinity maximum of the Subtropical Lower Water in 150 m depth, the salinity minimum of the northern Intermediate Water in 600 m depth, and an oxygen minimum in 900 m depth. Because the sill depth of the Luzon Strait is about 2500 m, all these water masses can enter the China Sea and are observed there. A TS and a TO_2 diagram for the China Sea, based on observations of the DANA and of Japanese vessels, shows the Subtropical Lower Water as the uppermost water type practically forming the discontinuity layer. The salinity maximum lies in the Luzon Strait at temperatures of 23°C and oxygen values of 4.5 ml/L, fig. 6·18, when penetrating further to the southwest its salinity decreases by mixing primarily with the water above it, so that the maximum comes to lie at always lower temperatures and oxygen values. In the southernmost parts of the China Sea the salinity maximum is no longer well pronounced and lies at temperatures of 15°C and oxygen values of less than 2.5 ml/L, see plates 16 and 17. The relation between the decrease of salinity and oxygen content in the salinity maximum is completely linear, as shown in the SO_2 diagram, fig. 6·18, so that the decrease is caused by mixing only.

A remarkable feature in the China Sea is the well developed inversion of the oxygen content in the lower parts of the discontinuity layer just below the core layer of the salinity maximum; west of the Luzon Strait this inversion reaches a value of 0.9 ml/L. It decreases considerably to the southwest, and in the southeast of the region it is not found. It may be assumed that this inversion is not caused by biological processes, but is due to movements of water masses of different oxygen content. The centre of the inversion lies relatively uniformly at temperatures of 16°C, so that the water above it belongs to the Subtropical Lower Water and the water below it to the Intermediate Water. In these two water masses the oxygen content decreases considerably with increasing depth, and strong horizontal gradients of the oxygen content are present in the two water masses. If a rapid opposite movement of the two water masses occurs, Lower Water of relatively low oxygen content can come over Intermediate Water of relatively high oxygen content, so that such an inversion is observed at the boundary between the two water masses. Thus, it can be concluded that the two water masses must move in opposite direction. The depth of this inversion is about 200 m and corresponds well to the depth of the dynamic boundary between the two counter-moving layers, see table 10 and Section 7·7. The appearance of this inversion is certainly seasonal, but observations from other seasons are not available.

The salinity minimum also enters through the Luzon Strait and spreads in the China Sea towards the southwest, plate 20. During this movement its oxygen content decreases from 2.5 ml/L in the Luzon Strait to 1.5 ml/L in the south of the region, plate 21. The core layer of

the salinity minimum lies in about 400 to 500 m depth, essentially higher than outside of the China Sea, but at about the same temperature, between 7.5 and 9.5°C.

The distribution of the different factors shows the Intermediate Water as well as the Lower Water entering the China Sea from the Pacific Ocean. Consequently the question arises, in which depth does water leave the China Sea to maintain the balance. It is unlikely that an outflow occurs in depths below the Intermediate Water, because vertical movements would have to appear and such an effect should be visible in the stratification.

A dynamical consideration of the circulation in the China Sea as made in Section 7 · 7 shows that besides the Monsoon Currents a considerable vertical circulation which is comparable quantitatively with the Monsoon Current is produced by the winds. During the northeast mon-

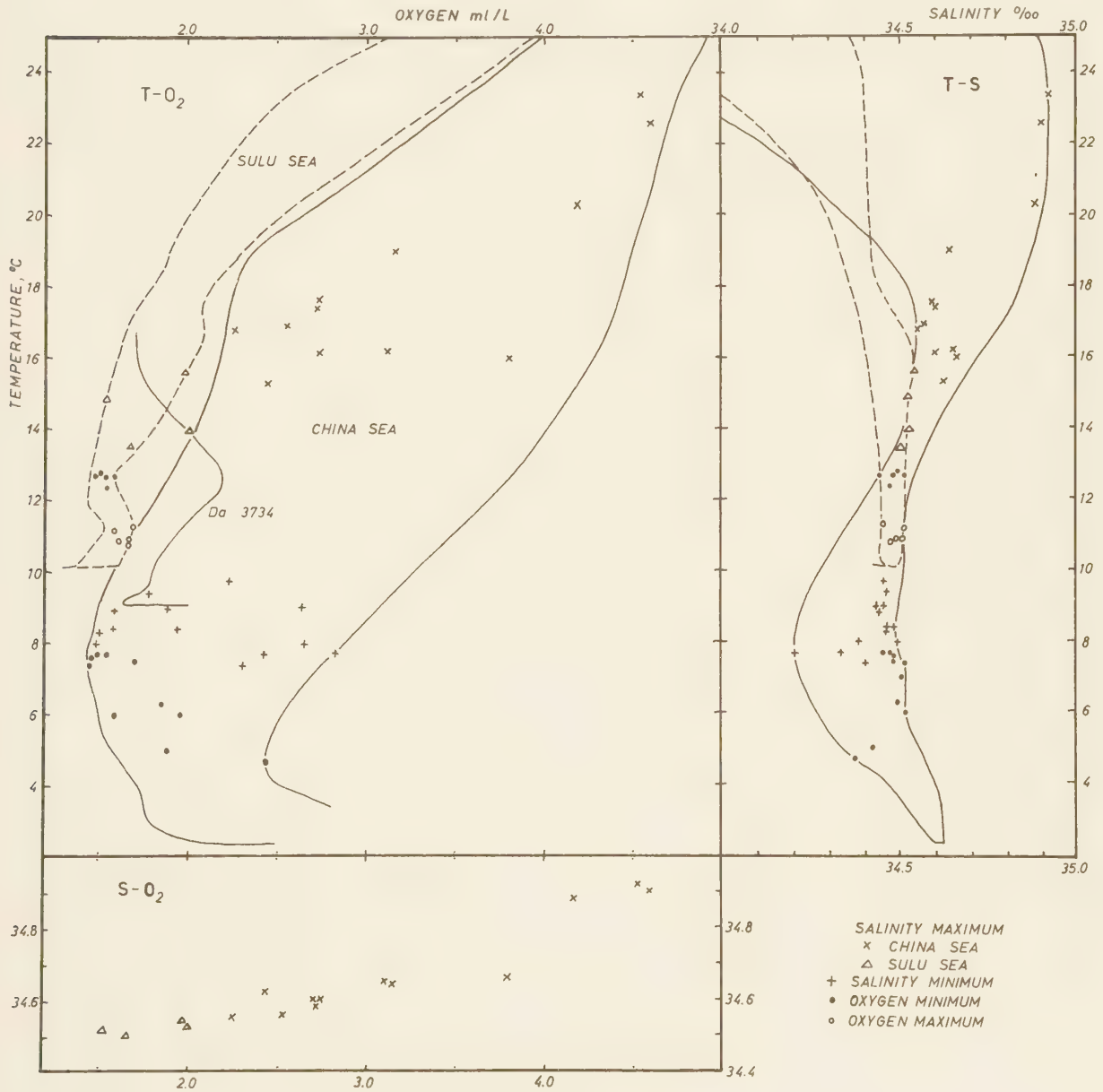

Fig. 6·18. Temperature-salinity and temperature-oxygen diagram of the core layers of the different water masses in the China Sea and in the Sulu Sea together with envelopes of the T-S and T-O_2 curves. Position of station Da 3734 see figure 6·19. Lower part: S-O_2 diagram of the core layer of the salinity maximum.

soon, surface water from the Pacific Ocean is transported into the China Sea. The vertical extent of this layer is about 200 m, as shown in fig. 7 · 12, so that the Lower Water also is transported into the China Sea during this season. It spreads according to the surface currents chiefly along the west side of the China Sea, plate 16. During this period the discontinuity layer sinks in the average about 50 m (fig. 7 · 20). Below this zone of sinking the movements are directed to the northeast and parts of the Intermediate Water flow out of the China Sea in depths between 400 and 900 m during this season.

During the southwest monsoon the conditions are just reversed. The surface water flows towards the northeast and takes with it parts of the discontinuity layer. So the salinities in the salinity maximum are reduced, and simultaneously, the discontinuity layer rises. Below about 300 to 400 m water masses flow into the China Sea; these belong to the Intermediate Water and consequently the salinity in the salinity minimum decreases during this season. The spreading of the salinity minimum takes place along the east side of the China Sea, plate 20, and is favored by the development of temporary counter currents along this side.

Consequently the inflow of the Lower Water and of the Intermediate Water into the China Sea occurs alternately during different seasons. During the northeast monsoon surface water and Lower Water flow into the China Sea and Intermediate Water flows out of it in the deeper layers. On the other hand surface water and Lower Water leave the China Sea during the southwest monsoon and Intermediate Water enters in intermediate layers. A detailed knowledge of these processes can, however, only be expected from further systematic investigations in this region during the different seasons.

Below the Intermediate Water the oxygen minimum lies in a depth of about 600 m. It enters like the Intermediate Water through the Luzon Strait, plates 23 and 24. It is a branch of the oxygen minimum of the North Pacific Ocean and there is no indication that it is formed in the China Sea. Its oxygen content, however, is lowered within the China Sea like that of the other water masses. The lowest oxygen values occur in the south and are below 1.5 ml/L. The water masses below it are very uniform in their structure. They belong to the Pacific Deep Water and have temperatures below 4°C and a salinity between 34.50 and 34.60‰. The oxygen content increases with decreasing temperature to values above 2.0 ml/L. In greater depths the typical basin conditions are found, the temperature minimum is reached in 3000 m depth with 2.38°C. A little below the sill depth of about 2500 m, the salinity rises to 34.63‰ the oxygen content to 2.4 ml/L, demonstrating the relatively good ventilation of the China Basin.

The SULU SEA is separated from the China Sea by a 420 m deep sill, and only water masses present in the China Sea above this depth can enter the Sulu Sea. Thus the last traces of the Lower Water with salinities of 34.55‰ are met entering the Sulu Sea, in about 200 m depth, plates 16 - 18. At some stations a maximum can no longer be recognized, which is also demonstrated by the envelopes of the TS-curves in the Sulu Sea, fig. 6 · 18. The salinity maximum is found at temperatures between 13° and 16°C, the oxygen content is only 1.5 to 2.0 ml/L. Here it must be pointed out that the oxygen content is lower in the whole Sulu Sea than in equivalent depths of the China Sea, as shown by the envelopes of the TO_2 relations of the two regions. In the SO_2 diagram, however, the dots are in clear continuation of the values in the China Sea, fig. 6 · 18. Below the salinity maximum the salinity is exactly the same as in the China Sea. Its variations are only small and the values remain between 34.45 and 34.51‰. At some stations in depths of about 300 m a weak salinity minimum can be recognized, indicating the last traces of the Intermediate Water. In the same depth an oxygen minimum occurs with oxygen contents of only 1.5 ml/L. This minimum seems to be present in the whole Sulu Sea. Below a depth of 300 m the oxygen content again in-

creases a little, reaching values between 1.6 and 1.7 ml/L. This oxygen maximum is in about the same depth as the sill, where a horizontal exchange is still possible. Below this depth the oxygen content decreases again like the temperature, which reaches its minimum in about 1000 m depth. Below this depth the typical basin conditions are found, as given in table 7.

An extensive investigation of the waters of the Philippines and the Sulu Sea was undertaken during the years 1947 - 1950, but the results are not yet published in detail. A preliminary study of the hydrographic conditions in the Sulu Sea is given by Graham (1952, 57), but brings practically no essentially new results. Moreover the effect of internal tides and waves has not been eliminated and the charts of the horizontal distribution of the properties are rather disturbed by them. Those of the dynamic topography especially give an inadequate picture. More interesting results, however, are to be expected from the publication of the chemical data taken at the stations.

Within the Philippines a number of basins are found, which are more or less isolated from the Sulu Sea. These are the Sibuyan Basin in the north and the Bohol Basin in the south, as well as some smaller ones with higher sill depths. The TS and TO_2 relations within these basins are given in fig. 6 · 19. Station Da 3731 west of Luzon, represents the conditions as those just outside the Sulu Sea. It shows a clear salinity maximum at a temperature of 18°C and higher values of oxygen content. The thick broken curve shows the envelopes of the TS and TO_2 relations in the Sulu Sea. In the TS diagram the curves of the other basins run completely within these envelopes. The bottom water in the

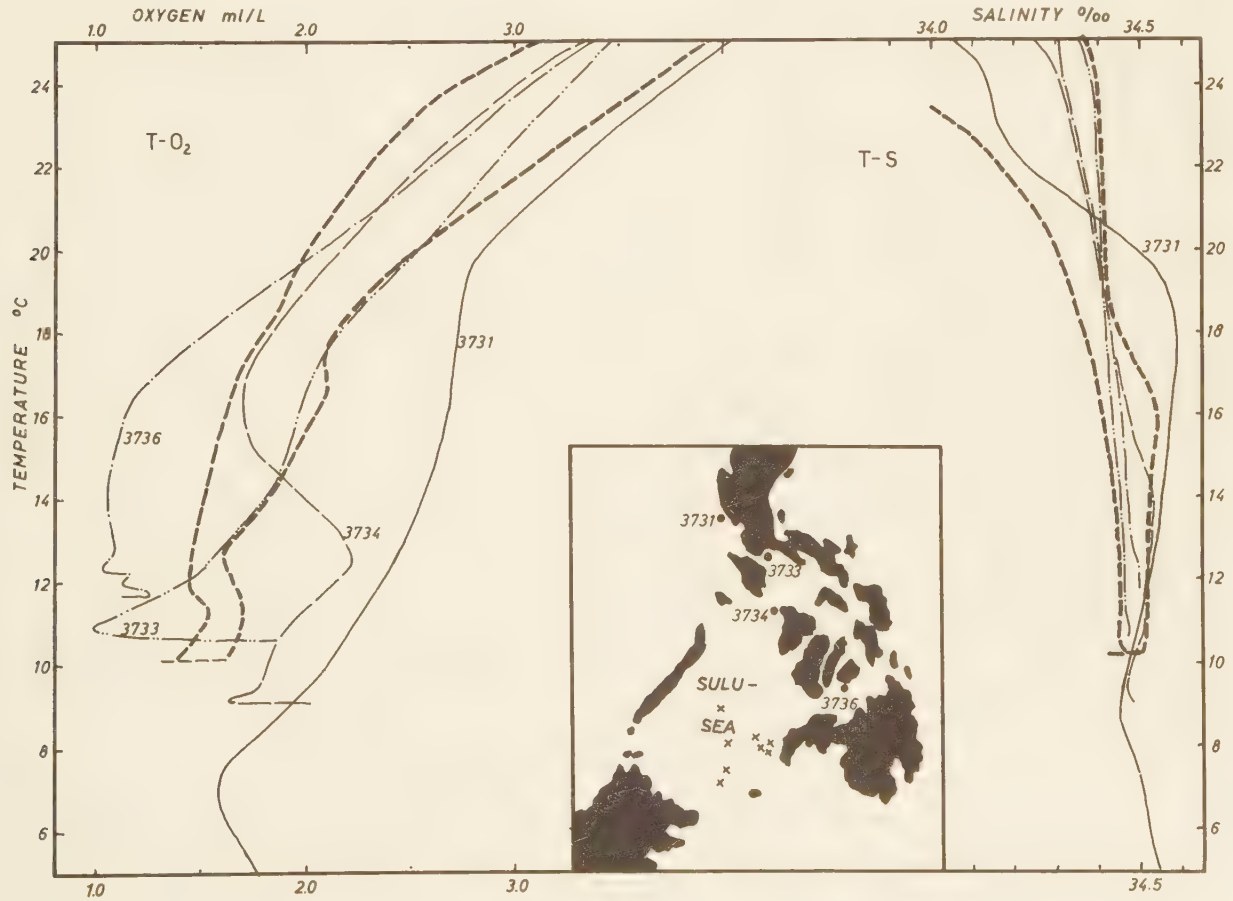

Fig. 6·19. Temperature-salinity and temperature-oxygen curves of different stations in the vicinity of the Sulu Sea and envelopes of T-S and $T-O_2$ curves for the Sulu Sea. Inset map shows positions of the stations.

Sulu Sea corresponds to the water of the same temperature at its entrance. In the oxygen content, on the other hand, considerable differences between the individual basins are to be noted, but they are all of lower oxygen content than the China Sea.

The station Da 3734, situated in the trench connecting the China and Sulu Seas, shows in its upper part a distribution corresponding to that in the Sulu Sea, while below 13°C the oxygen content is still relatively high and corresponds to the conditions at station Da 3731. The minimal temperature at station Da 3734 is 9.03°C, meaning that water which is found in the China Sea in a depth of 470 m, enters into this trench. The Sulu Sea on the other hand has a minimal temperature of 10.08°C, which is 1°C higher. Consequently, the sill of the Sulu Sea must be situated south of station Da 3734 and must be higher, 420 m.

The conditions in the Sibuyan Basin south of Luzon are represented by those at Station Da 3733. In the range of the sill depth an oxygen minimum is found with values of only 1.0 ml/L, in deeper layers the oxygen increases again to values of 1.8 ml/L. In the Bohol Basin, situated north of Mindanao and represented by station Da 3736, the oxygen content decreases in 200 m depth to 1.1 ml/L, but does not increase again. Some other smaller basins with higher sill depths and also higher bottom temperatures, but without an intermediate temperature minimum are found within the Philippines. They are all listed in table 7 and presented in plate 37. The properties of the water in the different core layers in the China Sea are presented in table 6.

6 · 4 THE SUBTROPICAL LOWER WATER IN THE EASTERN ARCHIPELAGO

The subtropical Lower Water forms in the whole region of the Eastern Archipelago a salinity maximum below the warm surface layer of low salinity. This water mass whose origin has already been discussed in Section 6 · 2 penetrates between Mindanao and New Guinea into the Eastern Archipelago and forms practically the water masses of the discontinuity layer. The position of the salinity maximum in the upper part of the discontinuity layer implies that it participates in the movements of the surface water. So the northern Subtropical Lower Water penetrates with the Mindanao Current into the Celebes and the Molucca Seas and the southern Subtropical Lower Water with the South Equatorial Current into the Halmahera Sea, and during this movement the salinity decreases rapidly to less than 34.7‰, plates 16 and 33, but the maximum can clearly be followed to the Lesser Sunda Islands.

An analysis of the TSO_2 values in the salinity maximum of the Lower Water shows clearly that its salinity is decreased by mixing with the warm, less saline water masses above and the cold less saline water masses below the salinity maximum, fig. 6 · 12, and the maximum is displaced to lower temperatures and oxygen values. This figure, as well as fig. 6 · 20 for the Eastern Archipelago, show that only the use of the oxygen values makes it possible to differentiate between the two Lower Waters. In the SO_2 and in the TO_2 diagrams two groups of dots are clearly distinguishable, and they are separated by a straight line, fig. 6 · 20. In the TS diagram they are interspersed and the separation line, which is repeated according to its TS values,

TABLE 6

Properties of subsurface water masses in the China Sea.

Water Type	Characteristic	T	S	O_2
Subtropical Lower Water	S maximum	15 - 24	34.5-34.9	2.2-3.5
Northern Intermediate Water	S minimum	7.5 - 9.5	34.3-34.5	1.5-2.6
	O_2 minimum	5 - 8	34.4-34.55	1.4-2.0
Deep Water	T minimum	$t_p = 2.38$	34.63	2.4

gives only the boundary of the northern Lower Water towards higher salinities. The geographical distribution of the two Lower Waters based on this analysis is also given in fig. 6 · 20.

The northern Subtropical Lower Water entering the Celebes Sea with the Mindanao Current has a higher oxygen content, but when it spreads westwards its oxygen content decreases, plate 17. With the current flowing to the south through the Macassar Strait it is transported into the Flores Sea and its salinity is reduced to 34.6‰. During the northwest monsoon it is picked up there by the Monsoon Current and is transported to the east, and its last traces can be recognized to the east point of Flores, meeting there the last traces of the southern Subtropical Lower Water. During the southeast monsoon this boundary lies probably further to the west, because then the currents in the Flores Sea flow in the opposite direction.

The depth of the salinity maximum in the Mindanao Current is in about 100 m and it deepens in the direction of its spreading, plate 18. In the Celebes Sea it is found in about 130 m and in the Flores Sea in 150 to 160 m depth. With the water masses of the Mindanao Eddy one branch of the northern Lower Water is transported into the Molucca Sea, which normally seems to be filled by it. Temporarily it is also found south of the Lifamatola Strait. This seems to happen, especially if the currents west of Halmahera are directed to the south.

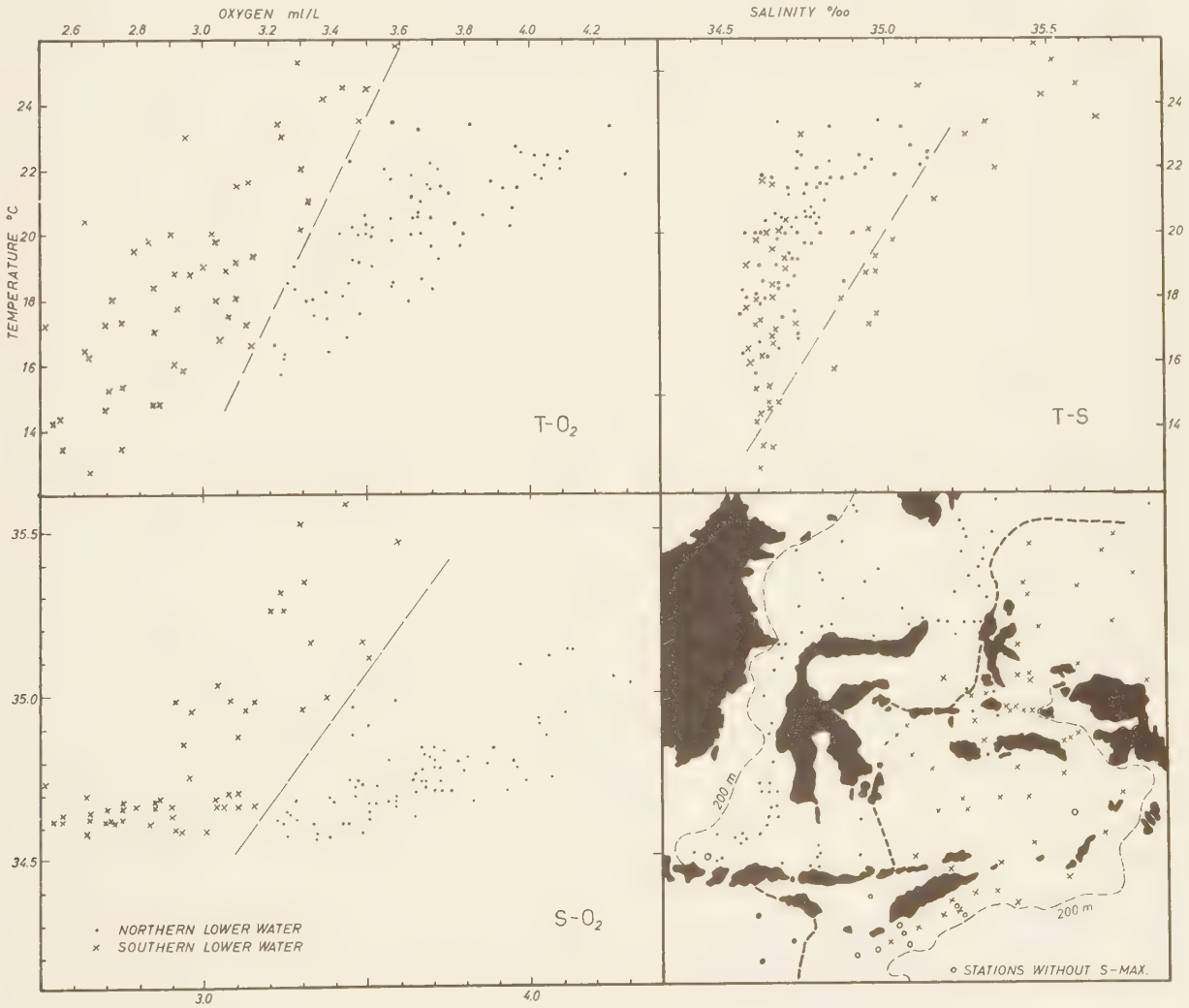

Fig. 6·20. Temperature-salinity, temperature-oxygen and salinity-oxygen diagram of the core layer of the salinity maximum in the Eastern Archipelago, demonstrating the subdivision into a northern and a southern Subtropical Lower Water. Map shows the distribution of both water types. Stations without salinity maximum are indicated.

The southern Subtropical Lower Water of lower oxygen content enters the Eastern Archipelago through the Halmahera Sea, especially during the southeast monsoon, when the South Equatorial Current is strongly developed. It spreads along the southwest coast of New Guinea towards the southeast, where its salinity remains unaltered above 34.8‰ for a relatively long distance. On the other hand the salinity decreases rapidly to the west, and only water below 34.7‰ enters the Banda Sea on both sides of the island of Buru. In large parts of the Banda Sea the salinity maximum is only weakly developed, but can still be identified in the vertical curves. Its salinity is between 34.60 and 34.65‰. The oxygen content is 2.6 to 2.7 ml/L and lower than that of the northern Lower Water in the Flores Sea. The last traces of the southern Lower Water can be recognized in the Sawu and Timor Seas. The Subtropical Lower Water of the Indian Ocean is found only west of 120°E and south of the Lesser Sunda Islands.

Along the boundary of the northern and the southern Lower Water to the north of the island of Halmahera, a double salinity maximum is found at some stations and can be explained simply by overlapping of the core layers of the two Lower Waters according to their density, Wyrtki (1956). Another double salinity maximum is observed in the Halmahera Sea and in the region north of New Guinea. It can be assumed, that it is formed, when from April to October the South Equatorial Current carries a new salinity maximum over the old one, which is still present from the last year. In this way both double salinity maxima can be explained simply by movements of water masses.

In some parts of the Eastern Archipelago an oxygen inversion is found within the Subtropical Lower Water in the lower part of the discontinuity layer. The formation of such an inversion seems to be related to the movements of water masses more than to biological processes, as already explained, when discussing the inversion in the China Sea, Section 6 · 3. The oxygen inversion in the Halmahera Sea seems to be caused by the same fluctuation of the circulation. Another also seasonally conditioned oxygen inversion is found in the Timor Sea, where values up to 0.4 ml/L are found, this inversion is due to the overlapping of different water masses, as explained in Section 4 · 4.

During the southeast monsoon locally, and perhaps only in individual years, water of high salinity above 35‰ is formed at the surface of the Arafura Sea or in the Gulf of Carpentaria, plate 13. It seems to be possible also, that water of higher density is formed, even if only in small quantities, which can sink down to the top of the discontinuity layer and form a salinity maximum there. The station Da 3675, south of the Aru Islands, indicates such a possibility, because in a depth of 75 m a salinity maximum of 34.62‰ occurs at a temperature of 27.5°C. This source, however, seems not to be very extensive or productive so that this maximum is not a stationary feature.

6 · 5 THE SALINITY AND THE OXYGEN MINIMA IN THE EASTERN ARCHIPELAGO

Below the discontinuity layer in a depth between 250 and 1200 m two salinity and two oxygen minima are found in the Eastern Archipelago. They are the last traces of the corresponding water masses in the Pacific and Indian Oceans and their formation and spreading there have already been discussed in Sections 6 · 1 and 6 · 2.

The upper salinity minimum is a branch of the northern Intermediate Water of the Pacific Ocean. It penetrates with the Mindanao Current into the Celebes Sea and fills it completely in a depth of about 300 m, plates 20 - 22. The salinities in the minimum are about 34.40‰ and as an effect of mixing, the oxygen content increases essentially in the direction of the flow. From the Celebes Sea the Intermediate Water penetrates further through the Macassar Strait towards the south into the Flores Sea. There it is picked up like the Subtropical Lower Water by the Monsoon Current during the northwest monsoon and spreads further to the east, where its last traces are found far east of Timor. On its way the

salinity increases only very slowly, it is 34.45‰ in the Flores Sea and rises to 34.55‰ in the region north and east of Timor. This small increase is due to the fact that the water masses above and below the minimum deviate only a little from its salinities. The spreading of the salinity minimum according to the surface currents shows that these are effective down to about 400 m, and that the zero layer lies below this level.

The oxygen content reaches its maximal values in the centre of the Celebes Sea, plate 21, these can be caused by mixing processes in the eddy present there. Further on the oxygen content remains relatively constant between 2.4 and 2.8 ml/L, and no systematic increase or decrease can be detected. Also the salinity values show a considerable scattering, plate 34, and among them often extremely low values occur. This leads to the conclusion that the inflow of the Intermediate Water is not continuous, but occurs in individual more or less large bodies of water. This feature in the Intermediate Water has already been mentioned in Section 6 · 2.

The salinity in the upper salinity minimum based on the SNELLIUS observations is presented in plate 34. In the regions, where no salinity minimum exists, the salinity in 300 m depth is given for comparison. It is essentially higher in the Molucca Sea, due to the relatively deep position of the salinity maximum there. In the Banda Sea the boundary cannot be given quite clearly, and stations with and without a salinity minimum are found alternately. In general, however, the stations with a salinity minimum have salinities below 34.57‰, while those without a minimum have salinities above this value. Conditions are different in the Timor Sea, where the salinity in 300 m depth corresponds to that in the minimum of the neighboring stations. At these stations the salinity maximum of the Subtropical Lower Water is also lacking. In the TS and TO_2 diagram, fig. 6 · 21, the dots of the upper salinity minimum are found between 12° and 9°C and at salinities below 34.6‰. The oxygen content varies considerably between 2.1 and 3.0 ml/L.

The upper salinity minimum in the Indian Ocean on the other hand does not penetrate into the Eastern Archipelago. Its last traces are found at the entrances of the Timor and Sawu Seas. Because in this region the Subtropical Lower Water is also found with its last traces and salinities below 34.6‰, the water masses are practically isohaline from the surface to greater depths. Therefore the salinities of some SNELLIUS stations in the Sawu and Timor Seas vary between 100 and 1000 m depth only between 34.45 and 34.60‰, without indicating a maximum or a minimum. So this is the actual hydrographic boundary between the water masses of the Pacific and Indian Oceans.

The upper oxygen minimum occupying the lower parts of the Intermediate Water penetrates

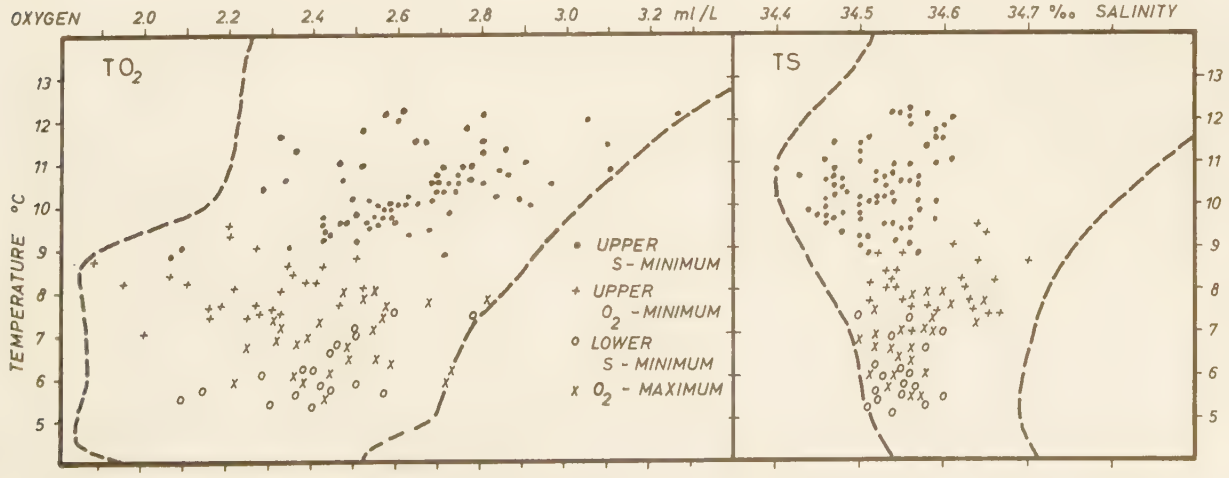

Fig. 6·21. Temperature-salinity and temperature-oxygen diagram of the core layers within the intermediate layer in the Eastern Archipelago together with envelopes of the T-S and T-O_2 curves.

only a little into the Eastern Archipelago. It also follows the Mindanao Current, but its spreading is limited to the Celebes Sea, plates 23 and 24. There it lies between 400 and 450 m depth at temperatures between 9° and 7°C. Its oxygen content varies between 2.0 and 2.4 ml/L and is essentially lower than that of the salinity minimum. Further to the south in the Macassar Strait oxygen values of less than 2.4 ml/L are found in the same depth, but a minimum is no longer developed, because the decrease of oxygen content with depth is too sharp. The position of the oxygen minimum in the TS and TO_2 diagram is given in fig. 6 · 21, and shows at lower oxygen values a displacement towards lower temperatures and higher salinities compared with the salinity minimum. The two groups of dots are clearly separated from one another.

The lower salinity minimum is identical with the southern Intermediate Water of the Pacific Ocean, which appears in the region north of New Guinea and penetrates only a little north and west of Halmahera into the Molucca Sea, plates 28 - 30. It has salinities between 34.50 and 34.60‰ at temperatures between 7° and 5°C and lies in depths between 600 and 750 m, and its oxygen content in the Molucca Sea is about 2.4 ml/L. In the TS and TO_2 diagram its position is clearly below the upper salinity minimum. The Intermediate Water at its origin is a water mass of high oxygen content, as already stated in Section 6 · 2. So it is not surprising that oxygen maxima occur in the vicinity of its core layer at individual stations. In the region where the upper and the lower oxygen minima are overlapping, an oxygen maximum must develop between them. The values corresponding to this maximum are recorded in the TS and TO_2 diagrams, fig. 6 · 21 where it can be seen that they fall into the same range as the values of the lower salinity minimum, so that their identity is proved.

The lower oxygen minimum is spread over the whole Eastern Archipelago, plates 31 and 35, but consists of two different water types. From the Pacific Ocean, where the lower oxygen minimum lies in the lower parts of the southern Intermediate Water, it enters the Celebes Sea in depths between 1000 and 1200 m with temperatures between 4° and 5°C and penetrates into

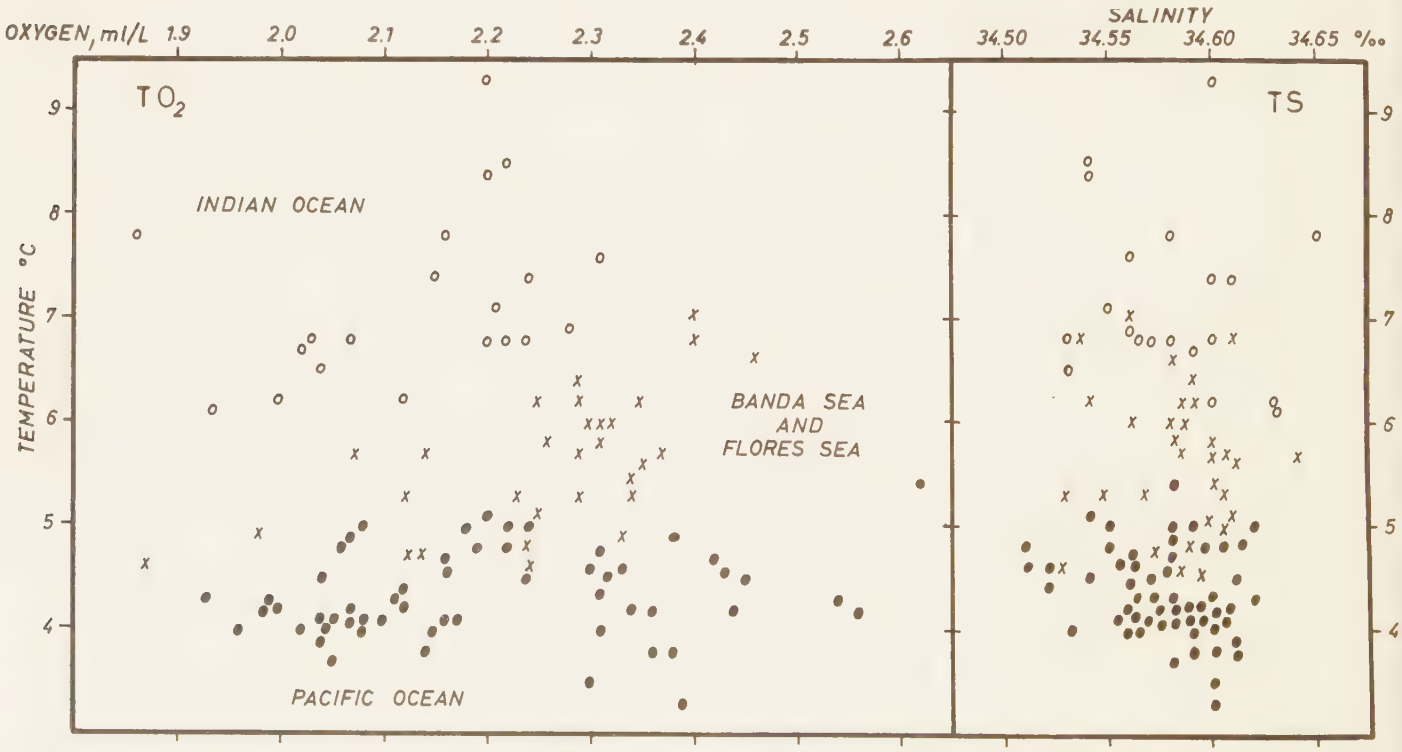

Fig. 6·22. Temperature-salinity and temperature-oxygen diagram of the core layer of the lower oxygen minimum in the Eastern Achipelago, demonstrating the subdivision into the oxygen minimum of the Indian Ocean, present also in the Sawu and Timor Seas, the oxygen minimum of the Pacific Ocean, present also in the Celebes and Molucca Seas and the oxygen minimum in the Banda and Flores Seas, originating by mixing of the former.

the Macassar Strait, on its way the oxygen content decreases from 2.1 to 1.9 ml/L. A further penetration to the south is prevented by a ridge closing the Macassar Strait at its southern end in this depth. Another branch penetrates west of Halmahera into the Molucca Sea, where its oxygen content increases up to 2.4 ml/L. This water penetrates on both sides of the island of Buru into the Banda Sea, where it ascends to 800 m, plate 32.

In the Indian Ocean south of Java in depths of 600 m an oxygen minimum is also present. It extends with oxygen values of about 2.1 ml/L at temperatures between 8° and 6°C into the Sawu and Timor Seas. It penetrates through the Timor Trench into the Aru Basin and its last traces can be followed up to the north of the island of Ceram. Through the Sawu Sea and through the passages east of Timor the oxygen minimum of the Indian Ocean invades the Banda Sea, but this penetration seems to occur by lateral mixing rather than by a real flow. In the TS and TO_2 diagram, fig. 6·22, the two groups of dots are presented, which belong to the oxygen minimum of the Pacific Ocean and of the Indian Ocean, respectively. In the Banda Sea the last traces of the two oxygen minima meet, and by mixing a water mass is formed, which corresponds in its salinity and oxygen content to the original water masses, but occupies a mid-position in respect to its temperature. It varies between 7° and 5°C, as seen in the TS and TO_2 diagram. This water mass spreads from the Banda Sea towards the west into the Flores Sea, on its way its temperature and oxygen content decrease continuously, plate 35.

This study was completed when a survey of the water masses and their movements in the upper and intermediate layers of the Eastern Archipelago was published by Postma (1958) in the Reports of the SNELLIUS Expedition. The results of this survey agree in detail with the analysis given here.

These two oxygen minima are formed in the two oceans by biological processes, which consume oxygen. In this process extensive water bodies of low oxygen content are formed, which are nearly without motion, so that the replacement of oxygen occurs by mixing only, and therefore minimal oxygen values are caused. From these water bodies of low oxygen content, which lie below the cores of the Intermediate Waters, branches penetrate with the Intermediate Waters into the Eastern Archipelago forming there also an oxygen minimum. It must not be assumed that these oxygen minima are formed within the Eastern Archipelago by biological processes, but it is likely that the oxygen content is further decreased, especially in regions such as the Flores and the Celebes Seas, with only a small water exchange in these depths. The penetration of the oxygen minima, especially of that from the Indian Ocean seems to occur by lateral mixing more than by a real flow. It cannot be said, however, that the layer of minimal oxygen content is completely identical with the "layer of no motion", even if it is relatively close to the zero layer, which lies in the Archipelago in about 500 to 800 m depth. But on the other hand it must be said, that the whole layer of minimal oxygen content is also a layer of minimal horizontal movements. It will be shown by the author in another place, that between two moving layers in a water mass, where oxygen consumption and vertical mixing are assumed, a layer of minimal oxygen content is formed in the layer of minimal horizontal movements.

6·6 THE WATER MASSES IN THE DEEP LAYER

At depths of about 1000 m the different parts of the Eastern Archipelago are separated from one another and connected only by narrow passages, plate 36, so that large scale water exchange is impossible. The Celebes Sea is connected with the Pacific Ocean only by four narrow passages, and it is separated in the south from the Flores Sea. The inflow of water into the Banda Sea is possible only by one passage, the Lifamatola Strait between the islands Mangole and Obi. With the Indian Ocean a narrow connection still exists through the Sawu Sea and the Timor Trench. The hydrographic conditions

in this depth are therefore much equalized. The temperature varies between 4.4° and 4.8°C and the salinity between 34.51 and 34.62‰. In the Pacific Ocean the lowest salinities are found, which is an influence of the salinity minimum, situated a little higher between 700 and 900 m depth. This water, having on the average a salinity of 34.55‰, fills the whole Celebes Sea at this depth, plate 36. On the other hand the salinities in the Banda Sea, especially in its eastern parts are a little higher, they usually reach 34.60‰ so it must be assumed, that the salinity in this region is increased by vertical mixing, or that ascending movements bring the water of deeper layers into the 1000 m level.

In the Indian Ocean a clearly distinguished salinity minimum is found in 1000 m depth with lowest salinities in the region south of the Sawu Sea. Because the TSO_2 values within this minimum correspond to those in the Sawu and Timor Seas in 1000 m depth, fig. 6 · 7, an origin of this water type from the Eastern Archipelago is indicated. Its spreading into the Indian Ocean is already discussed in Section 6 · 1 and the existence of this water mass is simultaneously an indication, that water movements take place from the Pacific to the Indian Oceans in the 1000 m level. This is, however, not a more or less direct flow from the Pacific to the Indian Oceans, but an extremely slow spreading process. Probably vertical movements in connection with the replacement of the water masses in the deep sea basins are decisively engaged in this process. The water flowing from the Pacific Ocean over the different sills into the deep sea basins must cause ascending movements in the other parts of the basins, and the ascending water masses must be transported away in horizontal directions. In this way the appearance of higher salinities in the eastern Banda Sea can be explained.

From the Pacific Ocean the replacement of the water in the Banda Sea and in the other basins of this group takes place over the 1900 m deep sill of the Lifamatola Strait. If this water sinks towards the bottom, an equivalent quantity must ascend in the other parts of the basins. This water leaves through the Sawu and Timor Seas in a horizontal direction towards the Indian Ocean, where it forms the salinity minimum, having approximately the properties of the water in the Banda Sea. This process is presented schematically in fig. 6 · 30. The actual transported masses seem to be very small, but the spreading of the Mediterranean water in the Atlantic Ocean shows how far reaching such processes can be. It is also likely that the outflow of the water ascending out of the basins towards the Indian Ocean does not take place continuously, but is related to the monsoon circulation at the surface and occurs periodically. This interaction of the surface and the deep circulation is specially discussed in Section 7 · 5 in connection with the upwelling in the Banda Sea.

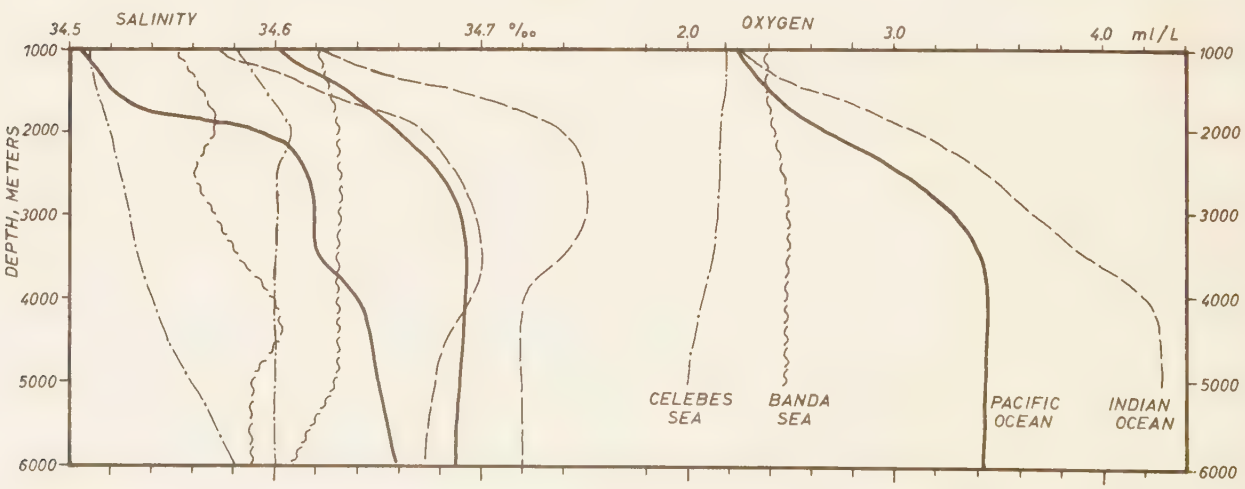

Fig. 6·23. Vertical distribution of salinity and oxygen content in the deep and bottom water of the Eastern Archipelago and the adjoining parts of the Indian and the Pacific Oceans.
Left: range of the variation of salinity with depth.
Right: average distribution of oxygen content.

Below about 1000 m depth the salinity as well as the oxygen content increase again in the two oceans. These conditions are illustrated in fig. 6·23 by means of the vertical salinity and oxygen distribution. In the two oceans the layer between 1000 and 3000 m depth is the transition area between the less saline Intermediate Water and the Bottom Water of relatively high salinity, high oxygen content and minimal temperature. In the western Pacific Ocean the salinity increases from about 34.55‰ in 1000 m depth to 34.67‰ in 3500 m depth and the oxygen content increases in the same interval from 2.2 to 3.4 ml/L. In 3500 m depth practically the properties of the bottom water are reached, being homogeneous in greater depth. In the eastern Indian Ocean the salinity increases from 34.60‰ in 1000 m depth to an intermediate maximum of 34.73‰ in about 2750 m depth, but decreases later again to 34.70‰. The oxygen content on the other hand increases continuously from about 2.2 ml/L in 1000 m to over 4.2 ml/L in depths below 4000 m.

The deep sea basins of the Eastern Archipelago, however, are separated from the open ocean in depths above 2000 m, so that the deep water of the two oceans cannot enter them. Only water masses of the transition layer, in which the oxygen content as well as the salinity increase and the temperature decreases, can pass the different sills of the basin. Consequently the water masses in the deep sea basins are of lower salinity and oxygen content than those in the same depth in the two oceans, fig. 6·24.

In the Celebes Sea the salinity varies between 34.52 and 34.61‰ and corresponds to the low values above the sills. The salinities in the Molucca Sea are the same as in the Pacific Ocean. South of the Lifamatola Strait, in the Buru and Banda Basins, the salinities are about 34.60‰ with a variation of ± 0.03‰. The appearance of relatively low salinities between 34.55 and 34.58‰ in the Flores and Sawu Basins is remarkable. This could be a mixing effect with the water masses in higher layers, but it is also possible that these water masses date from an earlier period, when the basins were filled with water of lower salinity, which has not yet been replaced by ascending movements. It must, in general, be assumed that long periodic fluctua-

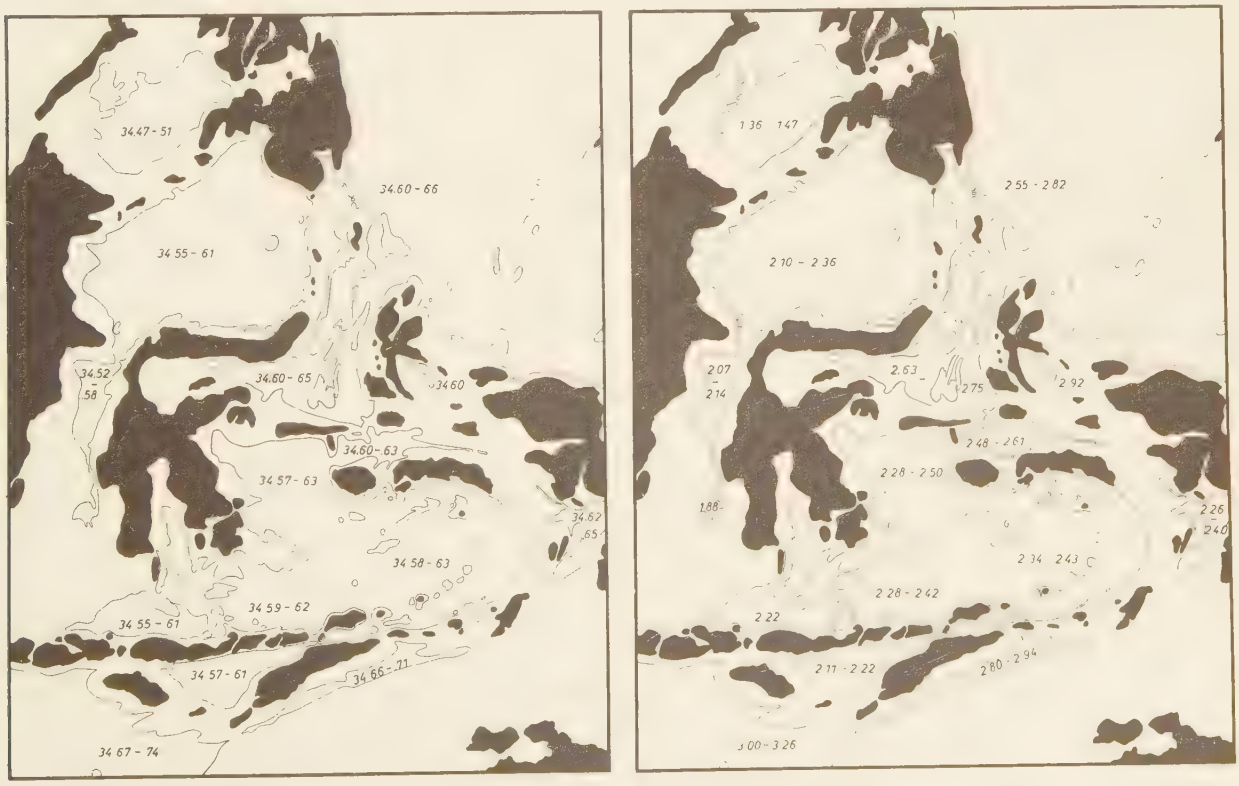

Fig. 6·24. Distribution of salinity and oxygen content in 2000 meters depth in the Eastern Archipelago. Full line gives contour of the 2000 meter line.

tions of the properties occur in these basins. This, however, can be verified only by long series of observations.

The Timor Trench is filled with water of higher salinity from the Indian Ocean, so that values up to 34.71‰ occur. The Aru Basin seems to get its water from the Timor Trench as well as from the Buru Basin and with salinities between 34.62 and 34.65‰ has a mid position.

The distribution of the oxygen content in 2000 m depth, fig. 6 · 24, in general shows the same picture. Oxygen values between 2.1 and 2.2 ml/L in the Celebes Basin, which decrease to less than 2.0 ml/L in the Macassar Strait, are in contrast to values between 2.6 and 2.7 ml/L in the Pacific Ocean. Also in the Banda and Flores Basins the oxygen values are 2.2 to 2.4 ml/L, and lower than those in the Molucca Sea at the same depth. The high value in the Halmahera Sea is caused by the high position of the sill, lying above the oxygen minimum. Very low oxygen values are observed in the Sawu Basin. In general a clear decrease of the oxygen content is found as distances from the sills increase. The consumption gradients are 0.25 10^{-3} ml/km in the Celebes Basin and 0.5 10^{-3} ml/km in the Banda Basin in agreement with those found by Wattenberg (1939) in the Atlantic Ocean. Very clearly the process of oxygen consumption can be seen in the longitudinal section through the Celebes Sea, plate 38. The oxygen content of the invading water is 2.2 ml/L and decreases in the direction of its spreading to less than 2.0 ml/L. The zone of low oxygen content also extends continuously upwards.

6 · 7 THE WATER MASSES IN THE DEEP SEA BASINS

The conditions in any deep sea basin are governed by the water flowing over the sill, and sinking down into the depths. Because of the continuous flow of heat from higher layers downwards, the water within the deep sea basins becomes warmer and its density is decreased, so that new heavier water can subsequently invade the basins. Thus, descending movements must occur in the immediate vicinity of the entrances and extremely slow ascending movements in other parts. By this circulation the water within the basins is renewed continuously, although the process may be extremely slow. That such a replacement of the water really occurs, is indicated by the high values of the oxygen content within the basins.

When considering the replacement of the water in the basins, two types of basins must be differentiated, these are primary basins which are those receiving their water directly from the open ocean, and secondary basins which are receiving their water from another basin, which is closed from the ocean at a higher level. The water of these secondary basins will generally deviate only a little from the properties of the primary basin.

The different deep sea basins within the Southeast Asian Waters are listed in table 7. They are numbered, and these numbers are used in future reference to the basins, the primary basins are indicated in cap type. The next columns give the reference station, the maximal depth, and the sill depth. The next three columns deal with the observed temperature minimum, giving depth, temperature and potential temperature. Column 8 gives the minimal observed potential temperature, column 9 shows the fluctuations of salinity, and column 10 those of oxygen content below the temperature minimum. These figures give the values of all important properties in the different basins. The position and shape of the basins and the observed minimal temperatures are presented in plate 37.

The information is based in the Eastern Archipelago on the observations of the SNELLIUS, which are carefully worked up by van Riehl (1934) with respect to the spreading of the bottom water. In the China Sea, the Sulu Sea and the waters of the Philippines the investigations are chiefly based on DANA stations and on the information given by Villadolid (1952).

The first group of deep sea basins, which are supplied by water from the Pacific Ocean, is formed out of the China Basin, the Sulu Basin

and some smaller basins in the Philippines. In the Pacific Ocean east of the Luzon Strait a temperature minimum is found in a depth of between 3500 and 4000 m. The deep water situated above this minimum can invade the China Basin (1) through the Bashi Channel and causes there in 3000 m depth a temperature minimum of 2.38°C. Below it the normal basin conditions are found. A comparison of the vertical curves of temperature inside and outside the basin gives a sill depth of only 2000 m, while the soundings in the Bashi Channel make a connection probably deeper than 2500 m. To solve this discrepancy new soundings are required in the Bashi Channel, which may lead to the discovery of a new higher sill. The China Sea itself is a large uniform basin, in its southern part an extended reef area is situated. Between these reefs and the steep continental slope off Borneo and Palawan the Palawan Trough (2) is situated. It is connected with the China Basin (1) by a deep channel of about 2050 m sill depth through the reef area. It can be expected that detailed soundings in this reef area may find new smaller isolated basins.

The water invading the Sulu Sea from the China Sea passes first a sill with a depth of 470 m southwest of Mindoro. In the following Panay Trough (3) the minimal temperatures, observed at the bottom, are 9.03°C, the oxygen content at the bottom is even somewhat higher than in the China Sea. The water invading the Sulu Basin (4) has to pass another sill of about 420 m west of Panay. In the Sulu Basin the temperature minimum is observed at 1000 m depth which is considerably below the sill. The potential temperature, however, decreases further to the bottom. The salinity is 34.48‰, it is very uniform and corresponds to that in the Intermediate Water of the China Sea, which practically supplies the bottom water of the Sulu Sea. The oxygen values are low, but this does not necessarily indicate an insufficient ventilation of the Sulu Basin, because the oxygen content of the inflowing water is also low.

The Sibuyan Basin (5) being up to 1600 m deep, is connected with the Panay Trough (3) over a sill of 400 m sill depth. The low oxygen values indicate only a weak ventilation. From the Sibuyan Basin the water enters, over a 126 m deep sill, the 602 m deep Ragay Gulf (6). The observed temperature of 17.15°C is associated with the high position of the sill in the depth of the stable tropical discontinuity layer. This causes the oxygen content to reach zero, so the ventilation of this basin is insufficient.

From the Sulu Basin water penetrates over a 412 m deep sill into the Bohol Basin (7) with a maximal depth of 2031 m. In this basin the temperature minimum is developed deeper than in the Sulu Basin, in 1500 m. Also the oxygen values are lower than in the Sulu Basin because of the longer passage of the invading water. From the Mindanao Sea also the two shallower basins within the Philippines are supplied by water. The Tanon Strait (8) with maximal depths of 547 m is supplied with water of 18°C, the oxygen content of only 0.17 ml/L is very low, as in the Ragay Gulf. The sill depth of the 850 m deep Canotes Trough (9) is 260 m so that water with temperatures of 13.3°C can invade it. The oxygen content indicates a better ventilation than in the two shallower basins of the Philippines.

In the region south of Mindanao and in the Molucca Sea several shallow, but deep lying, basins are found, into which the deep water of the Pacific Ocean can flow. East of the island of Talaut the relatively flat Talaut Trough is situated, this is only proved by soundings. Its sill depth is about 3130 m and its maximal depth 3450 m. It is not likely that a temperature minimum is developed within it. North of the island Talaut the deep water has entrance over an approximately 2050 m deep sill into the Sangihe Trough (10) with maximal depths of 3820 m. To the north of Morotai a 2340 m deep sill separates the Morotai Basin (13) from the Pacific Ocean. This basin is 3890 m deep, but is connected below its sill depth with other secondary basins. These are the Ternate Trough (14), the Batjan Basin (15), the Mangole Basin (16)

and the Gorontalo Basin (17). All these basins have maximal depths above 3400 m, their sill depths are between 2550 and 2710 m, that is deeper than the sill of the Morotai Basin. Remarkable is the increase of the potential temperature in the direction of the spreading of the water, while the salinity and the oxygen content decrease. This increase of temperature can be explained as a mixing effect with the water masses in higher levels, which is especially strong when the waters pass the sills. Between Halmahera and the island Batjan the 2048 m deep Patientie Trough (18) is situated, which is connected with the Obi Strait at about 490 m. The observations in this trough, however, do not reach down to the bottom.

The Celebes Basin (11) with maximal depth of 6220 m is separated from the Pacific Ocean by a ridge connecting Celebes and Mindanao, which has three thresholds with sill depths of about 1400 m. Water of relatively low salinity and oxygen content from the Pacific Ocean enters through these. The temperature in the minimum at 2500 m depth is about 3.58°C. The oxygen content decreases gradually in the direction of the spreading. The deep Celebes Basin continues into the Macassar Strait, in which northern part a flat depression, the Macassar Trough (12), is situated, this is a secondary basin of the Celebes Sea. Its maximal depth of 2540 m lies only a little below its sill depth of 2300 m, so that a temperature minimum is not observed.

The Molucca Sea is closed in the south by a ridge connecting Celebes with New Guinea, having a threshold with a sill of 1880 m, the Lifamatola Strait, over which the whole Banda Sea is supplied with deep and bottom water. This water penetrates first into the Buru Basin (19) and spreads from there into all basins in the Banda and Flores Seas. The sills of the connected basins, even that of the Sawu Basin, are all deeper than the Lifamatola Strait, so that they are secondary basins, whose hydrographic conditions are governed by the sill of the Lifamatola Strait. In spite of this they show some differences, which allow conclusions to be made on the spreading of their bottom water. Because the potential temperature is not constant within the basins, but increases upwards due to the downward conduction of heat, the individual basins have slightly different bottom temperatures according to their sill depth.

The Banda Basin is divided into three large basins, the North Banda Basin (20), the South Banda Basin (21) and the Weber Deep (22). From the Buru Basin bottom water penetrates over a 3130 m deep sill first into the North Banda Basin with depths of 5800 m. This basin is connected by a long relatively narrow channel having depths of about 4200 m with the South Banda Basin, which has maximal depths of 5400 m. South of the Banda Islands the bottom water can flow over another sill of 4300 m into the 7440 m deep Weber Deep. The connections of these three basins are all below the sill depth of the entrance, which is 3130 m, so that they are occupied by a nearly homogeneous water mass. The temperature minimum lies in about 3000 m depth above the connection of all basins. The temperature in it increases only a little in the direction of the spreading, from 3.04°C in the North Banda Basin to 3.08°C in the Weber Deep, plate 37. South and east of the island of Buru two smaller basins are situated, the Ambalau Basin (23) and the Manipa Basin (24), which are supplied with bottom water from the North Banda Basin. The temperature minimum in the Ambalau Basin lies in 3500 m and deeper than in the North Banda Basin, in spite of the fact that its sill depth is also 3500 m. The Manipa Basin is closed by a sill in 3000 m depth, so that its temperature minimum, 3.15°C, is warmer than that in the Banda Basin. From the South Banda Basin the Butung Trough (25) with 4180 m depth is reached over a sill of 3600 m, but no observations are available from this basin.

From the South Banda Basin the Flores Basin is reached over a 2300 m deep sill, which leads first into the East Flores Trough (26) with 3350 m depth and over a second sill of 2450 m

into the Flores Basin (27). Because of these two sills the minimal temperature in the East Flores Trough is 3.19°C and in the Flores Basin 3.23°C, but the minimum lies only a little below the sill depth in 2500 m. North of the Flores Basin is situated the only primary basin in this region, the Salajar Trough (30), with a maximal depth of 3370 m and a sill of 1350 m. Because of the higher position of the sill the minimal temperature is 3.86°C.

From the Weber Deep a narrow channel leads over a 2400 m deep sill into the Wetar Basin (28) with 3460 m maximal depth and from there over a 2100 m deep sill into the Sawu Basin (29). The temperature minimum is found in a depth of 2500 and 2250 m only a little below the sill depth with temperatures of 3.17° and 3.39°C, respectively. The two basins are secondary basins of the Banda Basin.

The Halmahera Basin (31) is supplied with bottom water directly from the Pacific Ocean over a sill about 700 m deep. Because of the comparatively high position of the sill the temperature is 7.7°C and a minimum is not observed in the 2040 m deep basin, and the oxygen content shows rather high values indicating an intensive water exchange. A certain exception is the 502 m deep Kau Bay (32), which is filled with water of the Pacific entering over a sill only 45 m deep. Below a depth of 350 m H_2S is observed, van Riehl (1943). The insufficient ventilation of this bay can be explained by the fact that it is filled with water of the surface layer, and that it takes a rather long time until again comparably high densities are reached at the surface to renew the bottom water in the bay. Thus, basins with their sills below the discontinuity layer seem to be much better ventilated than those with their sills in or above the discontinuity layer. This has already been shown in the discussion on the basins with shallow sill depths in the Philippines.

In the Indian Ocean, in the 7140 m deep Java Trench, potential temperatures of only 0.77°C are observed, the temperature minimum lies in about 4500 m, deeper than in the Philippines Basin. Also the salinity and the oxygen content of the bottom water are higher in the Java Trench. The Andaman Basin (33) is supplied with water from the Indian Ocean over a sill of about 1800 m depth, but no hydrographical stations reaching that depth are available in it. From the Indian Ocean deep water enters also the Timor Trough (34) over a 1940 m deep sill. The temperature minimum lies only a little below the sill depth and the oxygen content is relatively high. The Aru Basin (35) with a maximal depth of 3680 m is connected with the Timor Trough as well as with the Buru Basin (19) by two channels about 1500 m deep, which are rather long and small, so that the replacement of the water occurs very slowly from both sides. Thereby the water from the Indian Ocean forms the bottom water and the water of Pacific origin remains in higher levels, as shown by van Riehl (1943). The potential temperature of 3.63°C is relatively high, the oxygen content with 2.3 ml/L relatively low.

The distribution of the potential temperature in a longitudinal section from the Pacific Ocean through the Molucca, Banda and Sawu Seas into the Indian Ocean is presented in fig. 6 · 25. The horizontal run of the isotherms can be seen clearly in the 1000 m level. Below it deep water of the Pacific Ocean with temperatures below 3°C enters the different basins. The isotherms show a considerable vertical displacement, when passing the different sills. The 3.2°C isotherm, for instance, lies in the Pacific Ocean in 1450 m depth, falls in the Banda Basin to 1800 m and in the Sawu Basin to 2300 m. This feature can be explained as an effect of the conduction of heat, coming from the layer above the sill depth and causing a continual heating of the water masses in the basins. A similar effect can be observed at the 1.8°C isotherm in the Molucca Sea. The position of the temperature minimum is also indicated in fig. 6 · 25 by circles, it is normally below the sill depth. The relation between the depth of the temperature minimum and the bottom depth, which is mentioned by van Riehl (1956), seems not to be an effect of the bottom topography, but is caused by a more intensive

TABLE 7

HYDROGRAPHIC CONDITIONS IN THE DEEP SEA BASINS OF SOUTHEAST ASIA

Primary basins are in cap and small cap type. Values in brackets refer to deepest observation at stations without a temperature minimum

	Name of Basin	Reference Station	Max. Depth	Sill Depth	Observed Temperature Minimum			Minimum of t_p	S ‰	O_2
					Depth	°C	t_p		Below Temperature Minimum	
	Philippine Basin	Sn 262	10800	—	3470	1.58	1.31	1.16	34.67 — .69	3.47 — 3.36
1	China Basin	Da 3714	5016	<2500	3000	2.38	2.13	2.08	34.63	2.50 — 2.22
2	Palawan Trough	Da 3687	3475	2050	(2000)	(2.60)	(2.44)	—	(34.63)	(2.00)
3	Panay Trough	Da 3734	1400	470	(1150)	(9.03)	(8.89)	8.89	(34.48)	(2.02)
4	Sulu Basin	Sn 66	5580	420	990	10.08	9.96	9.84	34.46 — .49	1.67 — 1.30
5	Sibuyan Basin	Da 3733	1600	400	(575)	(10.63)	(10.55)	—	(34.47 — .48)	(1.12 — 0.83)
6	Ragay Gulf	—	602	126	(550)	(17.15)	—	—	(34.45)	(0.0)
7	Bohol Basin	Da 3736	2031	412	1500	11.70	11.48	11.48	34.50	1.25 — 1.16
8	Tanon Strait	—	547	91	(500)	(18.00)	—	—	(34.43)	(0.17)
9	Canotes Trough	—	850	260	(800)	(13.32)	—	—	(34.43)	(0.90)
	Philippine Trench	Sn 270	10800	—	2980	1.56	1.34	1.16	34.66 — .69	3.47 — 3.36
10	Sangihe Trough	Sn 296	3820	2050	2550	2.39	2.19	2.15	34.63 — .65	2.73 — 2.63
11	Celebes Basin	Sn 301	6220	1400	2500	3.58	3.36	3.26	34.56 — .60	2.26 — 1.94
12	Macassar Trough	Sn 311	2540	2300	1990	3.60	3.44	3.44	34.55 — .58	2.14 — 1.88
13	Morotai Basin	Sn 284	3890	2340	2490	1.81	1.63	1.55	34.65 — .68	3.06 — 2.96
14	Ternate Trough	Sn 347	3450	2710	2760	1.85	1.64	1.64	34.66 — .67	3.04 — 3.01
15	Batjan Basin	Sn 80	4810	2550	2970	2.05	1.81	1.78	34.64 — .66	2.75 — 2.63
16	Mangole Basin	—	3510	2710	—	—	—	—	—	—
17	Gorontalo Basin	Sn 337	4180	2700	2740	2.19	1.98	1.95	34.62 — .65	2.73 — 2.55

MOLUCCA SEA GROUP

BANDA SEA GROUP	18	Patientie Trough	Sa 25	2048	490	(1160)	(7.97)	(7.84)	—	(34.65)	(2.6 — 2.5)
	19	Buru Basin	Sn 229	5320	1880	2990	3.02	2.76	2.66	34.60 — .63	2.58 — 2.51
	20	North Banda Basin	Sn 218	5800	3130	3000	3.04	2.78	2.73	34.59 — .61	2.51 — 2.44
	21	South Banda Basin	Sn 245	5400	4200	2990	3.08	2.82	2.75	34.60 — .62	2.46 — 2.39
	22	Weber Deep	Sn 321	7440	4300	2990	3.07	2.81	2.72	34.59 — .62	2.40 — 2.34
	23	Ambalau Basin	Sn 251	5330	3500	3470	3.08	2.77	2.72	34.59 — .60	—
	24	Manipa Basin	Sn 253	4360	3000	2990	3.15	2.89	2.85	34.58 — .60	—
	25	Butung Trough	—	4180	3600	—	—	—	—	—	—
	26	East Flores Trough	Sn 317	3350	2300	2500	3.19	2.98	2.97	34.61	2.44 — 2.42
	27	Flores Basin	Sn 180	5130	2450	2500	3.25	3.04	2.97	34.55 — .60	2.28 — 2.21
	28	Wetar Basin	Sn 377	3460	2400	2500	3.17	2.96	2.92	34.61 — .63	2.40 — 2.36
	29	Sawu Basin	Sn 159	3470	2100	2250	3.39	3.20	3.13	34.54 — .59	2.26 — 1.86
	30	Salajar Trough	Sn 187	3370	1350	1750	3.86	3.72	3.66	34.60	2.22 — 2.17
	31	Halmahera Basin	Sn 353	2040	700	—	—	—	7.54	34.60 — .63	2.95 — 2.86
	32	Kau Bay	Sn 278	502	45	75	28.17	28.15	28.15	34.14 — .48	3.00 — H_2S
		Java Trench	Sn 146	7140	—	4475	1.17	0.80	0.77	34.69 — .72	4.33 — 4.22
	33	Andaman Basin	—	4360	~1800	—	—	—	—	—	—
	34	Timor Trench	Sn 118	3310	1940	2250	2.77	2.60	2.57	34.68 — .69	3.06 — 2.88
	35	Aru Basin	Sn 104	3680	1500	2240	3.89	3.70	3.63	34.63 — .65	2.37 — 2.25

mixing in the central parts of the basins than along their periphery. The depth of the temperature minimum increases due to the mixing in the direction of the flow of the deep water.

Some remarks may be made about the conditions within the primary and the secondary basins. In a primary basin the minimal temperature will always be found below the sill depth because of the mixing effect. The difference between sill depth and the depth of the temperature minimum can be a measure of the intensity of the replacement with bottom water, the more intense the water exchange is, the smaller this difference must be. Thus, the minimum in the certainly well ventilated Morotai Basin is only 150 m below the sill, while in the poorly ventilated Celebes and Banda Basin the minimum is about 1000 m below the sill, and in the insufficiently ventilated Kau Bay as in some smaller basins within the Philippines, no minimum is found. A secondary basin on the other hand will have almost the same conditions as its primary

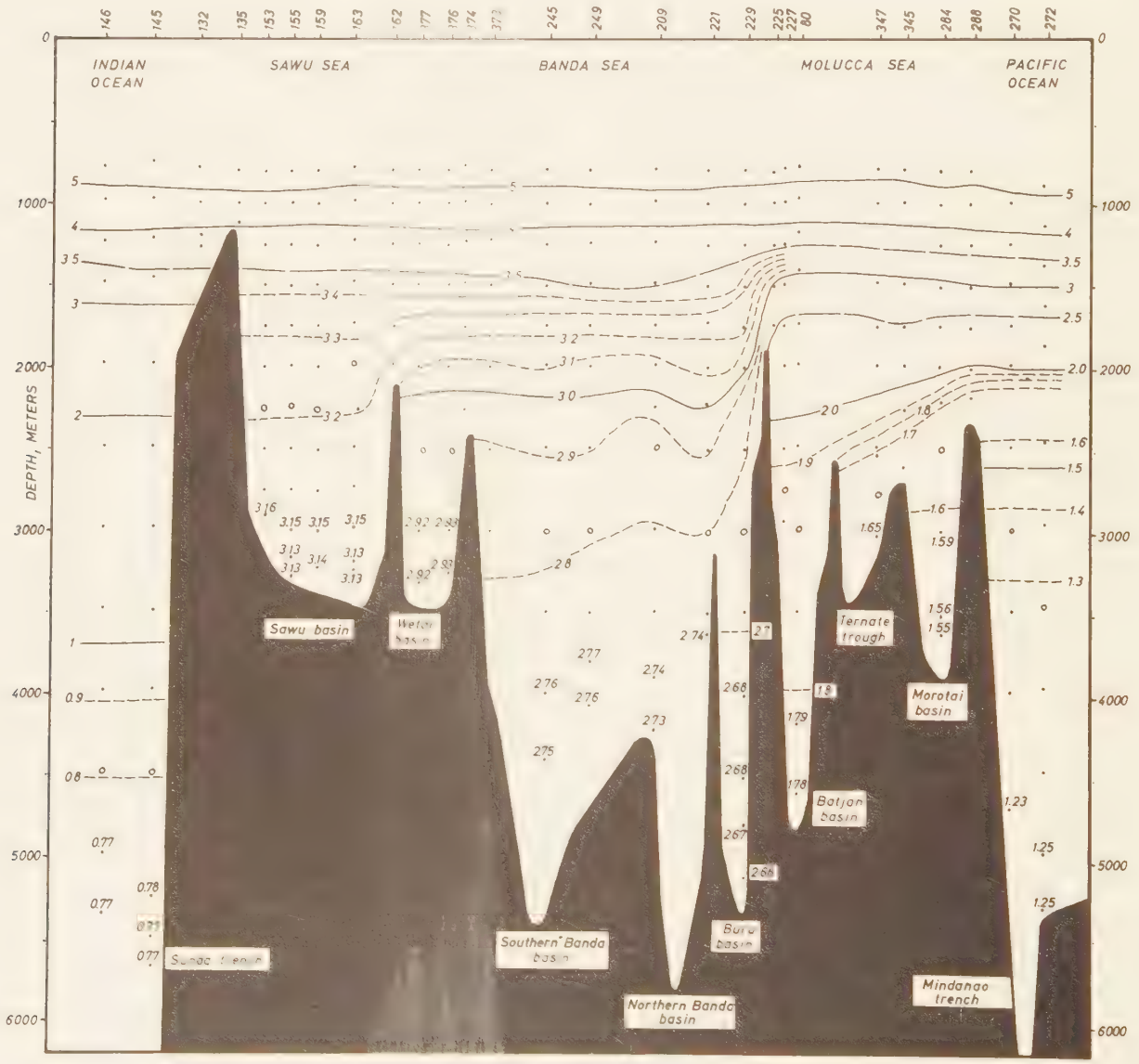

Fig. 6·25. Section of the potential temperature through the Eastern Archipelago from the Pacific to the Indian Ocean. Values give potential temperature, dots indicate observations, circles the depth of the observed temperature minimum.

basin, if the connection is below the temperature minimum, as it is in the case of the three basins of the Banda Sea. A small increase of the temperature in the minimum and of its depth, must, however, be neglected. But if the sill of the secondary basin lies above the depth of the temperature minimum in the primary basin, the minimum in it must have a higher temperature according to the circulation in it. Such a case is found in the Wetar and Sawu Basins.

The vertical distribution of the potential temperature in some basins of the Banda and Molucca Seas is presented in figure 6 · 26. It shows the typical exponential decrease of potential temperature with depth, which approaches the asymptotic value of constant potential temperature. The shape of the curves is given by the conduction of heat penetrating into the basin from higher levels and by the ascending motion of the water masses in the basin. A theoretical treatment of the problem is given in the following.

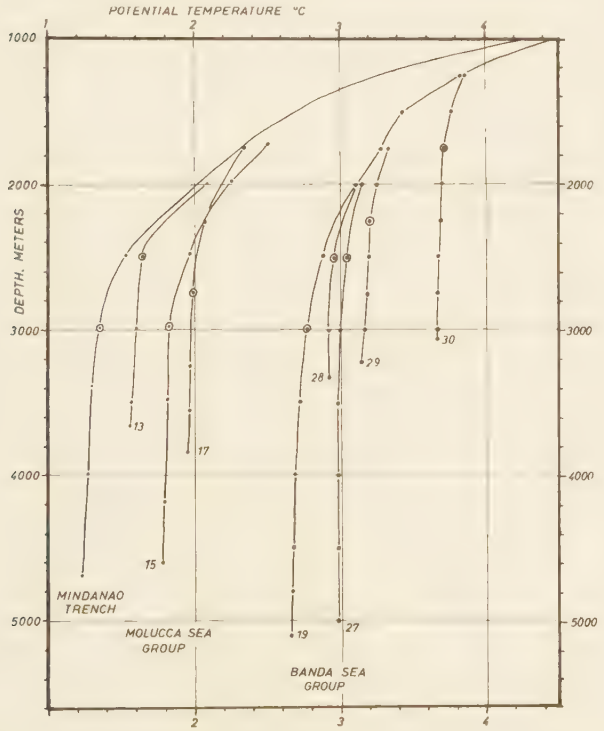

Fig. 6·26. Vertical distribution of potential temperature in different deep sea basins. Numbers refer to those used in table 7. Circles indicate depth of the observed temperature minimum.

Into a basin of depth D and area F with vertical walls a current with transport T (cm^3/sec) may flow over a sill and sink down to the bottom. To maintain the balance this downward movement must be compensated for by ascending motions with the average velocity w in the other parts of the basin. For the water balance of the basin it follows

$$T = F w$$

The inflowing water may have the temperature t_i so that if c is the specific heat of the water a quantity of heat $c T t_i$ enters the basin. The heat given off by the ascending movement in the depth z is then $c F w t$, and is bigger, because in all observed temperature distributions the potential temperature decreases down to the bottom. This flow of heat is, however, opposed by a turbulent conduction of heat from higher levels into the basin, which transports a quantity of heat equal to $c F A \frac{dt}{dz}$ downwards, where A is the coefficient of vertical eddy conductivity. The equation of the heat balance of the basin is therefore

$$T t_i = F w t - F A \frac{dt}{dz}$$

For the temperature t the potential temperature must be used, which is independent of vertical movements. From the two equations the relation

$$A \frac{dt}{dz} = w \ (t - t_i)$$

follows. If the vertical distribution of the temperature is known, the value of the quotient w/A can be calculated, because

$$\frac{w}{A} = \frac{1}{t - t_i} \frac{dt}{dz}$$

The vertical distribution of the temperature should follow the equation

$$t = t_i + t_o \, e^{\frac{w}{A} z}$$

To verify this, the logarithm of the potential temperature in four basins is plotted against the

depth in fig. 6·27. For w/A values between 1.2 and 1.8 10^{-5} result. Assuming a vertical eddy conductivity A = 4, as determined by Defant (1936) for the deep and bottom layer of the South Atlantic Ocean in nearly homogeneous water, vertical velocities of w = 5 to 7 10^{-5} cm/sec result. These values are of the same order as the average of w = 3 10^{-5} cm/sec derived by Stommel (1958) for the entire ocean. This value indicates, that the water exchange in these deep sea basins is comparatively intensive.

The curves given in fig. 6·27 demonstrate that the exponential decrease of the temperature starts in the Banda Sea in a depth of 1500 m. Above this level another value of w/A is found and it must be assumed that horizontal movements are of importance above this depth, so that the vertical flow of heat is no longer free of divergence. In the Sawu Sea this boundary is also found in 1500 m depth, essentially above the sill depth of the Banda Sea, but deeper than the connections with the Indian Ocean, which are 1100 m deep. In the Celebes Sea the break in the curve is in 1250 m depth, only a little above the sill at 1400 m. The only exception is the Sulu Sea, where the break in the curve is in about 1000 m while the sill is in 420 m. In the Sulu Sea above 1000 m also the highest value of w/A is found with 4.5 10^{-5}. With the assumption of the same velocity w for the ascending motion above and below 1000 m this indicates a smaller vertical eddy conductivity above 1000 m, which may be caused by the stronger density gradient and the higher stability in this layer. It must be remarked, that the break in the curve is just in the temperature minimum.

In general it can be said, that vertical distribution of potential temperature in the deep sea basins follows the theoretical required exponential decrease of temperature. The minimum of the temperature *in situ* develops in that depth, in which the vertical gradient of the potential temperature is equal to the adiabatic gradient. Assuming a certain value for A, the water exchange of the different deep sea basins can be calculated. From the velocity of the ascending motion w and the area F of the basin results the exchanged water volume T. In table 8, these values are calculated for four basins under the assumption A = 4.

The calculated transports vary between about 0.02 and 0.2 million m^3/sec, which are considerable quantities in these depths. A simple estimation of the transport over a sill gives, with a velocity of 5 cm/sec, a width of 20 km and a vertical extent of the current of 100 m a transport T of 0.1 million m^3/sec, which is of the same size. With these values it is also possible

Fig. 6·27. Relation between the depth and the logarithm of the potential temperature, referred to the lowest potential temperature, in four deep sea basins.

to estimate the time in which the water within a deep sea basin is renewed. At an ascending motion with the velocity w = 6 10^{-5} cm/sec the water in a 2000 m deep basin is renewed in

about 100 years. These values agree completely with those calculated by Postma (1958) from the distribution of specific alkalinity.

It is also of interest to estimate the influence of the conduction of heat through the ocean bottom on the temperature distribution in the deep sea basins. Numerically the conduction of heat from the interior of the earth is $Q = 0.1$ cal/cm^2/day $\approx 1.2\ 10^{-6}$ cal cm^{-2} sec^{-1}, according to Revelle and Maxwell (1952). Through the bottom of a deep sea basin of the area F flows the heat Q F. On the other hand the water volume T enters the basin in the same interval of time and absorbs this heat, when considering that the water is simultaneously distributed over the whole bottom of the basin. The increase of the temperature Δt is therefore given by the equation $Q\,F = c\,T\,\Delta t$, where c is the specific heat. Because of the relation $F\,w = T$, where w is the ascending velocity of the water in the deep sea basin, it follows $\Delta t = \frac{Q}{c\ w}$. With $w = 6\ 10^{-5}$, according to table 8, it results in an increase of the temperature of the ascending water by 0.02°C. Thus, under stationary conditions the water in a short distance above the bottom should be 0.02°C warmer than the invading water, but this temperature difference is difficult to observe. However, it is well known that in nearly all deep sea basins the potential temperature decreases down to the bottom with its lowest values directly above the bottom. Consequently, the influence of the heat conduction from upper layers is more important for the shape of the temperature curve in deep sea basins than the conduction of heat through the ocean bottom.

On the other hand the water invading the deep sea basin can flow a long distance in a relatively narrow band along its bottom. Considering a bottom current of transport T and a width b flowing over a distance L, the increase of the temperature Δt is given by the equation $Q\,b\,L = c\,T\,\Delta t$. With a transport $T = 0.1\ 10^{12}$ cm^3/sec of a width $b = 100$ km over a distance $L = 2000$ km follows an increase of the temperature of the bottom current by 0.024°C. But this increase is practically not observable, because it is near the limits of the accuracy of the temperature observations and a very careful elimination of the adiabatic effect would be necessary because the bottom currents normally do not flow horizontally. Moreover it must be mentioned that this bottom current, which extends over a width of 100 km at a transport of 0.1 million m^3/sec has a velocity of 2 cm/sec, when considering its vertical extent to be 50 m. It would need three years to flow over the distance of 2000 km. Concluding, it can be said that the conduction of heat through the ocean bottom has no measurable influence on the temperature distribution in the deep sea basins, if they are of comparatively small size.

Further conclusions on the processes in deep sea basins can be drawn from the distribution of the oxygen content. Upon first examination of the data it is surprising to note that the oxygen content is rather high in almost all deep sea basins and that it is often nearly constant below the sill. This fact indicates a quite good ventilation of all basins, but also a very low rate of consumption.

Considering first the vertical distribution of

TABLE 8

Values of the water exchange in four deep sea basins.

Basin	w/A	w cm/sec	F cm^2	T cm^3/sec
Banda Basin	$1.4\ 10^{-5}$	$5.6\ 10^{-5}$	$32\ 10^{14}$	$18\ 10^{10}$
Celebes Basin	1.8	7.2	22	16
Sawu Basin	1.6	6.4	4	2.6
Sulu Basin	1.2	4.8	12	5.8

the oxygen content n, it is governed by the differential equation

$$w\frac{dn}{dz} - A\frac{d^2n}{dz^2} = -e$$

if all horizontal gradients are vanishing. The rate of consumption of oxygen is -e. The solution of this equation is

$$n - n_0 = -\frac{e}{w}z + n_2 e^{-\frac{w}{A}z}$$

The constants n_0 and n_2 are definitely determined, if the values of the oxygen content n are given in two levels, for instance at the bottom and in the sill depth. Above the sill depth normally horizontal gradients and movements are present, so that the equation is no longer applicable.

The four possible types of the vertical distribu-

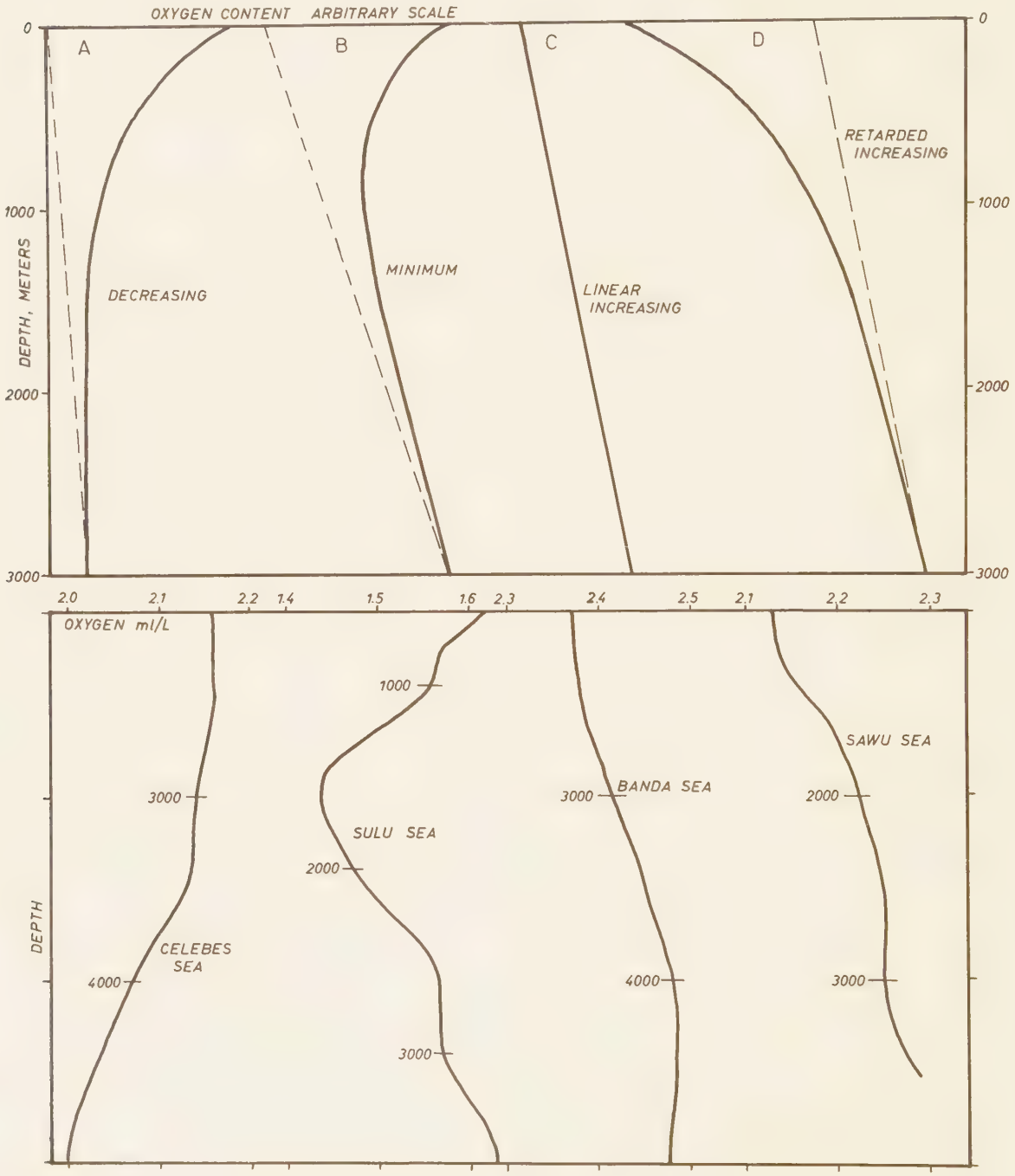

Fig. 6·28. Upper part: Possible vertical distribution of oxygen content in deep sea basins below sill depth according to theory.
Lower part: observed oxygen distributions.

tion of oxygen are presented in fig. 6 · 28 and show a simple decrease (A), a curve with a minimum (B), a linear increase (C), or a retarded increase (D) of the oxygen content below the sill. Four observed curves are presented for comparison and show that such oxygen distributions are actually observed, even if the scattering of the values is rather high. The value $w/A = 1.5\ 10^{-5}$ is taken for the exponent, as it is determined from the temperature distribution. In the Celebes Basin a more or less continuous decrease of the oxygen content with depth is observed so that the bottom water is of lowest oxygen content. This means that here the inflowing water is of lowest oxygen content and that the increase of the oxygen is caused by the turbulent diffusion from higher levels. In the Sulu Basin an oxygen minimum is observed in about 1500 m depth, the distribution corresponds to the curve (B). Here the bottom water is relatively rich in oxygen, which is partly consumed during the ascent of the water, until in the higher parts the turbulent flow of oxygen from the upper layers causes again an increase of the oxygen content. This process causes a minimum in a certain depth. The two curves in the Banda and Sawu Basins show maximal values of oxygen at the bottom and a continual decrease to higher levels. Here a turbulent flow of oxygen from higher levels is not possible, because an oxygen minimum lies a little above the sill depth. Therefore the inflowing water is of highest oxygen content, which is decreased during the ascending motion and passes over into the oxygen minimum.

The curves from observed data compared with the theoretical formula allow the estimation of the magnitude of the oxygen consumption $-e$. The oxygen gradient $\frac{dn}{dz}$ is smaller than 0.2/3000 m as shown in fig. 6 · 28. With a vertical upward velocity $w = 6\ 10^{-5}$ the value $0.4\ 10^{-10}$ for $-e$ results. This value corresponds well with that of $0.42\ 10^{-10}$ found by Riley (1951) in the Atlantic Ocean in 2000 m depth. Assuming a consumption of $0.4\ 10^{-10}$, an oxygen content of 2.0 ml/L in a deep sea basin without renewing its water would reach zero after 1700 years. This is a time much longer than the normal climatic fluctuations, and it must be assumed, that at least during each of them a renewing of the water in the basin occurs. On the other hand it could be shown from the distribution of temperature, that the water within the basins is renewed continuously during a period of the order of 100 years, but this is much faster than the consumption of oxygen would take. Thus, the distribution of the oxygen content in most of the deep sea basins seems to be determined more by an inflow of water of varying oxygen content than by the consumption. This explains also the fact, that the oxygen content is relatively independent of the depth and shows usually maximal values in the deepest layers. It must be mentioned, however, that immediately at the bottom an increased consumption of oxygen takes place, causing an oxygen minimum directly at the bottom, as observed at many stations of the SNELLIUS expedition.

The horizontal distribution of the oxygen content in the different deep sea basins shows a decrease in the direction of the flow of the bottom water. This decrease caused by consumption amounts in the Celebes Basin to about 0.1 ml/L in 500 km. Assuming a consumption of $0.4\ 10^{-10}$, as determined above, a velocity of the bottom current of $2\ 10^{-2}$ cm/sec results. Such an extremely small value, however, cannot be called a velocity, but demonstrates only how slowly the bottom water spreads in enclosed deep sea basins. On the other hand it cannot be assumed, that the spreading of the properties of the water occurs by mixing only, but it must be assumed, that real displacements of the water masses take place.

Very little is known about the process of the flow over the sills. The few direct current observations of the SNELLIUS, which were obtained over sills, give no conclusive proof of such currents. At some stations the observed velocities of above 20 cm/sec are rather high, but they are very often just at right angles to the expected direction of the flow over the sill. Tides seem to play an important role in the flow over the sills,

but also this is only an assumption. Using oxygen observations, Keunen (1948) has tried to show, that the water masses are deflected by the effect of the coriolis force during their spreading within the basins, so that the maxima of the oxygen content are displaced to the right in the northern hemisphere and to the left in the southern hemisphere. Also from this effect it must be concluded, that the spreading of the water masses is a real flow and is not due only to mixing.

6·8 SUMMARY: THE WATER MASSES AND THEIR MOVEMENTS IN THE EASTERN ARCHIPELAGO

The Southeast Asian Waters are a region, in which the last branches of water masses present in the two adjoining oceans are mixed. In the Pacific Ocean off the entrances to the Molucca Sea the water masses are still relatively differentiated, but in the eastern Indian Ocean at station Sn 146 and others off the entrances to the Sawu

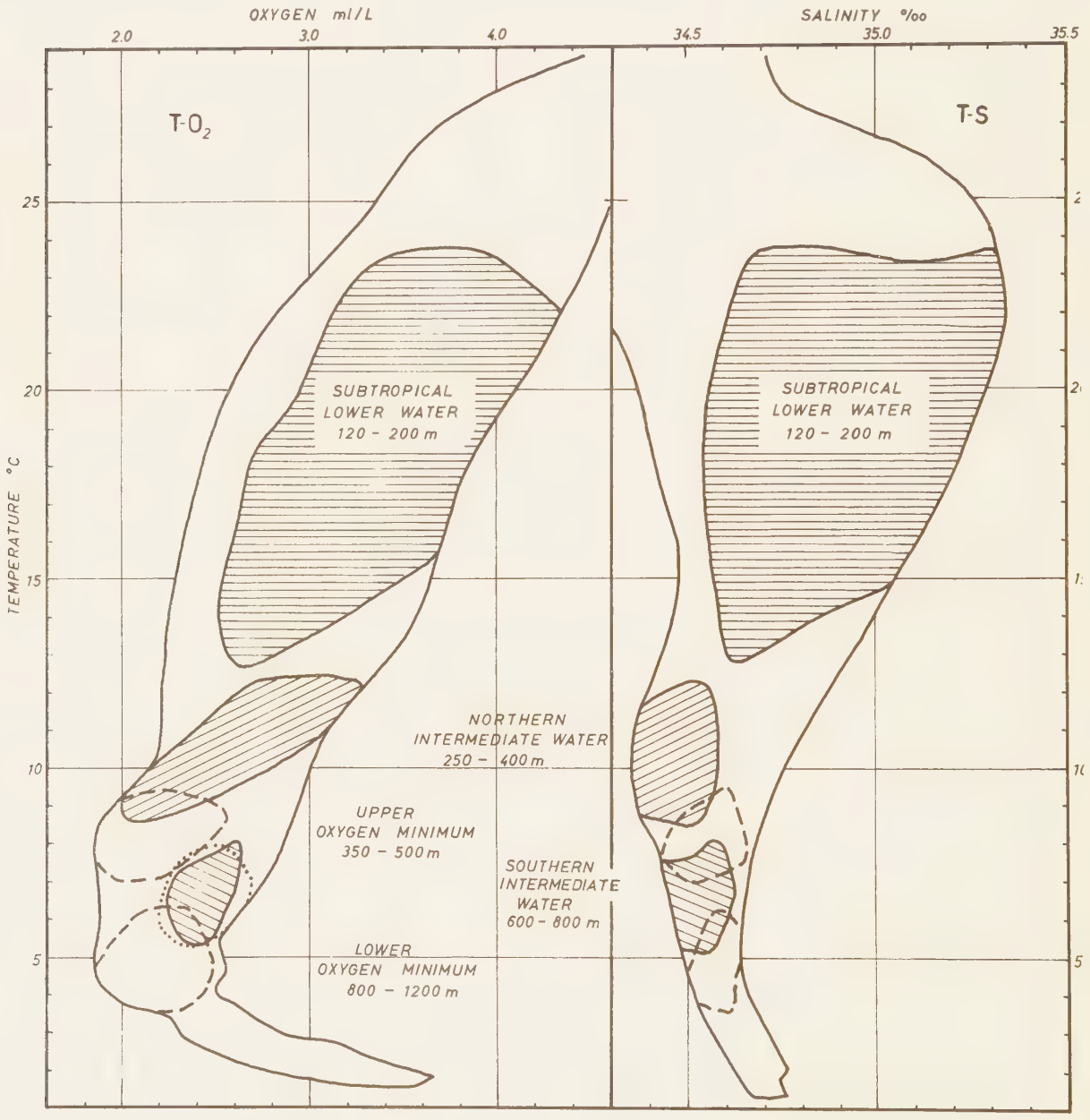

Fig. 6·29. Positions of the various core layers in the Eastern Archipelago within the T-S and T-O_2 diagram and envelopes of all T-S and T-O_2 curves. The dotted line gives the position of the intermediate oxygen maximum.

and Timor Seas, the salinity from the surface to the bottom is within an interval of 0.25‰. The Eastern Archipelago is therefore filled primarily with water of the Pacific Ocean, not only because of the deeper and wider entrances from the Pacific, but also because of dynamical conditions. Throughout the year the sea level in the western Pacific Ocean is higher than that in the region south of Java, so that a stationary slope from the Pacific to the Indian Ocean exists, as shown in Section 7·6. The hydrographic boundary between the two oceans lies practically at the southern entrances of the Sawu and Timor Seas, because the more important water masses of the Pacific Ocean can be followed to there.

Based on data from all SNELLIUS, DANA and SAMUDERA stations, the temperature-salinity and temperature-oxygen diagrams in fig. 6·29 were drawn to show the characteristics of these water masses. The envelopes of the TS and TO_2 relations of all stations are entered and show, below a surface layer with low salinities and high oxygen values, water masses of high salinity within the discontinuity layer. Below them a layer of lower oxygen content and lower salinity is found. Within this layer also the absolute variations of the properties become much smaller. Below a temperature of 4°C the oxygen content as well as the salinity increase again, but the variations of the properties converge towards the values of the bottom water.

Within the discontinuity layer the Subtropical Lower Water is situated in depths between 120 and 200 m, and is marked by a salinity maximum. The salinity in its core layer is higher than 34.6‰, its oxygen content is between 2.6 and 4.3 ml/L and the maximum occurs at temperatures between 24 and 13°C. Below it, in the layer of lower salinity and oxygen content, the two Intermediate Waters are found each with a salinity and an oxygen minimum. The northern Intermediate Water is found in depths between 250 and 400 m at temperatures between 9° and 12°C. The salinity in its core varies only a little between 34.4 and 34.6‰. The oxygen content in its core is relatively high, but in every case higher than in the oxygen minimum below it. This is an indication that this water mass was of high oxygen content at its formation. At the lower boundary of the Intermediate Water an oxygen minimum is found in depths between 350 and 500 m. The salinity in its core is higher than in the core of the Intermediate Water, the oxygen content is everywhere lower than 2.5 ml/L. In depths between 600 and 800 m the Southern Intermediate Water is found at temperatures between 5° and 8°C. The salinity is a little higher than that in the core of the Northern Intermediate Water and varies between 34.45 and 34.65‰. The oxygen content in the core of the Southern Intermediate Water varies between 2.2 and 2.6 ml/L and is higher than in the oxygen minima above and below it. Therefore the layer of minimal salinity is locally developed also as a layer of maximal oxygen content. This is in accordance with the origin of the Southern

TABLE 9

Properties of subsurface water masses in the Eastern Archipelago.

Water Type	Characteristic	T	S	O_2
Northern Subtropical Lower Water	S maximum	23-15	34.6 -35.1	3.3-4.3
Southern Subtropical Lower Water	S maximum	24-13	34.6 -35.3	2.6-3.6
Northern Intermediate Water	S minimum	12-9	34.4 -34.6	2.0-3.3
	O_2 minimum	9-7	34.45-34.65	1.8-2.5
Indian Ocean Oxygen Minimum	O_2 minimum	8.5-6	34.50-34.65	< 2.3
Southern Intermediate Water	S minimum	8-5	34.45-34.65	2.2-2.6
	O_2 minimum	6-4	34.5 -34.6	1.8-2.5
Deep Water	T minimum	< 4	34.65-34.75	different

Intermediate Water at the surface as a water mass of high oxygen content. The lower oxygen minimum is found throughout the Archipelago, but consists of two water types. One is of Pacific origin and lies at the lower boundary of the Southern Intermediate Water in depths between 800 and 1200 m. The other type originates from the Indian Ocean and lies slightly higher, but the oxygen content remains everywhere below 2.5 ml/L. Table 9 summarizes the properties of these water masses.

To follow the inflow and the spreading of the different water masses within the Eastern Archipelago two longitudinal sections (plate 38) were constructed demonstrating the distribution of salinity and oxygen content. Section I runs from the region south of Mindanao through the Celebes Sea, the Macassar Strait over the ridge at its southern entrance into the Flores Sea. Section II runs from the region north of Halmahera through the Molucca Sea, the Buru Sea into the Banda Sea and from there through the Timor Sea into the Indian Ocean. The two sections pass through rather deep basins, but the more interesting features appear in the upper layers, so a logarithmic scale was used for the depth. Thus, the depth between 100 and 500 m appears the same size as the depth between 1000 and 5000 m, so distorting the bottom topography. Section I shows in depths between 100 and 200 m the spreading of the Northern Subtropical Lower Water with the salinity maximum in its core. Within this water mass the oxygen content decreases continuously with depth. In depths between 250 and 500 m occurs a zone with salinities below 34.5‰ whose core is the salinity minimum of the Northern Intermediate Water. Also within this water mass the oxygen content decreases progressively downwards until it reaches an oxygen minimum at its lower boundary. But this is developed only south of Mindanao and in the Celebes Sea, later it is no longer recognizable because the oxygen content decreases too rapidly with depth. In this section the Southern Intermediate Water no longer appears as a salinity minimum. But the lower oxygen minimum is found as in the whole Archipelago and lies in 1000 m depth. Outside the Celebes Sea the oxygen content below the minimum increases again and the salinity also increases to over 34.65‰. Water masses of less than 34.6‰ and of an oxygen content below 2.2 ml/L only penetrate into the Celebes Sea, they originate out of the range of the oxygen minimum. The oxygen minimum itself has values between 2.0 and 2.1 ml/L and its increase with depth is therefore only small. In the southern part of the Macassar Strait the oxygen content is lower than 2.0 ml/L, indicating that the replacement of the water masses takes place very slowly, this is caused by the ridge at its southern entrance, which prevents a water exchange below 800 m depth. The observations, however, indicate that parts of the water of lower salinity ascend and penetrate over this sill into the Flores Sea. The relatively low oxygen content of the Celebes Basin seems to be completely explained by the unfavorable position of its sill in the depth of the oxygen minimum.

In its northern part section II shows the layer of maximal salinity of the Subtropical Lower Water in depths between 100 and 400 m. In the region northwest of Halmahera two maxima are to be observed, the upper belonging to the northern, the lower to the southern Lower Water. The spreading of these two branches of the Lower Water ends in the Molucca Sea off the Lifamatola Strait. The branch of the Lower Water, visible again in the Ceram and Banda Seas in about 200 m depth, comes through the Halmahera Sea and spreads southwards through the Buru Sea. It belongs to the Southern Subtropical Lower Water. The depth to which the water of high salinity extends, which is 500 in the Buru Sea, is remarkable. This is due to the absence of the Northern Intermediate Water and to the deep position of the Southern Intermediate Water in about 800 m. South of the Banda Sea the Lower Water can no longer be identified as a uniform water mass, even though it is recognizable at individual stations. In the region north and west of Halmahera in depths between 500

and 1500 m the layer of the Southern Intermediate Water is found, where the salinity decreases below 34.6‰. The core of this layer is in about 800 m depth.

The oxygen content decreases from the surface continuously to depths between 600 and 1000 m. In the northern part of the section it reaches its minimum in about 1000 m depth below the core layer of the Southern Intermediate Water. The oxygen values in the minimum are below 2.4 ml/L, the water itself is part of the Southern Intermediate Water. In the southern part of the section and in the Banda Sea the oxygen minimum is higher in depths between 500 and 800 m. The oxygen values are lowest with less than 2.0 ml/L in the Indian Ocean and increasing to more than 2.2 ml/L in the Banda Sea. This distribution of the oxygen content indicates that the minimum in the Banda Sea has been influenced by the Indian Ocean. But it must be assumed, that not real movements, but mixing processes allow penetration of the layer of minimal oxygen content between 500 and 700 m into the Banda Sea. It is also likely that the processes usually causing the formation of an intermediate oxygen minimum in the oceans, are effective here. A conclusion about this question can only be expected after the biological processes causing such intermediate oxygen minima have been examined. In the Eastern Archipelago the layer of minimal oxygen content is also a layer of minimal horizontal movements.

In this longitudinal section the oxygen minimum lies considerably above the sills and water of higher oxygen content can enter the basins. Consequently, in all deep sea basins essentially higher oxygen contents are found than in the oxygen minimum, in contrast to the conditions in the Celebes Sea. The salinity in the depth is everywhere higher than 34.6‰, in the Timor Sea values above 34.7‰ are found in the bottom layer as an influence of the Indian Ocean. In the southern part of the section the first traces can be recognized of the water flowing out of the Timor Sea at a depth of 1000 m and forming a salinity minimum in the Indian Ocean. It lies clearly below the oxygen minimum, which originates in the Indian Ocean.

The spreading of the different water types within the Eastern Archipelago is presented schematically in fig. 6 · 30 and 6 · 31 in a longitudinal section from the Pacific to the Indian Ocean and in six charts showing the horizontal movements within the different core layers. The Subtropical Lower Water, which is divided into three different types, spreads within the discontinuity layer between 100 and 200 m depth. The northern Lower Water of the Pacific Ocean spreads over the Celebes Sea and the Molucca Sea and penetrates through the Macassar Strait into the Flores Sea. The Southern Lower Water penetrates through the Halmahera Sea into the Ceram Sea and spreads from there at both sides of the islands Buru and Ceram into the Banda and the Arafura Seas and penetrates to the Timor Sea. The boundary against the Northern

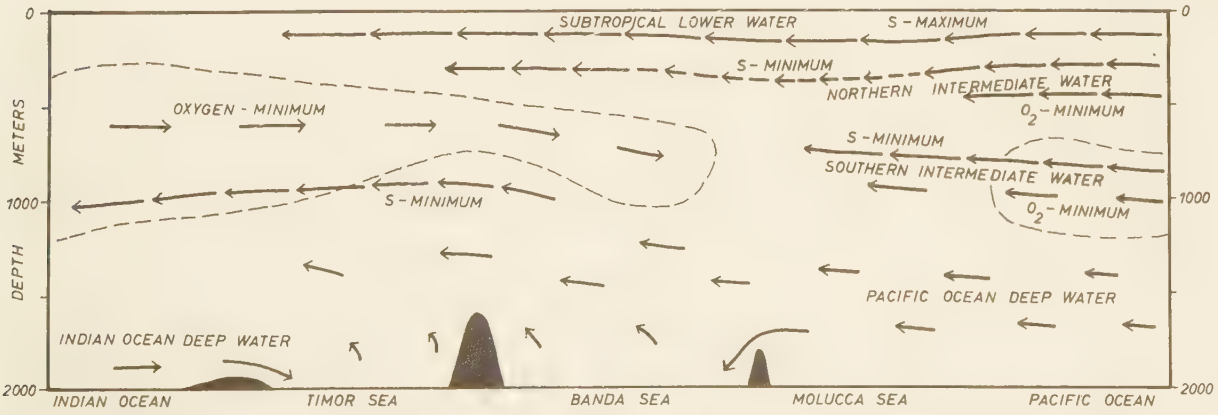

Fig. 6·30. Schematic representation of the position of the core layers of the different water masses in a section from the Pacific to the Indian Ocean.

Fig. 6·31. Schematic representation of the horizontal distribution and the movements of the different water masses in the Eastern Archipelago.

Lower Water in the Flores Sea seems to be subject to considerable annual variations, because the lower water is still under the influence of the monsoon circulation in the surface layer. The Subtropical Lower Water of the Indian Ocean is restricted to it, in the Sawu and Timor Seas the salinity maximum of the Lower Water is found at only few stations.

Below the discontinuity layer the Northern Intermediate Water is situated. It enters the Celebes Sea with the Mindanao Current and penetrates through the Macassar Strait into the Flores Sea. From here it spreads further than the Lower Water into the Banda Sea and its last traces can be recognized in the Timor and Arafura Seas, but it does not penetrate into the Molucca Sea and the northern parts of the Banda Sea. This fact is indicated by broken arrows showing the spreading of the salinity minimum in the schematic longitudinal section (fig. 6 · 30). Immediately below the salinity minimum the oxygen minimum is situated in the lower parts of the Northern Intermediate Water, but it is found only in the Celebes Sea.

The salinity minimum of the Southern Intermediate Water of the Pacific Ocean is well developed in the region north of New Guinea, but it penetrates only a little into the Molucca Sea, and in the Celebes Sea it is not found as a salinity minimum. An oxygen minimum below its core layer belongs to the Southern Intermediate Water. In the Banda Sea no lower salinity minimum is found, but it occurs again in the Indian Ocean, where water masses of low salinity penetrate from the Sawu and Timor Sea and form a minimum in 1000 m depth. Here it must be mentioned that the oxygen minimum of the Southern Intermediate Water of the Pacific Ocean and that of the Indian Ocean are not the same water mass, although the isolines in the oxygen section II could indicate this. The oxygen minimum of the Pacific Ocean lies in the lower parts of the Southern Intermediate Water and penetrates with it into the Molucca Sea. The oxygen minimum of the Indian Ocean on the other hand lies at essentially higher temperatures, and it is questionable whether this water mass has a distinct direction of movement. It originates, however, from the Indian Ocean, as indicated in the longitudinal section (fig. 6 · 30). The water entering the Indian Ocean in 1000 m depth can hardly be considered to be the extension of the Southern Intermediate Water, but it is more a new water mass formed by mixing of the Intermediate Water and deep water, which penetrates into the Indian Ocean.

The deep water between 1000 and 1500 m depth is a water mass flowing very slowly from the Pacific to the Indian Ocean and is carrying away simultaneously the water masses ascending out of the deep sea basins. The passages between the different basins in this depth are, however, so small that these movements must be extremely slow, especially over the large basins. One branch of the deep water enters the Celebes Sea on both sides of the Sangihe Islands and penetrates further into the Macassar Strait. At its southern end it must ascend and pass the ridge connecting Celebes and the Sunda Shelf. This does seem to happen and is indicated in section I. Another branch enters through the Molucca Sea and passes through the Lifamatola Strait, which is the only connection with the Buru Basin. Here it can split off to three sides and comes into the Banda Sea and the Arafura Sea. Through the very narrow passages east of Wetar the deep water then flows into the Sawu and Timor Seas and to the Indian Ocean.

The flow of the bottom water has already been discussed by van Riehl (1934). It enters the Celebes Sea north of the Sangihe Islands and flows probably along the northern side of the basin. In the Molucca Sea the bottom water flows within the trough along the west coast of Halmahera to the south, turns off the Lifamatola ridge to the west and enters the Gorontalo Basin from the south. The water masses passing the Lifamatola Sill come into the Buru Basin and into the Banda Basin and spread to all sides, into the Manipa Basin, into the Weber Deep, into the Flores Basin and into the Salajar Trough. From the Weber Deep the bottom

water penetrates over the sill northeast of Timor into the Wetar and the Sawu Basins. Another branch of the bottom water spreads from the Buru Basin into the Aru Basin. From the Indian Ocean the Timor Trough is supplied with bottom water and one branch penetrates to the Aru Basin. The water masses passing the different sills seem to sink behind them relatively rapidly to the bottom of the basins and there spread further along the bottom. Consequently in the other parts of the basins ascending movements must take place to compensate for these water masses. This ascending water is carried away horizontally as soon as it comes into the range of the deep current. This process is schematically indicated in fig. 6 - 30. Naturally all these movements are extremely slow, this is obvious from the transports of the magnitude of 0.2 million m^3/sec replacing the water in the deep sea basins.

In general the following picture results for the circulation within the Southeast Asian Waters. At the surface the monsoon circulation exists, which is subject to strong annual variations. It has, however, one branch, the Timor Current continuously giving off water to the Indian Ocean. Below these layers the spreading of the Subtropical Lower water and of the Northern Intermediate Water takes place according to the general surface gradient from the Pacific to the Indian Ocean, but with decreasing intensity with depth. Below them and especially in the southern parts of the region a nearly motionless layer seems to exist, in this the oxygen minimum is situated. In the deep layer again movements from the Pacific to the Indian Ocean take place, which also replace the water of the deep sea basins. Thus in all layers with the exception of that of the oxygen minimum, movements from the Pacifc to the Indian Ocean predominate.

LITERATURE

Bruneau, L., N. G. Jerlov and F. F. Koczy

1953. Physical and chemical methods.
Rep. Swed. Deep-Sea Exped. 3(4) : 99-112.

Carlsberg Foundation, Copenhagen.

1937. Hydrological observations made during the "Dana" expedition, 1928-30, with an introduction by Helge Thomsen.
Dana Rep. 2(12) 46 pp.

Defant, A.

1936. Ausbreitungs- und Vermischungsvorgänge im antarktischen Bodenstrom und im subantarktischen Zwischenwasser.
Dtsch. Atlantische Exped. Meteor 1925-27. 6 (2) : 55-96.

Germany. Reichsmarineamt.

1909. Die Forschungsreise S.M.S. Planet, 1906-1907. Berlin.

Graham, H. W.

1952. A contribution to the oceanography of the Sulu Sea.
Proc. 7th. Pacif. Sci. Congr. 3 : 225-266.

1957. The topography of the sea surface in the region of the Philippines.
Proc. 8th Pacif. Sci. Congr. 3 : 673-8.

Indo Pacific Fisheries Council

1952. Philippine fisheries, Manila, 185 pp.

Japan. Hydrographic Department.

1950-55. Hydrogr. Bull. Spec. Nos. 3-16.

Koenuma, K.

1937. On the hydrography of the southwestern part of the North Pacific and the Kurosio.
I. General Oceanographic features of the region.
Mem. Mar. Obs. Kobe. 6 : 279-331.

1938. II. Characteristic water masses which are related to this region and their mixtures, especially water of the Kurosio.
Mem. Mar. Obs. Kobe. 6 : 349-413.

1939. III. Oceanographic investigations of the Kurosio area and its outer region, development of ocean currents in the North Pacific.
Mem. Mar. Obs. Kobe. 7 : 41-114.

KUENEN, P. H.
1948: Influence of the earth's rotation on ventilation currents of the Molucca deep sea basins.
Proc. Kon. Ned. Akad. Wet. 51 : 417-426.

MEGIA, T. G., and D. V. VILLADOLID
1953. A contribution to the knowledge of the structure and composition of the water masses off eastern Philippines.
Philipp. J. Fish. 2 (1) : 59-67.

MÖLLER, L.
1929. Die Zirkulation des Indischen Ozeans.
Veröff. Inst. Meeresk. Univ. Berlin NFA. 21, 48 pp.

POSTMA, H.
1958. Chemical results and a survey of water masses and currents.
Snellius Exped. 2 (8) 116 pp.
1959. Tables. Oxygen, hydrogen ion, alkalinity and phosphate.
Snellius Exped. 4 35 pp.

RAO, C. P.
1956. Water masses in the Bay of Bengal.
Curr. Sci. 25 : 51-33.

REVELLE, R., and A. E. MAXWELL
1952. Heat flow through the floor of the eastern North Pacific Ocean.
Nature, Lond. 170 : 199-200.

VAN RIEHL, P. M.
1932. Einige ozeanographische Beobachtungen im Roten Meer, Golf von Aden und Indischen Ozean.
Ann. Hydrogr. Berl. 1932 : 401-7.
1934. The bottom configuration in relation to the flow of bottom water.
Snellius Exped. 2(2) 63 pp.
1943. The bottom water. Introductory remarks and oxygen content.
Snellius Exped. 2(5) 1. 77 pp.
1956. The bottom water. Temperature.
Snellius Exped. 2(5) 2. 60 pp.

VAN RIEHL, P. M., HAMAKER, H. C., and L. VAN EYCK
1950. Serial and bottom observations.
Snellius Exped. 2(6) 44 pp.

RILEY, G. A.
1951. Oxygen, phosphate and nitrate in the Atlantic Ocean.
Bull. Bingham Oceanogr. Coll. 13(1) : 1-26.

SCHOTT, G.
1926. Die Tiefwasserbewegungen des Indischen Ozeans.
Ann. Hydrogr. Berl. 1926 : 417-431.
1935. Geographie des Indischen und Stillen Ozeans.
Hamburg. C. Boysen. 413 pp.

STOMMEL, H.
1958. The abyssal circulation.
Deep-Sea Res. 5(1) : 80-82.

SVERDRUP, H. U., F. M. SOULE, J. A. FLEMING, and others.
1944-45. Observations and results in physical oceanography.
Sci. res. Carnegie cruise VII Oceanography 1A VII, 156 pp.
Pub. Carnegie Inst. 545.

SVERDRUP, H. U., M. W. JOHNSON, and R. H. FLEMING
1942. The oceans, their physics, chemistry and general biology.
New York, Prentice-Hall, 1,087 pp.

THOMSEN, H.
1933. The circulation in the depth of the Indian Ocean.
J. Cons. Int. Explor. Mer. 8 : 73-79.
1935. Entstehung und Verbreitung einiger charakteristischer Wassermassen in dem Indischen und südlichen Pazifischen Ozean.
Ann. Hydrogr. Berl. 1935 : 293-305.
1937. Hydrological observations.
Dana Rep. 2(12). (SEE CARLSBERG FOUNDATION).

THORADE, H.
1931. Strömung und zugenförmige Ausbreitung des Wassers.
Gerlands Beitr. Geophysik 34 : 57-76.

Uda, M.
1957. On the circulation in the North Pacific in relation to pelagic fisheries.
Proc. 8th. Pacif. Sci. Congr. 3 : 663-672.

Villadolid, D. V.
1952. Philippine fisheries, Manilla. 185 pp.

Wattenberg, H.
1939. Die Entstehung der sauerstoffarmen Zwischenschicht im Ozean.
Ann Hydrogr. Ber. 1939 : 257-266.

Wüst, G.
1929. Schichtung und Tiefenzirkulation des Pazifischen Ozeans auf Grund zweier Längschnitte. Veröff. Inst. Meeresk, Berl. N.F.(A) 20. 64 pp.

1935. Zur Frage des indischen Tiefenstromes.
Naturwissenschaften 23 : 137-9.

1935. Die Stratosphäre.
Dtsch. Atlantische Exped. Meteor 1925-27. 6(1) 288 pp.

Wyrtki, K.
1956. The subtropical lower water between the Philippines and New Guinea.
Mar. Res. Indonesia 1 : 21-45.

Wyrtki, K.
1956. 1957. Oceanographic station list 1956, 1957.
Mar. Res. Indonesia 2 : 49-55. 3 : 57-69.

Chapter 7

THE DYNAMICS OF THE CIRCULATION

The description of currents, given in Chapter 3, can naturally not satisfy for a geophysical study which requires a comparison of the observed movements with the forces producing them and the derivation of numerical relations. The wind as an external force and the field of mass as an internal force lead to the deformation of the sea surface and to currents. The hydrodynamical differential equations combine these factors and, if the forces are known, permit the calculation of the currents and the topography of the sea surface, but the wind is the only independent factor, while the field of mass, the currents and the topography of the sea surface influence one another. Thus, normally it is not possible to treat these factors separately, because they form a unit and the circulation becomes only understandable by their interaction.

The theoretical treatment of such problems requires initially the confirmation of the validity of the theory by comparison of the observations with the theoretical results so that a physical statement may be made. However, the application of a theory may give quantitative information, which would be difficult to derive from observations, or may permit forecasts. In oceanography, quantitative information on mass transport and on the distribution of current velocity is of particular interest but it is difficult to secure from observations. On the other hand, it is simple to observe winds and sea level, and even the observation of the distribution of mass is much easier than that of the distribution of velocity.

The object of a dynamical investigation is therefore the determination of the mass transports in the different current branches. In a region like the Southeast Asian Waters, in which the circulation varies considerably under the influence of the changing monsoons, the annual variation of the circulation and of the transports will be of greatest interest. These waters are subdivided into many individual regions, which are connected in different ways, so that strong opposite influences between the various seas result, causing difficulties in the determination of the transports and their annual variations. On the other hand, some conclusions can be drawn from the equation of continuity, because the sum of all in- and out-flowing water in an individual sea must vanish.

The hydrodynamical differential equations form the basis for a theoretical treatment of the circulation. Disregarding the friction, they lead to the dynamical theory, which has been widely used for the calculation of transports. This theory permits the calculation of the mass transports from the known distribution of mass. The pressure gradients are balanced by the coriolis force. But in the vicinity of the equator the coriolis force becomes very small and vanishes at the equator, so that the theory no longer gives acceptable solutions. Thus, in the equatorial belt friction can no longer be neglected, because the pressure gradients are balanced by friction. Also when treating wind currents, the friction must be considered, because the action of the wind stress causes a continuous addition of energy, which must be compensated by friction. Because the Southeast Asian Waters are strongly subdivided and shallow in large parts, the frictional influences resulting from these boundaries cannot be disregarded.

Friction can be considered in different ways in the hydrodynamical differential equations, as lateral friction, bottom friction, vertical eddy viscosity or friction at internal boundaries. But it is not the purpose of these investigations to give special information about friction and therefore the friction is simply taken proportional to the velocity. If the transports and not the vertical distribution of the velocity are of more interest, some further simplifications of the hydrodynamical differential equations result.

The components of the mass transports between the surface and the depth D are given by

$$M^x = \int_0^D \rho\, u\, dz$$

(1)

$$M^y = \int_0^D \rho\, v\, dz$$

where ρ is the density and u and v the components of the velocity in the x and y direction. The differential equations of the stationary movements neglecting convective terms are

$$-f M^y + r M^x = \tau^x - P_x$$
$$f M^x + r M^y = \tau^y - P_y$$

(2)

$$P = \int_0^D p\, dz$$

$$p = \int_{-h}^{z} \rho\, g\, dz$$

$$M^x_x + M^y_y = -\rho\, w_D$$

where $f = 2\omega \sin\varphi$ is the coriolis parameter, r the friction coefficient, τ the wind stress, g the acceleration of the earth, p the pressure in the depth z and w_D the vertical velocity in the depth D. The lower indices indicate differentiations in x- and y- direction. These equations permit the calculation of the mass transport M without integrating differential equations, if the wind stress and the distribution of mass are given. The function P has to be calculated from the distribution of mass in the usual way. Simultaneously the vertical movements in the depth D are given by these equations. These vanish only if the mass transport M can be presented as the components of a stream function. If, however, the depth D is the very bottom, such a presentation is always possible. The system (2) has a solution also at the Equator, where $f = 0$. There the vector of the mass transport falls into the resultant wind vector and surface gradient.

In many cases it is possible to consider the density ρ to be constant within the layer D. In this case the equations become even simpler. If h is the topography of the sea surface, it follows $p = \rho\, g\, (z + h)$. The system (2) then becomes

$$-f M^y + r M^x = \tau^x - \rho\, g\, D\, h_x$$
$$f M^x + r M^y = \tau^y - \rho\, g\, D\, h_y$$

(3)

$$P = \rho\, g\, D\, (\frac{D}{2} + h)$$
$$M^x_x + M^y_y = -\rho\, w_D$$

The special properties of this system, the factor between transport and acting forces and the angle between both, have been discussed by Wyrtki (1956), where also numerical values of the friction coefficient r are given.

In the Southeast Asian Waters channel-like seas are often found with a flow in only one direction and without any remarkable cross circulation. In this case the system (3) can be integrated across the channel. Putting the X-axis in the direction of the channel and integrating over its width b, one obtains

$$\int_0^b M^y\, dy = 0 \text{ and } \int_0^b M^x\, dy = T$$

because the mass transport across the channel must vanish. T is the volume transport through the channel in m^3/sec. With the assumption of a wind independent of y, one obtains

$$r \rho T = b \tau^x - \rho\, g\, D\, b\, h_x$$

(4)

$$f \rho T = b \tau^y - \rho\, g\, D\, \Delta h^y$$

where Δh^y is the sea level difference between both coasts. These two equations will be used widely for the calculation of the transports in the following. The system (4) makes immediately clear the connection between wind, transport and sea level. A wind τ^x in the direction of the channel causes a transport T in this direction, its amount is determined by the friction r. A slope h_x present in the direction of the channel can intensify this transport, but also can bring it completely to rest, if it is strong enough and against the wind. The transport present in the direction of the channel induces a cross slope h_y because of the deflection due to the coriolis force. This cross slope can be intensified or diminished by a wind component τ^y across the channel. All these effects must be considered, when treating

the relations between wind, sea level and transports.

7 · 1 RELATIONS BETWEEN WINDS, SEA LEVEL AND CURRENTS

As already demonstrated in the discussion of the currents at the surface, the monsoon circulation within the Southeast Asian Waters takes place in either direction along the line China Sea-Java Sea-Flores Sea-Banda Sea. In this course the Java Sea is the sea with the smallest cross section. It is relatively narrow, of channel-like shape and always very shallow. The water masses are vertically homogeneous and the currents reach down to the bottom. Moreover the axis of the Java Sea lies about in the main wind direction during the two monsoons. So it is really the ideal region to be made the starting point of calculation of the transports within the monsoon currents.

The sea level observations used in the following are corrected for atmospheric pressure. Their relative heights are determined by comparing sea level differences with current observations. The given values refer to a levelling which is described in detail in Section 7 · 6 and adjusted to the 800 decibar surface.

For the JAVA SEA the annual variation of the sea level on the coast of Borneo (Musang Ketjil) and on the north coast of Java (Tuban) are presented in fig. 7 · 1 together with the sea level difference. During the southeast monsoon the sea level on the coast of Java is higher, due to the deflection of the water masses to the left in the southern hemisphere. From May to September the sea level falls at both stations, but the slope remains maintained. In October at the time of the change of the monsoons the slope practically vanishes and develops again but in the opposite direction in November and December. During the northwest monsoon the sea level is higher on the coast of Borneo. The wind over the Java Sea blows with a very high constancy from westnorthwest from November to March and from eastsoutheast from May to September. The currents are developed in the same direction and are given in fig. 7 · 1. In April and October the change of the monsoons takes place and also of the currents. The correlations between winds, currents and sea level differences are immediately visible, the relations between these factors are also presented. There is a clear relation between currents and cross slope, which allows the calculation of the transport according to equation (4). It is

$$f\,T = -g\,D\,\Delta h^y$$

and with the relation $T = b\,D\,v$, where v is the average velocity over the whole cross section, it results

$$f\,b\,v = -g\,\Delta h^y$$

Numerically, $f = 1.28\ 10^{-5}$ and $b = 3.3\ 10^7$ cm, and the relation between the velocity v and the cross slope Δh^y is

$$v = 2.3\ \Delta h^y$$

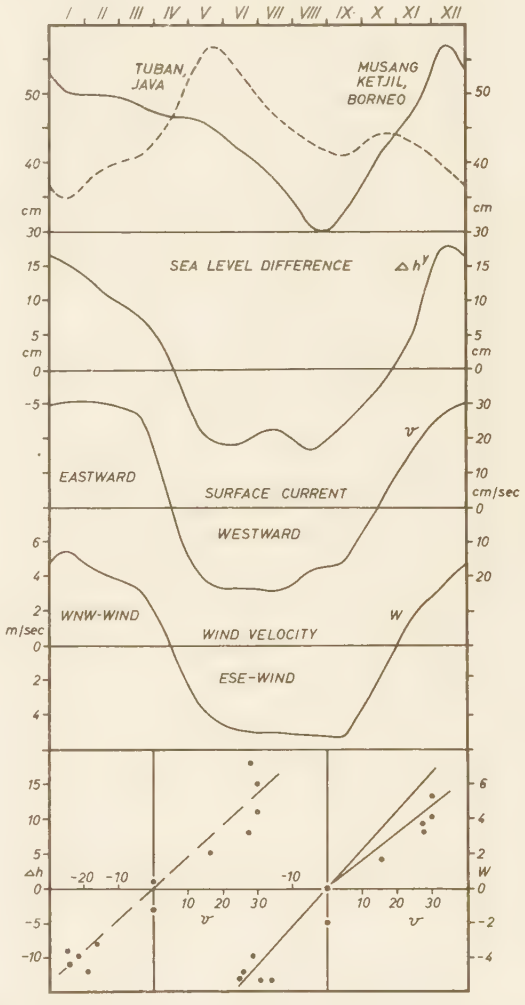

Fig. 7·1. Annual variation of dynamical factors in the Java Sea, demonstrating relations between sea level, sea level difference, current velocity and wind velocity.

This is in full agreement with the observations. The maximal transports at an average depth of 40 m amount to about 4.5 million m^3/sec during the northwest monsoon and to about 3.3 million m^3/sec during the southeast monsoon. These values correspond to those calculated by Berlage (1927) from current observations.

The relation between the wind and the current in the absence of a longitudinal slope is according to equation (4)

$$r \rho T = b \tau^x$$

or after the introduction of the velocity

$$r \rho D v = \tau^x$$

With a friction coefficient $r = 0.8\ 10^{-5}$ a velocity

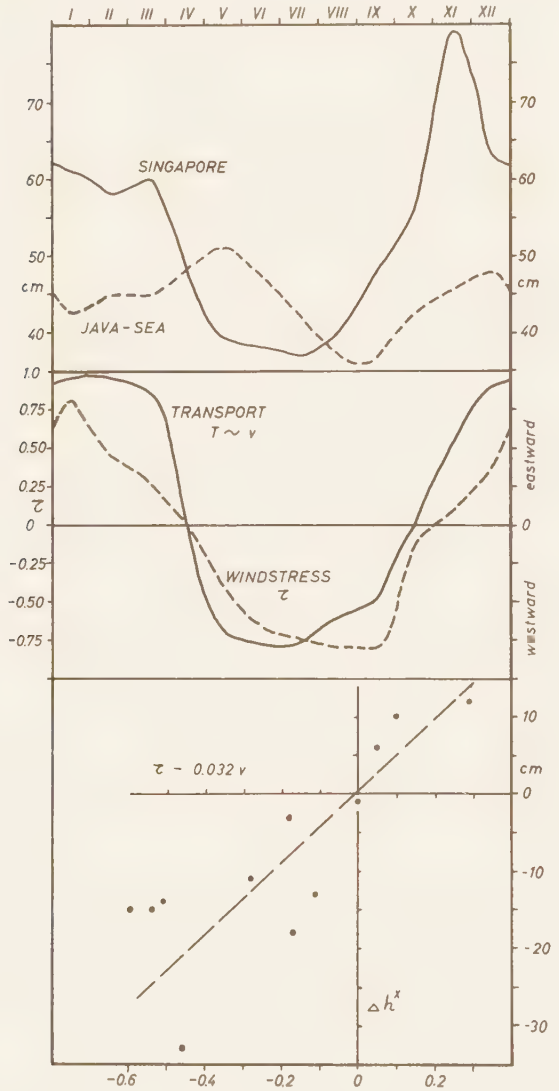

Fig. 7·2. Annual variation of sea level in the Java Sea, compared with sea level at Singapore, longtitudinal slope Δh^x, transports and wind stress.

$v = 22$ cm/sec is found during the southeast monsoon at an average wind stress $\tau^x = 0.7$. This is in agreement with the observations. During the northwest monsoon on the other hand the observed velocities are essentially higher than values calculated from wind observations. It must be assumed that during this season a slope towards the east exists in the direction of the flow.

In order to investigate such a longitudinal slope, the average sea level in the eastern Java Sea (average from Musang Ketjil and Tuban) is compared with the sea level in Singapore, fig. 7·2. This graph shows that the sea level in Singapore is higher than in the eastern Java Sea during the whole year with the exception of May, June and July, but especially during the northwest monsoon. For comparison the current velocity in the Java Sea, which might be proportional to the transports, is given, the wind stress is also added. Obviously, the transports are essentially higher during the northwest monsoon than could be expected from the winds, because during this season a longitudinal slope from Singapore to the eastern Java Sea reinforces the current. During the southeast monsoon from May to July, the westward transport is greater than calculated from wind data, because of the slope in wind direction. In August and September the slope acts against the current and the transports are smaller than expected from the wind stress.

To get numerical relations, the transport in equation (4) is replaced by the velocity

$$\tau^x - r \rho D v \fallingdotseq \rho g D h_x$$

With $r = 0.8\ 10^{-5}$ and $D = 40$ m results.

$$\tau^x - 0.032\ v = 4\ 10^6\ h_x$$

In fig. 7·2 the relation between Δh^x and $(\tau^x - 0.032\ v)$ is according to this equation. It demonstrates clearly the correlation, even if the scattering is relatively high, this might be due to uncertain wind and current observations. Even if the reason of this longitudinal slope cannot be discussed until later, both presentations demonstrate clearly the way in which winds cross and longitudinal slope work together in producing the currents.

In the southern parts of the China Sea, in the waters between Singapore and Borneo the conditions are different. Because the coriolis parameter vanishes, no cross slope can be expected to balance the current, and such a cross slope could only be induced by a wind component across the channel. Therefore the transport is maintained by the longitudinal component of the wind and by the longitudinal slope. Here the correlation between wind and current appears especially clear, fig. 7 · 3. The numerical relation is $v = 42\,\tau^x$ and because $\tau^x = r\,D\,v$ and $D = 30$ m, a friction $r = 0.8\,10^{-5}$ results, the same as in the Java Sea. Maximal transports of

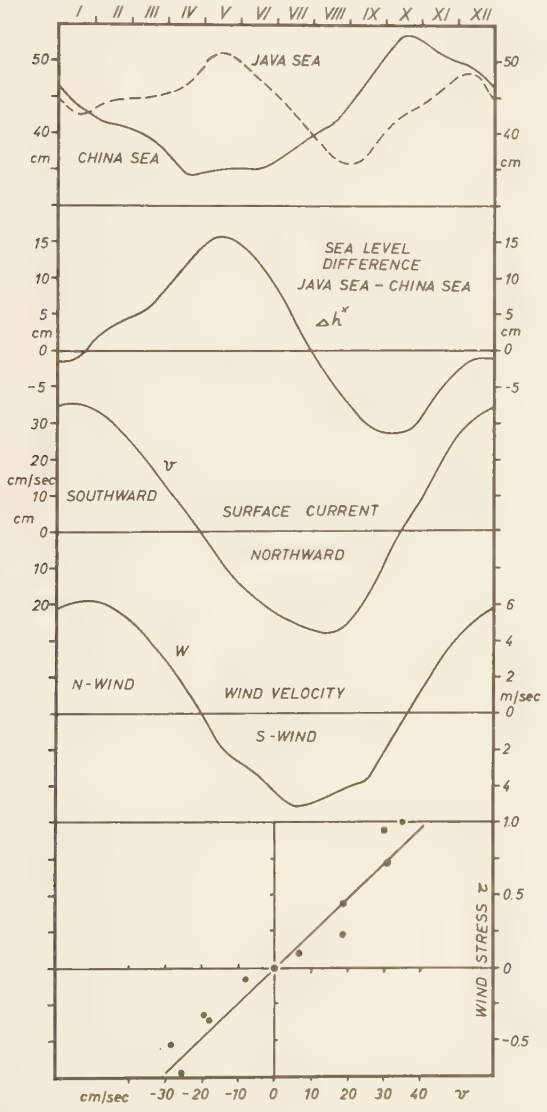

Fig. 7·3. Annual variation of the average sea level in the Java Sea and in the China Sea compared with surface currents and winds in the southern China Sea.

4.6 10^6 m^3/sec in January and of 3.4 10^6 m^3/sec in August agree with the values determined for the Java Sea.

To estimate the influence of a longitudinal slope the sea level in the Java Sea (average of Musang Ketjil and Tuban) and the sea level in the northern China Sea (average of Macao and Port Uson) are given in fig. 7 · 3 and show interesting relations. In the northern China Sea the sea level has a distinct annual variation with rising water during the southwest monsoon and falling water during the northeast monsoon. The Java Sea on the other hand has a distinct semiannual variation, the maxima occur at the beginning of both monsoon periods. Consequently the Java Sea has a higher sea level from February to July and the China Sea from August to November. In December and January there is practically no longitudinal slope. A comparison with the current shows that a close relation exists between the longitudinal slope and the change of the currents. From February to July, when the sea level in the Java Sea is higher, the southgoing current is first weakened, later reversed and develops finally into a northgoing current in the direction of the slope. The maximal longitudinal slope is reached, when the current changes direction. From August to November the sea level is higher in the China Sea than in the Java Sea and the northgoing current is weakened. Later in October the reversal of the current occurs simultaneously with the maximum of the slope. In November the southgoing current is developed.

The longitudinal slope is actually small, the maximal value in May is only 16 cm and gives, with a horizontal distance between both pairs of stations of 3000 km only a value of $5.3\,10^{-8}$, equal to 0.5 cm on 100 km. Such a slope would produce a current of 7.5 cm/sec, taking a friction $r = 0.8\,10^{-5}$, but this would be measurable. It must be considered, however, that the calculated slope is an average over the distance of 3000 km, and it is unlikely that it is distributed equally. A part of this slope has already been discussed in connection with the Java Sea, the other will be discussed with the conditions in the China Sea.

However, it is interesting that a longitudinal slope on such a long distance correlates well with the change of the currents and that its highest values occur at the time of the change of the direction of the currents.

The CHINA SEA is the largest region within the Southeast Asian Waters and the monsoon currents do not pass it in a simple way as they do in the Java Sea. An additional cross circulation is formed, as seen in the charts of the surface currents. Also in this region a close relationship is found between winds, currents and sea level fig. 7 · 4. The two stations Macao and Port Uson allow the calculation of the sea level difference

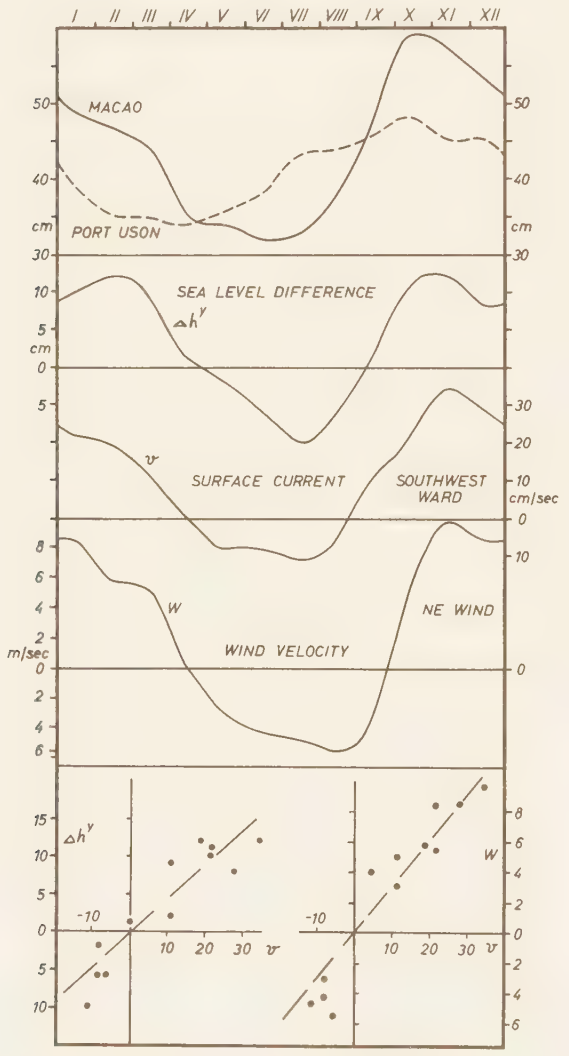

Fig. 7·4. Annual variation of dynamical factors in the northern China Sea, demonstrating relations between sea level, sea level difference across the current, current velocity and wind velocity.

across the northern China Sea rectangular to the monsoon current. The variations of the sea level in Macao are much higher than in the Philippines. The cross slope is clearly visible during both monsoons, the higher sea level is here, in the northern hemisphere, to the right of the current. Winds, currents and sea level show the same characteristic annual variation, but the correlation between winds and currents is weak, while it is much stronger between sea level differences and currents.

When investigating the numerical relations, a strong discrepancy is found. When calculating the transports according to the equation $f\,T = g\,D\,\Delta h^y$ with $f = 4.0\ 10^{-5}$ and $D = 50$ m, transports of only $1.5\ 10^6$ m³/sec result during the strongest development of the monsoons. On the other hand, from the relation $r\,T = b\,\tau^x$ transports of $10 - 12\ 10^6$ m³/sec follow with $r = 0.8\ 10^{-5}$ and $b = 1000$ km during the months August and February. This discrepancy needs an explanation. Because water masses of the magnitude of $10\ 10^6$ m³/sec can neither be delivered from the Java Sea during the south monsoon nor taken up during the north monsoon, a considerable part of the wind stress must be compensated by a longitudinal slope against the wind. Therefore a high piling up of water must accompany the development of the circulation.

Over the China Sea the winds blow almost in the direction of its axis and $\tau^y = 0$ might be assumed. Then the equations (4) reduce to

$$\rho\,r\,T = b\,\tau^x - \rho\,g\,D\,b\,h_x$$
$$f\,T = -\,g\,D\,\Delta h^y$$

In these equations the cross slope Δh^y, the friction r, the wind stress τ^x and the transport T might be assumed to be given, as well as the dimensions of the channel. The transport in the monsoon currents must be the same as already calculated for the Java Sea and the southern China Sea, because these regions cannot deliver or take up more water. The longitudinal slope h_x and the depth D of the current might be assumed to be unknown. The largest part of the China Sea is a deep sea basin and therefore the

depth of the current is not given *a priori* as in the Java Sea. Because of the great depth the bottom friction is not effective and the friction is therefore assumed to be only $0.6\ 10^{-5}$. With $f = 4.0\ 10^{-5}$, $b = 1000$ km, the observed cross slope Δh^y and the transports T, the depth D can be eliminated from the second equation. Then the first equation gives, with the wind stress and the transport, the value of the longitudinal slope h_x. These values have been calculated for February, August and November and given in table 10. The longitudinal slope is related to a distance of 2000 km.

These values show first the considerable vertical extension of the current, which goes deep down into the discontinuity layer. The pressure differences seem to vanish only at the lower boundary of the discontinuity layer. This fact has already been mentioned, when discussing the hydrographic conditions and the circulation in the depth of the China Sea (Section 6 · 3). A comparison of the fractions of the wind stresses, which are used for the development of the currents $\rho \frac{r}{b} T$ and for the piling up of the water $\rho\ g\ D\ h_x$ show clearly that the bigger part is used to set up the longitudinal slope against the wind. This piling up of the water masses reaches its highest value in November at the beginning of the northeast monsoon.

The relation between the winds and the longitudinal slope in the China Sea is demonstrated in fig. 7 · 5. During the southwest monsoon the sea level is higher in Formosa than in Singapore. The wind transports more water than is delivered from the Java Sea, and this causes a fall of the sea level in the southern China Sea. During the northeast monsoon on the other hand the water masses of the drift current, produced in the China Sea can only partly flow into the Java Sea and cause a considerable piling up of water in the southern parts of the China Sea.

The relation between the stress of the wind and the slope between Singapore and Formosa is shown in fig. 7 · 5, the numerical relation is $\Delta h^x = 11\ \tau^x$. From equation (4) the expression $\tau^x = \rho\ g\ D\ h_x$ follows for the balance between wind stress and longitudinal slope. With a distance of 2850 km between the two stations a depth $D = 260$ m results for the vertical extension of the influenced layer. This high value indicates a deep going influence of the wind, and demonstrates that the pressure differences are balanced only at the lower boundary of the discontinuity layer. But no importance can be attributed to this value of D, because there is not only simply a piling up effect, but also a considerable transport in the direction of the wind. Moreover the depth varies considerably and the whole southern part is a shallow sea with a depth of less than 100 m, and this had to be considered. All these questions will be discussed, when dealing with the dynamics of the water movements in the China Sea in Section 7 · 7.

Through the **Formosa Strait** a part of the water exchange between the China Sea and the Pacific Ocean takes place. This water transport causes a slope across the strait. Unfortunately there exist no suitable sea level stations directly on the strait and the two stations Takao and Macao are used. From the data of these two stations a rather good correlation results between the currents and the cross slope, as shown in fig. 7 · 6. Numerically the relation is $v = 2.3\ \Delta h^y$.

TABLE 10

Values of dynamical factors in the China Sea.

	T	Δh^y	D	τ^x	$\rho \frac{r}{b} T$	$\rho\ g\ D\ h_x$	h_x	Δh^x	Δh^x_{obs}
	m^3/sec	cm	m		g cm^{-1} sec^{-1}		10^{-7}	cm	cm
Febr.	4.0	12	133	0.94	0.24	0.70	0.53	10.6	18
Aug.	—3.0	—6	200	—0.85	—0.18	—0.67	—0.33	—6.6	—11
Nov.	5.0	12	167	2.75	0.30	2.45	1.47	29.4	29

The theoretical relation is according to equation (4) $f v = g h_y$. With $f = 5.5\ 10^{-5}$ and a width of the channel $b = 80$ km the theory gives $v = 1.5\ \Delta h^y$. This means that the observed velocities are higher than the theoretical values, which might be an effect of the unfavorable position of the stations. The transports at the time of the strongest currents in July and December remain apparently below 1 million m^3/sec.

Through the SUNDA STRAIT a small exchange of water between the Java Sea and the Indian Ocean takes place. Because of its small cross section, the strait is only 24 km wide and 80 m deep at the narrowest point, and in spite of the relatively strong currents, the water transports seem to have little effect on the water balance of the Java Sea. An estimation shows, that these transports do not exceed 0.5 10^6 m^3/sec. Tidal currents predominate, but in spite of this the current observations result in a distinct annual variation of the velocity of the current (fig. 7·7), which is always directed towards the Indian Ocean. The maxima of the velocity occur in December and August, when the monsoons are strongest. During the time of the changing of the monsoons the currents are weak and it seems possible, that under certain conditions water of the Indian Ocean also penetrates into the Java

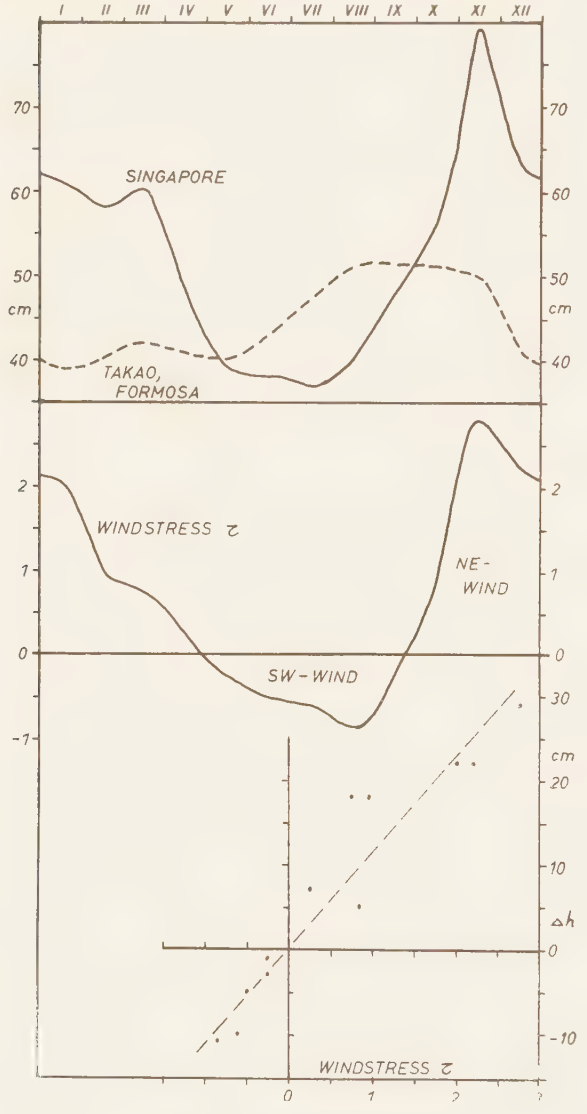

Fig. 7·5. Annual variation of the longitudinal slope in the China Sea compared with the wind stress.

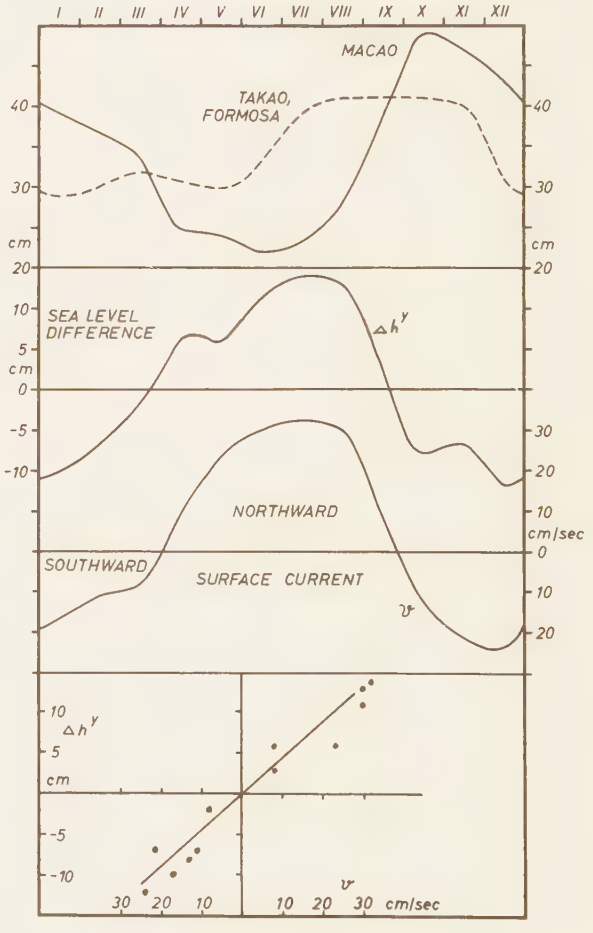

Fig. 7·6. Annual variation of dynamical factors in the Formosa Strait, demonstrating relations between sea level, sea level difference and current velocity.

Sea, but this may be an exception. To prove the reality of these currents determined from ships' observations in the Sunda Strait, which could be affected by tidal currents, the sea level difference between Tandjong Priok on the north coast of Java and Pelabuan Ratu on its south coast were investigated, fig. 7 · 7. Even if the values scatter considerably, a relation between the currents and the sea level difference is obvious. Moreover it is to be noted that both stations are situated about 120 km east of the strait.

In the MALACCA STRAIT, as in the Sunda Strait, the transports are of minor importance for general circulation. Also here tidal currents predominate and a northwest current is superimposed during the whole year, fig. 7 · 8. In June, July and August it is very weak and often opposite directions are recorded. Along the Malacca Strait a number of sea level stations are situated, and their data permit a comparison with the currents. The station Ko Ta Phao Noi on the coast of the Malayan peninsula and the station Belawan on the northeast coast of Sumatra show a nearly identical annual variation. This demonstrates the absence of a cross slope and of any transport worth mentioning. Also the two stations Singapore and Prigi at the southern entrance of the Malacca Strait show the same

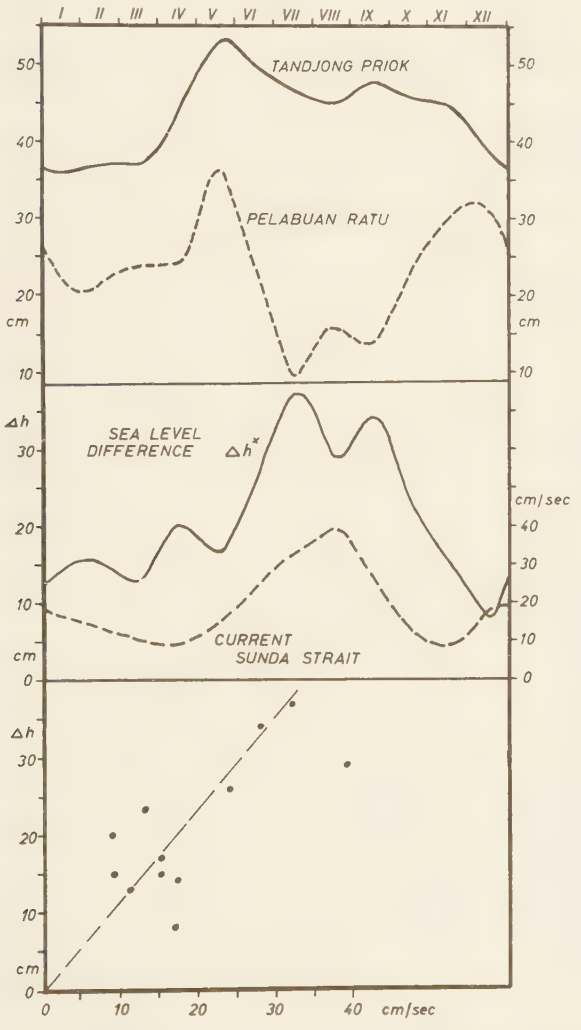

Fig. 7·7. Annual variation of dynamical factors in the Sunda Strait, demonstrating the relation between the sea level difference Java Sea-Java south coast and the currents in the Sunda Strait.

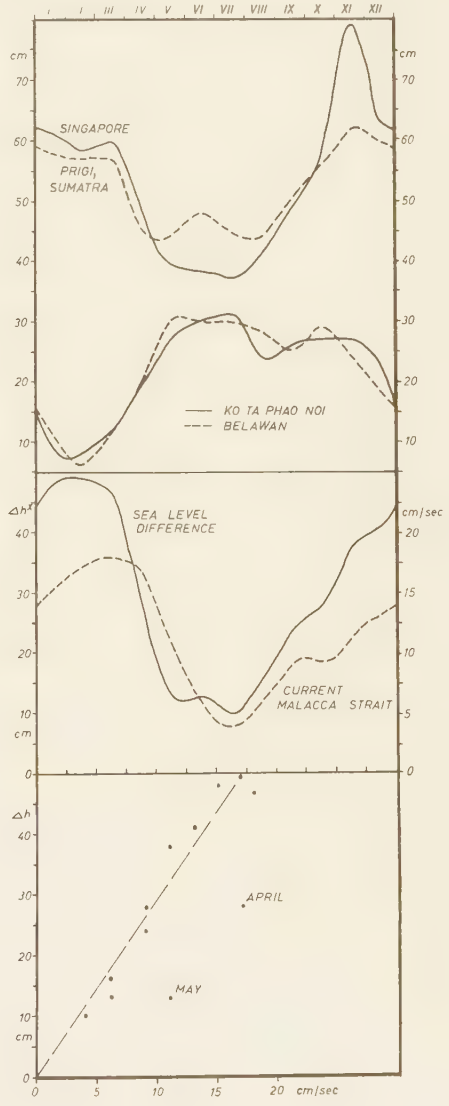

Fig. 7·8. Annual variation of dynamical factors in the Malacca Strait, demonstrating the relations between sea level, longitudinal slope and surface currents.

annual variation. They can be said to reflect the sea level in the southern China Sea, while the two stations at the northern entrance of the strait follow the sea level in the Andaman Sea. There the sea level is low during the northeast monsoon and high during the southwest monsoon, when the water is piled up in the Andaman Sea. From these annual variations of the sea level at both entrances of the strait a considerable longitudinal slope results, reaching up to 50 cm from January to March. Because of the length, narrowness and shallowness of the strait this strong slope produces only a relatively weak current. The correlation between the currents and the slope is rather close with the exception of the months of April and May. Its numerical expression is $v = 0.34\,\Delta h^x$. With the relation $r\,v = g\,h_x$ and a distance of 800 km between the two station pairs, for the friction the high value $r = 3.6\,10^{-5}$ results.

The foregoing investigations aim chiefly at the derivation of relations between the currents and the sea level, which permit the calculation of the transports as well as the determination of the relative position of the zero points of the different gauges. The purpose of further investigation is to join these results and to give a comprehensive picture of the transports in the different branches of the circulation and of the topography of the sea surface in these waters.

7·2 THE TOPOGRAPHY OF THE SEA SURFACE RELATIVE TO 800 DECIBARS

A representation of the topography of the sea surface based on the distribution of the density above a certain reference level is a method widely used in oceanography for the study of ocean currents. Even if the determination of the dynamic heights is an unequivocal process, the currents derived from it depend much on the selection of the reference level and on the applicability of the theory. The dynamic theory presumes stationary, frictionless currents, in which the pressure gradients are balanced by the coriolis forces. Therefore the theory loses its applicability in the vicinity of the equator, because here the effect of the coriolis force becomes smaller than other effects. Also in cases of sharply curved stream lines the theory is of limited applicaiton because here the convective terms of the hydrodynamic equations assume considerable importance. To date, however, this theory is the only method permitting the study of the movements in an inhomogeneous ocean.

For the Southeast Asian Waters and the adjoining parts of the Indian and the Pacific Oceans the topography of the sea surface relative to 800 dbar is presented for the north and the south monsoon periods, plates 39 and 40. These are based on the observations of the SNELLIUS (van Riehl, Groen and Weenink, 1957) within the Eastern Archipelago, of the DANA and the ALBATROSS in the northeastern Indian Ocean and of the Japanese surveys Nos. 35, 40, 42, 68 and 102 in the Pacific Ocean and in the China Sea. They are all related uniformly to 800 dbar, although the zero layer lies in the Eastern Archipelago partly in 500 to 600 m and in the range of the Pacific North Equatorial Current in 1000 to 1200 m depth. But the deviations from the absolute topography resulting from this change in the depth of the zero layer would normally be small, because the water movements in the depth are very weak. It must, however, be noted that the constant value of 130 dynamic cm has to be added to the values shown in plates 39 and 40, in order to get the anomaly of the dynamic depth relative to 800 decibar. This value had been subtracted to make the dynamical topographies comparable with the charts of the topography of the sea surface, derived from sea level observations, plates 1-6.

Another difficulty originates from the fact that the observations are from different months and years and without smoothing cannot be joined to give a uniform picture. The effect of such variations of the topography of the sea surface even within short periods has been demonstrated by Sverdrup (1946) when investigating the California Current. Other fluctuations are not caused by real variations of the circulation, but stimulated by the effect of internal tides and internal waves, which are strongly developed within these

waters, Lek (1938). These can easily exceed 10 cm, as shown by Sverdrup (1946) using the observations of the anchor station Sn 253a. In the vicinity of the equator the topography of the sea surface is very flat, because already a small slope causes rather strong currents, and therefore the presentation of the topography is difficult. Under consideration of these facts the presentation of the topography of the sea surface might be really representative only in the range of the stronger branches of the circulation. Within the Archipelago, where the geographical subdivision of the region additionally complicates the conditions, a real representation seems almost impossible.

The main features of the circulation are clearly visible in both representations. In the Pacific Ocean the North Equatorial Current flows westwards between 8° and 20°N, and splits off, when approaching the coast of the Philippines. This happens about along the line of 40 dyn cm. The water masses between 10 and 40 dyn cm pass into the Mindanao Current and the water masses between 40 and 80 dyn cm are deflected northwards and form the root of the Kuroshio. The depression, east of Mindanao, seems to be a stationary feature, even if its position varies. In January it occurs in 135°E and in May very close to Mindanao in 130°E. This depression is the centre of a large eddy, in which the water masses of the North Equatorial Current are deflected into the Mindanao Current and further into the Counter Current. It is more strongly developed in May than in January, in agreement with the results shown in fig. 3 · 3. The Counter Current becomes weaker and weaker from December to February and starts in May again with great power. Investigations of this large eddy might be a highly interesting dynamical problem, but for this, quasisynoptical observations within its whole range are required. The Japanese investigations do not extend westwards enough, while those of the SNELLIUS do not reach far enough into the Pacific Ocean. The far spreading of the Mindanao Current to the south before it turns into the Counter Current is also remarkable, and this feature is shown in fig. 7 · 12 and will be discussed later.

Another stationary feature in this region is the high in about 4°N, north of New Guinea. It is well developed in both seasons with about 40 dyn cm, and also the few stations of the DANA confirm its presence in August. North of this high, the Counter Current sets eastwards, and south of it the topography is highly equalized. Here at the equator, strong surface gradients are unstable. They would produce strong currents in the direction of the slope, because the coriolis deflection is lacking, and would diminish the slope. The observations here presented are from February and May, when the water movements in this region are rather irregular. A presentation of the conditions in August during the full development of the South Equatorial Current would be much more interesting, but the number of DANA stations is too small.

In the Indian Ocean both diagrams show the South Equatorial Current as the main feature of the circulation, even if the number of stations is rather scanty. In September, plate 40, it flows south of the dynamic isobath of 15 dyn cm, but seems to extend further south than the station network. Southwest of the Sunda Strait it is deflected towards the north, so that its northern boundary lies at 5°S in about 95°E. North of it, at the equator the topography is again much equalized, the dynamic heights are about 20 dyn cm. Along the southwest coast of Sumatra a considerable longitudinal slope exists, causing a strong coastal current, which is found also in the chart of the surface currents of October. The Counter Current is not reached by the net of the DANA stations, its influence in this season is limited to the region west of 95°E.

Quite different are the conditions in March, plate 39. At 88°E the South Equatorial Current flows in a narrow band westwards with a slight southerly component. Its northern boundary lies in about 8°S at values of only 5 dyn cm, south of Java it meanders slightly at about 10°S. Assuming the stream lines to be parallel to the dynamic isobaths, the line of 25 dyn cm is approximately

the boundary between the water coming from the east and the water masses of the Counter Current coming from the north. The Counter Current lies at 88°E about between 8°S and 6°S, but further to the north there seems to be a second branch of the current. The turning of the Counter Current into the South Equatorial Current happens east of 90°E in the region west of Sumatra. North of the equator again a small rise of the sea surface is to be noted indicating the North Equatorial Current. In the region south of the Lesser Sunda Islands a depression is developed with dynamic heights of less than 25 dyn cm. South of this depression the South Equatorial Current flows westwards, reinforced by water from the Sawu and Timor Seas.

In the China Sea observations are available only for the southwest monsoon period. They show clearly the slope across the current with a low sea level in the northwest and a high sea level in the east along the coast of the Philippines, and the westward intensification of the current, which is effective also during the southwest monsoon. This representation of the topography is in complete agreement with the current chart for June, plate 3. For the Sulu Sea, which is closed in a depth of 400 m from the China Sea, Graham (1957) has given presentations of the dynamic topography for both monsoons, but they seem to be highly disturbed by tides and internal waves, and give practically no useful pattern of the circulation. Currents up to 100 cm/sec, often in opposite directions, appear in the Sulu Sea only as tidal currents, but not as residual currents reflecting the general circulation. The material could be used for an analysis of the circulation only after a careful elimination of the effects of internal waves, as done by Defant (1950) for the California Current.

A branch of the Mindanao Current enters the Celebes Sea, plate 40, and splits off in its southwestern part, part of it turns northwards and flows into the Sulu Sea, part of it flows into the Macassar Strait and a small part flows back to the east along the north coast of Celebes. The presentation of the dynamic topography is in full agreement with that of the surface currents, plate 3. Through the Macassar Strait a southward transport takes place during the whole year according to the longitudinal slope. This slope and the wind alone can produce the current, because the strait crosses the equator in a north-south direction. Among the islands of the Molucca Sea a presentation of the dynamic topography is practically impossible, because the observations are from different months and also an elimination of the internal tides seems to be rather hopeless.

In the Flores and Banda Seas a current flows eastwards during the northwest monsoon, this is clearly shown in the dynamical topography, plate 39. In the Banda Sea it has a northward component, confirming the result that considerable parts of the water masses of the Monsoon Current pass through the Molucca Sea into the Pacific Ocean. Although the observations are rather scanty, the dynamic topography during the southeast monsoon shows a nearly reversed picture. The dynamic isobath of 30 dyn cm runs from the island of Buru into the Flores Sea indicating a transport in this direction. But the distribution of the numerous oceanographic stations obtained by the SNELLIUS Expedition in the Flores, Banda and Arafura Seas is so unfavorable, that it is impossible to draw the dynamic topography for only one single season. Considering the large annual variation of the circulation it would have been necessary, at least from the dynamical point of view, to cover the region as a whole two or three times with a net of stations, even if they were more widely spaced. But the observations in the Flores Sea are from February and March, in the central parts of the Banda Sea from April and May and in the eastern parts of the Banda Sea and in the Arafura Sea from October of two different years. Because February falls in the northwest monsoon and May in the southeast monsoon the observations cannot be used together and October falls just in the changing season. Although a presentation of the dynamic topography would be desirable for this region of strong seasonal upwelling, it is impossible in spite of the numerous observations.

TABLE 11

Dynamical Values of different currents in the Southeast Asian Waters. For symbols see text.

Current System	Month		Stations	Latitude	1/f	r	$\frac{f}{\sqrt{f^2+r^2}}$	D	v	T_f	T_r	T_{150}	T_{est}	I_D	I_{150}
				φ	10^{-5}	10^{-5}	10^{-5}	m	cm/sec		Million m^3/sec			$10^6 g\ sec^{-2}$	$10^6 g\ sec^{-2}$
A Mindanao Current	May	Sn	263-266	6 N	0.65	1.2	0.40	1250	135	(41.2)	25.3	15.2	10-15	634	380
B Counter Current	May	Sn	271-273	4 N	0.98	1.2	0.41	1250 (250)	200	(31.9)	13.4	12.1	10-15	325	295
C Celebes Sea	Aug.	Sn	53-56	3 N	1.32	1.0	0.48	600	25	(33.0)	12.0	6.2	3-6	250	130
D Monsoon Current Flores Sea	Feb.	Sn	196-198	8 S	0.49	0.8	0.43	400	83	4.8	4.2	3.9	4-6	98	93
E Monsoon Current Flores Sea	Feb.	Sa	42-44	8 S	0.49	0.8	0.43	500	88	6.8	6.0	2.5	4-6	139	57
F Formosa Current	May	Da	3716-3719	20 N	0.20	1.0	0.193	1000	28	53.0	51.0	20.0	35-40	2650	1040
G Luzon Current	Aug.	J	99/40-45	20 N	0.20	1.0	0.193	400	20	9.1	8.7	5.4	6-8	454	282
H Luzon Current	Feb.	J	20/37-41	20 N	0.20	1.0	0.193	300	60	12.3	11.9	9.4	6-9	614	490
J South Equatorial Current	Nov.	Sn	146-147	11 S	0.36	0.6	0.34	500	13	5.6	5.3	3.4	3-5	156	101
H South Equatorial Current	Oct.	Da	3844-3852	9 S	0.44	0.6	0.41	700	10	27.9	26.3	14.8	20-25	642	361
L Timor Current	Oct.	Sn	119-123	10 S	0.39	0.8	0.36	400	22	(7.1)	6.4	4.5	2-3	181	125

7·3 THE VERTICAL DISTRIBUTION OF THE VELOCITIES AND THE TRANSPORTS

The vertical distribution of velocity in ocean currents is calculated according to the dynamic theory from the differences of the dynamic values of two stations. Such a calculation gives the relative current and only the knowledge of a zero layer allows the calculation of the absolute current. In the simplest cases it is possible to select the depth of the zero layer (Defant, 1941) in such a way, that in its vicinity the vertical variation of the difference of the dynamic values vanishes. By integration from the zero layer to the surface also the absolute transports can be calculated. But the velocities as well as the transports are reciprocally proportional to the coriolis parameter, which has very low values near the equator. This makes an overestimation of the velocities and of the transports likely. For this reason, the differences of the dynamic heights, not the velocities, are given in the fig. 7·9 and 7·10. In table 11 are listed the stations on which the calculations are based, together with their average latitude, the value of the coriolis parameter $f = 2\ \omega \sin \varphi$ the depth D of the zero layer and the values of the two integrals

$$I_D = \int_0^D (\Delta D_a - \Delta D_b)\ dz$$

and

$$I_{150} = \int_0^{150} (\Delta D_a - \Delta D_b)\ dz$$

representing the transports above the zero layer and in the upper 150 m. ΔD_a and ΔD_b are the anomalies of the dynamic values at both stations a and b. The surface velocities v calculated with the coriolis parameter f and the transports above the zero layer T_f are also given and set in parentheses in cases of unlikely high values. From the value of 1/f it can be easily noted that the same distribution of mass causes in 8° latitude 2.5 times the transport than in 20° latitude, this is an effect of the neglect of the friction. But when taking the friction into account and proportional to the velocity (Wyrtki, 1956) then the dynamic theory can be applied also in lower latitudes. In this case the factor 1/f is to be replaced by the factor $\frac{f}{f^2 + r^2}$. At the equator the mass transport parallel to the dynamic isobaths vanishes and currents are possible only in the direction of the slope. The friction r and the factor $f/(f^2 + r^2)$ are also given in table 11 together with the transports T_r above the zero layer and T_{150} in the upper 150 m. In addition the transports T_{est} are given, which are estimated from observations on the velocity, depth and width of the current. The positions of the section are entered into chart fig. 7·15.

In the Mindanao Current a slope of 30 dyn cm exists across the current and the velocities often exceed 100 cm/sec at the surface, fig. 7·9A. The current is of considerable depth and reaches down to 600 m, transporting also the northern Intermediate Water. Below it a zone of counter movements is found. The layer of no motion lies rather deep in about 1250 m. The vertical extent of the Counter Current, in which large parts of the Mindanao Current pass over, is only 300 m, fig. 7·9B. Below it also a layer of opposite movements exists between 500 and 1000 m

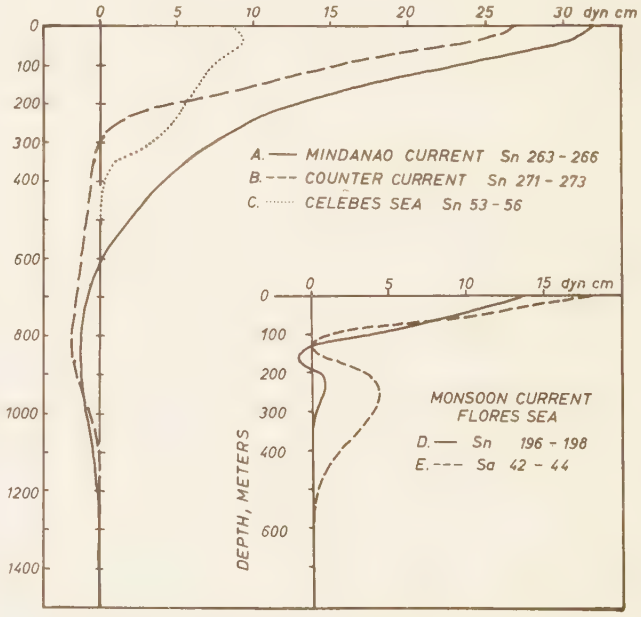

Fig. 7·9. Vertical distribution of current velocity in different current systems, demonstrated by differences of dynamic heights. Positions of the sections are given in figure 7·15.

depth. The dynamic theory gives in both currents, situated in about 5° latitude, extremely large transports, which are certainly unreal. But with the assumption of a friction $r = 1.0\ 10^{-5}$ the transports reduce to 25 million m^3/sec in the Mindanao Current and to 13 million m^3/sec in the Counter Current. These values, but especially those within the upper 150 m, correspond much better to the values estimated from current observations of about 10-15 million m^3/sec. This justifies the use of such a high friction, which must be higher in the system of the Mindanao eddy than in the open ocean and in parallel currents.

A part of the water masses of the Mindanao Current enters the Celebes Sea. The depth of this current is only 300 m, that is about the depth of the lower boundary of the discontinuity layer, fig. 7 · 9C. Also the zero layer lies in the Celebes Sea higher at 600 m than in the range of the Mindanao eddy. But the transports of this current, situated in 3° latitude, give completely misleading values, when applying the dynamical theory. When consideration is given to the friction, however, values result, which come closer to those estimated from current observations.

Two sections through the Monsoon Current in the Flores Sea in February show that this current is rather flat and reaches only down to the center of the discontinuity layer, fig. 7 · 9D and E. Below this current the movements are weak and irregular and the zero layer lies in 400 to 500 m depth. The transports agree well with those calculated for the Monsoon Current in the Java Sea and are about 4 million m^3/sec.

Of special interest is the calculation from Japanese station data of the transports of the currents between Luzon and Formosa flowing in and out of the China Sea. The vertical distribution of the differences of the dynamic heights shows in February an inflow between the surface and 300 m depth and in deeper layers an outflow from the China Sea, reaching its maximum in about 500 m depth, fig. 7 · 10H. In August the conditions are just reversed, but the outflow at the surface extends down to 400 m and the maximum of the inflow is in 600 m depth, fig. 7 · 10G. The zero layer lies in about 1000 to 1200 m depth. The calculated transports are rather high and the influence of friction is practically unimportant in these latitudes. But these big transports can be explained easily by the unfavorable position of the stations, which include parts of the Formosa Current flowing with high velocity northwards. A more favorable selection of the stations is impossible, because the Japanese investigations concerned the Formosa Cur-

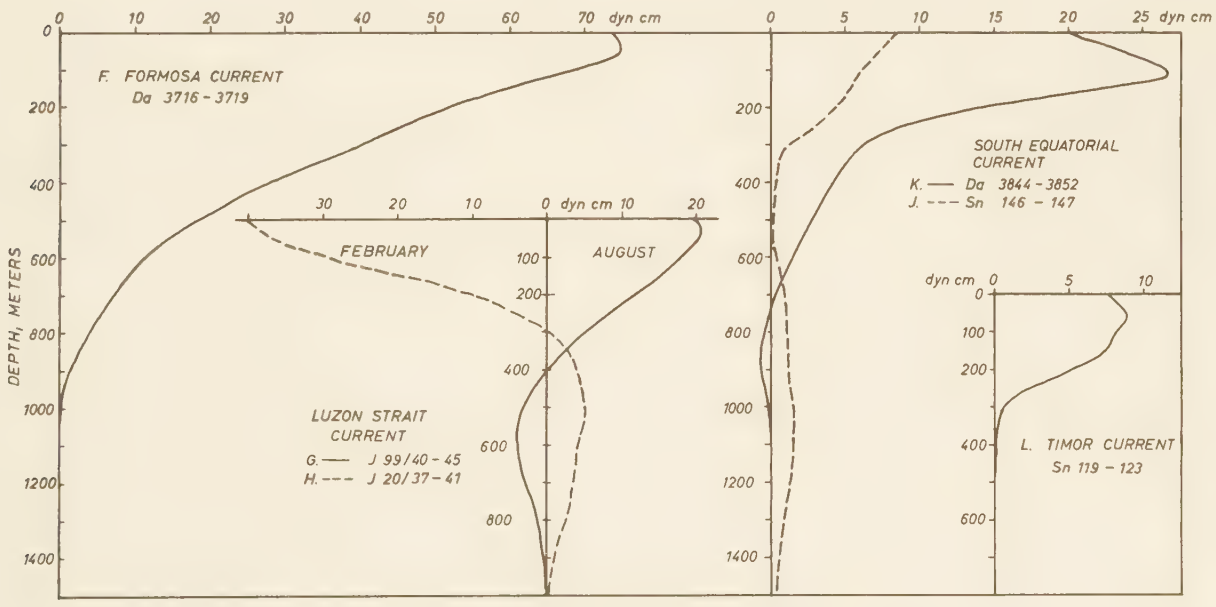

Fig. 7·10. Vertical distribution of current velocity in different current systems, demonstrated by differences of dynamic heights. Positions of the sections are given in figure 7·15.

rent in its role as root of the Kuroshio and were not planned to collect information about water entering and leaving the China Sea. Only comprehensive investigations on this flow could answer the various questions of the hydrography of the China Sea.

The vertical distribution of the velocity in the Formosa Current shows its immense depth (fig. 7 · 10F). Only in 800 to 1000 m depth the velocities become unimportant. The calculated transport is 50 million m^3/sec, but the real transport can be assumed not to exceed 40 million m^3/sec. The overvaluation of the transport seems to be caused by the use of only two stations for the calculation, which makes it impossible to consider the change of the depth of the zero layer. Moreover the current suffers a considerable change in its direction and the effects of these accelerations remain neglected.

In the Indian Ocean the South Equatorial Current is the most important branch of the circulation, some DANA stations north of the Cocos Islands lie in its range. The cross slope is 25 dyn cm, but the current seems to reach further to the south of the islands. The average velocity at the surface is only 10 cm/sec. The current extends down to 300 m depth, and below it only weaker movements occur (fig. 7 · 10K). The transport of 26 million m^3/sec seems to reflect the real conditions. For the Counter Current, Jerlov (1953) calculates a transport of 15 million m^3/sec, its vertical extent is about 250 m. Another section through the South Equatorial Current south of the island of Sumbawa is possible by using two SNELLIUS stations. The depth of the current is 300 m, the velocity decrease is almost linear (fig. 7 · 10J). Below this current an almost motionless layer extends from 400 to 600 m depth, and between 600 and 1400 m depth weak movements to the west are found. These are in agreement with the spreading of the lower salinity minimum from the Timor Sea into the Indian Ocean, see Section 6 · 1. The transport of the south Equatorial Current through this section is about 5 million m^3/sec.

The South Equatorial Current receives a part of its water masses from the Timor Sea. A section across the Timor Current based on the SNELLIUS stations Sn 119 and Sn 123 shows a current down to 250 m depth (fig. 7 · 10L). But in this region internal tides seem to play an important role and affect the observations, as can be seen from a comparison of other pairs of stations. But the two stations used were made with an interval of about 24 hours and the effect of the tides might be negligible, but even with this a transport of 6.4 million m^3/sec results, which is rather large.

The coastal current south of Java has been investigated by the SAMUDERA in two cross sec-

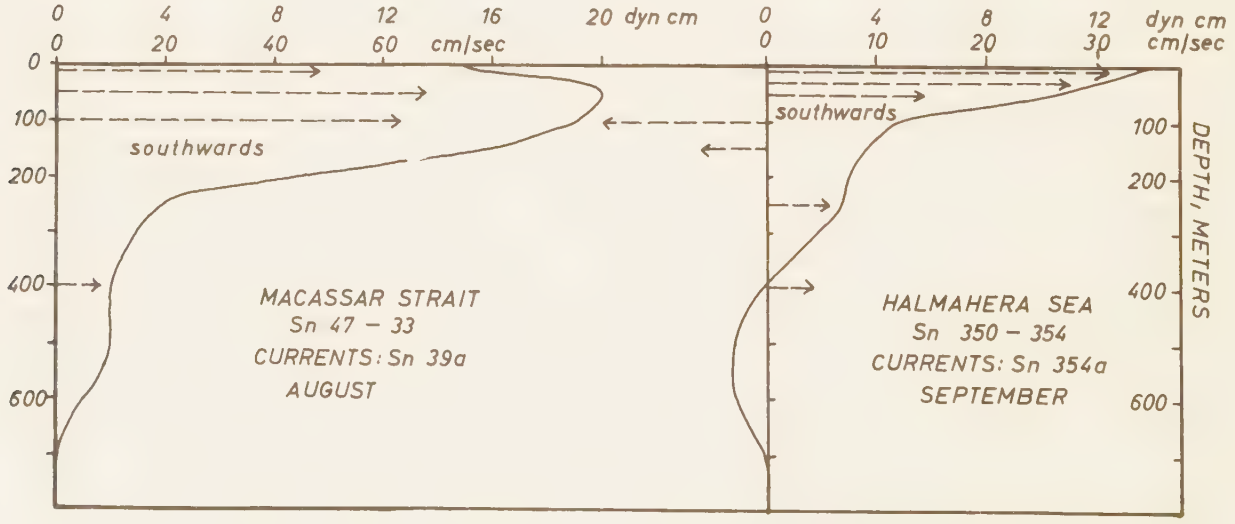

Fig. 7·11. Vertical distribution of differences in dynamic heights between stations in the northern and southern entrance of the Macassar Strait and the Halmahera Sea compared with resulting currents measured at anchor stations.

tions in February 1957 at the time of its strongest development. Considerable transports of 4.7 and 5.6 million m^3/sec have been calculated by Soeriaatmadja (1957). The depth of the current is about 200 m and along its boundary with the South Equatorial Current upwelling seems to occur.

Across the equator currents are possible only in the direction of the winds and of the slope, because the coriolis force vanishes. The acting forces are balanced by the friction, the relation between them results from equation (4)

$$\rho\, r\, T = b\, \tau^x - \rho\, g\, D\, b\, h_x$$

As an example the water movements through the Macassar Strait and through the Halmahera Sea are considered. Both cross the equator at right angles and the transports are from north to south. In the Macassar Strait the distribution of the differences of the dynamic heights between the station Sn 47 at the northern entrance and the station Sn 33 at the southern entrance indicates a current to the south down to 200 m depth (fig. 7 · 11). The maximal velocities are reached in 50 to 100 m depth, which is in agreement with the current measurements at the anchor station Sn 39a, and might be caused by a weak southerly wind. Disregarding the wind, the relation between current and slope is $r\, v = g\, h_x$, where v is the average velocity of the current. With a distance of 720 km between the stations and a friction of $r = 0.6\ 10^{-5}$ a maximal velocity of $v = 45$ cm/sec results in 75 m depth. This value is essentially smaller than the resultant current of 84 cm/sec measured at anchor station Sn 39a in a depth of 50 m. But the velocity derived from the slope gives an average over the whole cross section, while the anchor station might be situated in the current axis, where higher velocities may be expected. With an average velocity of 40 cm/sec in the upper 150 m and a width of the current of 50 km a transport of 3 million m^3/sec results, which is rather large. The average surface current in August determined from ships' observations is 36 cm/sec to the south.

In the Halmahera Sea the current is not so deep, as shown by the differences of the dynamic heights of the two stations Sn 350 at the northern and Sn 354 at the southern entrance of the sea. With a distance of 300 km between the two stations and a friction $r = 0.8\ 10^{-5}$ a surface velocity of 57 cm/sec results. But the resultant current at anchor station Sn 354a when measured is only 31 cm/sec and might be affected by the position of the station at the southern entrance, where the current is already dissolved and weakened. But it seems possible too, that the dynamical values are affected by internal tides. The distribution of the resultant currents at anchor station Sn 354a shows, in accordance with the dynamical values, an immediate decrease of the velocity from the surface to 100 m depth. The current measurements in 100 and 150 m depth even show movements in an opposite direction, and below 200 m the movements are only weak. When calculating the transports within the upper 100 m at an average velocity of 40 cm/sec and a width of 75 km, 3.0 million m^3/sec result. This observed southward transport of water through the Halmahera Sea in September is in accordance with the inflow of water masses from the Pacific Ocean into the Banda Sea, plates 4 and 5, which supply the Monsoon Current.

The inflow of water from the Pacific Ocean into the Eastern Archipelago between Mindanao and New Guinea is one of the most interesting problems of the oceanography of these waters, but a detailed investigation of these processes is still pending, because a complete knowledge of the structure and the dynamics of the Mindanao eddy is the necessary condition. In this eddy the North Equatorial Current is first deflected into the Mindanao Current and later into the Counter Current. A part of the water masses is given off into the Eastern Archipelago in the course of this turning. By means of data from the stations of the SNELLIUS the southwestern part of this eddy is represented in fig. 7 · 12, where the deflection of the Mindanao Current into the Counter Current takes place. The dynamic topography of the sea surface, the 150, 300 and 800 decibar surfaces have been determined relatively to the

1250 decibar surface. The vertical distribution of the differences of the dynamic heights of neighboring stations shows that these remain constant in the range between 1000 and 1500 m, consequently the zero layer is assumed to be in 1250 m depth.

The Mindanao Current flows in a small band southwards, in the latitude of the south point of Mindanao it splits off, one branch flowing southwestwards along the coast, while the main branch flows straight on towards the Talaut Islands. The first eastward deflection of this current occurs in the vicinity of these islands and in the region northeast of Morotai. North of Morotai a branch of the South Equatorial Current joins with these water masses and forms the Counter Current, which has here a northern component. In 150 m depth, where the Subtropical

Fig. 7·12. Dynamical topography of the surface, the 150, 300 and 800 decibar surfaces relative to the 1250 decibar surface in the Mindanao eddy. 1000 meter line dotted.

Lower Water spreads, the conditions have changed, the water coming from the north penetrates partly into the Celebes Sea, the rest is turned eastwards nearly completely north of the Talaut Islands. South of the Talaut Islands the movements are only weak and north of Morotai the South Equatorial Current extends further to the north.

In a depth of 300 m the movements are essentially weaker, and in this depth the core layer of the northern salinity minimum is transported with the Mindanao Current. This water enters the Celebes Sea south of Mindanao with a sharp turn to the west. South of the Talaut Islands only weak movements to the east occur, which probably transport water out of the Molucca Sea, and in this region also the salinity minimum is not present (plates 20-22). North of Morotai these water masses join with those coming from the southeast and with water, which is directly turned from the Mindanao Current into the Counter Current north of 6°N. The Counter Current is still developed in 300 m depth, and the strong northward displacement of its current axis with increasing depth is remarkable. At the surface the current axis lies with equal parts north and south of the station Sn 272, in 150 m depth lies the larger part and in 300 m depth the whole Counter Current north of this station. In 800 m depth the conditions are completely reversed, a current from the east enters the region and is deflected to the north off the Talaut Islands. The transported water masses belong to the southern salinity minimum, plates 28-30. The spreading of this water is in accordance with the run of the dynamic isobaths. The movements in this eddy are in full agreement with the theoretical results obtained by Defant (1929).

Another eddy of similar extent is developed northeast of Halmahera from May to October. During this time the South Equatorial Current flows along the north coast of New Guinea westwards and is deflected to the north, when meeting the island of Halmahera. Northeast of the island the water masses are further deflected to the east, they join with the water of the Mindanao eddy and form the Counter Current. But the number of available stations in this region is too small for an analysis of this eddy. Schott (1939) has mentioned the existence of this eddy, when dealing with the surface currents of this region, and Wyrtki (1956) discussed its role in connection with the spreading of the Subtropical Lower Water.

7 · 4 CHARTS OF THE MASS TRANSPORTS

The purpose of the investigations in the previous sections was to calculate the transports in the various current branches from observations of different factors, such as winds, sea level, current observations and dynamic calculations. In this section an attempt will be made to combine these results in order to get a comprehensive picture of the circulation within the Southeast Asian Waters. Extensive use is made of the equation of continuity, which demands the vanishing of the sum of all in- and outflowing water in a region. This means for the illustrations (plates 1-6) that the transport lines must be closed. But it seems advisable and necessary to restrict the presentations of the transports to the upper layers of the currents, because the information about the movements in the deeper layers is too scanty. Consequently, the charts give practically the transports above and within the discontinuity layer, relating to the upper 150 to 200 m. In this case it is naturally necessary to treat the regions of upwelling and sinking separately to fulfil the equation of continuity. Thus, in these regions the transport lines must begin or end, and they must further be regarded as stream lines and not as trajectories.

The charts of the transports are constructed for every second month and are presented together with the charts of the surface currents, plates 1 - 6. The numerical values of the transports in the diffeernt current branches are given in table 12.

Three almost separate circulations are distinguished. First the circulation in the Pacific Ocean, which affects the eastern parts of the region, but enters the Eastern Archipelago only in the range of the Celebes Sea. Second the circu-

lation of the Indian Ocean, where only the South Equatorial Current is included, but which has no influence on the Southeast Asian Waters. Third the circulation within the Southeast Asian Archipelago, which is determined by the monsoons. This monsoon circulation, as it might be called, is connected with the circulation in the Pacific Ocean to a small extent and linked with that of the Indian Ocean only by the Timor Current.

The monsoon circulation develops chiefly along the line China Sea - Java Sea - Flores Sea - Banda Sea, because these regions lie with their axis almost in the direction of the winds during both monsoons. The other regions, such as the Molucca Sea, the Macassar Strait, the Celebes Sea and the Sulu Sea are less favorably situated in respect to the wind. Through these regions compensating currents occur between the Pacific Ocean and the Monsoon Current. Therefore the Java Sea, which has the smallest cross section in the course of the Monsoon Current, is made the starting point of the calculations. To the north the China Sea is annexed, to the east the Flores Sea and the Macassar Strait.

During the full development of the north monsoon the transport of the Monsoon Current through the Java Sea is about 4 million m^3/sec (see the charts of February and December). In the China Sea the transport of the strong current branch off the coast of Vietnam is larger, because the transport of the eddy in the central parts of the China Sea has been added. The water masses of the Monsoon Current come during the north monsoon out of the North Equatorial Current and enter the China Sea chiefly through the Luzon Strait, smaller parts enter through the Philippines and the Sulu Sea. A rela-

TABLE 12

Transports (millions m^3/sec) of different currents in the Southeast Asian Waters

Current	Feb.	April	June	Aug.	Oct.	Dec.
Pacific Ocean						
North Equatorial Current	41	32	41	39	37	37
Mindanao Current	12	8	9	10	9	12
Formosa Current	24.5	37.5	35	30.5	27	21.5
Counter Current	9	—	15	16.5	14.5	9
New Guinea Coastal Current	5	—	—	—	—	5
South Equatorial Current	—	8	10	10	6	—
Southeast Asian Waters						
Luzon Strait, westwards positive	+2.5	0	—3.0	—2.5	+0.5	+3.0
Macassar Strait, southwards	1.5	1.0	1.0	1.5	1.0	0.5
China Sea, off Vietnam southwards positive	+5.0	+1.5	—3.5	—3.0	+2.0	+5.0
Java Sea, eastwards positive	+4.5	+0.5	—3.0	—3.0	+0.5	+4.0
Flores Sea, eastwards positive	+6.0	+2.0	—2.5	—2.0	+1.0	+4.5
Banda Sea, upwelling positive sinking negative	—2.0	—0.5	+2.0	+1.5	—0.5	—1.0
Timor Current, westwards	1.0	1.5	1.0	1.5	1.5	1.5
Halmahera Sea, southwards positive	—2.0	+1.0	+3.0	+3.5	+2.0	—1.5
Indian Ocean						
Source of the South Equatorial Current	16	12	8	10	14	14
Java Coastal Current	4	3	1	—	—	2
upwelling off Australia	—	3	5	4	—	—
South Equatorial Current southwest of the Sunda Strait	20.5	19.5	16.0	16.5	16.0	17.0
resultant flow from the Indonesian Waters to the Indian Ocean	1.0	1.5	2.0	2.5	2.0	1.0
Torres Strait, eastwards positive	+0.8	0	—0.6	—0.4	—0.3	+0.5

tively small transport of water occurs also through the Formosa Strait. The water masses leaving the Java Sea to the east join with those coming out of the Macassar Strait and flow to the east as a strong current along the north coast of Flores. When entering the Banda Sea the Monsoon Current dissolves, parts leave through the Molucca Sea and the Halmahera Sea into the Pacific Ocean and end in the New Guinea Coastal Current, flowing eastwards along this island during this season. Another part of the Monsoon Current ends in the Banda and Arafura Seas, where during the north monsoon descending water movements occur, these are discussed in Section 7 · 5 with the regions of upwelling. A third part of the Monsoon Current turns east of the Lesser Sunda Islands to the south and forms the Timor Current, which represents practically the whole water exchange at the surface with the Indian Ocean. The Java Coastal Current is well developed during this season.

During the change from the north to the south monsoon in April the whole circulation within the Southeast Asian Waters is only weakly developed, plate 2. In the China Sea two big eddies are found with a transport of 1 to 2 million m^3/sec each. The current still flowing eastwards in the Java Sea transports only 0.5 million m^3/sec, joins with the water coming out of the Macassar Strait and forms along the north coast of the Lesser Sunda Islands a rather strong current of 2 million m^3/sec. From the Pacific Ocean a weak transport occurs through the Philippines and the Sulu Sea into the China Sea. Another branch splits off from the Mindanao Current and flows through the Celebes Sea into the Macassar Strait. From the South Equatorial Current of the Pacific Ocean about 1 million m^3/sec of water penetrates southwards through the Halmahera Sea. The sinking region in the Banda Sea is only weakly developed, the larger parts of the Monsoon Current flow through the Timor Sea into the Indian Ocean.

During the south monsoon the conditions are nearly inverse to those during the north monsoon, but the average transports of the Monsoon Current are smaller. They amount in the Java Sea to only 3 million m^3/sec. The Monsoon Current is almost completely supplied by water masses of the Pacific Ocean, entering between Mindanao and New Guinea. One branch of about 2 million m^3/sec splits off from the South Equatorial Current and penetrates through the Halmahera Sea into the Banda Sea. Another branch splits off from the Mindanao Current and flows southwards through the Macassar Strait. When entering the Java Sea both branches join and together transport 3 million m^3/sec through the Java and China Seas. In the southern China Sea a small eddy exists, but its transport is only weak. Through the Luzon and the Formosa Straits the Monsoon Current finally leaves the China Sea and joins the water of the Formosa Current.

At the beginning of the south monsoon a transport of about 1 million m^3/sec takes place through the Sulu Sea from south to north. Later in August the sea level in the eastern parts of the China Sea is so high, that the currents are stopped and later a weak southward flow starts. In the Banda and in the Arafura Seas upwelling develops under the influence of the southeast monsoon. The ascending water masses flow nearly completely through the passages of the Lesser Sunda Islands and through the Timor Sea into the Indian Ocean.

In October the change from the south to the north monsoon takes place over most of the region, and over the northern China Sea the north monsoon has already started with considerable strength. The Monsoon Current along the coast of Vietnam is already developed and transports 2 million m^3/sec southwards, but the larger part of this water turns northwards before entering the southern China Sea and is transported back along the coast of Borneo. In the Java Sea the water movements are still variable, the eastgoing Monsoon Current is not yet established. From the Sulu Sea water masses flow southwards through the western parts of the Celebes Sea and through the Macassar Strait and join in the

Flores Sea with the current along the Lesser Sunda Islands. In the eastern parts of the Archipelago the water movements are still weak, only through the Timor Sea does a considerable current flow into the Indian Ocean.

Summarizing, the transport chart for October shows the formation of the Monsoon Current in the north monsoon season and the chart for April the decay of this current. The Monsoon Current of the south monsoon season is formed in May and decays by the end of September. For the China Sea it must be mentioned, that the transports caused by vertical circulation, as discussed in Section 7 · 7, are not entered in the transport charts.

In the adjoining Pacific Ocean the main branch of the circulation is the North Equatorial Current, which divides when it reaches the Philippines, where the main part of the current turns north. The estimated transports of these currents are entered in the transport charts, but these estimates will need revision in the future. The transports in both parts, in the Mindanao Current and in the Formosa Current, have been estimated by means of the observed velocity, the width and depth of the currents. The Formosa Current has a distinct maximum from April to June (see fig. 3 · 2), when the Mindanao Current is weak by comparison, consequently, the transports of the North Equatorial Current are relatively equalized. With the exception of April the Counter Current is developed throughout the whole year. From December to March it is supplied only by water of the northern hemisphere and from May to November it receives the larger part of its water from the South Equatorial Current. In April the newly developing South Equatorial Current seems to suppress the Counter Current. Then it is present only as a shrunken part of the Mindanao eddy.

In the Indian Ocean the estimations of the transports of the different current branches are still uncertain, because they are almost exclusively based on observations of the surface currents. The position of the current axis of the South Equatorial Current is indicated. From October to February it seems to divide into two branches, but not during the southeast monsoon period, the branch coming from the south shows a distinct annual variation of its transport with small values during the southeast monsoon. During this season the demand for water of the South Equatorial Current is high, and in combination with the offshore winds along the northwest coast of Australia upwelling develops. The South Equatorial Current receives a further supply throughout the year from the Timor Current, even if this source is only small. This balance between the flow from the south and the upwelling along the Australian coast causes a relatively equalized transport of the South Equatorial Current in the region southwest of the Sunda Strait, before its fusion with the water masses of the Counter Current occurs.

7 · 5 REGIONS OF UPWELLING AND SINKING

In recent years scientists engaged in marine research, have studied regions of upwelling both from biological and dynamical points of view. The biologists have been interested in the high plankton production, which is usually accompanied by high fish production. The oceanographers consider these regions as important links in the general circulation, and the junctions between surface and sub-surface circulation.

Where regions of upwelling are large, they are usually coastal and closely related with offshore winds or at least winds parallel with the coast, which blow the light surface water to the open sea and permit denser water of the deeper layers to reach the surface. But upwelling also occurs in the open ocean, particularly if zones of divergence are so strongly developed that, not only an upward curvature of the discontinuity layer occurs, but the vertical upward movements reach the surface. Regions of sinking have received less attention in tropical waters, although dynamically they are as important as regions of upwelling. These vertical movements can be well developed along lines of convergence, but, especially in tropical regions, they are normally ex-

tensive and cover a larger area, which makes them difficult to observe.

In order to understand the circulation in regions of upwelling they have been classified into three types.

1. **The stationary type.** In regions of this type upwelling occurs during the whole year, although there may be fluctuations in its intensity. There are steady ascending motions passing over into horizontal movements, as they reach the surface layer. The properties of the water masses are changed along the subsequent horizontal path by the climatic conditions and they do not reach the upwelling region again. Example: the region off the coast of Peru.

2. **The periodic type.** In these regions upwelling occurs only during one season. During the upwelling season the water masses of the surface layer are carried out of the region and denser water reaches the surface, which normally has a lower temperature and a higher salinity. During the season without upwelling a change of the properties of the already upwelled water is caused by the climatic conditions. This changed water is carried out of the region during the next upwelling season and again water of deeper layers reaches the surface. The difference between this and the stationary type is, that the change of the properties of the upwelling water occurs within the upwelling region during the season without upwelling. Example: the region northwest of Australia.

3. **The alternating type.** In these regions upwelling and sinking occur alternately. This means that during one season the light surface water is driven out of the region and denser water of deeper layers ascends to the surface, while during the other season surface water of lower density spreads over the upwelled water, which again sinks down. Example: the region of the Banda and Arafura Seas. In extreme cases the same water masses might always be engaged in this process, but this would be an exception.

The upwelling on the northwest coast of Australia* is developed from the end of March to the beginning of September, when the southeast monsoon blows northwestwards from Australia as an offshore wind. The water masses in the region, which have been heated during the previous period, are driven into the open sea and almost immediately after the beginning of the upwelling the temperature begins to drop, fig. 4 · 2. This drop of temperature from over 29°C in March to less than 24°C in August is partly caused by high evaporation due to dry, strong winds. The energy required for evaporation during this season is higher than the available radiation, so that a cooling of the water results (see Section 5 · 4). With the decay of the southeast

*See footnote on page 154.

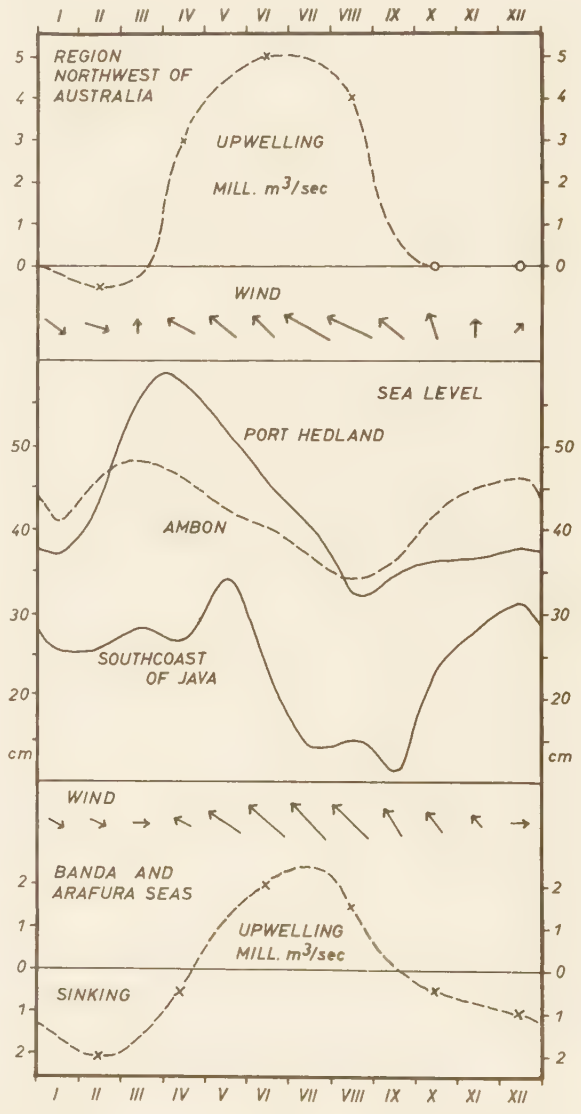

Fig. 7·13. Annual variation of the amount of upwelling, sea level and winds over the upwelling regions northwest of Australia and in the Banda and Arafura Seas.

winds in September/October also the upwelling becomes weaker, and later winds parallel to the coast and currents towards the northeast prevail. Thus the region is classified as the periodic type.

The sea level observations at Port Hedland, Australia, permit a certain insight into the dynamic conditions in this region (fig. 7 · 13). The sea level reaches its maximal height at the end of March and falls by 25 cm during the whole upwelling season. In October, when the winds come from south again, the sea level rises a little, but it remains at this low level until January, or as long as currents parallel to the coast to northeast prevail. The rise of the sea level occurs very rapidly from January to March when the northwest monsoon reaches its full strength in this region. The amount of the upwelling at the time of its full development in July and August might reach approximately 5 million m^3/sec. This water passes completely over into the South Equatorial Current and gives a considerable contribution to its supply. At an average upwelling of 4 million m^3/sec during five months the discontinuity layer would have to rise by 100 m in a region of fifty 1° squares, and the vertical upward velocity would be 0.8 10^{-3} cm/sec. Because a broad shelf lies off the Australian northwest coast and strong tidal currents occur on it, the conditions could be rather complicated. Probably the bulk of the upwelling does not occur along the coast, but along the edge of the shelf, although the maximal dropping of the temperature is observed along the coast.

In the Banda and Arafura Seas another upwelling region develops under the influence of the southeast monsoon. Based on observations of the SNELLIUS and the SAMUDERA made about at the beginning and at the end of the upwelling season in this region, it is possible to give a review of the change of the hydrographic conditions (fig. 7 · 14). By means of six pairs of stations, whose positions are given in fig. 7 · 14, the amount of upwelling can be determined. The SAMUDERA stations from March show a homogeneous layer up to 100 m of high temperature and low salinity. At the station Sa 64 a second layer, only 30 m deep, and of extremely low salinity lies at the surface, representing a branch of the Monsoon Current. The discontinuity layer is well developed at all stations, between 150 and 200 m the salinity maximum of the Subtropical Lower Water is found. In a depth of 200 m the temperature is everywhere lower than 18°C. In October at the end of the upwelling season the discontinuity layer is essentially higher at all stations, which can be seen easily from the distribution of temperature. The temperature at the surface is about 2°C lower than in March, a homogeneous layer does not exist with the exception of station Sn 321, but the temperature decreases directly from the surface. The salinity at the surface is everywhere at or above 34.4‰. This drop of temperature with a simultaneous increase of salinity is probably caused only partly by upwelling, because during this time the evaporation causes a small increase of the salinity and a cooling of the water (see Section 5 · 4).

An evaluation of the vertical curves of the temperature gives vertical displacements of the discontinuity layer between 50 and 70 m during the upwelling season. The region of upwelling is approximately limited by the area shown in fig. 7 · 14, stations further to the west show no raising of the discontinuity layer. The area of the upwelling region is therefore about 27 1° squares equal to 33 10^{14} cm^2. The upwelling takes place during the four months May to August and is of shorter duration than that along the Australian coast. The average upwards velocity is 0.6 10^{-3} cm/sec, the average amount of upwelling is 2 million m^3/sec. This upwelling region is therefore less intense than that on the Australian coast. In June the ascending water masses pass partly over into the Monsoon Current to the Flores Sea, partly into the Timor Current (see plate 3). But in August practically the whole upwelling water flows with the Timor Current into the Indian Ocean (see plate 4).

During the northwest monsoon on the other hand, in the period from November to March

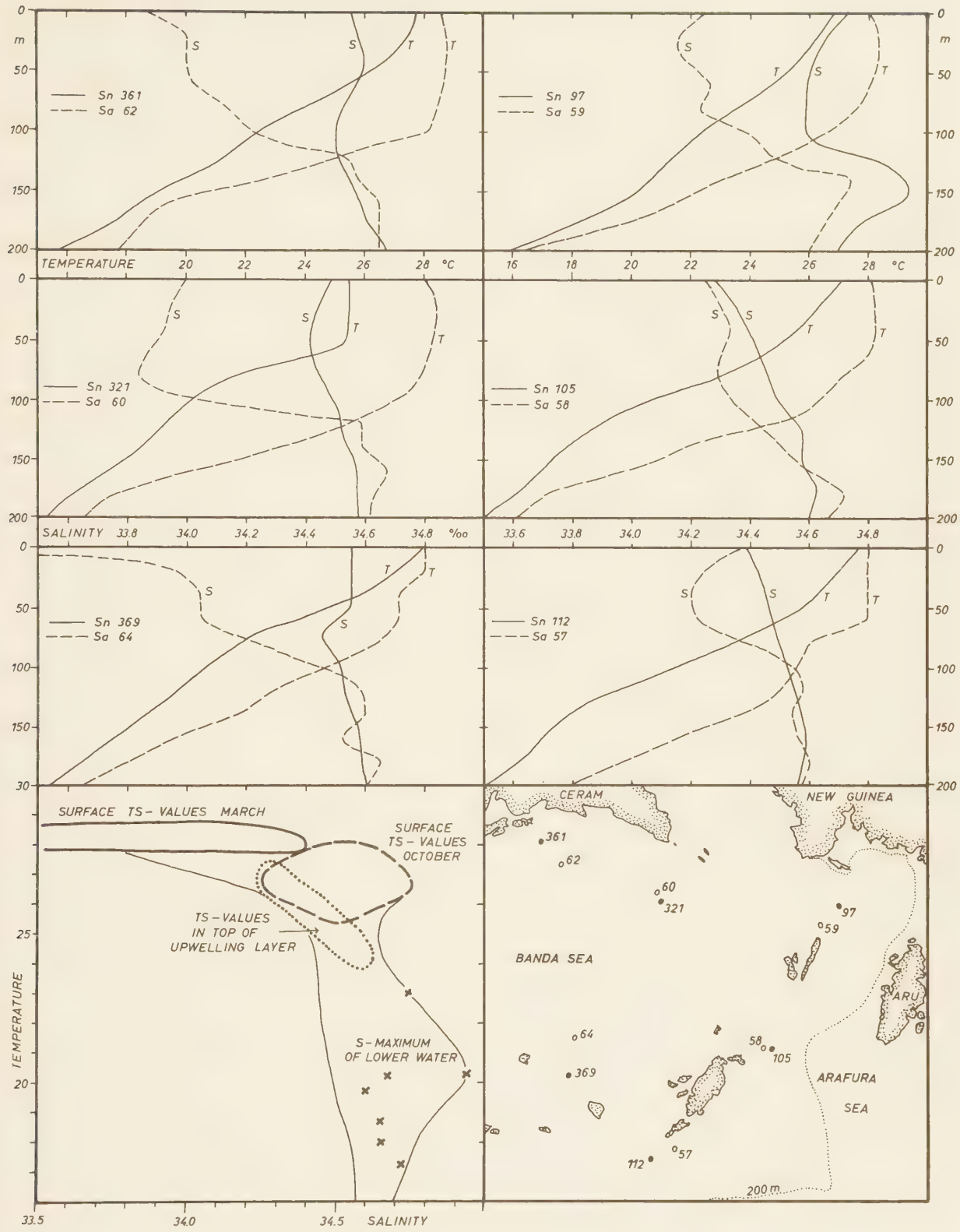

Fig. 7·14. Hydrographic conditions in the upwelling region of the eastern Banda Sea and the Arafura Sea. Upper part: Vertical distribution of temperature and salinity between the surface and 200 meters depth, comparing the observations of the SNELLIUS in October 1929 with those of the SAMUDERA in March 1957 at six positions. Stations are shown in the map below right. Lower part left: T-S diagram of the region, demonstrating the variation of the hydrographic conditions during the upwelling and sinking season.

descending movements occur in this region, classifying the region as an alternating type. The water masses of the Monsoon Current coming from the Flores Sea are piled up in the eastern Banda Sea and in the Arafura Sea and can disappear only partly through the Molucca Sea and the Timor Sea, consequently descending movements occur in the Banda and Arafura Seas. These movements seem to be balanced by an outflow of water from the Banda Sea into the Indian Ocean in a depth of 1000 m (see Section 6·6). The amount of these descending movements reaches its maximum in February with about 2 million m^3/sec and in the average seems to compensate approximately for the upwelling.

From these investigations on the upwelling and its connection with the general circulation, the role of this region in the water exchange between the Pacific and the Indian Oceans becomes evident. During the southeast monsoon upwelling is developed in this region and the ascending water passes at the surface to the Indian Ocean. Simultaneously an inflow of water from the Pacific Ocean occurs through the Halmahera Sea, which is not limited to the surface layer, but also carries the Subtropical Lower Water. Besides this, the continual spreading takes place of the Intermediate Water through the Macassar Strait and of the Deep Water through the Molucca Sea. These movements lead to a slow renewing of the water in the intermediate layers and allow the ascent of the discontinuity layer.

During the northeast monsoon on the other hand descending movements occur in this region, which are balanced by a flow of Banda Sea water into the Indian Ocean in a depth of 1000 m, causing a salinity minimum there. Generally during the southeast monsoon an inflow of water in intermediate layers into the Eastern Archipelago occurs together with upwelling in the Banda and Arafura Seas and an outflow at the surface into the Indian Ocean. On the other hand, during the northwest monsoon an inflow of surface water into the Eastern Archipelago occurs together with sinking in the Banda and Arafura Seas and in the depth an outflow into the Indian Ocean. This example demonstrates the close interrelation between the circulation at the surface and in the depth of the water exchange between the Pacific and the Indian Ocean, this has been discussed in detail by Wyrtki (1958).

The annual variation of the winds over this region, the amount of upwelling and the sea level in Ambon are given in fig. 7·13. It is to be noted that upwelling occurs after the beginning of the southeast winds and ends before them, and it corresponds with the period of falling sea level. The annual variation of the sea level in Ambon in general reflects that of Port Hedland with a smaller amplitude indicating the stronger upwelling off the Australian coast. The fall of the sea level in Ambon in January must be explained as a local effect, perhaps caused by the appearance of north winds in this month.

Remarkable in this connection is the variation of the sea level on the south coast of Java (fig. 7·13). In general it is similar to that of the two other stations, Ambon and Port Hedland, but shows certain deviations. The sea level is always lower, which is caused by a stationary depression at the northern boundary of the South Equatorial Current. The lowest sea level is reached simultaneously at all stations in August/September at the end of the upwelling season. Afterwards in October a rapid rise of the sea level occurs, indicating a filling of the low south of Java, when the southeast monsoon diminishes. The sea level rises gradually until December and this height remains stationary to April. During this period the Java Coastal Current has its strongest development, but the maximal height of the sea level is reached in May, when in Ambon and in Port Hedland the sea level is already falling. This feature might be explained by the fact, that the Java Coastal Current does not vanish before June and the South Equatorial Current touches Java first in July and causes then an extremely low sea level.

In the Andaman Sea another no less important region of upwelling seems to develop during the offshore northeast monsoon from December to March, giving considerable supply to the North Equatorial Current of the Indian Ocean. An evidence of this region is not only given by current observations, but by an increase of the salinity during this period (fig. 4·3). The temperature at the surface, on the other hand, rises, but this is understandable from the heat balance of the region (see Section 5·4). It is also likely that descending movements occur in this region during the southwest monsoon as in the Banda Sea, but no hydrographic observations are available from that region to verify this.

In the China Sea a considerable vertical circulation takes place, which is discussed in Section 7·7, causing, during the northeast monsoon, a piling up of water in the southern part and descending movements in the central part. On the other hand during the southwest monsoon ascending movements occur in the China Sea and especially along the edge of the shelf southeast of Vietnam, when the Monsoon Current leaves the shelf, flows over deep water and is strengthened by the winds in its further path to the northeast. Under these conditions water masses of the discontinuity layer are integrated into the horizontal movements, causing ascending motions along the edge of the shelf for compensation. It is unlikely that these movements reach up to the surface in larger areas, but along the left flank of the current, which has a wind produced component to the east, upwelling seems possible. Such effects have been observed along the coast of Vietnam, which is closely touched by the Monsoon Current. The temperatures of the surface water (fig. 4·2) off the coast of Vietnam in June and July show a drop of more than 1°C, which can be explained in this season only by upwelling.

In the region off Macassar temporary upwelling also appears probable, but its existence cannot yet be verified. During the southeast monsoon, water masses of the Flores Sea meet here with water coming out of the Macassar Strait and flow together into the Java Sea. Under these conditions it seems possible that immediately off the coast of Macassar the water masses of the surface are integrated into this flow, and water from deeper layers ascends, even if only in small quantities. The observations of the surface salinity in this region give evidence of this, they show in June and July often higher values off Macassar than in the surrounding area. This water cannot come from the Indian Ocean, as shown when discussing fig. 4·7, but in most years there is also no connection visible with the waters of higher salinity in the western Banda Sea, and upwelling seems to be the only explanation.

Besides in these regions, upwelling is also possible locally and temporarily at other places to a limited extent, as along the coast of China in the vicinity of Hong Kong during the northeast monsoon, or on the coast of Sarawak. On the other hand, upwelling in the region of the Philippines, in the Sulu and Celebes Seas is unlikely. The stationary high sea level in these regions might prevent ascending movements. In general the representations of hydrographic conditions in the different upwelling regions demonstrate the lack of information about so many of these features in this region, and the interesting possibilities they offer for further research. Because of the few observations from most of these upwelling regions, the information given here is only of a preliminary character.

Ascending movements occur also in the divergences of the main current systems. A region, in which such movements probably lead to upwelling, is the divergence between the Java Coastal Current and the South Equatorial Current. Here a considerable upward curvature of the discontinuity layer has been observed, (Soeriaatmadja 1957), and the surface salinity clearly shows higher values along this divergence. Other divergences are likely to be found along the boundaries of the main current systems of the Indian and the Pacific Oceans, but they are unlikely within the Southeast Asian Waters.

7·6. THE SEA LEVEL IN THE SOUTHEAST ASIAN WATERS

If it were possible to determine exactly the topography of the sea surface, many problems in physical oceanography would be solved. The deformations of the sea surface are the result of the effect of winds and of the distribution of mass in the ocean and are therefore closely related to circulation. Here the available data for the Southeast Asian Waters have been examined to determine the topography of the sea surface and to compare it with the results on circulation.

The basic materials are the observations on sea level published in monthly averages by the International Union of Geodesy and Geophysics (1940, 50, 53) and analyzed by Pattullo and collaborators (1955). There are approximately 50 stations in this region but they are very unequally distributed, they are rather dense in the Philippines and on Java and Sumatra, but are lacking completely in the southeastern parts of the region and in the central parts of the China Sea (see fig. 7·15). The observed heights z of the sea level in cm relative to the mean are corrected in respect to the atmospheric pressure p and a constant c is added, indicating the height of the average sea level. To determine these constants c it is necessary to relate the observations at the different stations to one another. In the following, the term $h = z + (p - 1000) + c$ expressed in centimeters, has always been used, this is a measure of the pressure in the geopotential surface zero, or the topography of the sea surface corrected for the atmospheric pressure. But it must be noted that the period of observations is rather short at most stations, see table 13.

For a determination of the constants c of the different stations quite good conditions exist in

TABLE 13

Adopted mean sea level heights (cm) for different stations in the Southeast Asian Waters Number of years with observations noted, and stations used in the dynamical nivellement are set off.

Station	Mean Height of Sea Level	Number of Years with Observations
Port Uson, Philippines	30	5
Philippines	30	2-30
Macao, China	30	10
Tacao, Formosa	31	40
Kirun, Formosa	31	21
Singapore	42	2
Prigi, east Sumatra	42	3
Palembang River	42	4
Gulf of Thailand	40	6-19
Tuban, Java north coast	34	3
Musang Ketjil, south Borneo	34	2
Semarang, Tandjong Priok, Java north coast	34	6-7
Macassar, south Celebes	30	7
Ambon, Molucca	32	3
Pelabuan Ratu, south coast Java	13	4
South coast Java	13	4-7
Southwest coast Sumatra	13	2-7
Belawan, north Sumatra	12	7
Phuket, Thailand	12	7
Bengkalis, Malacca Strait	25	3
Rangoon	20	5
Port Hedland, Australia	30	5

this region. As most currents are alternating, it is fairly simple to fix the relative zero points of two gauges by a comparison of their differences with the current between the two stations. This procedure has been applied to several gauge pairs in Section 7 · 1 and their positions are given in fig. 7 · 15. Based on this station network the more important gauges have been connected and the constants of the other gauges have been determined by comparison with stations in their vicinity. The "sea level" h determined in this way for the different stations has been used to construct the topography of the sea level in the different months. These results will be compared with the dynamic topography relative 800 decibar as obtained from the mass distribution as well as with the general circulation.

The waters of the Philippines, where the annual variation of the sea level is small, have been selected as the starting point for the determination of the constants c. To permit a direct comparison with the topography of the sea surface relative to 800 decibars, given in plates 39 and 40, the constant for Port Uson and the other stations in the Philippines is selected as c = 30 cm. A comparison of the sea level difference between Port Uson and Macao with the currents in the northern China Sea (fig. 7 · 4), gives for Macao also the value c = 30 cm. As the next station Tacao on Formosa can be connected with Macao by comparing the sea level difference between the two stations with the currents through the Formosa Strait (fig. 7 · 6), c = 31 is the value for Tacao, the same value is selected for Kirun at the north point of Formosa. A comparison of the wind over the China Sea with the longitudinal slope Tacao - Singapore (fig. 7 · 5), gives c = 42 cm for Singapore. For the Gulf of Thailand the value c = 40 cm is selected, permitting an acceptable presentation of the sea level during all seasons. For the two stations Prigi and Palembang River on east Sumatra the same value, c = 42 cm, as for Singapore is taken.

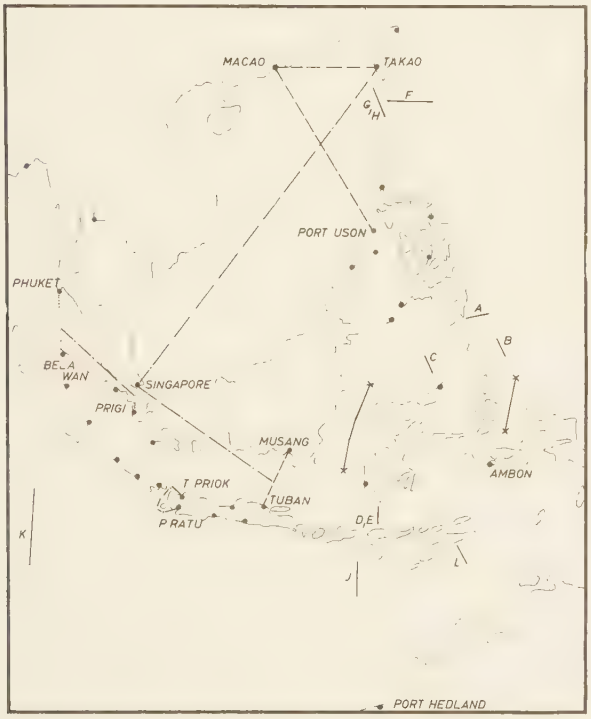

Fig. 7·15. Map showing the station network used for the dynamical nivellement, the sea level stations used in figures 7·1 - 7·8 and the positions of the dynamical sections figs. 7·9 - 7·11.

A comparison of the currents through the Java Sea with the cross slope between Tuban and Musang (fig. 7 · 1), gives for the two stations the same correction. But the determination of its value is only possible by comparing the longitudinal slope Java Sea - Singapore with the winds and the transports (fig. 7 · 2). The constant for the two stations is c = 34 cm and it is used too for the other stations along the north coast of Java. Macassar is connected with Musang in such a way that during the northwest monsoon it is never higher than Musang, resulting in c = 30 for Macassar. The constants of the two stations Menado and Ambon, which have only a relatively small annual variation and where no comparison with currents is possible, are selected in such a way that their sea level is the average between that of the Philippines and of the Java Sea, which gives c = 32 for these stations.

A connection of the stations of the Indian Ocean is only possible by means of a comparison of the currents through the Sunda and the Malacca Straits with the longitudinal slope in their direction. But such a comparison is complicated

by the fact that the currents have the same direction throughout the year. In figs. 7 · 7 and 7 · 8 these relations are shown. The longitudinal slope through the Sunda Straits gives for Pelabuan Ratu a correction c = 13 cm, which is also taken for the other stations along the south coast of Java. The longitudinal slope through the Malacca Strait gives c = 12 cm for Belawan and Phuket, that is practically the same value as that calculated for the south coast of Java. The correction for the gauge of Bengkal in the Malacca Strait is selected in such a way that the sea level in Bengkal is always lower than in Singapore and higher than Belawan, giving c = 25 cm. For Rangoon c = 20 cm is chosen, giving a small lowering of the sea level during the offshore northeast monsoon and a strong piling up of water during the southeast monsoon, according to Rao and Lafond (1953).

The selected values of the constants c are given in table 13 and show only small differences. The highest values in the vicinity of Singapore are only 12 cm above the sea level in the Philippines and the lowest values in the Indian Ocean only 18 cm lower than the average sea level in the Philippines. This result indicates the general piling up of water on the west coasts of the oceans.

The values h of the sea level, corrected for atmospheric pressure, are used to construct

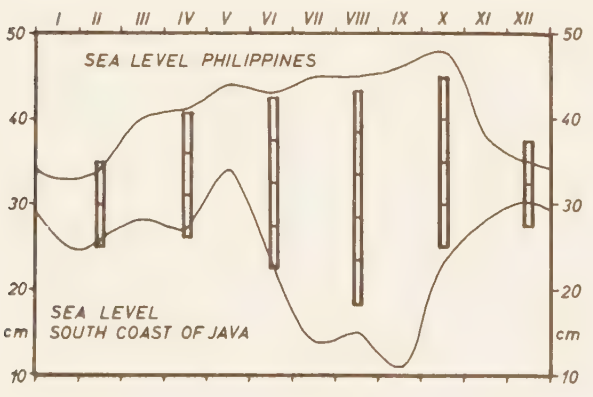

Fig. 7·16. Annual variation of the sea level in the Philippines and at the south coast of Java, showing the relation between the sea level difference Pacific Ocean-Indian Ocean and transports, as given in table 12. Transports are shown by vertical beams, one fraction equals 0.5 million m^3/sec.

charts of the topography of the sea surface. They are presented together with the charts of the surface currents and the transports (plates 1 - 6). In the adjoining parts of the Indian and the Pacific Oceans the charts for February, April and October are supplemented by the topography relative to 800 decibars. The topography of the sea surface as derived from the sea level observations as well as the dynamic topography, plates 39 and 40, show that the sea level in the Indian Ocean is about 20 cm lower than in the vicinity of the Philippines. From this a steady slope results from the Pacific to the Indian Ocean, which is represented in fig. 7 · 16 and shows a good correlation to the transports from the Eastern Archipelago into the Indian Ocean, as given in table 12. These transports are strongest during the southeast monsoon, when the sea level is lowered in the eastern parts of the Indian Ocean.

The three stations Jolo, Zamboanga and Menado on the Celebes Sea show only a very small annual variation of sea level in agreement with the stationary current system in the Celebes Sea. Accordingly the Mindanao Current should fluctuate only a little in its transports, this is confirmed by the observations. In the Flores Sea the Monsoon Current has in February a cross slope of 12 cm with low sea level along the coast of Flores in agreement with the dynamic topography. The eddy south of the island of Somba, which is also indicated by the observations of the SNELLIUS, is a stationary feature, as appeared when the charts of the sea level were drawn.

When comparing the charts of the topography of the sea level with those of the transports, the surface currents and the winds, many relationships between these factors become clear. In spite of this it must be mentioned that the construction of the charts of the transports and of the topography includes some hypotheses, particularly for the eastern parts of the Archipelago and north of Australia, from which almost no sea level observations are available. In these regions further observations and eventually

theoretical calculations will provide an improvement to the charts presented here.

In December and February at the full development of the north monsoon a strong southward transport takes place in the whole China Sea, but not all its water can flow into the Java Sea. Consequently, a piling up of water occurs in the southern China Sea and causes the development of counter currents in the central and eastern parts. The deflection of the current to the right and the piling up of water along the Asian coast with highest sea level in the Gulf of Thailand are clearly seen. In the southern China Sea at the equator no slope exists, the currents are pure wind drifts. In the Java Sea a considerable longitudinal slope develops from 58 cm in the Karimata Strait to only 40 cm south of Celebes. A cross slope exists and the higher values of the sea level are on the left side of the current in agreement with the conditions in the southern hemisphere. This cross slope persists along the whole Monsoon Current to the Banda Sea, there a part of the water masses sinks down, and another part is turned into the Timor Current and flows into the Indian Ocean. The depression of the sea level near the island of Sawu governs this flow. This depression is circulated clockwise, in the north by the Monsoon Current, in the east by the Timor Current and in the south by parts of the South Equatorial Current, which seems to cause and maintain this depression. Through the Macassar Strait chiefly wind-produced movements to the south occur, and a distinguishable slope does not exist. The information from the Molucca region may be questionable. The current chart shows transports to the north, these may be caused at the equator by a very weak slope, as is indicated in the topography. The low sea level in the Andaman Sea is related to the offshore northeast monsoon and to the upwelling.

During the changing of the monsoon in April the sea surface is relatively level. The area of high sea level in the southern China Sea has almost disappeared, the currents in this region are weak and irregular. Only in the Flores Sea remnants of the Monsoon Current are present and cause immediately a cross slope. This current is almost completely deflected into the Timor Current by the depression south of the Lesser Sunda Islands. In the Halmahera Sea the topography indicates a current to the north, but the observations do not verify this.

In June the Monsoon Current gets its water through the Halmahera Sea, through the Macassar Strait and from the upwelling region in the Banda Sea. The small slope from the Pacific Ocean to the Banda Sea indicates this flow. As soon as the Monsoon Current is formed in the Flores Sea, a cross slope develops, which is stronger in the Java Sea because of larger transports. In the southern and central parts of the China Sea the currents seem to be pure wind drifts and no slope is formed. Only in the northern China Sea a lowering of the sea level is found off the coast of China, and there is a slope across the Monsoon Current.

In August these conditions are more pronounced. In the Banda Sea the sea level is extremely low and strong upwelling occurs. The inflow through the Halmahera Sea is strengthened and accompanied by a strong slope. The tongue of high sea level extending from the Lesser Sunda Islands towards the northeast indicates that the Monsoon Current develops west of it and that the water masses of the upwelling region in the Arafura Sea flow chiefly into the Timor Current. The cross slope in the Flores and Java Seas is maintained, although the average sea level is 10 cm lower than in June. In the China Sea the piling up of water by the winds is higher along the coast of the Philippines. From the Celebes Sea water flows southwards through the Macassar Strait according to the slope (see also fig. 7 · 11). In the northeastern parts of the Andaman Sea the piling up of the water is strongest in this month due to the southwest monsoon. The water masses pressed against the coast flow away to the right along the coast of the Malayan Peninsula.

At the beginning of the northeast monsoon in October a piling up of water occurs in the south of the China Sea and along the coast of China. Through the Java Sea a flow to the east

occurs with the slope, because the winds are still weak and irregular during this month. Together with the water flowing southwards in the Macassar Strait with the slope, the water coming from the Java Sea forms in the Flores Sea a distinct current with a cross slope. East of Timor this current is almost completely turned southwards and flows into the depression present at the northern flank of the South Equatorial Current. Water flows with the slope from the Pacific Ocean through the Halmahera Sea to the south and also from the Philippines through the Sulu Sea into the Celebes Sea.

These charts demonstrate clearly the value of simultaneous plotting of the topography of sea level and of circulation for the understanding of their interactions. The inadequacies of this representation of the topography of the sea surface in such a strongly subdivided region are appreciated, and corrections of this picture will result in future. However, the high degree of correlation between the topography and the circulation shown here should encourage a more intensive use of data on sea level in oceanographic studies. Perhaps model experiments also could give important results about the circulation in such a highly subdivided region.

7·7 THE DYNAMICS OF THE WATER MOVEMENTS IN THE CHINA SEA

The China Sea, which is the largest enclosed region within the Southeast Asian Waters, is connected in the south with the Java Sea by very shallow straits, which permit an exchange of surface water only, but its connection with the Pacific Ocean through the deep Luzon Strait allows also an exchange of deep water. The axis of the China Sea lies approximately in the main direction of the winds during both monsoons, therefore the two connections with the Sulu Sea are of less importance. The southern part of the China Sea is very shallow and belongs to the Sunda Shelf, while the northern part is a deep sea basin, which is interspersed by a large number of island groups.

Because of these properties of the China Sea three different circulations can develop. First, a simple surface flow in longitudinal direction, which is driven by the monsoons. Second, because of its width the China Sea permits the development of a horizontal eddy, in which especially during the north monsoon the water which cannot flow into the Java Sea flows back. Third, a vertical circulation caused by the piling up of water in the direction of the wind. These

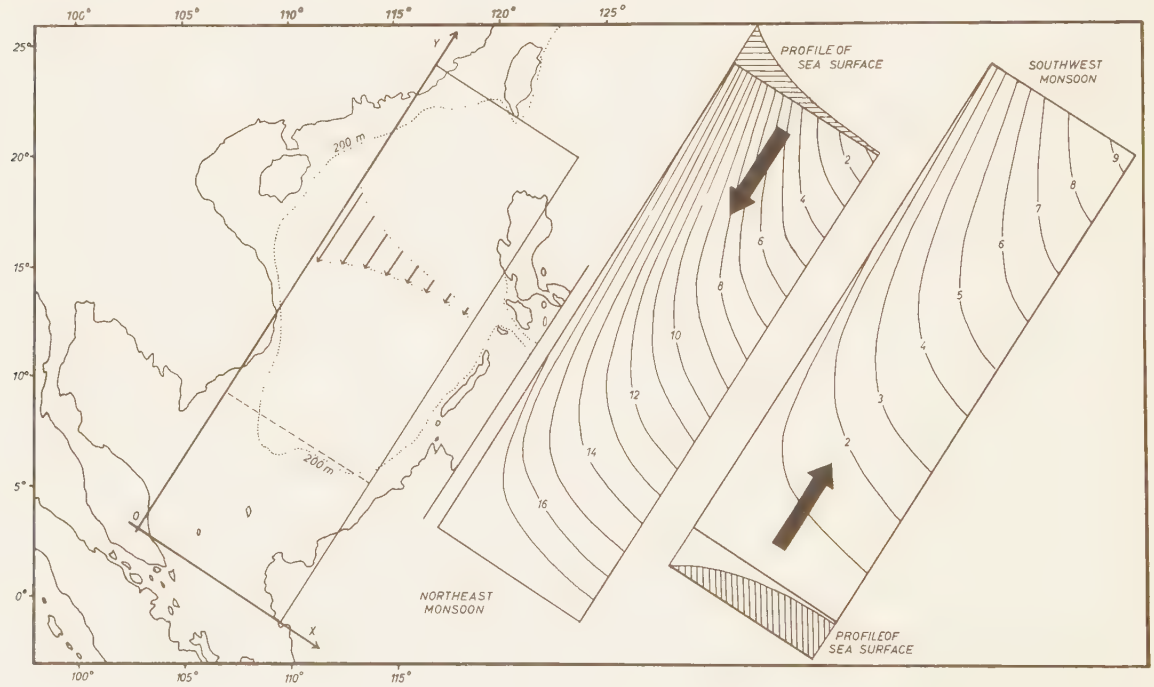

Fig. 7·17. Simplified model of the China Sea, showing the coordinates used in the calculations, the distribution of the current velocity and the topography of the sea surface in cm during the two monsoons.

three circulation systems are now investigated and their transports estimated. In connection with such investigations of the circulation the height of the piling up caused by the winds and also the topography of the surface are of interest.

Considering the China Sea in rough approximation to be a rectangular basin with the sides a and b, whose axis has an angle of 33° with the north direction, and which is open to the other regions in the northeast and southwest (fig. 7 · 17), the hydrodynamical differential equations can be solved under certain simple conditions in closed form. The equations of motion are used in the form (3), the mass transport across the channel is assumed to vanish, the transport in the direction of the channel may be a function of x only and the wind may blow with constant strength in the direction of the channel. Then the conditions are

$$M^x = 0,\ M^y = f(x),\ \tau^x = 0,\ \tau^y = \tau$$

Because the co-ordinate system is inclined against the north direction it must be considered, that for the geographical latitude the expression

$$\sin \varphi \approx \frac{y}{R} \cos 33° = 0.84 \frac{y}{R}$$

is valid, where R is the radius of the earth. With these assumptions the equations (3) simplify as following

$$-1.68\ \omega \frac{y}{R} M^y = -\rho\ g\ D\ h_x$$

$$r\ M^y = \tau - \rho\ g\ D\ h_y$$

A solution is obtained with the disposition

$$M^y = M_0\, e^{-\alpha \frac{x}{a}}$$

and

$$h = h_0 \frac{y}{b} + h_1 \frac{y}{b} e^{-\alpha \frac{x}{a}}$$

It follows for the unknown values

$$\alpha = \frac{1.68\ \omega\ a}{r\ R},\quad h_0 = \frac{\tau\ b}{\rho\ g\ D},\quad h_1 = -\frac{r\ b\ M_0}{\rho\ g\ D}$$

and the whole transport through the China Sea is

$$T = \int_0^a M^y\, dx = M_0 \int_0^a e^{-\alpha \frac{x}{a}}\, dx$$

$$= M_0 \frac{a}{\alpha}(1 - e^{-\alpha})$$

From this M_0 can be eliminated, if T is given. An impression of the properties of the solution is given by fig. 7 · 17. The current is concentrated along the west side and decreases exponentially to the east. The slope shows the same distribution across the current, having its highest values also along the west side. Two examples of the topography of the sea surface during the northeast monsoon in February and during the southwest monsoon in August are calculated with a friction $r = 0.6\ 10^{-5}$ and with the values of winds and transports given in table 10 and represented in fig. 7 · 17.

In February a considerable piling up of water which is about 18 cm, takes place towards the south in the China Sea. The lowest values of sea level occur in the eastern parts, where the water is driven away, the water masses are pressed against the west side by the wind and cause a strong current off the coast. Clearly the effect of variation of the coriolis force is seen, which requires a smaller slope in lower latitudes for the same transport. At the equator itself the cross slope would vanish completely. Over the southern shallow part of the China Sea the variation of the sea level is small and the energy of the wind is practically used only to maintain the transport. A comparison with the topography of the sea surface, as derived from sea level observations (plate 1), shows a surprisingly good agreement between the calculated and observed topography, so it may be assumed that the applied simplifications are justified.

In August the conditions in the China Sea are practically reversed. In the southern parts the sea level is lowered by the wind, in the eastern parts a piling up takes place. Because the transport is smaller, the cross slope is also smaller. The strongest currents develop again along the west side in agreement with the current observations. Over the southern parts the variation of sea level is again smallest, the absolute values agree well with the topography given in plate 4. Small deviations are seen near the entrances to the Sulu Sea, where a part of the piled up water can flow away.

This theoretical treatment of the currents shows the monsoons causing a transport of water

in the longitudinal direction of the China Sea, which is strongest along the west side and a piling up of water to the right of the wind. The calculated values of the topography agree with the observations. Schematically the topography of the sea surface during both monsoons is presented in fig. 7 · 18.

The China Sea is wide enough for the development of its own horizontal circulation, in so far as the necessary dynamic conditions are fulfilled. As shown by theory a horizontal circulation is possible in an enclosed sea only if the rotation of the wind stress vector does not vanish identically. By crosswise differentiation of the two first equations of the system (2) and neglecting variation of f it follows

$$r \operatorname{curl} M = \operatorname{curl} \tau \tag{5}$$

connecting the rotation of the wind stress vector and of the mass transport. To estimate the size of such a circulation a simple example can be constructed. In a rectangular basin with sides a and b, a circulation may exist with the velocity potential

$$\psi = T \sin \frac{\pi x}{a} \sin \frac{\pi y}{b}$$

where T is the transport of this rotating current. The components of the transport are

$$M^x = \psi_y \quad \text{and} \quad M^y = -\psi_x$$

When assuming that the cross component of the wind vanishes and the longitudinal component is only a function of x, likewise in the form

$$\tau^y = -\tau_0 - \Delta\tau \cos \frac{\pi x}{\alpha}$$

By differentiation and entering in (5) it results

$$r T \left(\frac{\pi^2}{b^2} + \frac{\pi^2}{a^2}\right) \sin \frac{\pi x}{a} \sin \frac{\pi y}{b} = \Delta\tau \frac{\pi}{a} \sin \frac{\pi x}{a}$$

Because this relation must also be valid in the average, and because the integral of sin y over a half period is 2, for the transport T caused by an asymmetrical wind distribution the expression

$$T = \frac{\Delta\tau\, b^2\, a}{2\pi r\,(b^2 + a^2)}$$

results. Using for the China Sea the values $b = 3a$, $a = 8^\circ = 890$ km, $r = 0.6\,10^{-5}$ and $\Delta\tau = 0.1$ a transport $T = 2.1$ million m³/sec results. Thus, a wind distribution having in the west a stress 0.2 g cm^{-1} sec^{-2} higher than in the east causes in the China Sea a horizontal counterclockwise circulation of 2.1 million m³/sec. Such a value can be reached especially during the northeast monsoon, which is much stronger off the coast of China than off the coast of Borneo. During the southwest monsoon such a difference is unlikely. Schematically such a circulation is presented in fig. 7 · 18. In the center of this counterclockwise circulation a depression of the sea surface appears. Practically the current in the west along the coast of Vietnam is strengthened, while off the coast of Borneo a current towards the northeast will develop flowing against the wind. This circulation is clearly expressed too in the charts of the surface currents and transports during the northeast monsoon. But the values given there are only 1 to 1.5 million m³/sec. It is possible, however, that the transports are underestimated or that the asymmetry of the wind distribution is overvalued.

The piling up of water in the China Sea caused by the monsoons, as discussed above, is not a stationary feature. Even if in such current systems

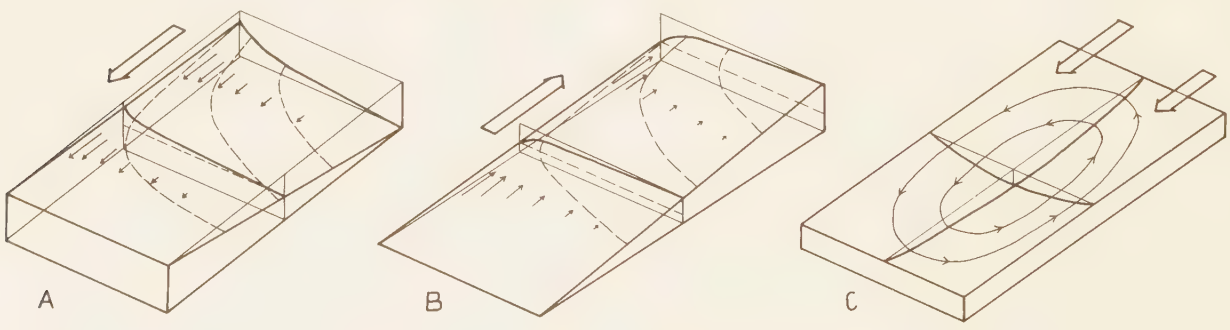

Fig. 7·18. Schematic representation of the topography of the sea surface and of the currents in the China Sea during the northeast monsoon (A), during the southwest monsoon (B) and of the rotating circulation due to the variation of wind stress across the China Sea (C).

the integral of the velocity from the surface to the bottom, that is the transport, vanishes, this does not mean that the velocity vanishes. On the contrary, there is a surface layer with a transport in the direction of the wind, while in the depth a flow back takes place. In a homogeneous water mass these movements are treated in a simple way, as shown by Hansen (1951). In the upper third of the depth the motion is in the direction of the wind, below this in the opposite direction and a maximum of the return flow is reached in two thirds of the depth. In a channel closed at one end such movements cause considerable vertical motions, which are possible without any complication in a homogeneous water mass. In stratified water such movements would result in a continual displacement of the discontinuity layer and lead to a disturbance of the equilibrium. Consequently, other methods must be used in a stratified water body. The discontinuity layer, whether it is in one third of the depth or not, will be the boundary between two independent movements. Because vertical movements must occur in a completely or partly closed channel, it might be convenient to estimate first their size.

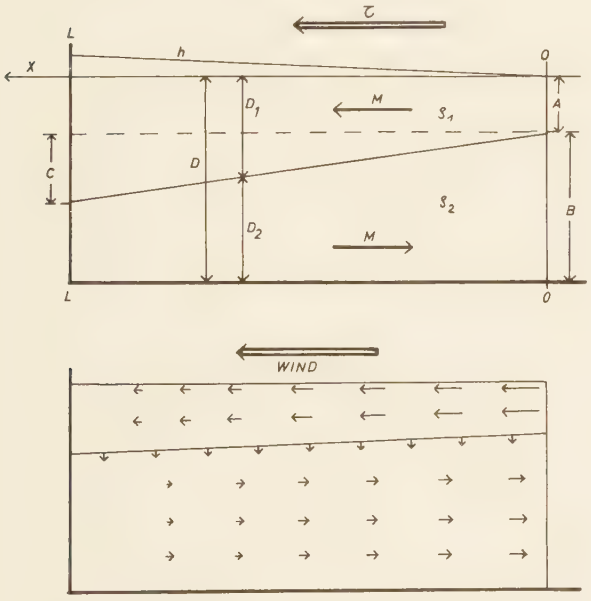

Fig. 7·19. Schematic representation of the vertical circulation in the China Sea.
Upper part: symbols used in the calculations.
Lower part: schematic distribution of currents during the northeast monsoon.

Assuming that the inflow in the surface layer is 5 million m^3/sec, and the same outflow takes place in the depth, the vertical velocity of the boundary surface, which is about 120 one degree squares (equal to $140\ 10^{14}\ cm^2$) is $w = 3.6\ 10^{-4}$ cm/sec. The duration of a full monsoon period is about 4 months or 10^7 sec, and with this value a vertical displacement of the discontinuity layer by 36 m results during a monsoon period. This is a considerable amount, but it does not change essentially the hydrographic conditions. This value is in agreement too with the information given in Section 4 · 1 about the extent of the homogeneous layer in the China Sea, which is 70 m at the end of the northeast monsoon and 40 m at its beginning.

To treat the conditions in the China Sea theoretically, it may be assumed, that over a sea of length L and depth D a wind blows with the stress τ. The channel may be closed at its left end, the surface layer of density ρ_1 may be A meters thick at the open end and A + C meters at the closed end (see fig. 7 · 19). The deviation h of the sea level from its undisturbed position, the thickness of the surface layer D_1 and of the deep layer D_2 as well as the mass transport M may be functions of x. The influence of the width of the channel and with it that of the coriolis force may be neglected. The transports in the surface layer may be opposite to those in the deep layer. With these assumptions the equations of motion are in the surface layer

$$(6) \qquad rM = \tau - \rho_1 g h_x D_1$$

and in the deep layer

$$(7) \quad -rM = -\rho_1 g h_x D_2 + (\rho_2 - \rho_1) g D_2 \frac{\partial D_1}{\partial x}$$

In addition the conditions $D_1 + D_2 = D$, $M = 0$ for $x = L$ and $M = M_0$ for $x = 0$ must be fulfilled. For the longitudinal slope from (6) the equation

$$(8) \qquad \rho_1 g h_x = \frac{1}{D_1} (\tau - rM)$$

results, indicating that it vanishes, if the energy of the wind is used completely to maintain the transport, and that it reaches its maximum if the

transport vanishes. Introducing (8) into (7) we get

$$(9)\quad rDM = \tau(D-D_1) - \Delta\rho g (D-D_1) D_1 \frac{\partial D_1}{\partial x}$$

This is a differential equation for D_1, if M is given, but its solution is difficult and it is simpler to calculate M for different values of D_1. In the simplest case D_1 can be considered to increase linearly, $D_1 = A + C\frac{x}{L}$. Introducing this into (9) leads to

$$(10)\quad r\,D\,M = \tau\left(D - A - C\frac{x}{L}\right) - \Delta\rho\, g\,\frac{C}{L}\left(D - A - C\frac{x}{L}\right)\left(A + C\frac{x}{L}\right)$$

The condition $M = 0$ for $x = L$ gives an equation for C, which is the amount by which the discontinuity layer falls in the direction of the surface flow

$$(11)\quad C = -\frac{A}{2} + \sqrt{\frac{A^2}{4} + \frac{L\,\tau}{\Delta\rho\, g}}$$

Because A is always > 0, it follows for C the condition

$$C < \sqrt{\frac{L\,\tau}{\Delta\rho\, g}}$$

For the transport M_0 at the open end of the channel it follows

$$M_0 = \frac{B}{r\,D}\left(\tau - \frac{\Delta\rho\, g\, A\, C}{L}\right)$$

By this value also the strength of the circulation is given, because the whole transport is $T = b\,M$, where b is the width of the channel. This equation shows the circulation being caused by the wind and being diminished by a term resulting from the stratification, which is practically the energy necessary to keep the discontinuity layer inclined. For the transport M the relation

$$(12)\quad M = M_0 - \beta\frac{x}{L} + \gamma\left(\frac{x}{L}\right)^2$$

results with

$$\beta = \frac{C}{r\,D}\left[\tau + \frac{\Delta\rho\, g\, C}{L}(B - A)\right]$$

and

$$\gamma = \frac{\Delta\rho\, g\, C^3}{r\,D\,L}$$

For a calculation of M and h knowledge of the difference of the density $\Delta\rho$, of the friction r and of the depth of the surface layer A at the open end of the channel is necessary besides the dimensions of the channel. For the China Sea the following values are valid: $L = 2\ 10^8$ cm, $D = 10^5$ cm, $r = 0.6\ 10^{-5}$ sec^{-1}, $\Delta\rho\, g = 4$, $\tau = 0.9$ g cm^{-1} sec^{-2}. The calculation of C from (11), M from (12) and h from (8) is made for three different values of A, the results are shown in table 14.

This table shows clearly that, with decreasing depth of the surface layer, the circulation becomes stronger, the inclination of the discontinuity layer and the piling up by the wind become larger. The decrease of the transport in the direction of the current is practically linear, the influence of the quadratic term is unimportant. The real value for the strength of this circulation in the China Sea is approximately 4 million m^3/sec, the depth of the surface layer, which is the boundary of the movements, lies at 80 m at the beginning and at 120 m depth at the closed end of the channel.

The effects of this circulation can easily be

TABLE 14

Numerical values of properties describing the vertical circulation in the China Sea in three cases

depth of the surface layer at the open end of the channel	A	50	100	150 m
amount of the decline of the discontinuity layer	C	46.6	33.5	25.6 m
strength of the circulation at the open end of the channel	$M_0\ 10^4$	6.87	3.45	1.87
term of the linear decrease of the transport	$\beta\ 10^4$	7.21	3.58	1.92
term of the quadratic increase of the transport	$\gamma\ 10^4$	0.34	0.12	0.05
transport of the whole circulation	T million m^3/sec	6.1	3.1	1.7
piling up at the closed end of the channel	h	18.8	13.5	10.1 cm

seen from the change of the hydrographic conditions at the entrance to the China Sea (fig. 7 · 20). In August during the southwest monsoon, water of low salinity from the southern China Sea has penetrated far to the north and the homogeneous layer is thin. On the other hand the salinity minimum in 500 m depth is well developed, indicating an inflow of water in this depth. In February during the northeast monsoon the conditions are reversed. At the surface, water of high salinity enters the China Sea from the Pacific Ocean, the homogeneous layer is about 80 m thick and the discontinuity layer as a whole is displaced downwards, as seen from the vertical curves of the temperature. This displacement amounts to about 50 m in a depth between 100 and 400 m depth. The maximum of the salinity in 200 m is increased, this must be considered as an influence of the inflow at the surface, which extends into the discontinuity layer. The outflow from the China Sea in the depth is of higher salinity than the inflow during the southwest monsoon. It is a layer of homogeneous salinity flowing outwards between 400 and 800 m depth, while the inflow shows clearly a salinity minimum. Also clear relations exist to the currents through the Luzon Strait as dynamically calculated, fig. 7 · 10.

This treatment of the dynamics of the water movements in the China Sea shows that three circulations, different in principle, occur.

1. The Monsoon Current, flowing through the China Sea as a whole. It is strongest along the west side, its transports are between 3 and 4 million m^3/sec during the southwest monsoon and between 4 and 6 million m^3/sec during the northeast monsoon.

2. A horizontal circulation, caused by the variation of the wind stress across the China Sea. It occurs chiefly during the northeast monsoon, the counter current flows north of the coast of Borneo. Its transport is between 1 and 3 million m^3/sec.

3. The vertical circulation, which causes opposite equal water transports at the surface and in the deep layer, as well as vertical displacements of the discontinuity layer. The transports in the surface layer are in the direction of the wind. This circulation occurs during both monsoons, but seems to be stronger during the northeast monsoon. The transports are between 3 and 6 million m^3/sec, they are omitted from the transport charts (plates 1 - 6).

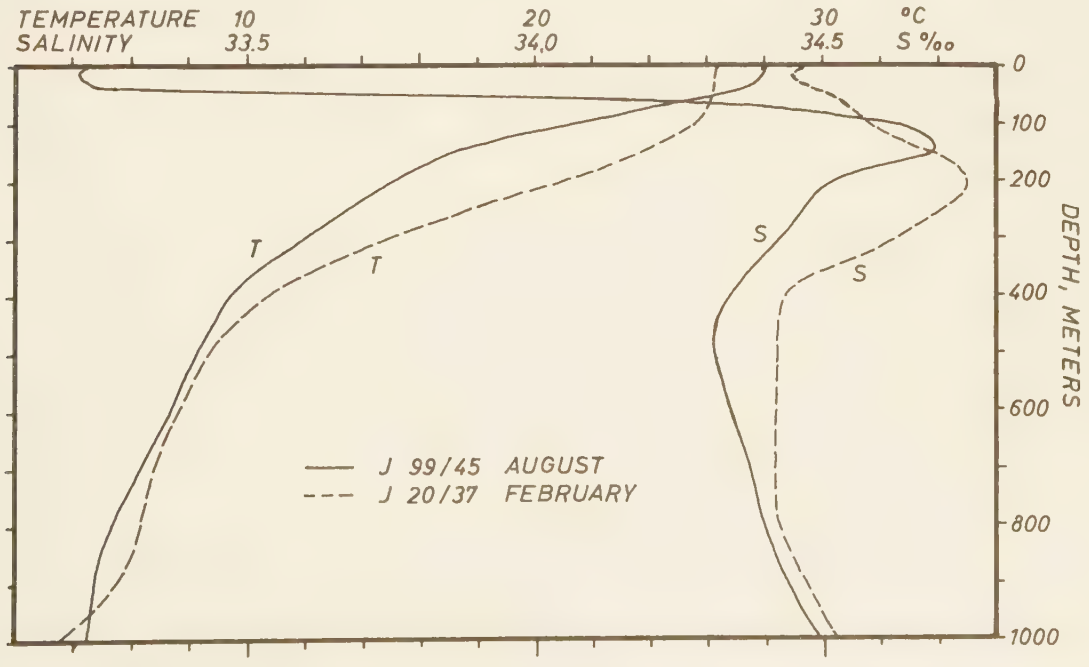

Fig. 7·20. Vertical distribution of temperature and salinity in the northern entrance of the China Sea in February and August, showing the variation of the conditions during the monsoons.

LITERATURE

BERLAGE, H. P.

1927. Monsoon currents in the Java Sea and its entrances.
Verh. Magn. Met. Obs. Batavia 19. 28 pp.

DEFANT, A.

1929. Stabile Lagerung ozeanischer Wassermassen und dazugehörige Stromsysteme.
Veröff Inst. Meeresk. Univ. Berl. 19. 33 pp.

1941. Die absolute Topographie des physikalischen Meeresniveaus im Atlantischen Ozean.
Wiss. Ergebn. dtsch. Atlant. Exped. Meteor. 6 (2) : 191-260.

1950. Reality and illusion in oceanographic surveys.
J. Mar. Res. 9 : 120-138.

GRAHAM, H. W.

1957. The topography of the sea surface in the region of the Philippines.
Proc. 8th Pacif. Sci. Congr. 3 : 673-678.

HANSEN, W.

1951. Beobachtungen des Windstaues und Triftstromes im Modellkanal.
Dtsch. Hydrogr. Z. 4(3) . 81-91.

JERLOV, N. G.

1953. The equatorial currents in the Indian Ocean.
Rep. Swed. Deep-Sea Exped. 3(5) : 115-125.

LEK, L.

1938. Die Ergebnisse der Strom- und Serienmessungen.
Snellius Exped. 1929-30. 2(3) 169 pp.

PATTULLO, J., W. MUNK, R. REVELLE, and E. STRONG

1955. The seasonal oscillation in sea level.
J. Mar. Res. 14 : 88-155.

RAO, R. P. and E. C. LA FOND

1953. Variations of sea level in the Bay of Bengal.
Curr. Sci. 22 : 333-4.

VAN RIEHL, P. M., P. GROEN, and M. P. H. WEENINK

1957. Quantitative data concerning the statics of the East Indonesian waters.
Snellius Exped. 2(7) 45 pp.

SCHOTT, G.

1939. Die äquatorialen Strömungen des westlichen Stillen Ozeans.
Ann. Hydrogr. Berl. 67 : 247-257.

SVERDRUP, H. U., M. W. JOHNSON, and R. H. FLEMING

1942. The oceans, their physics, chemistry and general biology.
New York, Prentice Hall, 1,087 pp.

SOERIAATMADJA, R. E.

1957. The coastal current south of Java.
Mar. Res. Indonesia 3 : 41-55.

WYRTKI, K.

1956. The Subtropical Lower Water between the Philippines and Irian (New Guinea).
Mar. Res. Indonesia 1 : 21-45.

1956. The computation of oceanic and meteorological fields of motion with friction proportional to the velocity.
Mar. Res. Indonesia 2 : 1-26.

1958. The water exchange between the Pacific and the Indian Ocean in relation to upwelling processes.
Proc. 9th Pacif. Sci. Congr. 16 : 61-66.

UNION GEODESEQUE et GEOPHYSIQUE INTERNATIONALE
Association d'Oceanographie Physique.

1940. Monthly and annual mean heights of
1950. sea-level.
1953. Publ. Sci. Nos. 5, 10, 12.

*Recent investigations in the area between Java and the northwest coast of Australia have shown that the bulk of the upwelling during the southeast monsoon does not occur along the coast of Australia, but rather south of Java and Sumbawa along the northern flank of the South Equatorial Current. These results will be published in the *Australian Journal of Marine and Freshwater Research*.

CHAPTER 8

TIDES AND TIDAL CURRENTS

The tides within the Southeast Asian Waters are cooscillating tides of the Pacific and the Indian Oceans. Because of the extremely strong subdivision of this region the pattern is manifold and in each basin a different oscillation is primarily stimulated. So diurnal tides predominate in the China and Java Seas, and mixed tides in the Eastern Archipelago and in the Philippine Waters. In the Andaman Sea and over the shelf northwest of Australia, on the other hand, the semidiurnal tides of the Indian Ocean are predominant.

The observations in this region are dense, and, as many of them are made on islands, they are suitably distributed, to allow a detailed presentation of the tides. These are based on the tidal constants as given in the British Admiralty Tide Tables and in the Dutch Pilots. The positions at which observations were made are given in plates 41 and 43. The four most important partial tides, M_2, S_2, K_1 and O_1 give a relatively complete picture of the tidal pattern at a station, so that their representation seems to be sufficient for general information. Their periods T and their coefficients k are:

	T	k
M_2 semidiurnal principal lunar	12.42	0.4543
S_2 semidiurnal principal solar	12.00	0.2120
K_1 diurnal luni-solar	23.93	0.2655
O_1 diurnal principal lunar	25.82	0.1886

For a geographical consideration of the tides, however, the two diurnal and the two semidiurnal tides can be dealt with together. According to the treatment of the tides of all oceans as given by Dietrich (1944) the following factors are presented:

1. $M_2 + S_2$ the sum of the amplitudes of the two most important semidiurnal tides, indicating the amplitude of the semidiurnal tide at spring tide, plate 41.
2. The phase of the M_2 tide, given by cotidal lines related to Greenwich time, plate 42. The phase of the S_2 tide deviates from the M_2 tide less than 1.5 hours.
3. $K_1 + O_1$ the sum of the amplitude of the two most important diurnal tides, indicating the amplitude of the diurnal tide at spring tide, plate 43.
4. The phase of the K_1 tide, given by cotidal lines related to Greenwich time, plate 44. The phase of the O_1 tide deviates from the K_1 tide less than 2 hours.

The four charts are based on the available material, the charts of the cotidal lines for the adjoining parts of the Indian and the Pacific Oceans are prepared from the representations given by Dietrich (1944) and by Fairbairn (1954). Based on these figures the penetration of the tides from the two oceans into the Southeast Asian Waters is discussed in the following section.

8·1 THE SEMIDIURNAL TIDE

In the region between Japan and New Guinea the semidiurnal tide (plates 41 and 42) is developed as a standing wave with a nodal line in north-south direction between 140° and 150°E. The high water occurs simultaneously along the whole east coast of Formosa and the Philippines with a phase of 9.5 hours. In the south of this region, in the vicinity of the Palau Islands it occurs half an hour later, which leads to the conclusion, that the wave is deflected and comes from the north. The amplitudes are about 60 cm. On both sides of Formosa the wave is strongly refracted, when coming into shallow water, so that it enters the Formosa Strait simultaneously from north and south. Consequently high amplitudes are caused in the centre of the shallow strait, exceeding 200 cm. The wave entering the Luzon Strait advances into the China Sea relatively slowly and with a small amplitude of only 20 cm. It meets the

Sunda Shelf exactly 6 hours after the high water in the Luzon Strait. A part of this wave enters the Gulf of Tonkin without forming an amphidromic region, as shown in other publications. The distribution of the cotidal lines shows clearly a simple progressive wave reaching the edge of the shelf with a phase of 3 hours and the inner parts of the bay 9 hours later, the amplitudes rise to 52 cm. Along the coast of China, between Hong Kong and Hainan Strait, high amplitudes of more than 100 cm are found as an effect of the shelf, which is met by the tidal wave almost under the same phase and causes a considerable increase of its amplitude.

When meeting the Sunda Shelf the velocity of the tidal wave is decreased. Especially off the coasts of Vietnam and Borneo the wave is refracted and high amplitudes develop. Off the mouth of the Mekong the amplitude reaches 119 cm and in the Datuk Bay even 222 cm. But the observations on the islands off the coast show that the increase of the amplitude reaches far into the shelf and is not limited to a small region close to the coast. The wave takes 8 hours from the time it passes the edge of the Sunda Shelf until it reaches the coast of Malaya. There it splits off into two branches, one moves northwards into the Gulf of Thailand and the other southwards and enters the Riau Archipelago. The part of the wave entering the Gulf of Thailand forms there an amphidromic region with a clockwise circulation. Its centre is in 9°18′ N, 103°28′E at the island Palau Panjang. This point is much displaced to the east, which may be caused by the asymmetric arrival of the wave and by the loss of energy due to friction. The amplitudes are less than 20 cm in the whole amphidromic region. But in the northern part a wave separates which does not participate in the amphidromic circulation, but moves directly towards the north. It causes strong tides at the northern coast of the bay, reaching 82 cm at the mouth of the Menam.

The part of the wave moving southwards in the China Sea turns anticlockwise around an amphidromic point in 0°30′N, 106°30′E. But the cotidal lines are all concentrated west of this point, the amphidromic region is developed asymmetrically. The wave begins its turn with a phase angle of 11 hours, reaches the Riau Archipelago with a phase of 4 hours and the island of Banka with 10 hours. Here it joins with the wave coming from the Java Sea and practically disappears. In the whole amphidromic region the amplitudes are small, only within the Riau Archipelago they are a little higher, but this seems to be partly an influence of the tidal wave entering through the Malacca Strait from the Indian Ocean. Here in the region between Borneo and Sumatra the influence of the tidal wave coming from the Pacific Ocean practically ends.

South of Mindanao another branch of the tides of the Pacific Ocean enters the Celebes Sea with a phase of 10 hours. In the northern entrance of the Macassar Strait and in the region east and west of Halmahera this wave meets the wave coming from the Indian Ocean, the amplitude is about 80 cm in the area where the two waves meet. In the Celebes Sea off the coast of Borneo the amplitudes increase up to 139 cm, when the tidal wave reaches the shelf. To the north the tidal wave enters the Sulu Sea and needs 4 hours to pass the Sulu Archipelago. In the whole Sulu Sea and in the Philippines the high water occurs practically simultaneously with a phase of 2 hours. This leads to the assumption that the tides in this region have the character of a standing wave. The amplitudes in the whole region are between 50 and 80 cm. The tidal wave of the China Sea seems not to enter the Sulu Sea. Also the immediate influence of the tides of the Pacific Ocean on the waters of the Philippines seems to be shielded by the small and shallow straits between Luzon and Mindanao. The cotidal lines are concentrated in these straits so strongly that a change of phase of nearly 5 hours occurs and strong tidal currents are the result.

In the Indian Ocean the semidiurnal tides are well developed. From an amphidromic point

west of Australia a bundle of cotidal lines runs to Ceylon and touches Sumatra. This means that in the Gulf of Bengal as well as in the region between Java and Australia an approximately standing wave is present. In the two regions high water occurs with a phase of 2 hours. The amplitudes are considerable and amount in the open ocean to 50 cm at the Christmas Island and to 90 cm at the Andaman Islands. When the wave enters the shelf off Burma, the amplitudes increase off the mouth of the Ganges to 180 cm and in the Gulf of Martaban to 220 cm. Essentially stronger, however, is the increase of the amplitude over the shelf off the northwest coast of Australia. Here the amplitude reaches more than 200 cm over large parts of the shelf and increases at some coastal places to more than 400 cm.

From the Andaman Sea a part of the tidal wave enters the Malacca Strait, where it advances slowly. Because of the contraction of the strait the amplitudes rise from 80 cm at the entrance to more than 250 cm in the narrowest part. Later the amplitude decreases again and the rest of the wave passes over into the amphidromic region in the southern China Sea.

The Lesser Sunda Islands are reached by the semidiurnal tide wave with a phase of 3 hours, the amplitudes are between 70 and 140 cm. A part of this strong wave passes the various straits between the islands, another part enters the Banda Sea through the Timor Sea. In the whole Banda Sea high water occurs with a phase of about 4.5 hours, the amplitudes are 70 cm. Between the islands in the Flores Sea the wave advances slowly northwards, one part is deflected to the west when reaching the Sunda Shelf. A smaller part advances further into the Macassar Strait, where it meets the wave of the Pacific Ocean with a phase of about 10 hours. The wave entering the Java Sea is weak and the amplitudes remain below 20 cm, only off the south coast of Borneo do the amplitudes rise above 40 cm.

From the Banda Sea the tidal wave enters the Molucca Sea, where its amplitude decreases. West and east of Halmahera it meets the wave coming from the Pacific Ocean. In the Timor Sea the tidal wave advances faster over the deep Timor Trench than over the shelf off Australia, which causes a considerable refraction of the wave. The Arafura Sea is reached under a phase of 7 hours with amplitudes of about 60 cm. Over the shelf the wave proceeds slowly but on a broad front. Locally along the coasts an essential increase of the amplitudes occurs, caused by the morphology. It reaches 168 cm at Merauke in New Guinea and 207 cm in the north of Australia. The Torres Strait is reached by this wave 14 hours after it has passed the edge of the Sahul Shelf. About the conditions in the Gulf of Carpentaria information cannot be given because of lack of observations. The amplitudes are between 40 and 80 cm.

8·2 THE DIURNAL TIDE

In large regions of this archipelago diurnal tides predominate (plates 43 and 44). The tidal wave of the Pacific Ocean reaches the Philippines and New Guinea with a phase of 6 hours and with amplitudes between 20 and 40 cm. When entering the China Sea high water occurs nearly simultaneously. The amplitudes of this standing wave are 50 to 60 cm. Contrary to the M_2 tide no intensification of the diurnal tide occurs in the Formosa Strait, because the strait is passed directly from north to south by the tidal wave. The conditions are different in the Gulf of Tonkin, where the diurnal tide develops an amphidromic region, in which the circulation is counterclockwise. The amphidromic point is situated close to the coast of Vietnam, the whole northern part of the Gulf has amplitudes above 100 cm, which increase up to 216 cm in its northeastern corner.

High water reaches the Sunda Shelf in the China Sea with a phase of 13 hours, but the wave advances relatively fast. Coming closer to the coast of Malaya it splits off like the M_2 wave into a north going and a south going branch. The branch moving into the Gulf of Thailand causes there an amphidromic region with an anticlockwise circulation. The amphidromic

point is displaced to the west close to the Malayan coast where the amplitudes are smaller. The highest amplitudes are observed in the northern part of the gulf with 113 cm. The part of the tidal wave moving southwards in the southern China Sea advances slowly, but its amplitudes increase, they reach more than 100 cm along the coast of Sumatra and Banka. In the Gaspar and Karimanta Straits this wave meets the wave coming from the Java Sea, and the amplitudes increase to 80 cm. An amphidromic region is not formed in the southern China Sea.

South of the Philippines the diurnal tidal wave entering the Celebes Sea is retarded, when it meets the first island groups, but advances quickly over the deep Celebes Sea. High water occurs almost simultaneously along all coasts of the Celebes Sea with a phase of 10 hours, the amplitudes are about 30 cm. When passing the Sulu Archipelago the wave is again retarded like the M_2 tide, high water occurs in the whole Sulu Sea and in the Philippines simultaneously with a phase of 13 hours, the tide is here of the standing type, also the amplitudes are very uniform and about 60 cm high. No wave seems to penetrate directly from the Pacific Ocean through the Philippines nor does the wave of the China Sea seem to have any influence.

Contrary to the M_2 wave the diurnal tidal wave penetrates into the Molucca Sea and the Macassar Strait. Through the Macassar Strait it penetrates into the Flores Sea and meets there the wave of the Indian Ocean penetrating through the passages between the Lesser Sunda Islands. Thereby its amplitude is intensified up to 50 cm in the Flores Sea. In the Molucca Sea the tidal wave penetrates on both sides of Halmahera southwards, but it advances slowly. The amplitude increases in this direction and reaches 45 cm, when the wave leaves the Molucca Archipelago in the south. In the Banda Sea finally it meets the wave of the Indian Ocean with a phase of 13 hours.

The diurnal tidal wave of the Indian Ocean circles around an amphidromic point south of Ceylon and is relatively weak. Along the whole south coast of Sumatra and Java high water occurs with a phase of 11 hours and with amplitudes of only 20 cm. At the west corner of Sumatra the cotidal lines are concentrated and very small amplitudes appear. Also in the Gulf of Bengal and in the Malacca Strait the amplitudes remain at about 20 cm. When the tidal wave meets the Lesser Sunda Islands and the Australian Shelf the amplitudes increase and reach 40 to 50 cm at the Sunda Islands and up to 90 cm along the Australian coast. Through the passages between the Lesser Sunda Islands and through the Timor Sea it penetrates into the Flores and Banda Seas. In the Flores Sea the wave meets the stronger wave coming from the Pacific Ocean, there the two waves are refracted and enter the Java Sea. Here they advance at first quickly and later slowly, and the amplitudes reach 80 cm on the north coast of Java and up to 100 cm on the south coast of Borneo. In the range of the stronger concentration of the cotidal lines in the western Java Sea the amplitudes decrease to only 20 cm. Later, when approaching the Karimanta Strait, this wave meets the wave coming from the China Sea and the amplitudes rise again to 80 cm.

Another part of the tidal wave of the Indian Ocean penetrates eastward over the Sahul Shelf. Due to shallow water this wave advances slowly. Along the coast of New Guinea the amplitude is increased, and reaches 224 cm off the mouth of the Digul river. In the Gulf of Carpentaria an amphidromic point seems to be situated in 12°S and 138°30′E and the circulation around it is clockwise. However, because of the small number of stations this assumption is still uncertain.

Summarizing, it may be said, that the semidiurnal tides as well as the diurnal tides of the two oceans penetrate deep into the Southeast Asian Waters. The tides of the Pacific Ocean govern the whole China Sea, the Philippine waters and the Celebes Sea, while those of the Indian Ocean govern the Timor Sea, the Banda Sea and the Sahul Shelf. The Molucca Sea, the

Macassar Strait and the Java Sea are the boundary regions between the two waves, but the semidiurnal tide penetrates further to the north than the diurnal tide. In the Java Sea the diurnal tide is the last trace of the wave of the Pacific Ocean penetrating through the Macassar Strait, while the semidiurnal tide is produced by the wave of the Indian Ocean.

A comparison with the charts given by Ogura (1928) and by Rauschelbach (1933, 1943) in the German Pilots, shows almost complete agreement. Only in the Gulf of Thailand and in the Gulf of Tonkin differences occur, which may be explained by an increase of the number of observations. The M_2 tide in the Gulf of Thailand is shown by Ogura as a simple progressive wave, while Rauschelbach draws a traverse oscillation. But these two oscillations are practically combined in plate 42 by drawing an amphidromic region with a clockwise circulation according to the observations. In the Gulf of Tonkin, Ogura also assumes for the M_2 tide a progressive wave, which is verified now by the more comprehensive observations, but in the charts of Rauschelbach a clockwise rotating amphidromic region appears.

The K_1 tide in the Gulf of Thailand rotates counterclockwise in agreement with Rauschelbach. On the other hand the presentations of Rauschelbach and of Ogura show in the Gulf of Tonkin a progressive wave, but an amphidromic region with a counterclockwise circulation now results as in the Gulf of Thailand, plate 44.

Remarkable too is the direction of the rotation around the amphidromic points. It should be counterclockwise in the northern and clockwise in the southern hemisphere, but this is not fulfilled in all cases. In the Gulf of Thailand the K_1 tide rotates counterclockwise according to the theory, but the faster M_2 tide rotates clockwise. This seems to be caused by the tidal wave coming from the China Sea advancing almost as a progressive wave in the western parts of the Gulf. It returns as a very weak wave in the eastern parts of the gulf around the amphidromic point, which is much displaced to the east. The K_1 tide in the Gulf of Tonkin rotates counterclockwise according to the theory. Remarkable too is the rotation of the M_2 tide around the amphidromic point in the southern China Sea just at the equator. It is counterclockwise, but the amphidromic region is developed asymmetrically, which may be caused by the meeting of three different waves. In the Gulf of Carpentaria the K_1 tide rotates clockwise around the amphidromic point according to the theory.

The tidal waves of the two oceans enter the various seas of the Southeast Asian Waters in quite different ways and many forms of waves and amphidromic regions appear. Theoretical studies of the tides in these waters have not yet been done, but there is an interesting field to study the reasons for various effects and thus to improve or verify many of the interpretations given in this book based solely on observations. A theoretical study of the tides in a region with such a highly complicated morphology would be difficult but it could give essentially new knowledge.

8 · 3. THE GEOGRAPHICAL DISTRIBUTION OF TIDAL TYPES

Only a study of the interaction of the diurnal and the semidiurnal tides can give a picture of the tidal pattern at any one place, this is most simply described by means of the quotient of their amplitudes. For this the proved expression $\frac{K_1 + O_1}{M_2 + S_2}$ is used, being the quotient of the sums of the amplitudes of the two most important diurnal and semidiurnal tides. This quotient can have values between zero and infinity, corresponding to a pure semidiurnal and a pure diurnal tide, respectively. For the presentation of the geographical distribution of the tidal types (fig. 8 · 2) the division given by Dietrich (1944) is used. Examples for the tidal variations of the sea level at four stations with different tidal types during a period of 16 days are given in fig. 8 · 1 the positions of the stations

are entered in fig. 8 · 2. The four tidal types are characterized in the following way:

0 — 0.25 semidiurnal tide. Daily, two high waters and two low waters almost equally high.
Example: Bagan Siapiapi, Malacca Strait.

0.25 — 1.5 mixed tide, prevailing semidiurnal. Daily, two high waters and two low waters, but different in high and high water time.
Example: Sandakan, Sulu Sea.

1.5 — 3.0 mixed tide, prevailing diurnal. Temporarily only one high water and one low water daily, but temporarily also two high waters and two low waters, which differ much in high and high water time.
Example: Hon Nie Nieu, Vietnam.

3.0 — 00 diurnal tide. Only one high and one low water daily.
Example: Cua Cam, Gulf of Tonkin.

The geographical distribution of the tidal types in fig. 8 · 2 shows the semidiurnal tides dominant in the Indian Ocean. The Gulf of Bengal, the Andaman Sea, the Malacca Strait and the shelf off northwest Australia have pure semidiurnal tides, and all the other regions, such as the south coast of Sumatra and Java and the Lesser Sunda Islands, have mixed, prevailing semidiurnal tides. In the western Pacific Ocean the diurnal tide is more pronounced, even if the mixed prevailing semidiurnal type is still dominant. But this changes immediatly when the tides enter the Southeast Asian Waters. Almost the whole China Sea has a mixed, prevailing diurnal tide, because the amplitudes of the semidiurnal tide are small. Only in the Formosa Strait, where local conditions cause a considerable strengthening of the M_2 tide, are semidiurnal tides found. In other regions the diurnal tide is amplified. Thus in the Gulf of Thailand, in the Gulf of Tonkin and in the waters between Sumatra and Borneo an almost pure diurnal tide is found. Also the Java Sea has a

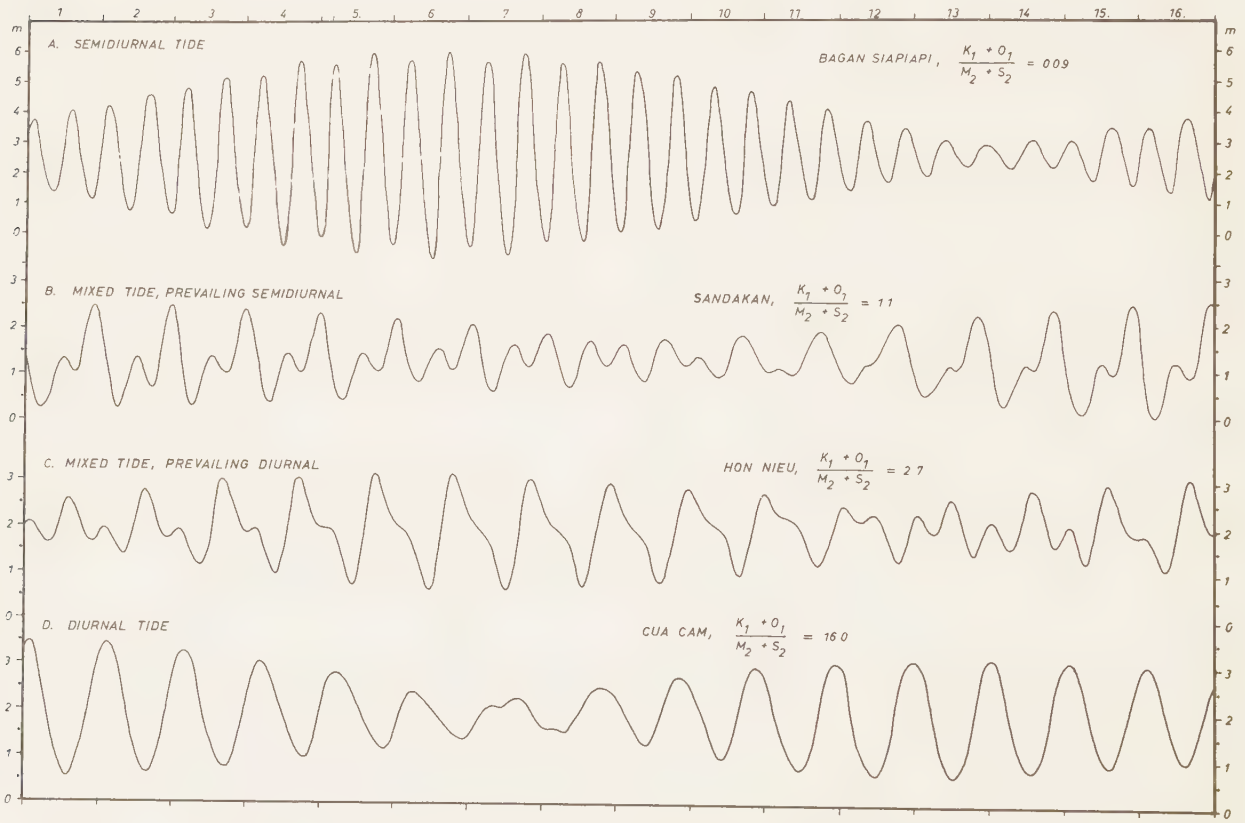
A. SEMIDIURNAL TIDE
BAGAN SIAPIAPI, $\frac{K_1 + O_1}{M_2 + S_2} = 0.09$
B. MIXED TIDE, PREVAILING SEMIDIURNAL
SANDAKAN, $\frac{K_1 + O_1}{M_2 + S_2} = 1.1$
C. MIXED TIDE, PREVAILING DIURNAL
HON NIEU, $\frac{K_1 + O_1}{M_2 + S_2} = 2.7$
D. DIURNAL TIDE
CUA CAM, $\frac{K_1 + O_1}{M_2 + S_2} = 16.0$

Fig. 8·1. Typical tidal curves in the Southeast Asian Waters, representing the four types of tides during a period of 16 days.

prevailing diurnal tide. On the other hand in the eastern parts of the Archipelago the mixed, prevailing semidiurnal tide is dominant, being an influence of the Indian Ocean. Only off the southwest coast of New Guinea and in the Sulu Archipelago, regions develop with prevailing diurnal tides, due to local conditions.

8·4. TIDAL CURRENTS AND INTERNAL WAVES

Tidal currents are very common in the Southeast Asian Waters, especially in the numerous narrow passages, and they reach considerable strength. Because of their importance for navigation they are well known at the surface and discussed in detail in the different Pilots. Record values of the tidal currents of about 10 knots are observed in the Tjaipololu Strait and are harmonically analysed by Rauschelbach (1931). But also in the passages between the Lesser Sunda Islands, in the Philippines and in the Torres Strait tidal currents of 5 to 6 knots occur at spring tide. In the other passages the tidal currents normally do not exceed 3 knots. Also in the open sea, especially over the shelves tidal currents are observed, but they normally remain below 1 knot, that is below 50 cm/sec. Over

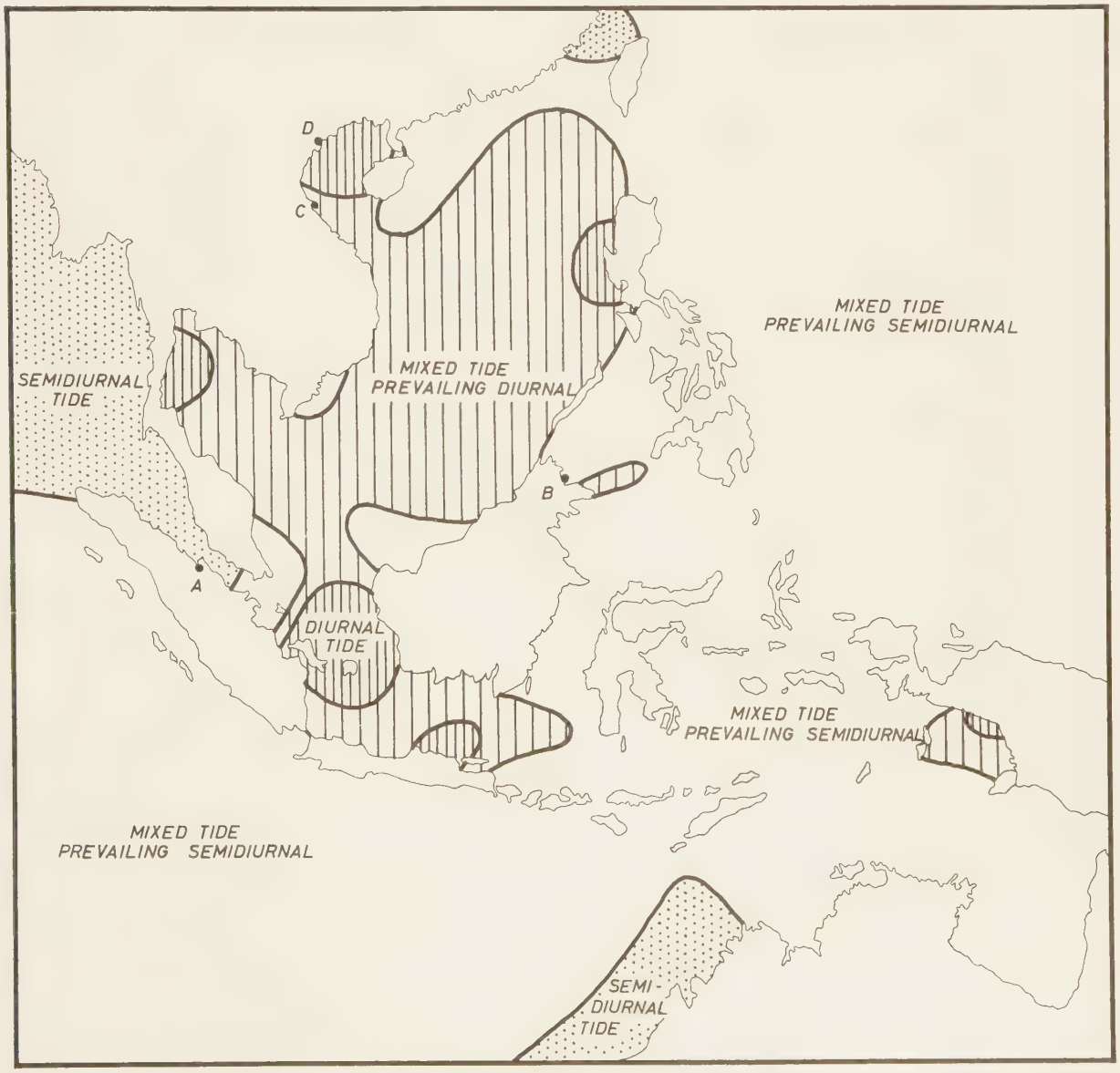

Fig. 8·2. Geographical distribution of tidal types in Southeast Asia.

the deeper regions in the Eastern Archipelago the tidal currents are even weaker. The SNELLIUS expedition has obtained, for the semidiurnal tidal current at the surface, amplitudes between 3 and 25 cm/sec and for the diurnal tidal current amplitudes between 6 and 27 cm/sec at its seven anchor stations, Lek (1938). For the Torres Strait extensive tidal current observations were made and published by the British Hydrographic Department (1931), the daily current figures are presented by Horn (1952) and demonstrate the highly complicated conditions in the tidal current pattern.

Over the shelf it can be expected, and is verified by some observations (van Weel 1923), that the current has practically the same direction and velocity from the surface to the depth, with the exception of a small layer near the bottom due to friction. Over the deep water the anchor stations of the SNELLIUS show that tidal currents, often with amplitudes exceeding those at the surface, are to be observed in all depths. But their phases normally vary considerably with the depth, as shown by Lek (1938), so that the resulting transport, that is the integral of the velocity from the surface to the bottom, does not reach high values. A review of the velocities in the main directions of the current ellipses in different depths, as calculated from the SNELLIUS data is given in table 15.

This table demonstrates that the semidiurnal tide is also more strongly developed in the depth than the diurnal tide. Further the averages show a slight decrease of the amplitudes with the depth. The values of the velocity indicate the strongest tidal currents occurring above and in the discontinuity layer and weaker movements in the deeper layers. But most observations are made in relatively narrow passages and therefore the velocities in the open seas may be smaller.

In connection with these tides and tidal currents, internal waves of tidal period occur in stratified water, as well as internal waves of other periods. These numerous oscillations cause a current pattern, which is so highly confused, that no conclusions can be drawn without a comprehensive analysis. Only a careful treatment of the current measurements, as done by Lek and Fjeldstad (1938) for the anchor stations of the SNELLIUS, can give results about the actual periods, vertical movements and amplitudes of the current in the different depths. It could be shown that the internal waves with

TABLE 15

Amplitudes of the tidal currents (cm/sec) in the main directions of the current ellipses for the Diurnal and the Semidiurnal Tides in different depths of the Eastern Archipelago

Depth	Semidiurnal Tide				Diurnal Tide			
25 - 100 m	5.0	6.5	8.7	10.2	6.0	7.0	8.3	9.3
	10.5	12.5	16.4	17.7	9.3	9.7	12.1	13.2
	25.6	26.1	35.4	35.4	13.3	13.8	15.5	21.6
	36.7							
	average : 18.7				average : 11.6			
125 - 250 m	4.4	4.9	5.5	9.7	5.1	6.1	6.4	9.6
	11.4	15.2	16.0	22.3	11.4	12.4	14.9	22.6
	26.4	44.2						
	average : 16.0				average : 11.4			
300 - 600 m	3.3	7.0	7.6	13.2	3.8	5.2	5.9	6.2
	14.0	18.4	20.9	22.3	6.3	7.8	7.8	9.0
	26.0				9.5	11.7	15.0	
	average : 15.8				average : 8.0			
> 600 m	1.6	3.4	8.7	14.7	8.5	10.0	12.4	
	average : 7.1				average : 10.3			

tidal period are dominant in these waters. In connection with the currents the different layers are subject to considerable vertical movements with amplitudes of 5 to 10 m, in single cases even 20 m were observed. This corresponds to a vertical displacement of a certain layer by 40 m. Based on this analysis a number of theoretical results which are discussed by Sverdrup (1946) could be verified. As important as these results may be for the understanding of the tides and internal waves, investigations are lacking, which combine these currents with the tides observed along the coast.

The internal waves cause, especially within the discontinuity layer, considerable vertical movements of the water masses, which lead to a continual variation of their vertical structure. Consequently all hydrographic observations are subject to these variations, which especially disturb dynamical calculations. In unfavorable cases the variation of the dynamic height at one station can be more than 10 dyn cm, and this makes it impossible to use the observations for drawing the dynamic topography.

LITERATURE

Dietrich, G.

1944. Die Schwingungssysteme der halb- und eintägigen Tiden in den Ozeanen. Veröff. Inst. Meeresk. Univ. Berl. A.41.

1944. Die Gezeiten des Weltmeeres als geographische Erscheinung. Z. Ges. Erdk. Berl. 1.

Fairbairn, L. A.

1954. The semi-diurnal tides along the equator in the Indian Ocean. Phil. Trans. A. 247 : 191-212.

Great Britain Hydrographic Department.

1931. Report on the tides, currents and tidal streams in the southern part of the Torres Strait. H.D. 302. 16 pp.

Great Britain Admiralty.

1957. Tidal tables. London. H.M.S.O.

Horn, W.

1952. Tägliche Stromfiguren der gemischten, überwiegend halbtägigen Gezeitenströmung von Proudfoot Shoal, Torres Strasse. Landolt-Börnstein, Zahlenwerte u Funktionen. 3.

Lek, L., and J. E. Fjeldstad.

1938. Die Ergebnisse der Strom- und Serienmessungen. Snellius Exped. 1929-30. 2(3) 169 pp.

Marmer, H. A.

1945. The tide in Philippine waters. Proc. U.S. Nav. Inst. 71 : 543-9.

Ogura, S.

1928. On the tides in the seas of Eastern Asia. Proc. 3rd. Pacif. Sci. Congr. 1 : 167-182.

Rauschelbach, H.

1931. Ausführliche Vorausberechnungen der Gezeitenströme in der Enge der Tjapololu Strasse. Ann. Hydrogr. Berl. 59 : 168-171.

1933. Gezeiten. Handb. Ostindischen Archipel. Berlin.

1943. Gezeiten. Handb. Südchinesische Meer. Berlin.

van der Stok, J. P.

1911. Elementare Theorie der Gezeiten nebst den Gezeitenkonstanten der wichtigsten Orte des Indischen Archipels und anderer Hafenplätze. Ann: Hydrogr. Berl. 39 : 227-241, 303-317, 354-373.

Sverdrup, H. U., M. W. Johnson, and R. H. Fleming.

1942. The oceans, their physics, chemistry and general biology. New York, Prentice Hall. 1,087 pp.

van Weel, K. M.

1923. Meteorological and hydrological observations in the western part of the Netherlands East Indian Archipelago. Treubia 4 : 559 pp.

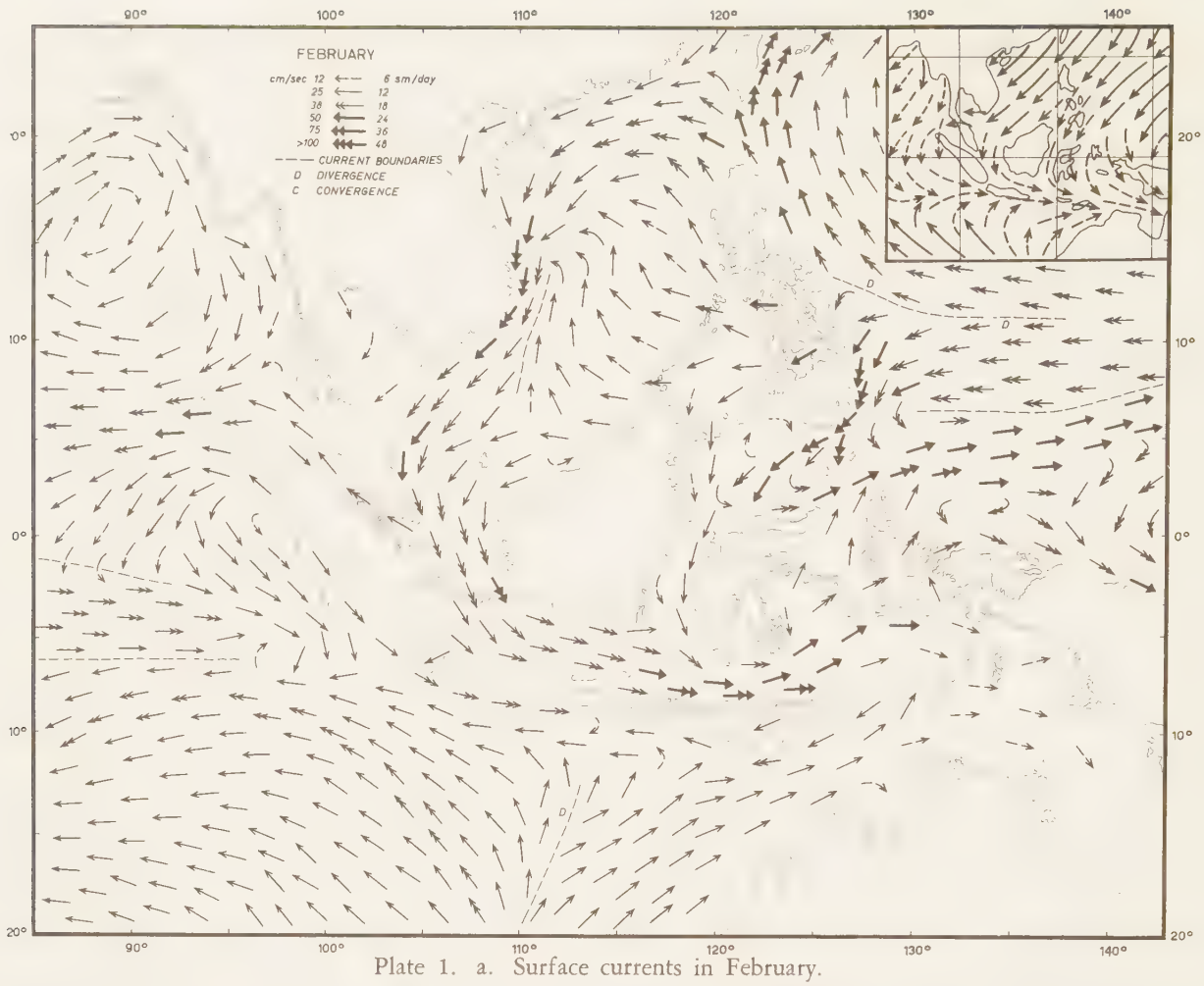

Plate 1. a. Surface currents in February.

b. Transports of surface circulation in million m^3/sec. + upwelling, o sinking.

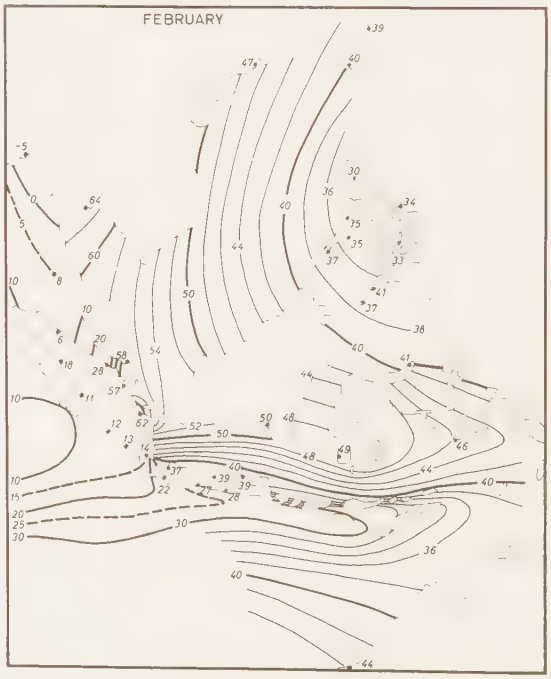

c. Topography of sea level in cm.

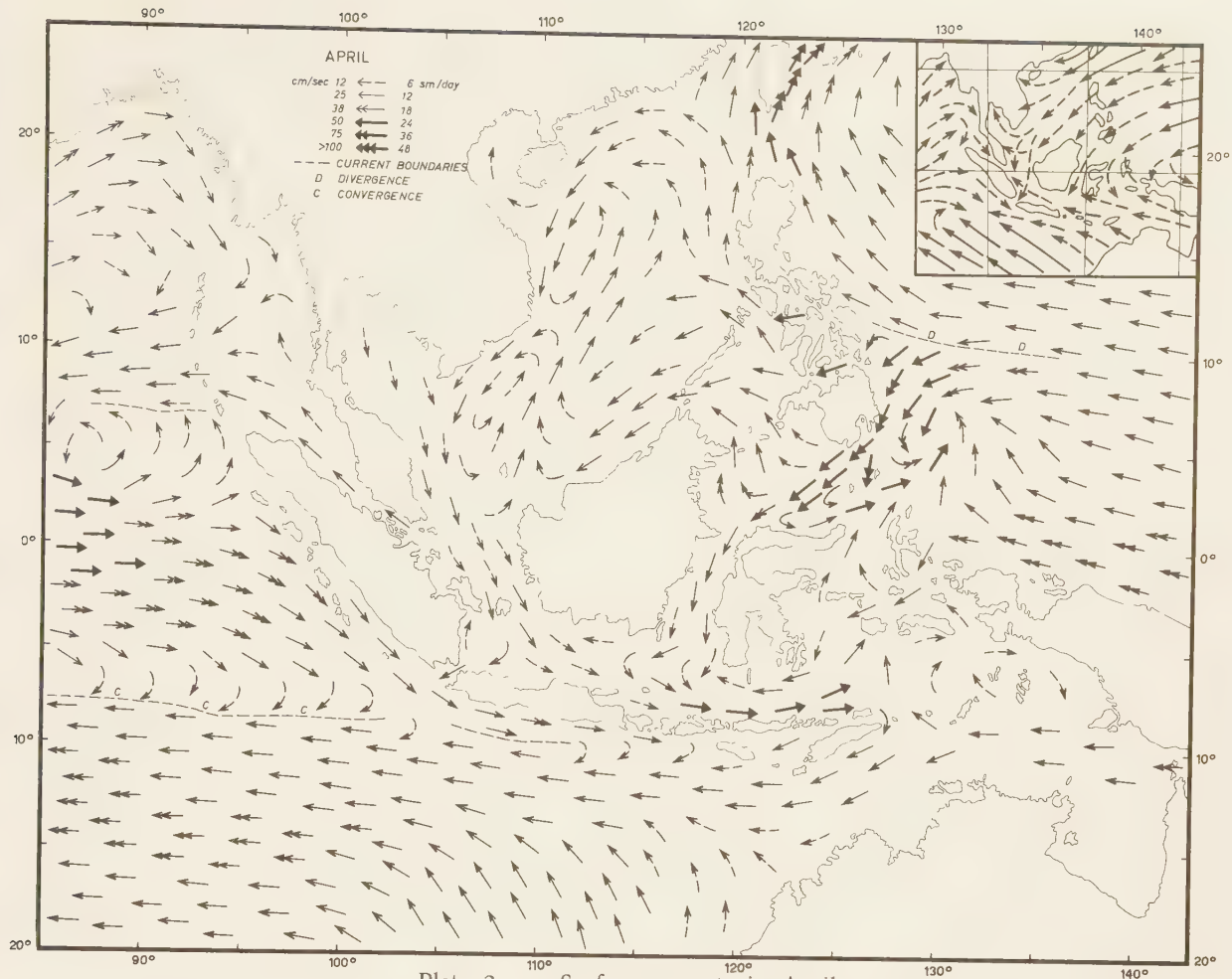

Plate 2. a. Surface currents in April.

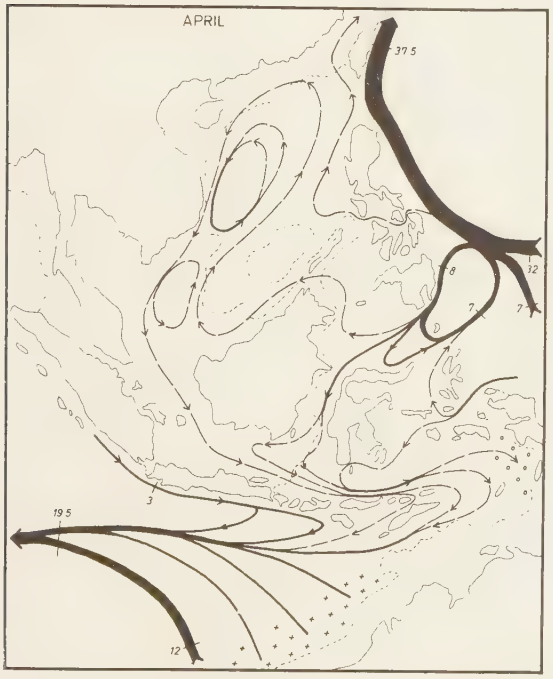

b. Transports of surface circulation in million m^3/sec. + upwelling, o sinking.

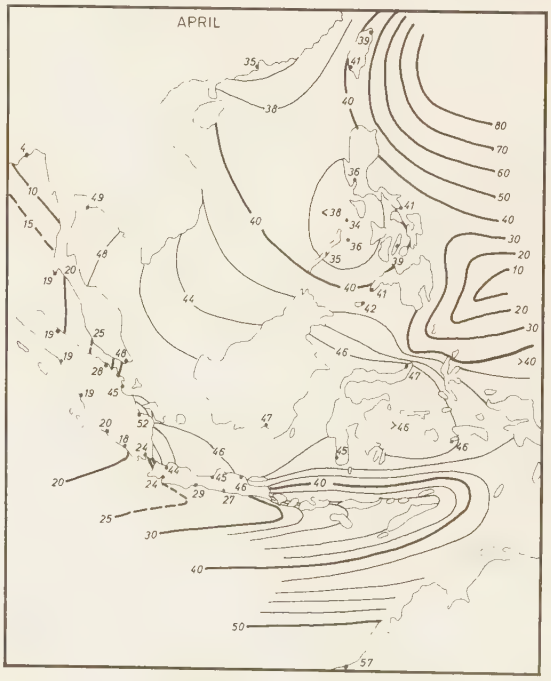

c. Topography of sea level in cm.

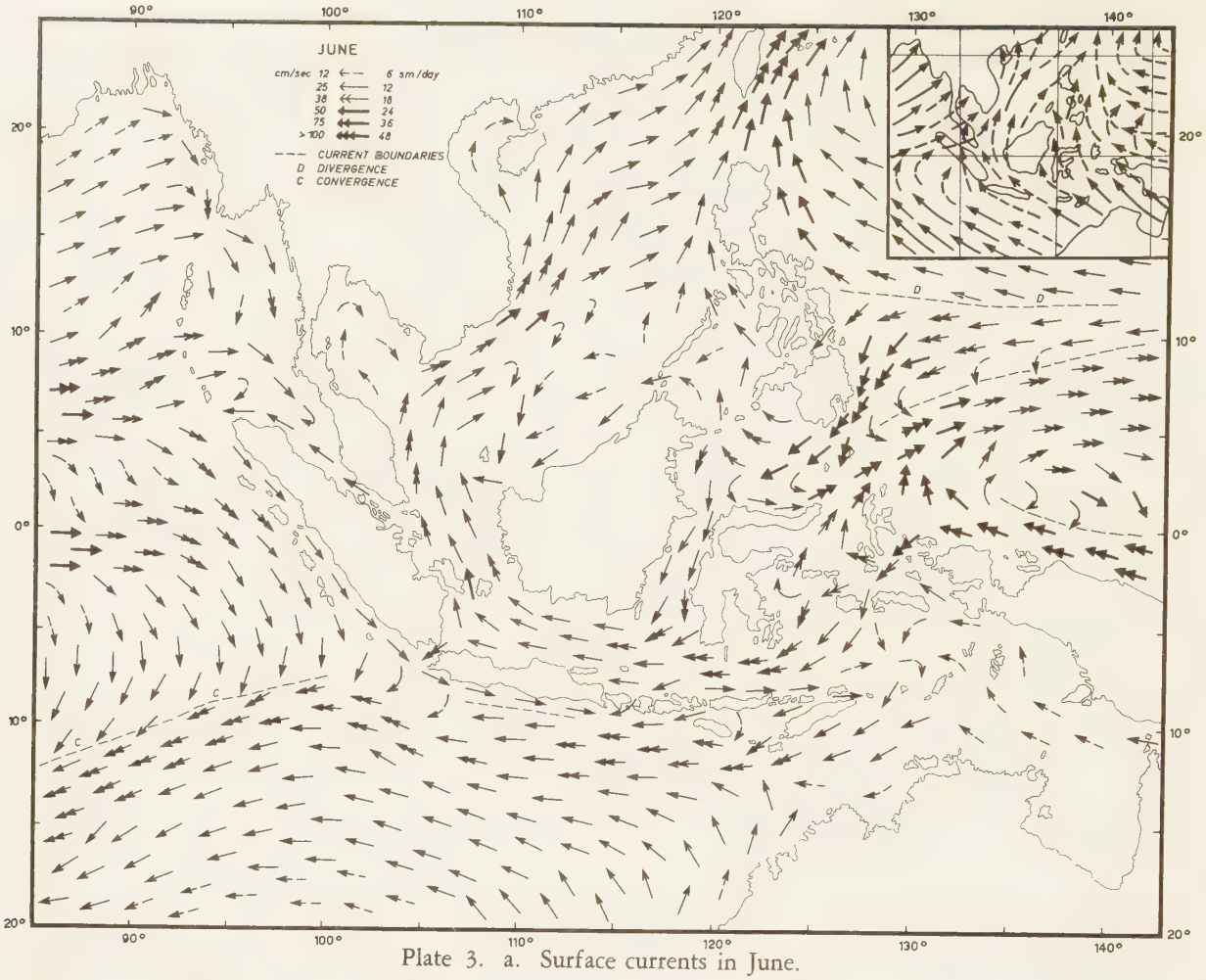

Plate 3. a. Surface currents in June.

b. Transports of surface circulation in million m^3/sec. + upwelling, o sinking.

c. Topography of sea level in cm.

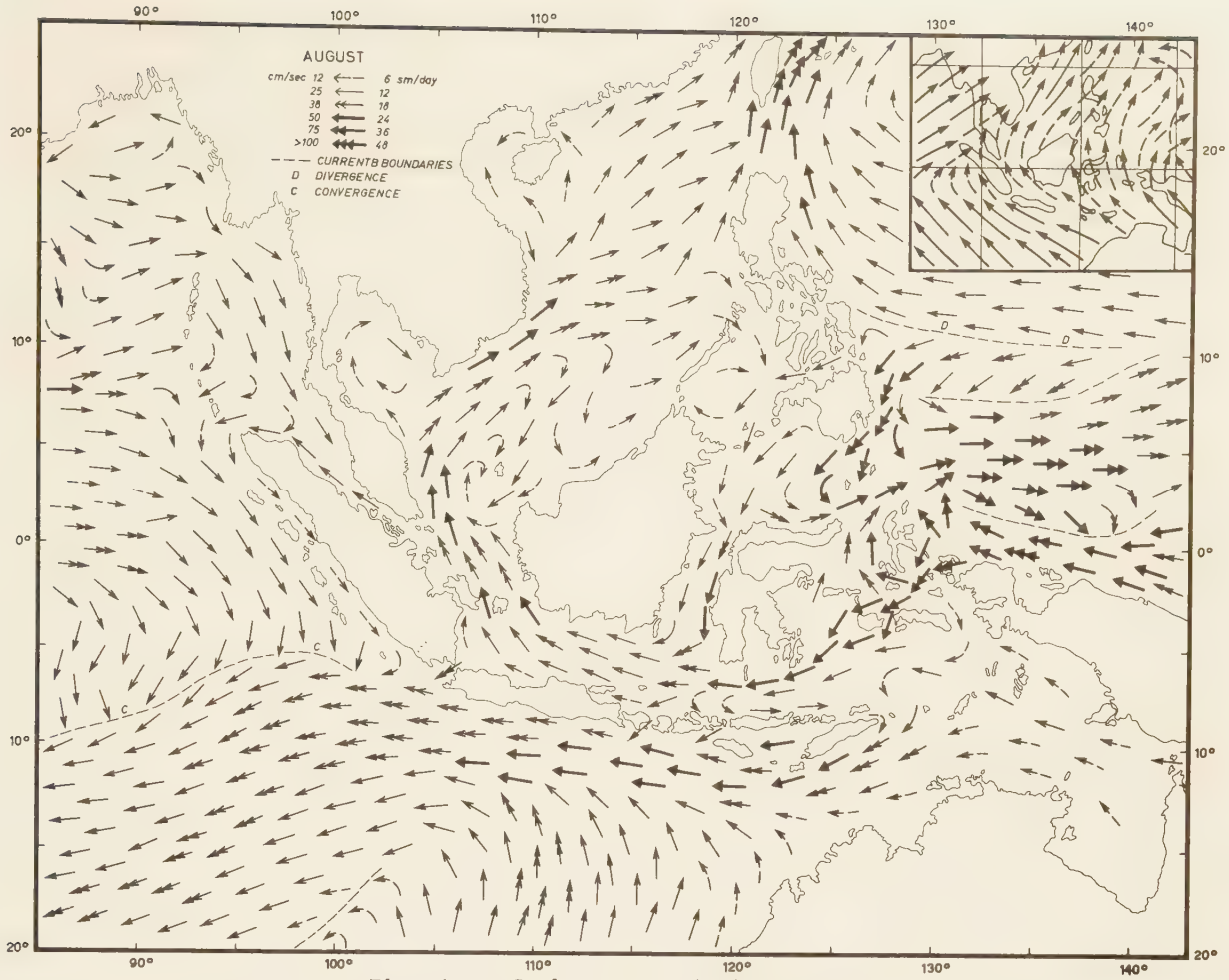

Plate 4. a. Surface currents in August.

b. Transports of surface circulation in million m^3/sec. + upwelling, o sinking.

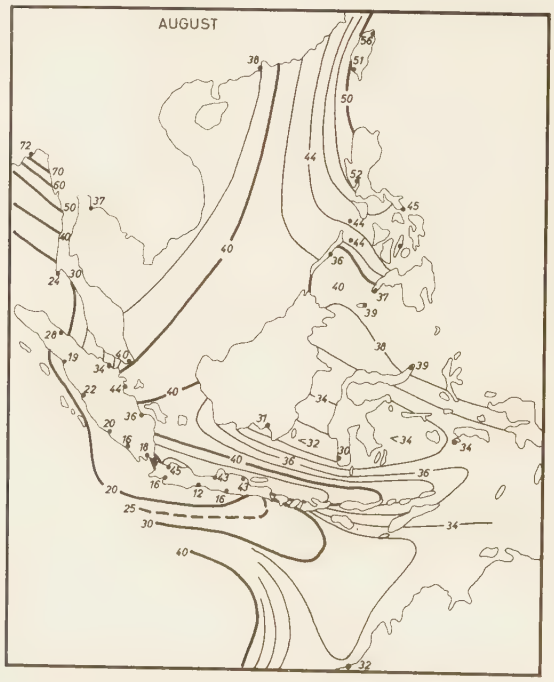

c. Topography of sea level in cm.

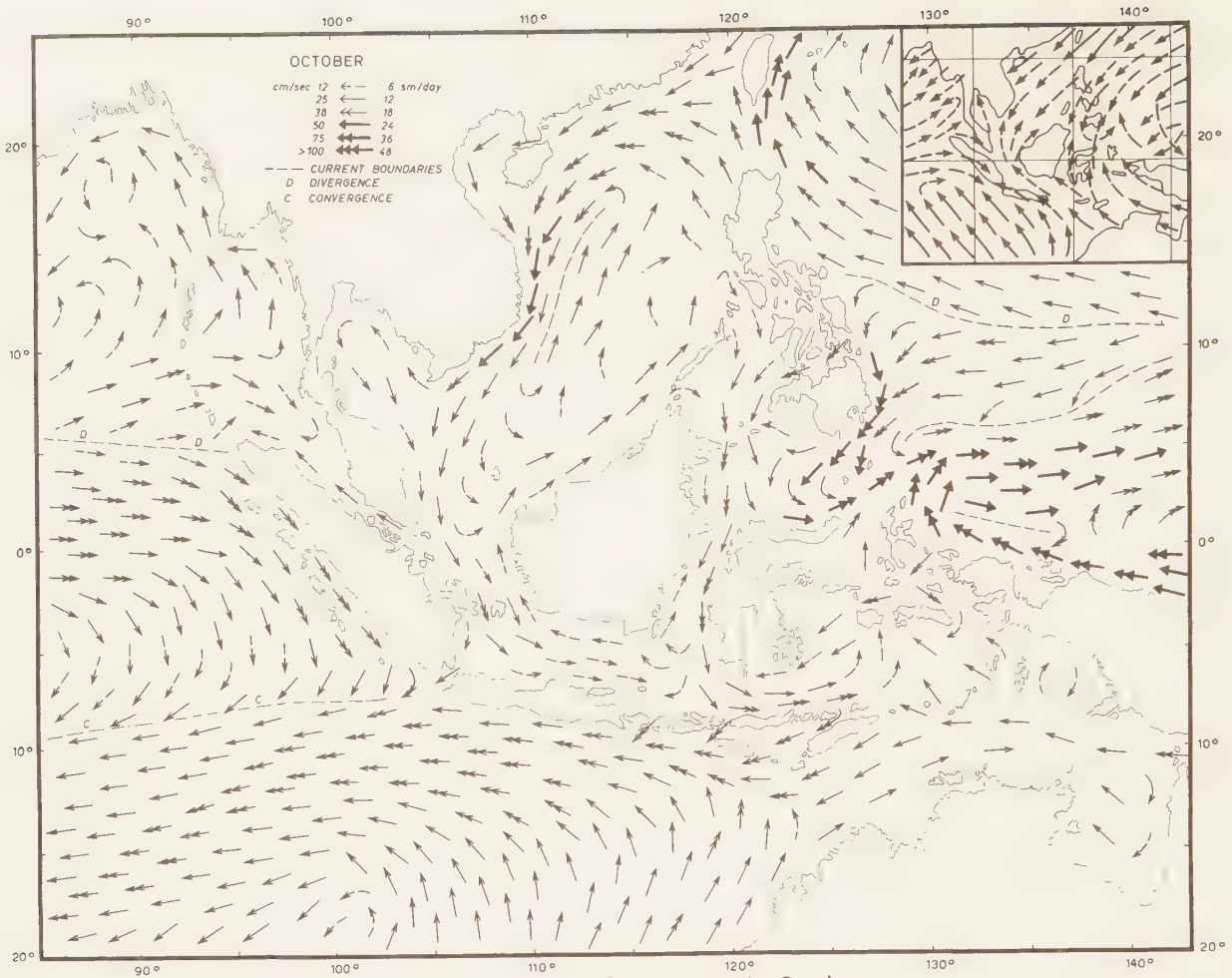

Plate 5. a. Surface currents in October.

b. Transports of surface circulation in million m^3/sec. + upwelling, o sinking.

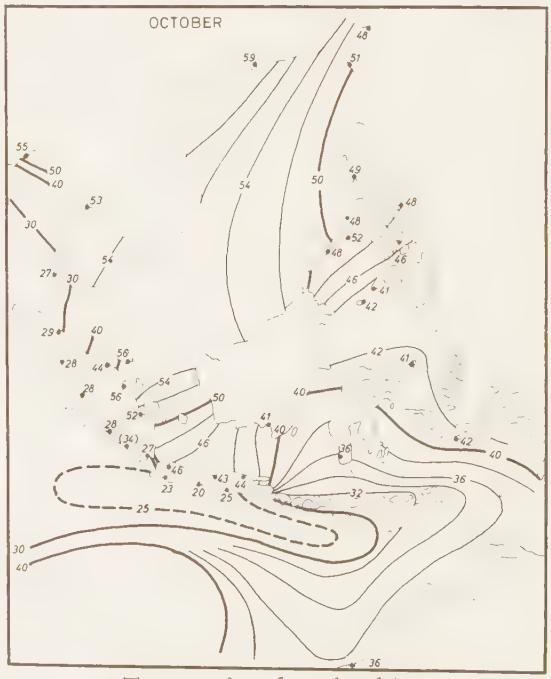

c. Topography of sea level in cm.

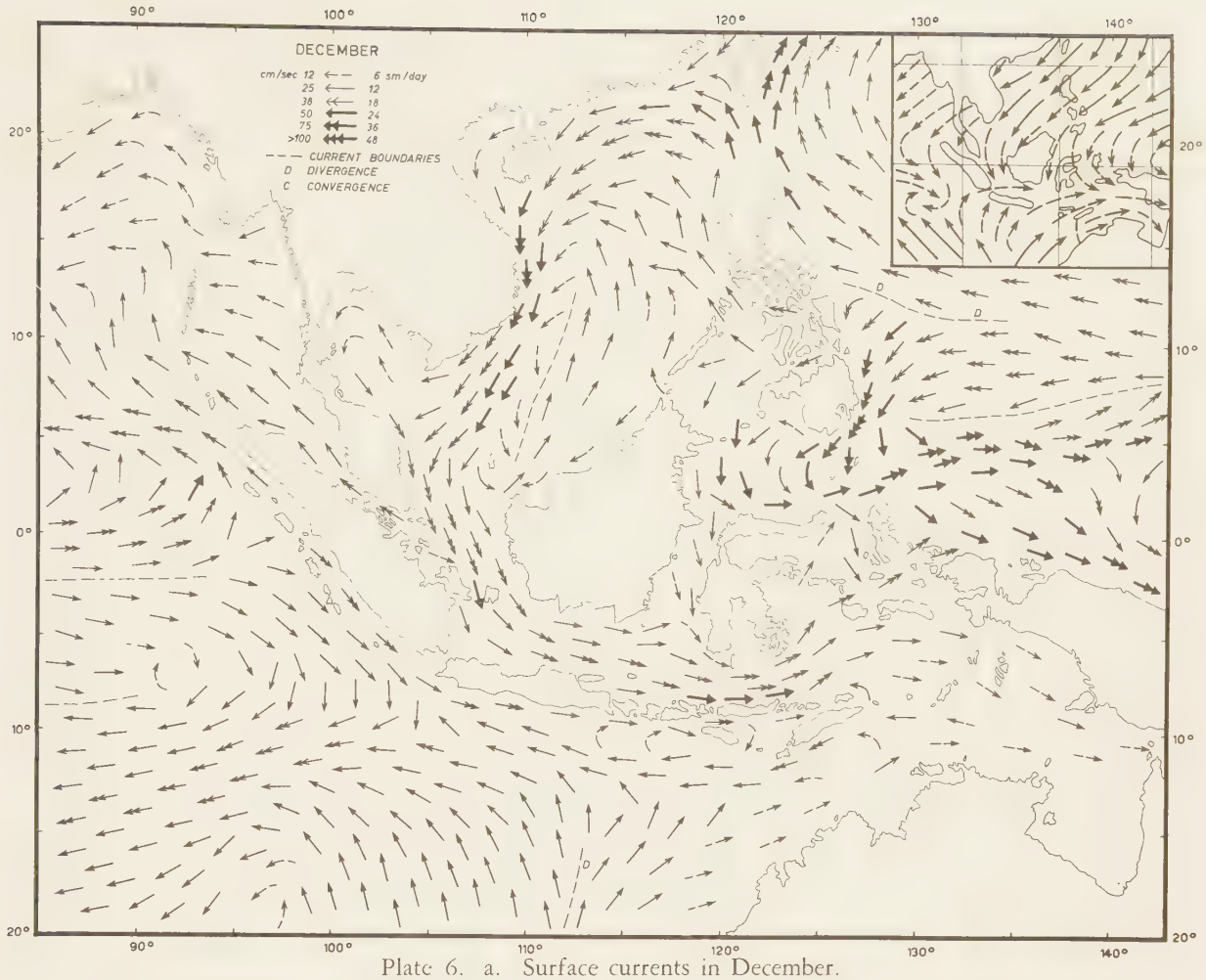

Plate 6. a. Surface currents in December.

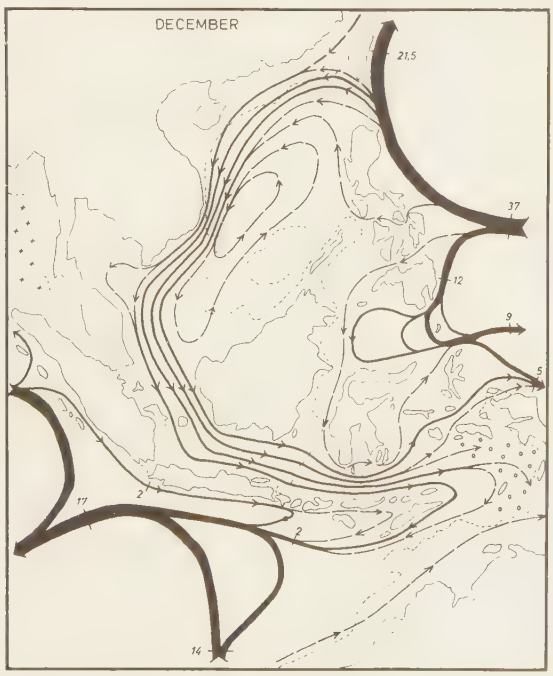

b. Transports of surface circulation in million m^3/sec. + upwelling, o sinking.

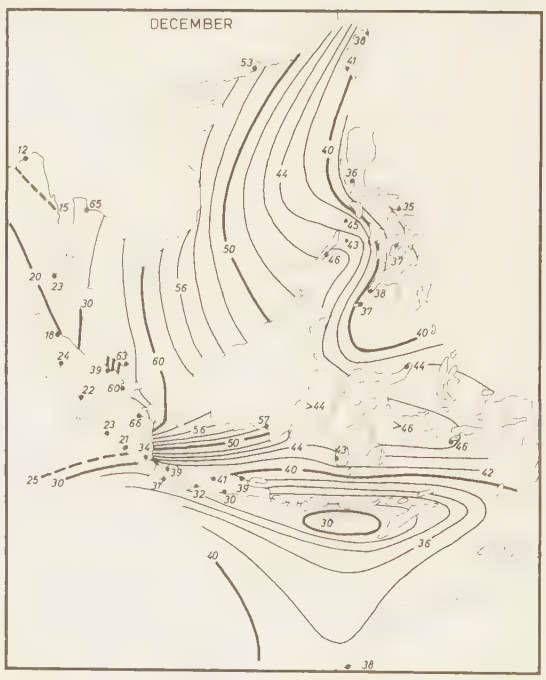

c. Topography of sea level in cm.

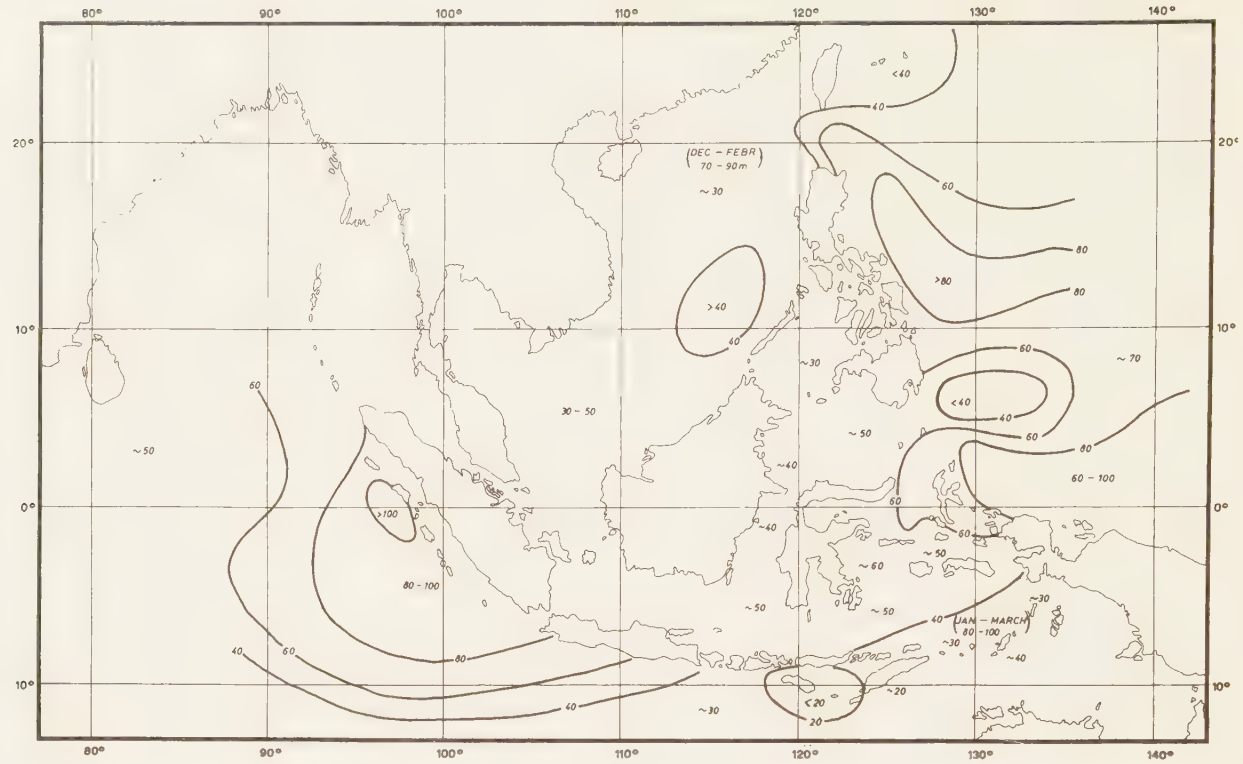

Plate 7. Average thickness (m) of the homogeneous layer (partly, only for one season, see Chapter 4).

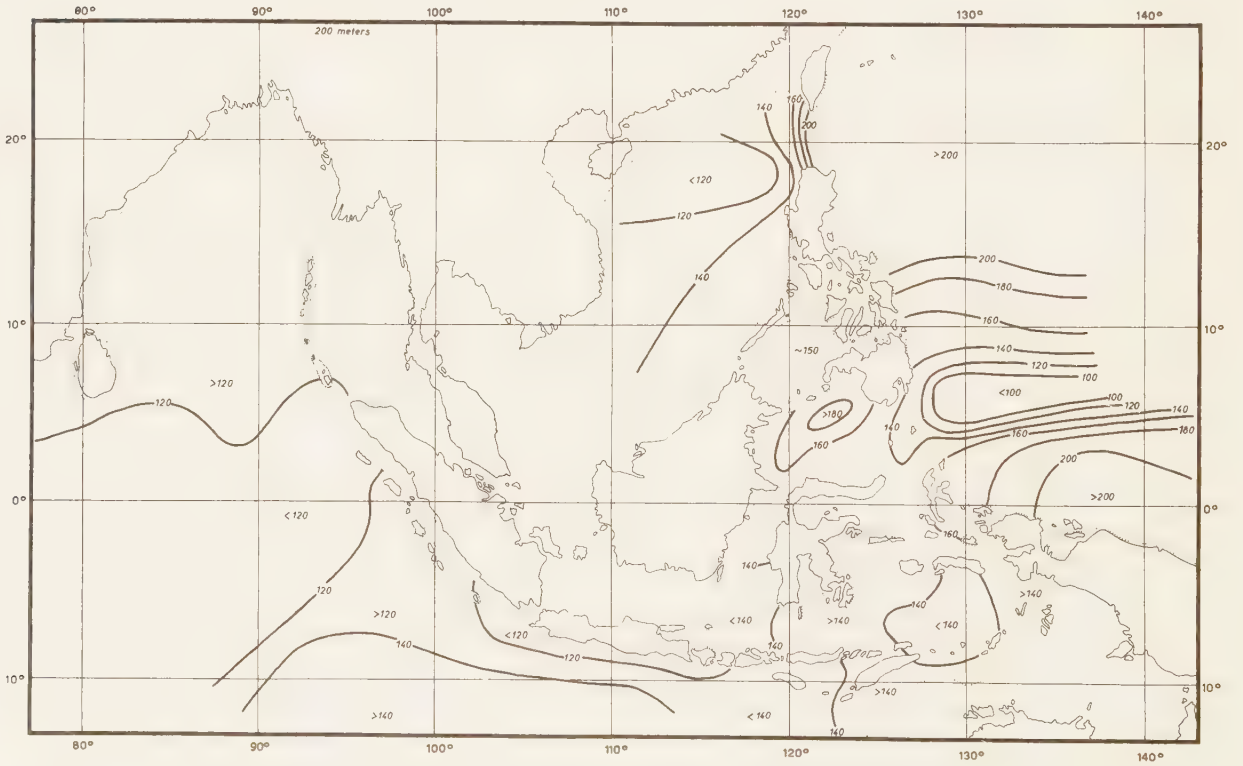

Plate 8. Average depth (m) of the maximal density gradient (partly, only for one season, see Chapter 4) Dotted line indicates 200 m line.

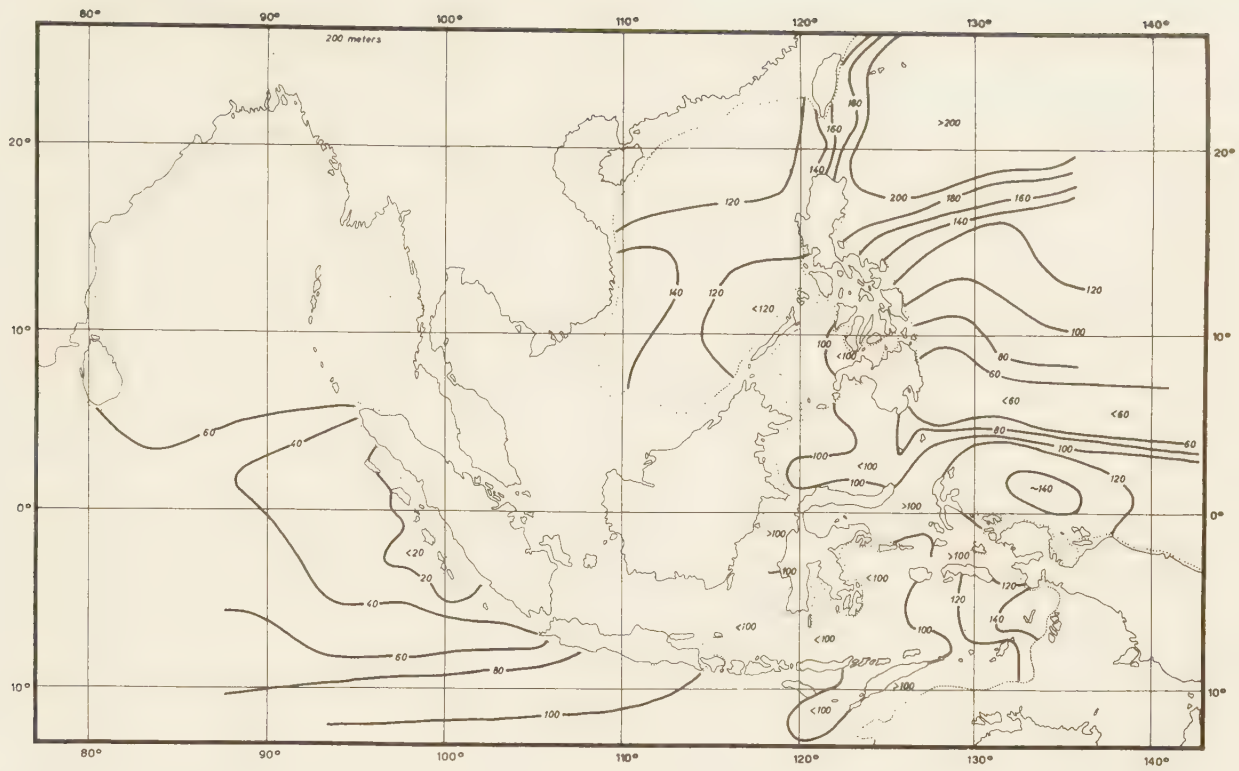

Plate 9. Average thickness (m) of the discontinuity layer, calculated from the distance between the 15° and 23° surfaces (partly, only for one season, see Chapter 4).

Plate 10. Average annual variation of the surface salinity (‰), drawn from observations in the years 1950-1955.

Plate 11. Average surface salinity (‰) in February, drawn from observations in the years 1950-1955.

Plate 12. Average surface salinity (‰) in August, drawn from observations in the years 1950-1955.

Plate 13. Maximal surface salinity (‰) observed in the period 1950-1955, drawn from monthly 1° square averages.

Plate 14. Minimal surface salinity (‰) observed in the period 1950-1955, drawn from monthly 1° square averages.

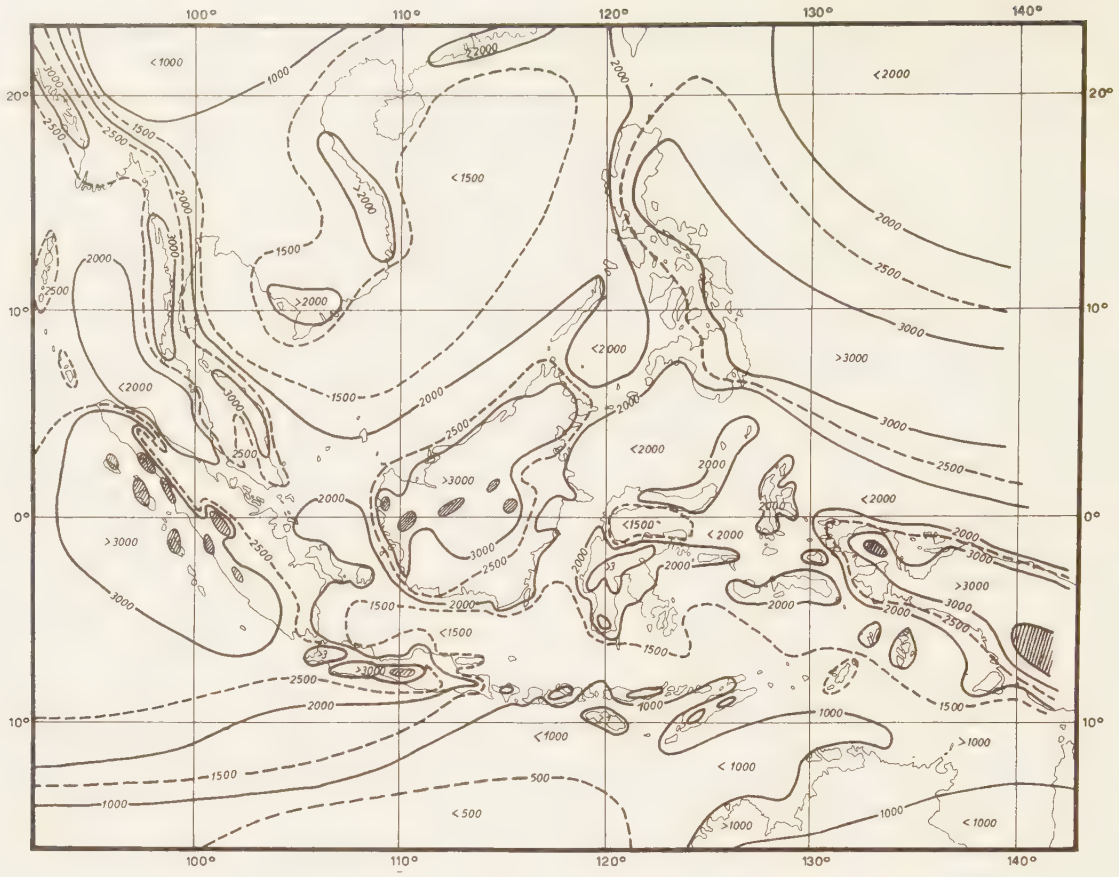

Plate 15. Average annual rainfall (mm), higher than 4000 mm shaded.

Plate 16. Salinity (‰) in the upper salinity maximum, core layer of the Subtropical Lower Water. Regions without salinity maximum are shaded, o indicates station without salinity maximum. See Plate 33 for the Eastern Archipelago.

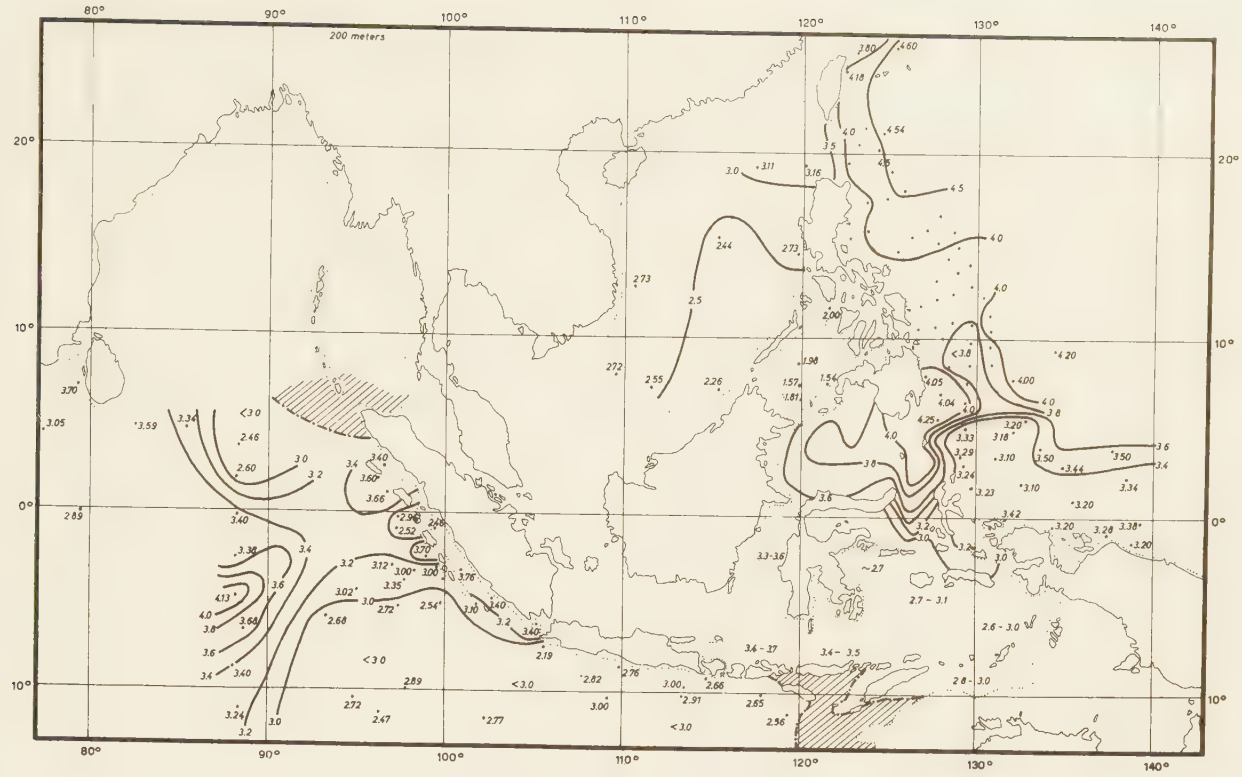

Plate 17. Oxygen content (ml/L) in the core layer of the Subtropical Lower Water (salinity maximum).

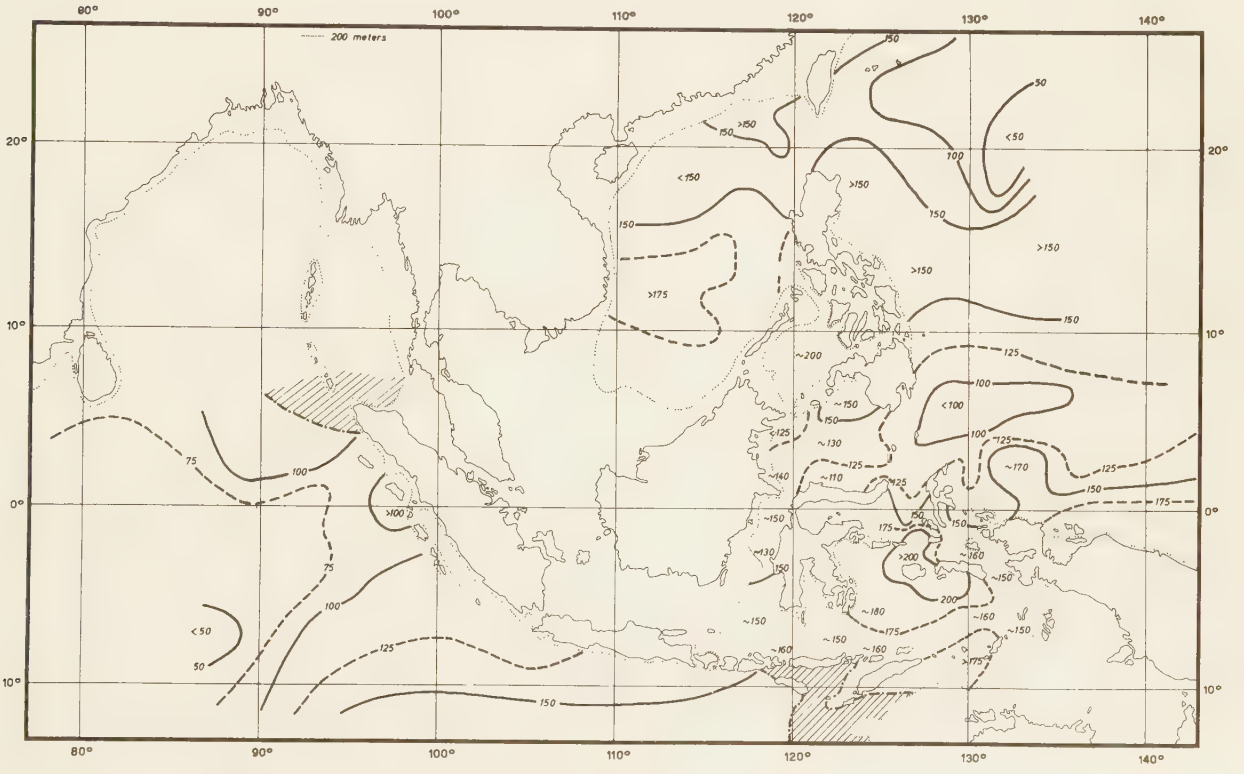

Plate 18. Depth (m) of the core layer of the Subtropical Lower Water.

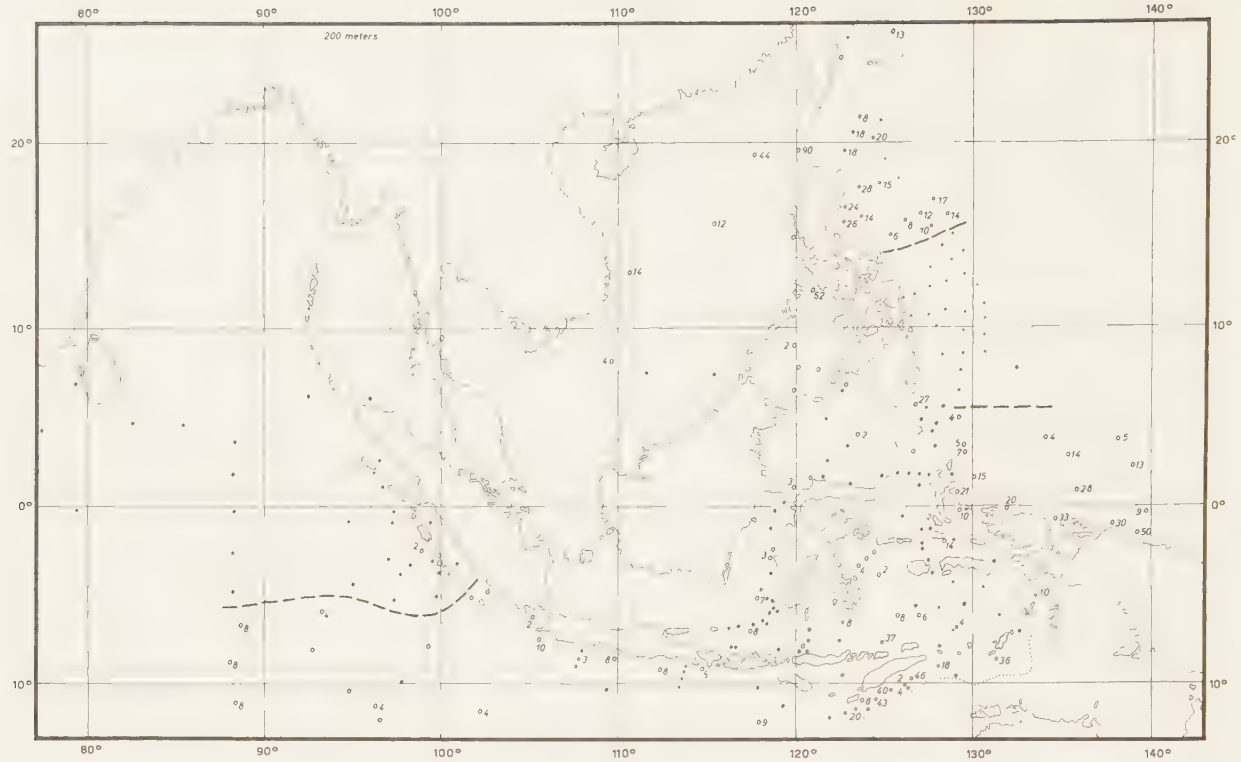

Plate 19. Oxygen inversion in the range of the Subtropical Lower Water in 0.01 ml/L. • indicates station without inversion.

Plate 20. Salinity (‰) in the upper salinity minimum. In the Pacific Ocean core layer of the northern Intermediate Water. o indicates station without salinity minimum.
See Plate 34 for the Eastern Archipelago.

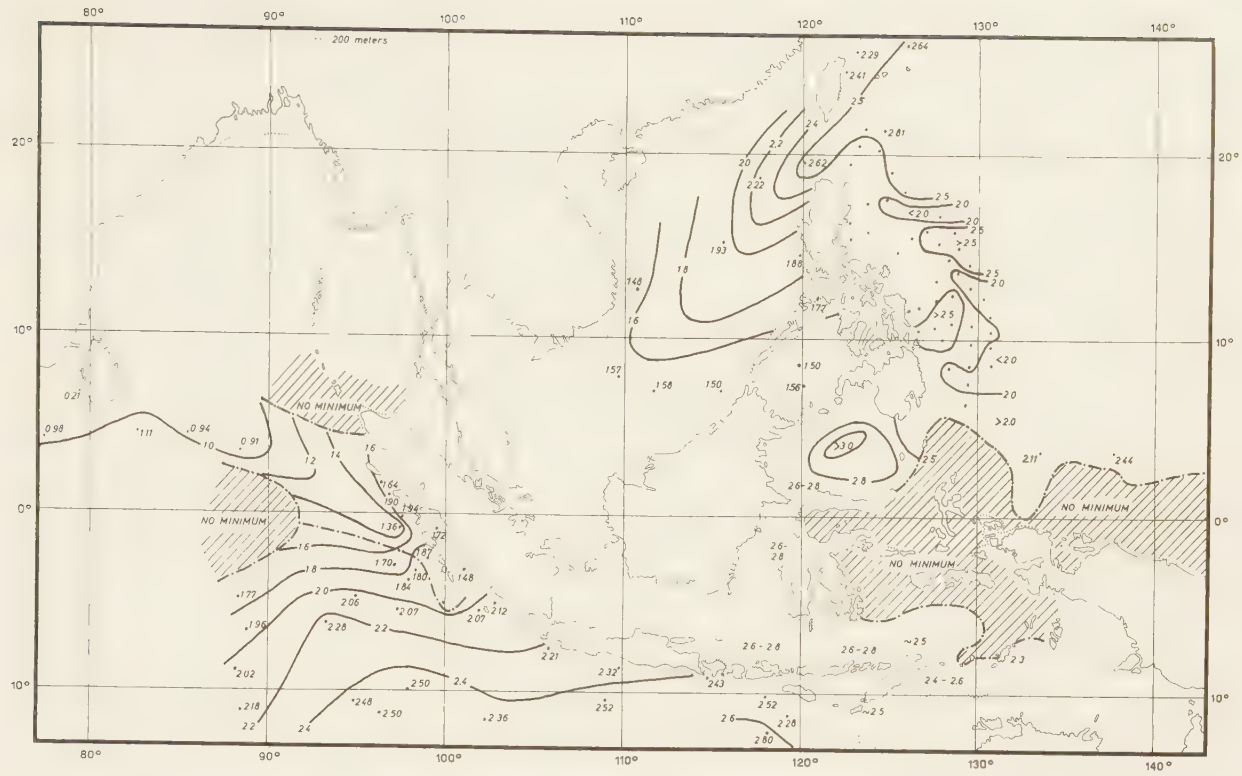

Plate 21. Oxygen content (ml/L) in the upper salinity minimum.

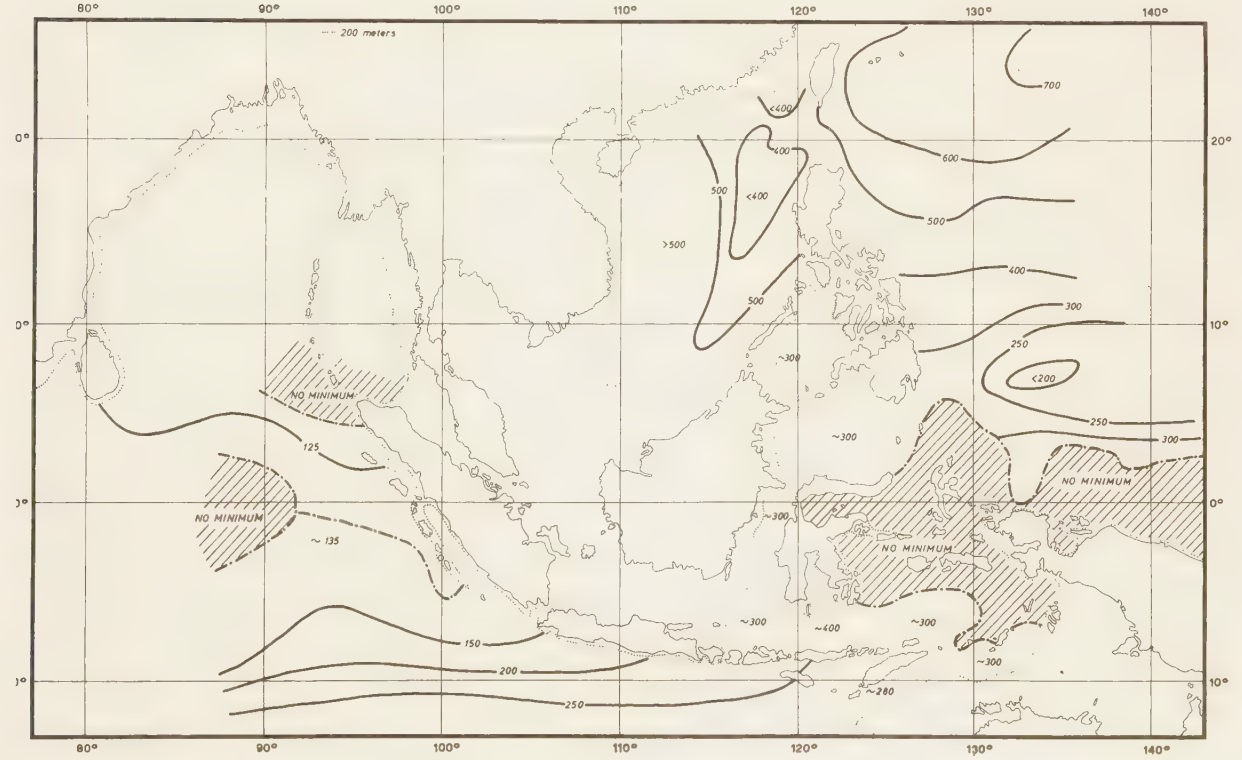

Plate 22. Depth (m) of the upper salinity minimum.

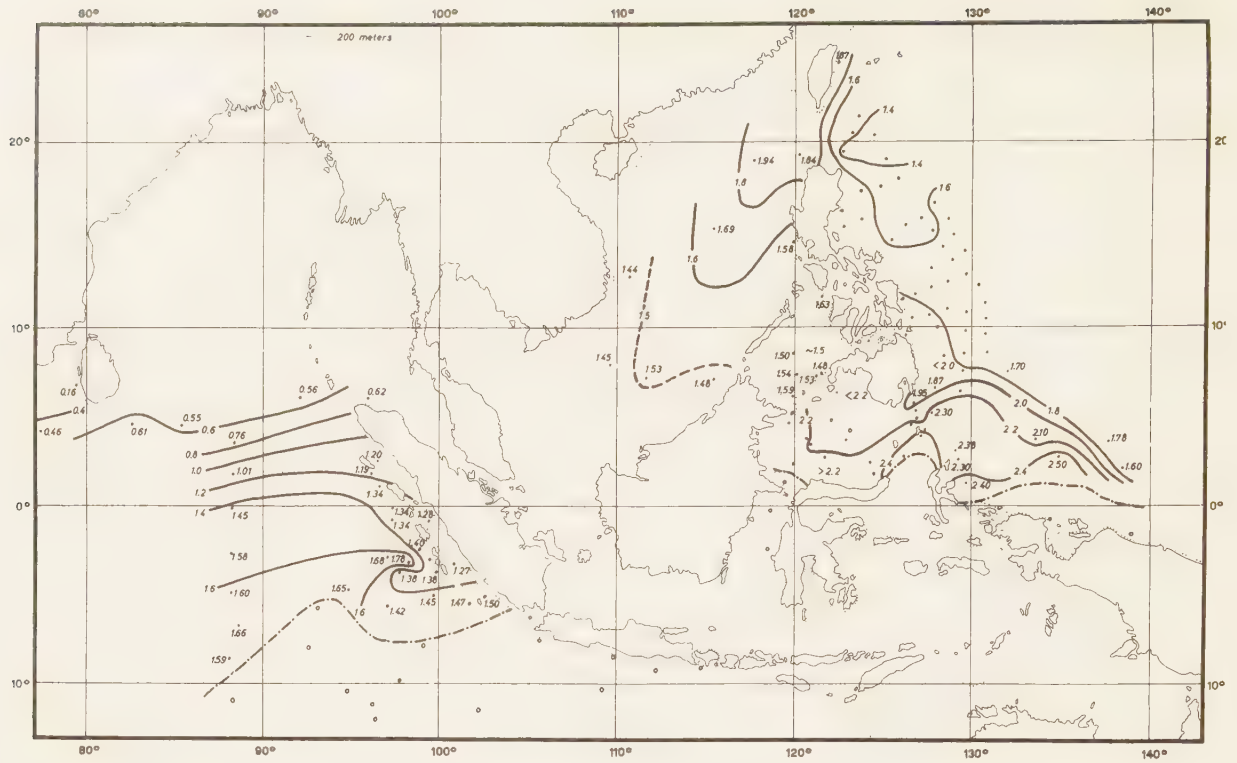

Plate 23. Oxygen content (ml/L) in the upper oxygen minimum. o indicates station without upper oxygen minimum.

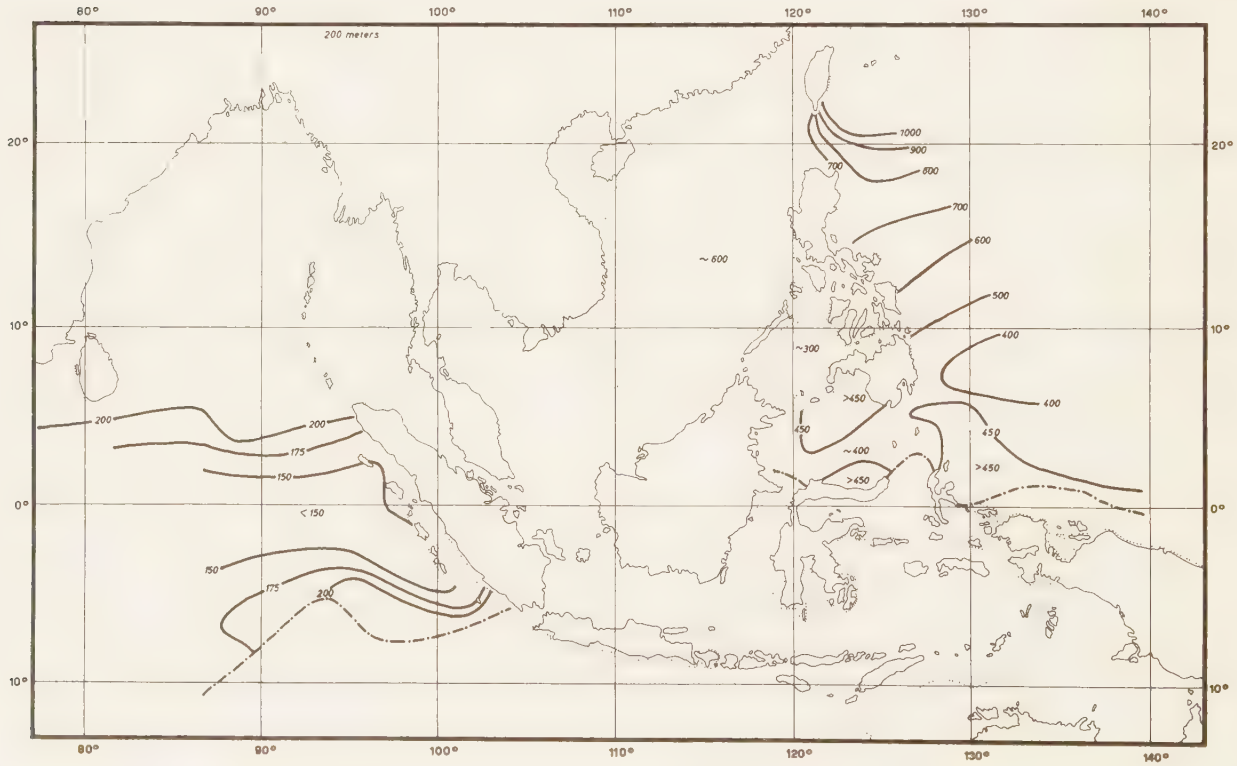

Plate 24. Depth (m) of the upper oxygen minimum.

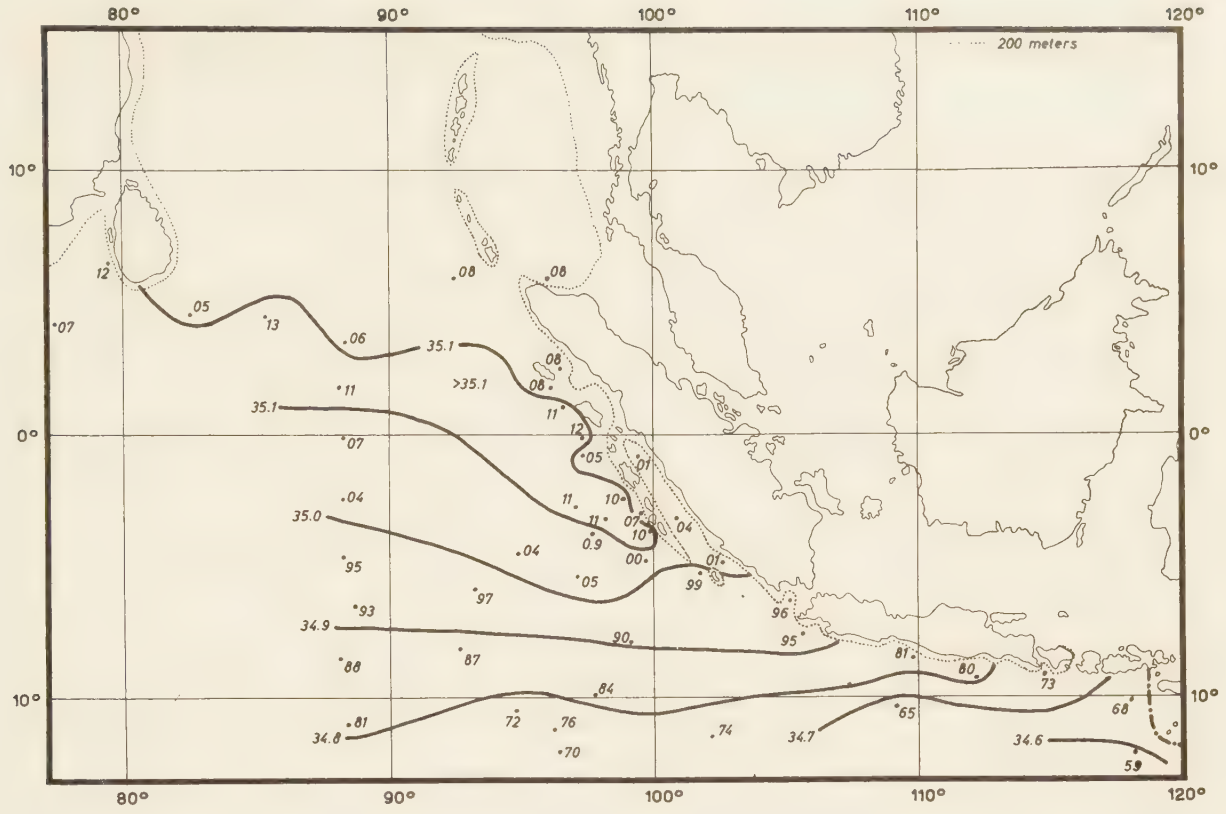

Plate 25a. Salinity (‰) in the upper salinity maximum, core layer of the Persian Gulf Water.

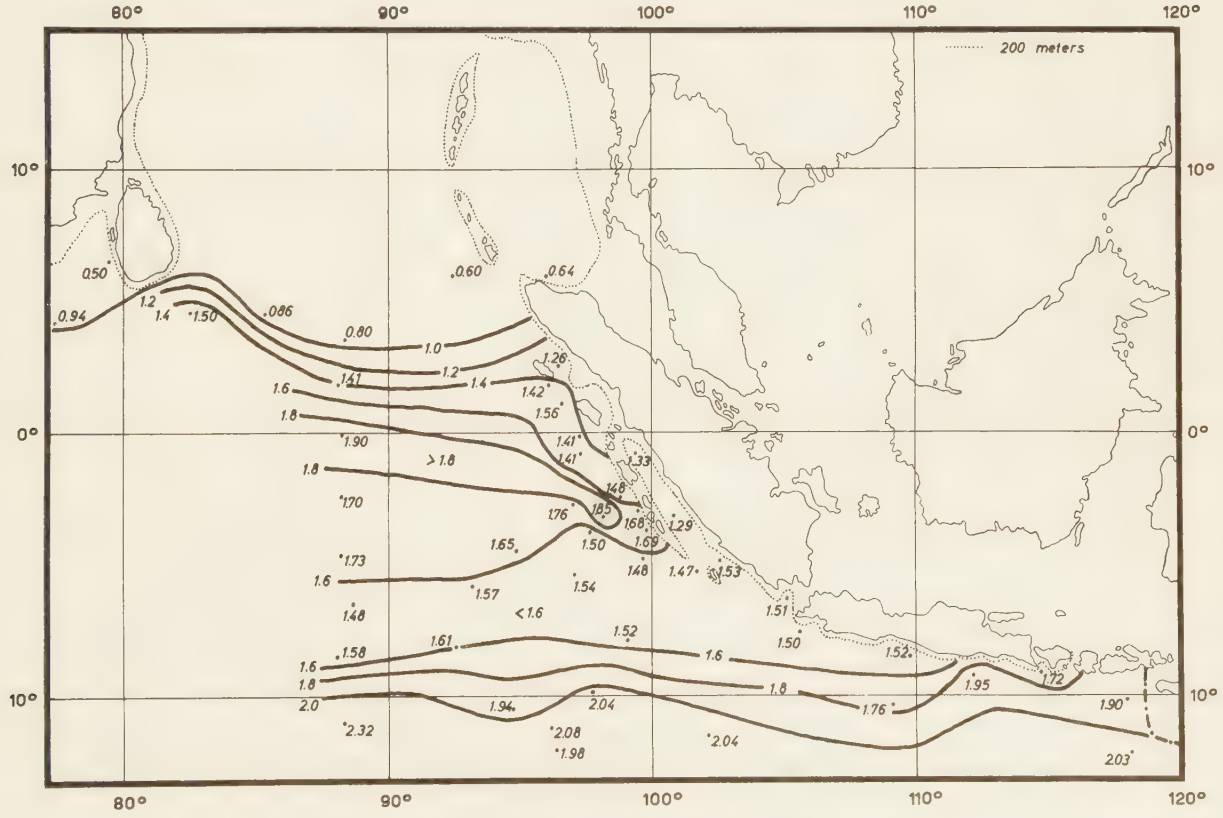

b. Oxygen content (ml/L) in the upper salinity maximum.

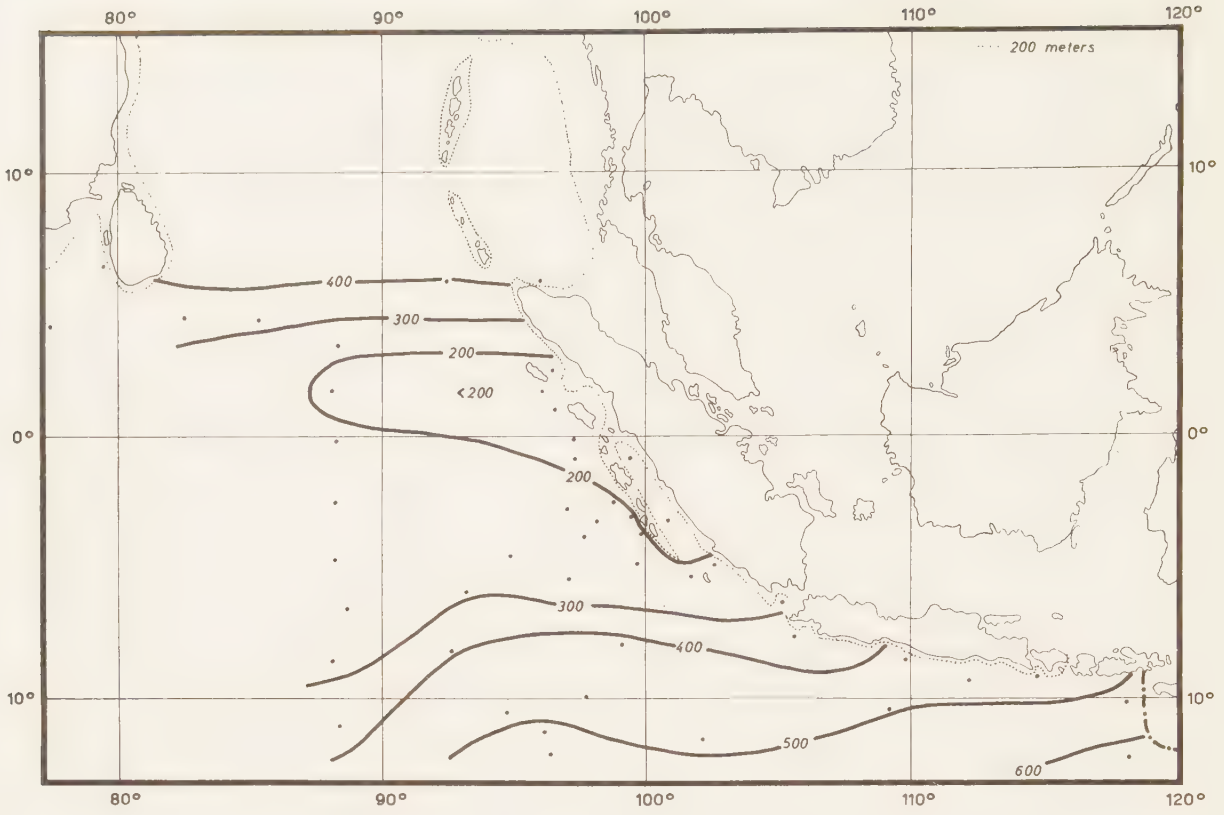

Plate 26a. Depth (m) of the upper salinity maximum.

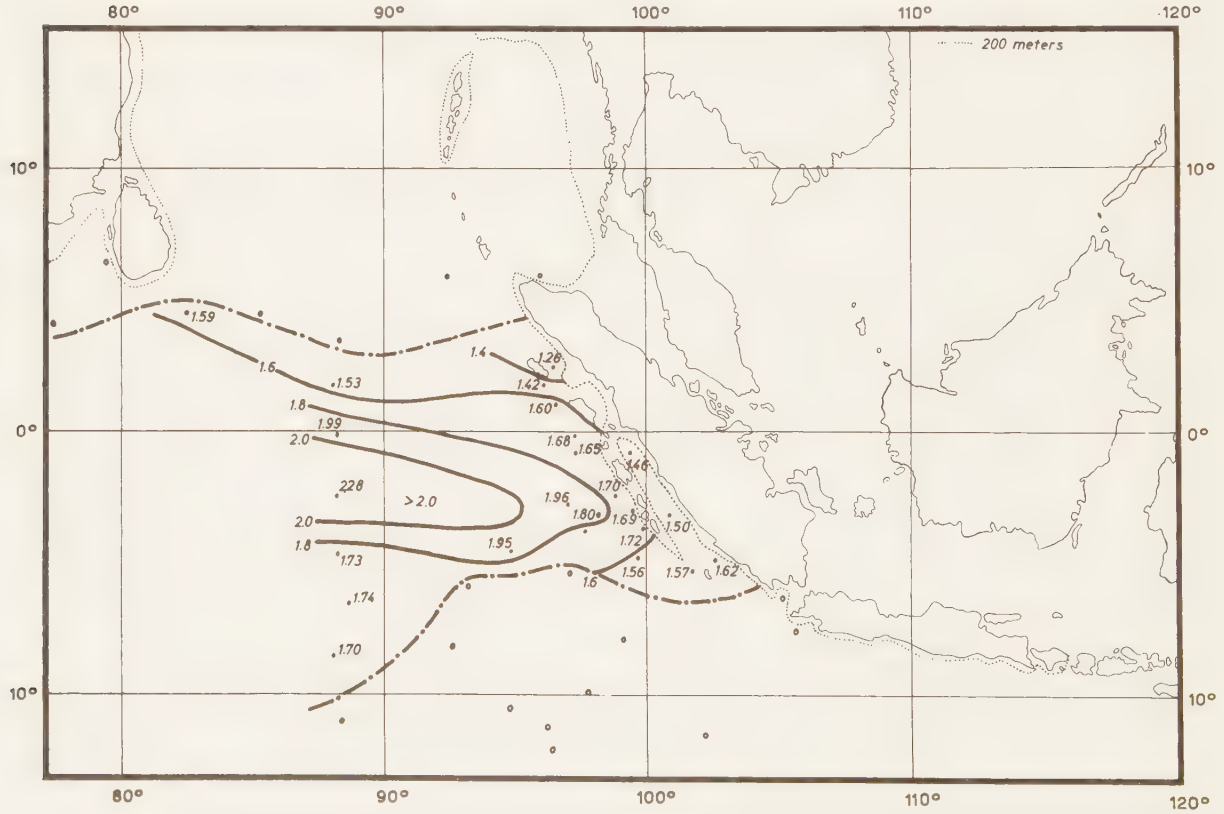

b. Oxygen content (ml/L) in the upper oxygen maximum. —·—·— Limits of the oxygen maximum, o station without oxygen maximum.

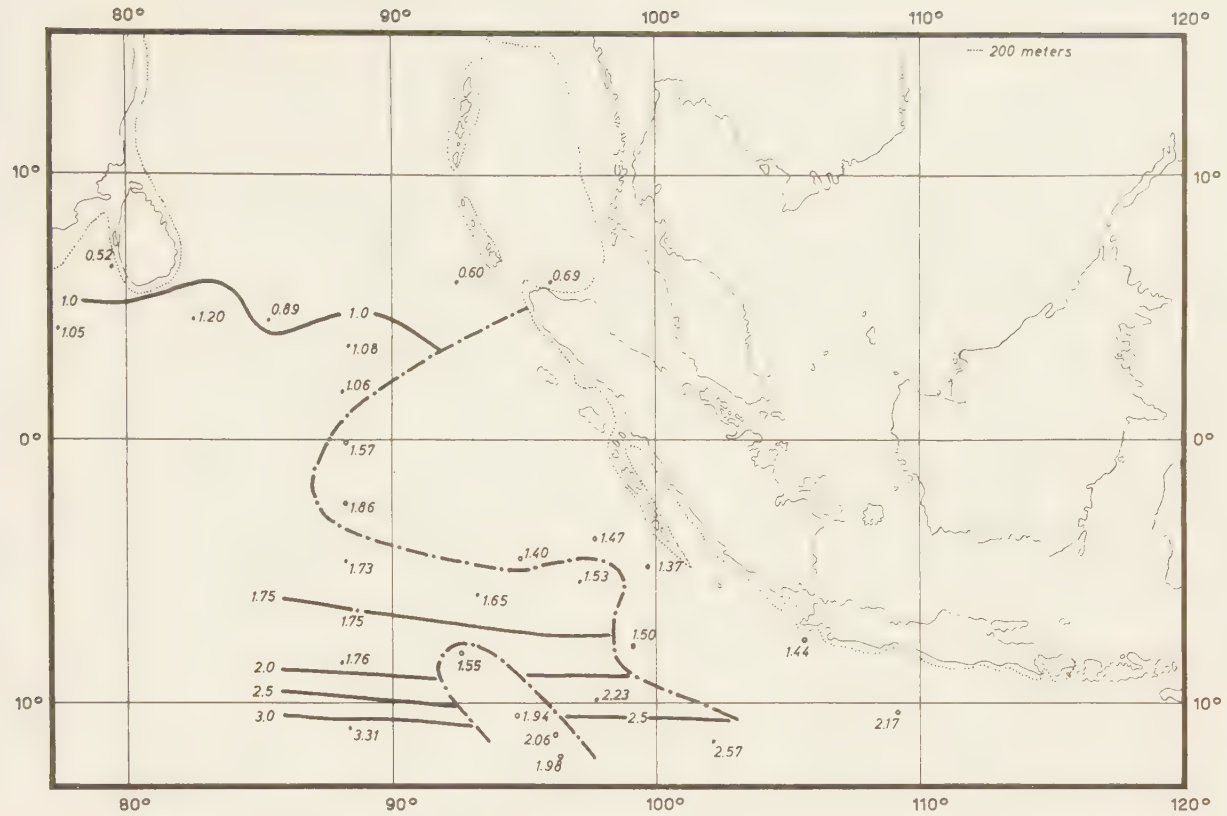

Plate 27a. Oxygen content (ml/L) in the lower oxygen maximum. o indicates station without oxygen maximum, but oxygen content at 500 m is given.

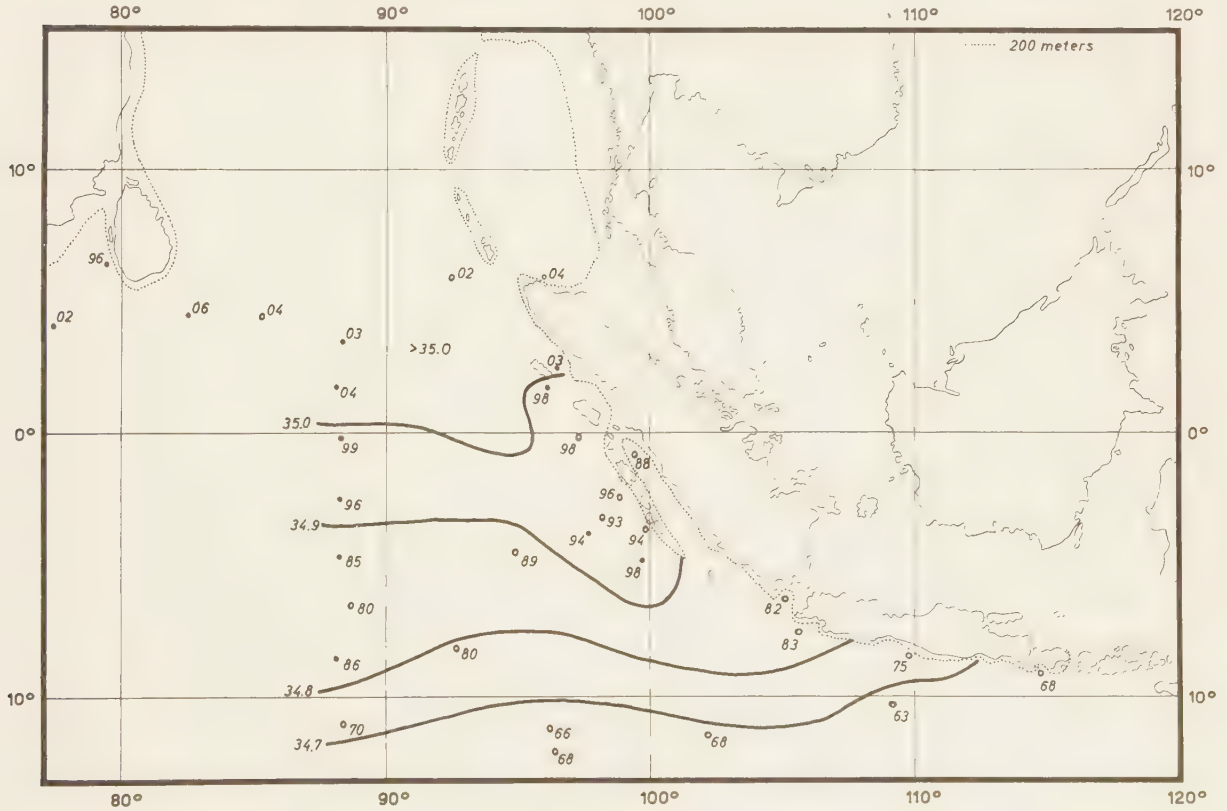

b. Salinity (‰) in the lower salinity maximum, core layer of the Red Sea Water. • indicates station with a real maximum, o station with only a break in the vertical curves of salinity.

Plate 28. Salinity (‰) in the lower salinity minimum. In the Pacific Ocean core layer of the Southern Intermediate Water, in the Indian Ocean core layer of the Banda Sea Water coming from the Eastern Archipelago.

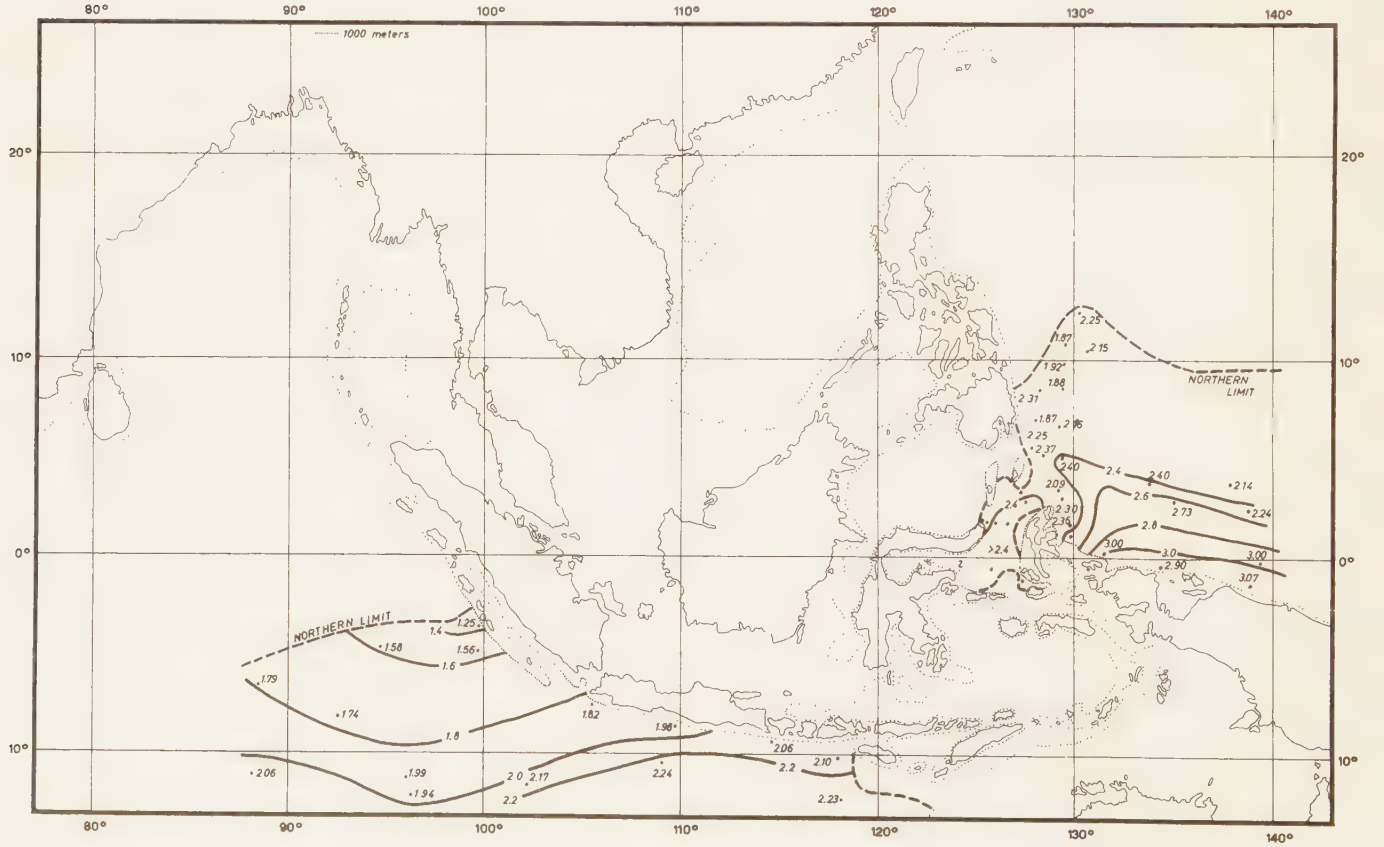

Plate 29. Oxygen content (ml/L) in the lower salinity minimum.

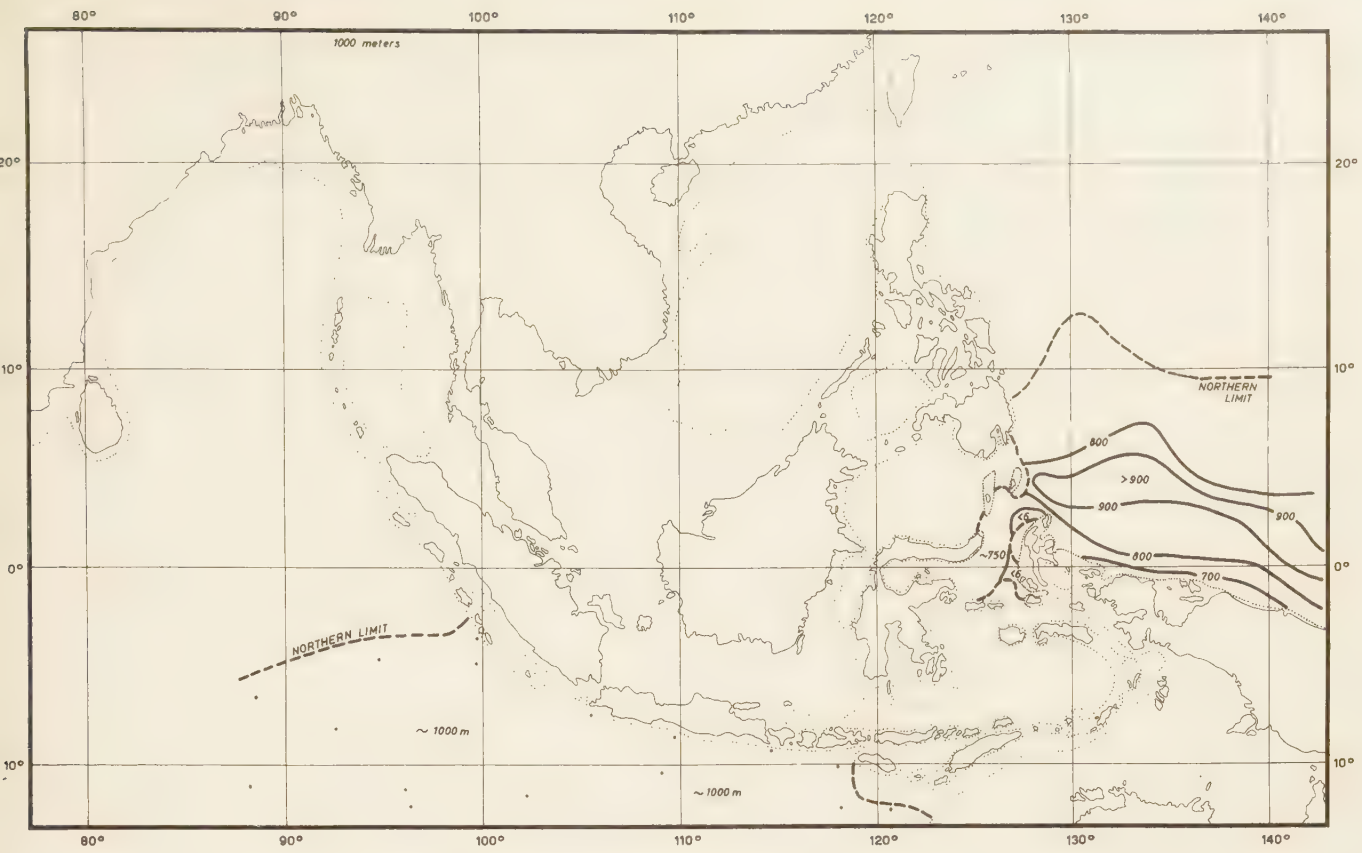

Plate 30. Depth (m) of the lower salinity minimum.

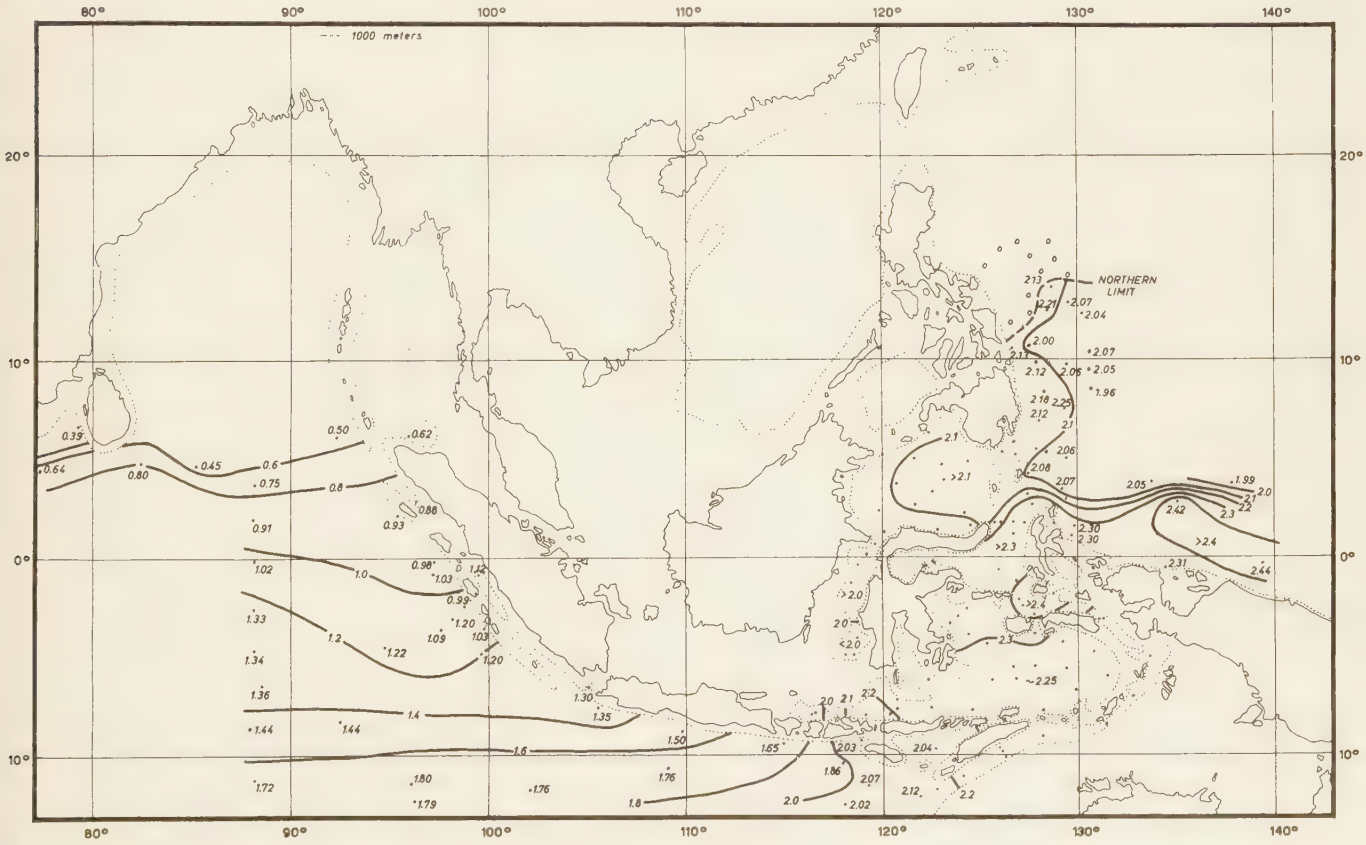

Plate 31. Oxygen content (ml/L) in the lower oxygen minimum. See Plate 35 for the Eastern Archipelago.

Plate 32. Depth (m) of the lower oxygen minimum.

Plate 33. Salinity (‰) in the upper salinity maximum, core layer of the Subtropical Lower Water, within the Eastern Archipelago based on SNELLIUS and DANA observations in 1929/30. o indicates station without salinity maximum.

Plate 34. Salinity ($^{0}/_{00}$) in the upper salinity minimum, core layer of the Northern Intermediate Water, within the Eastern Archipelago based on SNELLIUS and DANA observations in 1929/30. In regions without a salinity minimum stations are indicated by circles and the salinity in 300 m depth is given.

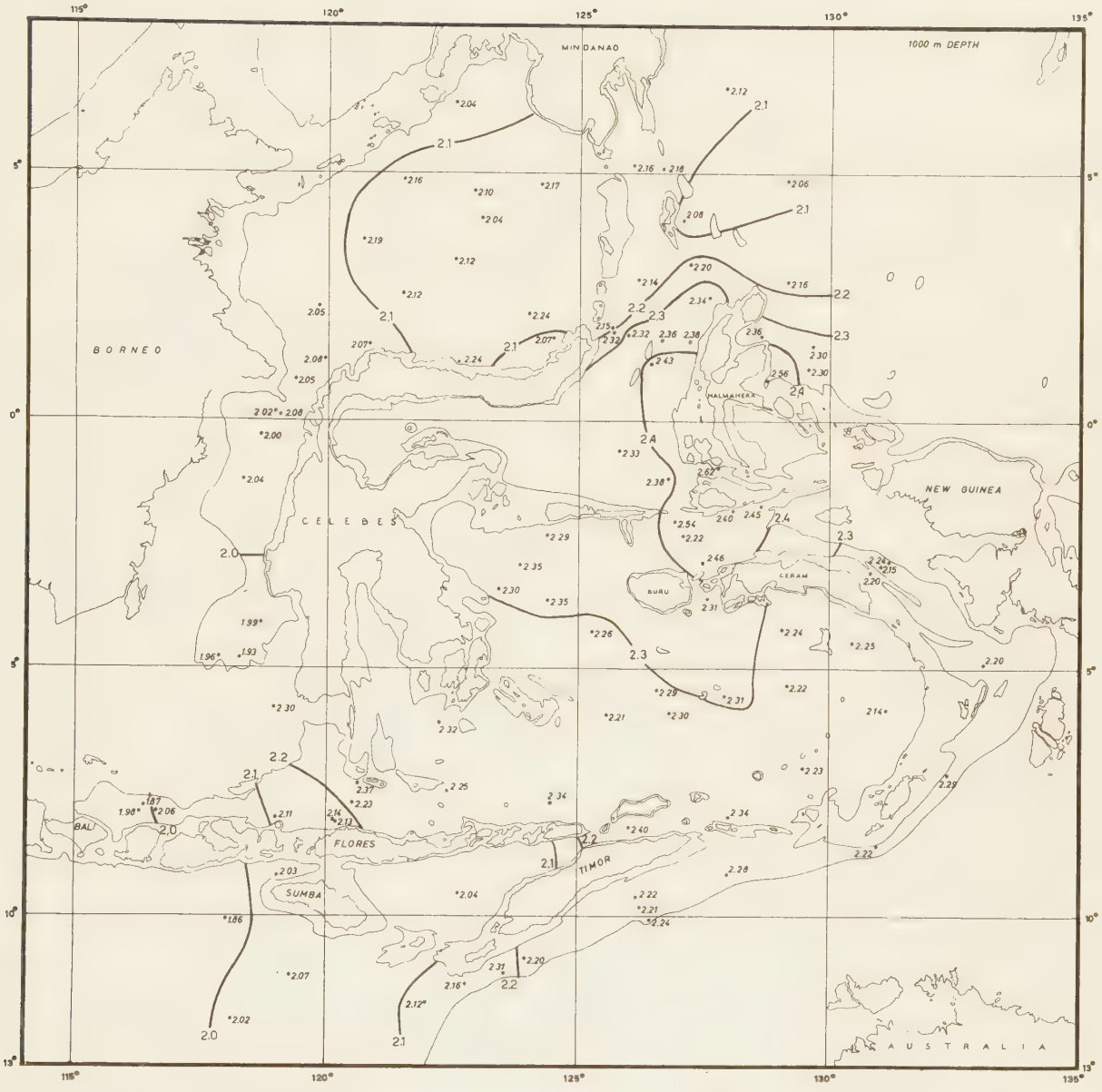

Plate 35. Oxygen content (ml/L) in the lower oxygen minimum within the Eastern Archipelago based on SNELLIUS, DANA and SAMUDERA observations.

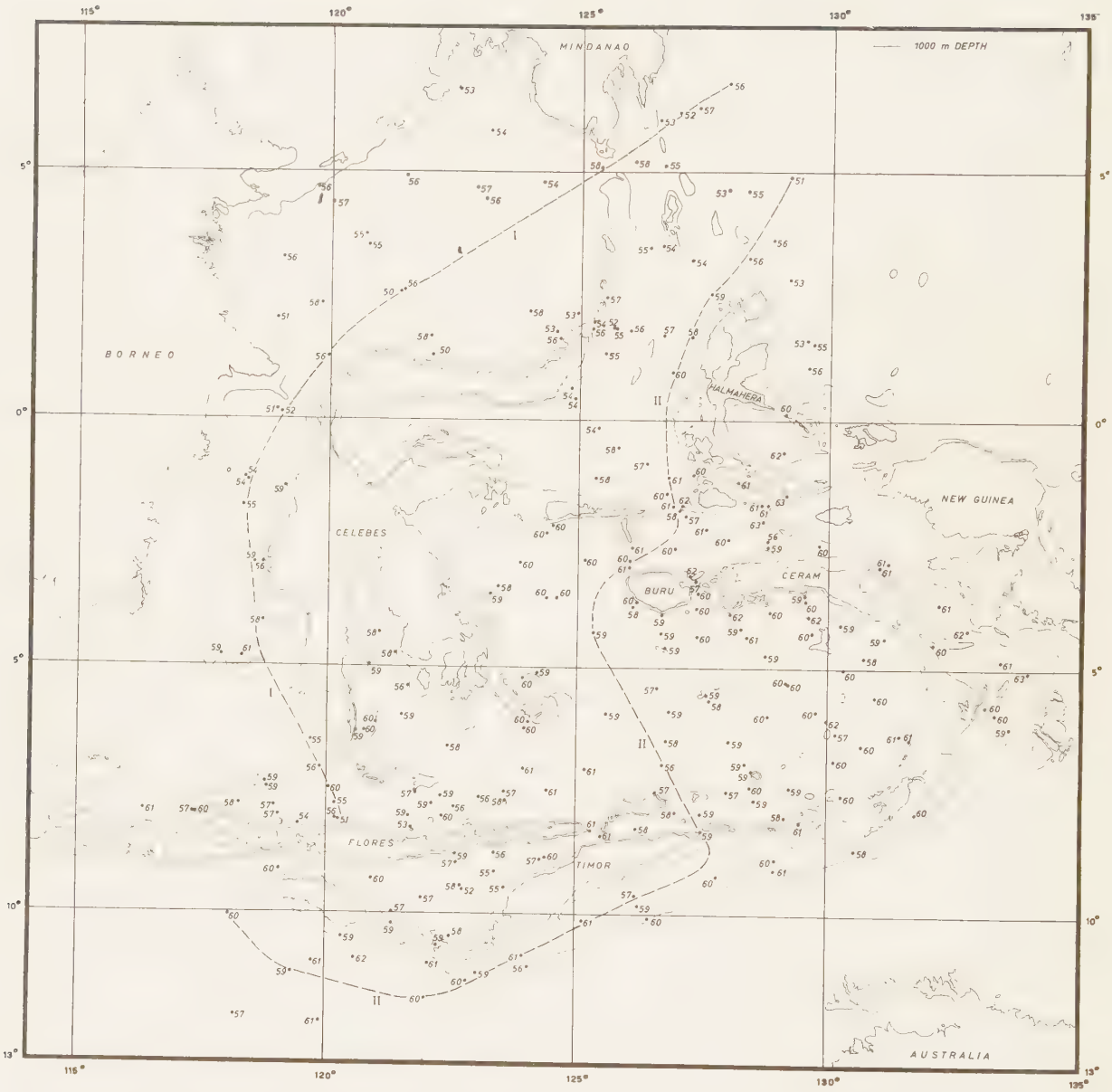

Plate 36. Salinity (‰) in a depth of 1000 meters in the Eastern Archipelago. Broken lines give positions of sections I and II in plate 38.

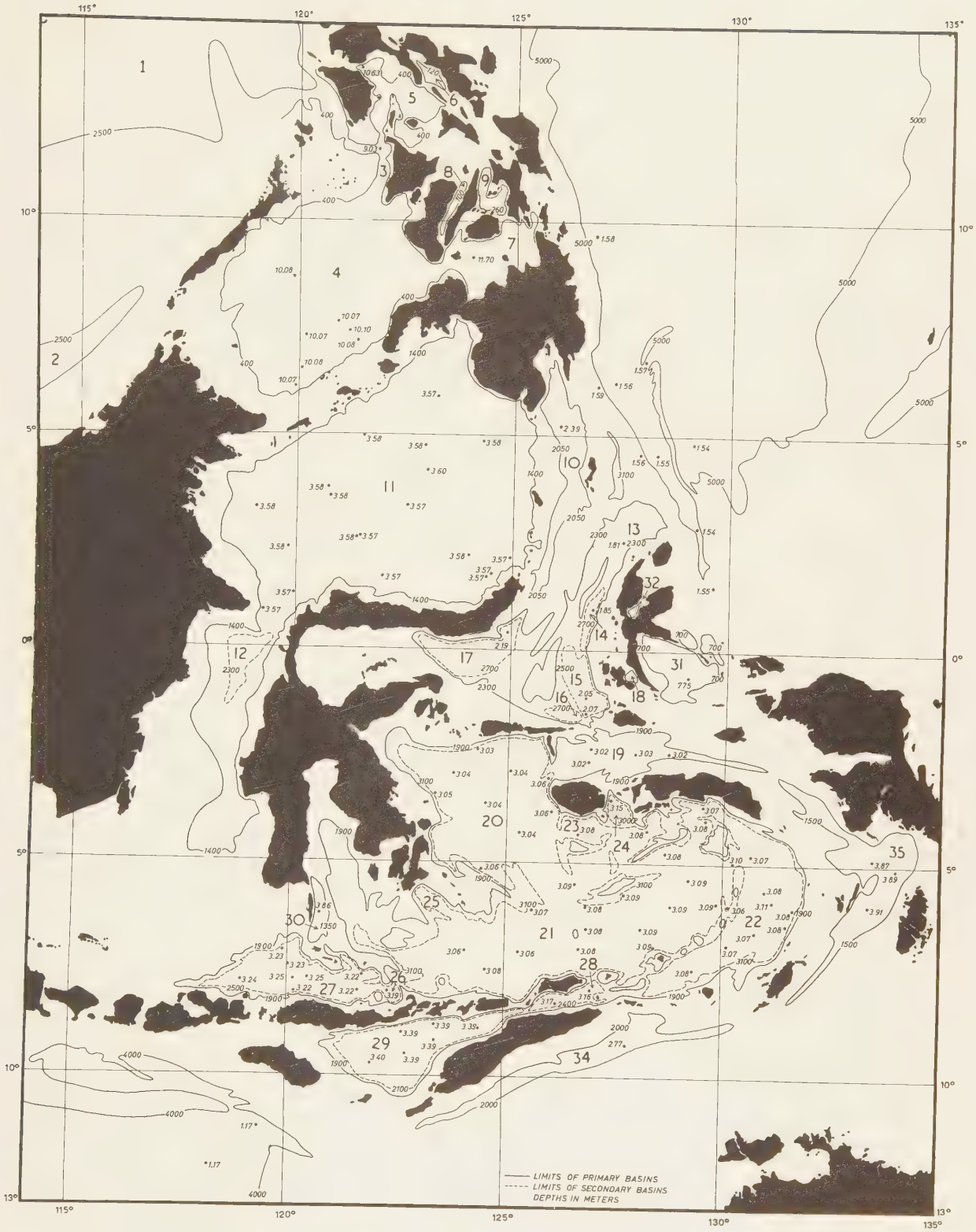

Plate 37. Temperature *in situ* in the observed temperature minimum. Depth contours are drawn for the sills of the different basins, full lines are used for primary basins, broken lines for secondary basins. Figures on contour lines indicate depth (m).

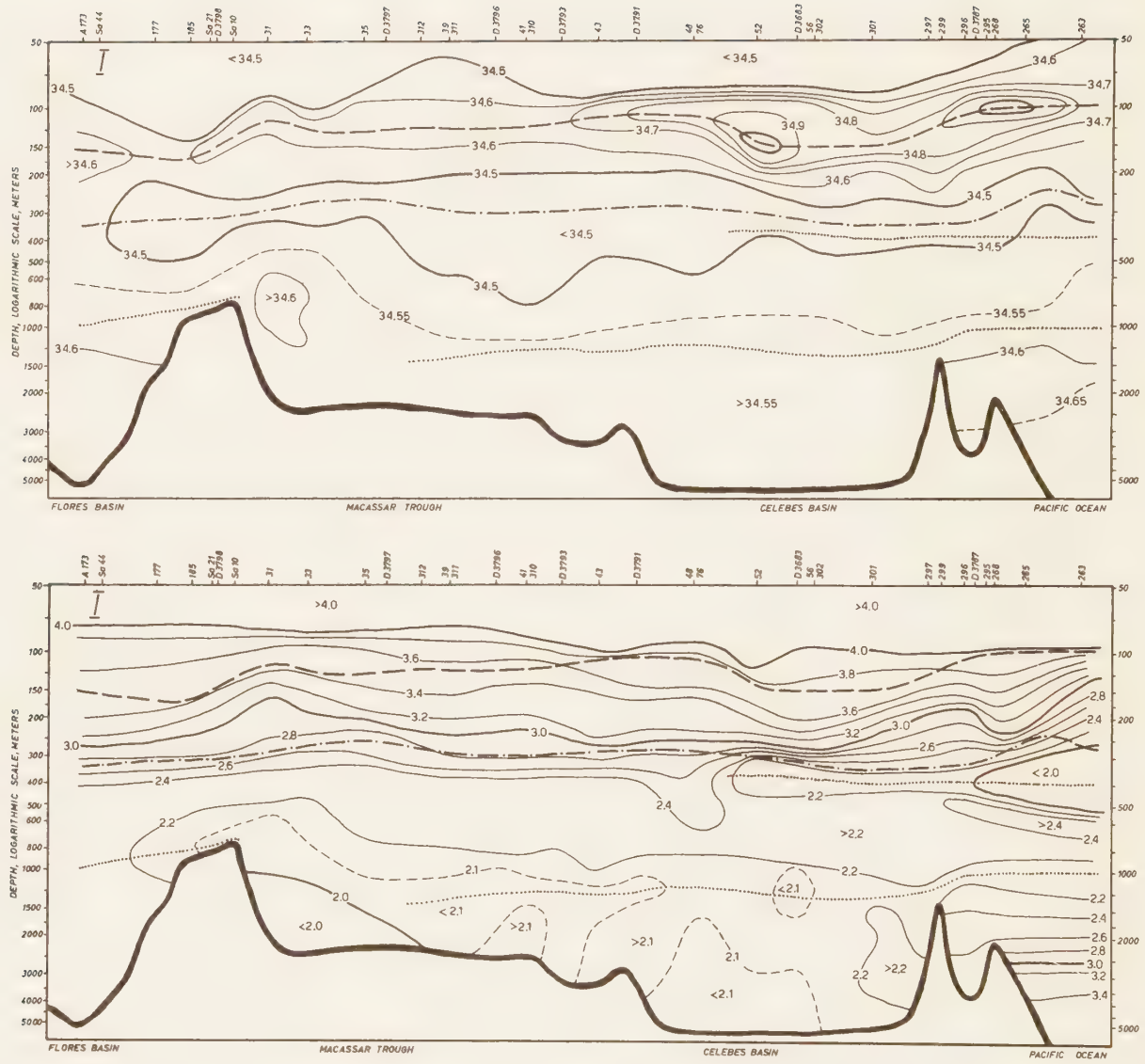

Plate 38. Section I. Distribution of salinity (‰) and oxygen content (ml/L) in a section through the Eastern Archipelago from south of Mindanao through the Celebes Sea and Macassar Strait to the Flores Sea. Core layers are indicated — — — — — salinity maximum, ·—·—·— salinity minimum, ····· oxygen minimum. Depth scale logarithmic. Stations indicated as follows: SNELLIUS, numbers only, DANA, D, SAMUDERA, Sa, ALBATROSS, A.

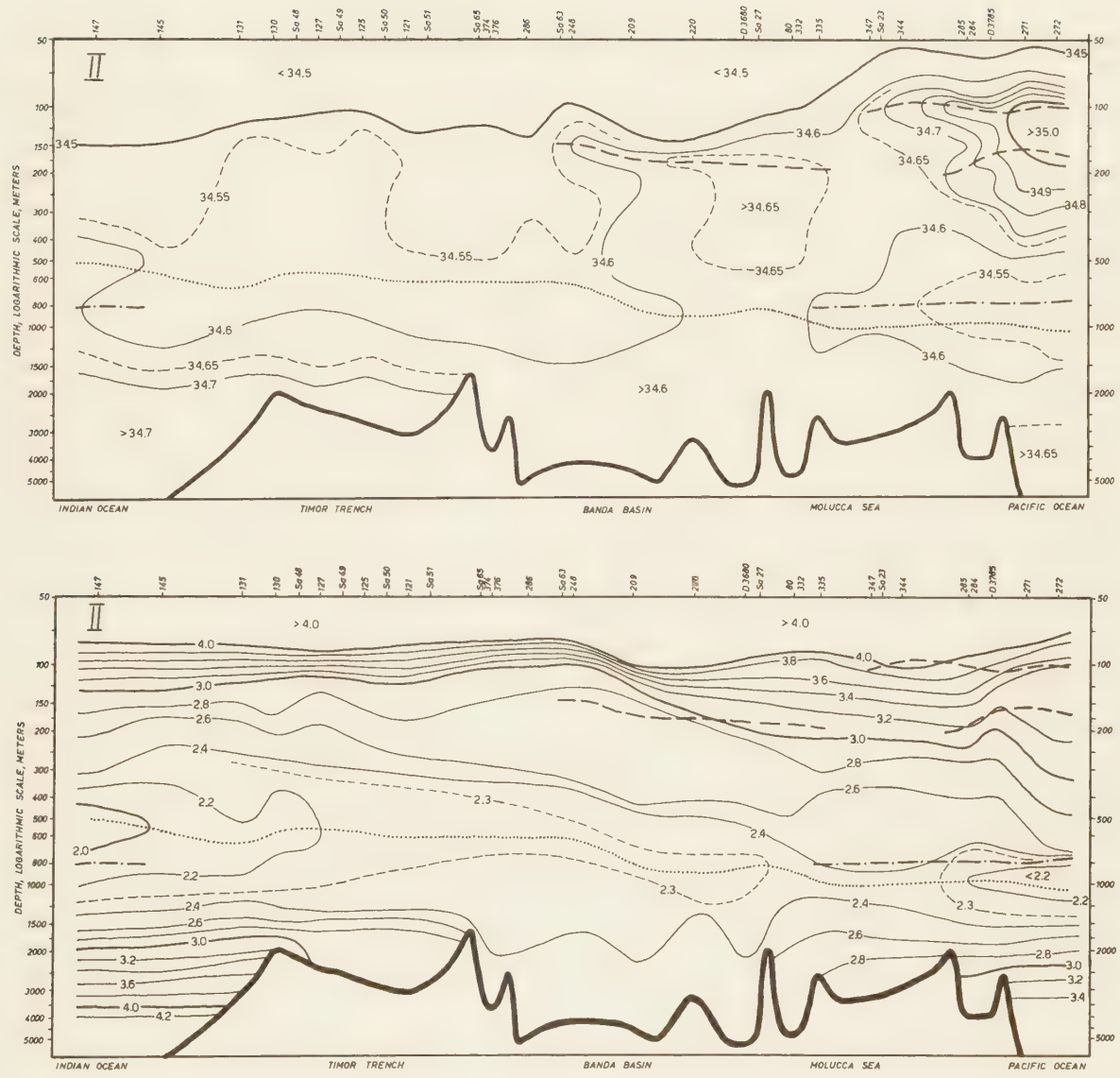

Plate 38. Section II. Distribution of salinity (‰) and oxygen content (ml/L) in a section through the Eastern Archipelago from north of Halmahera through the Molucca, Banda and Timor Seas into the Indian Ocean. Core layers are indicated — — — — — salinity maximum, ·—·—·— salinity minimum, ····· oxygen minimum. Depth scale logarithmic. Stations indicated as follows: SNELLIUS, numbers only, DANA, D, SAMUDERA, Sa, ALBATROSS, A.

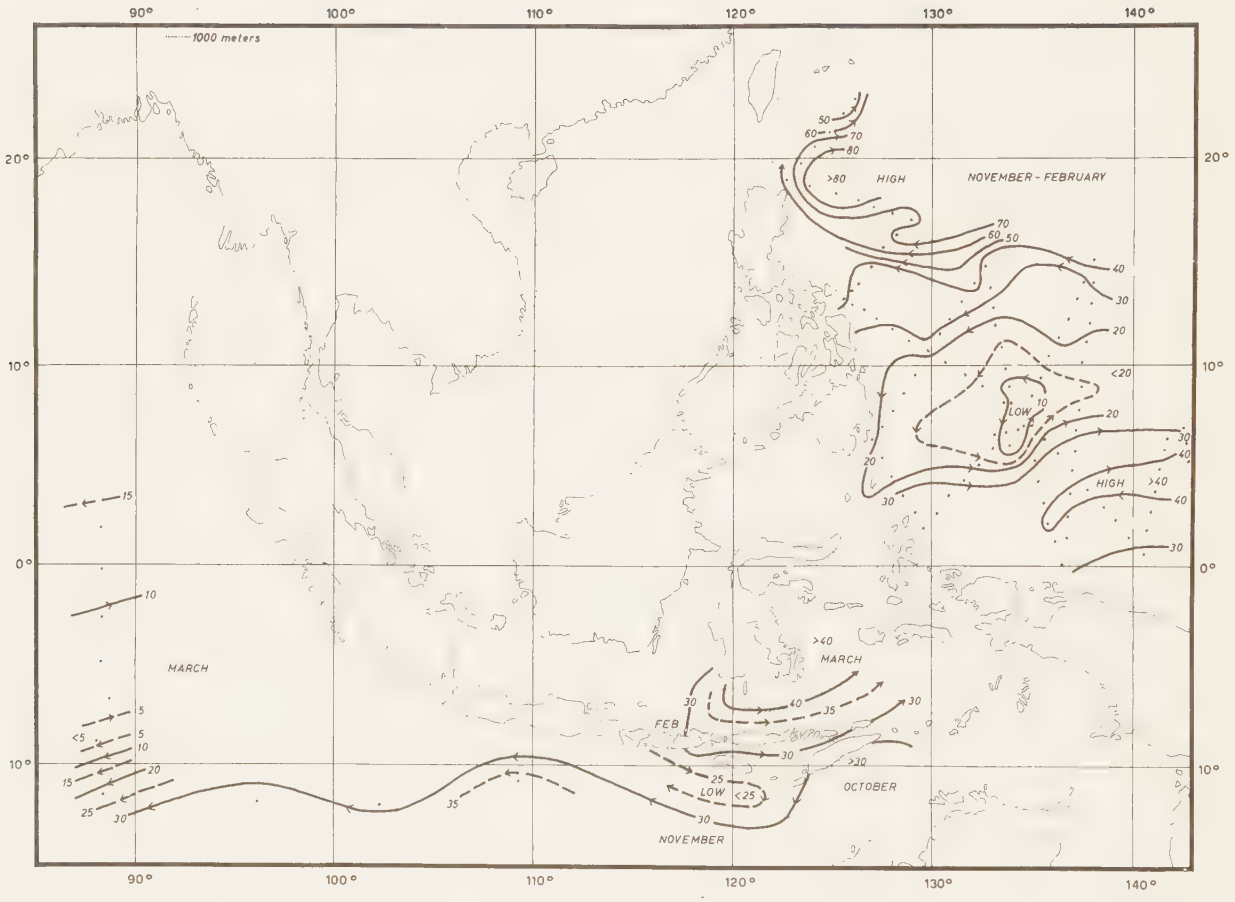

Plate 39. Dynamical topography of the sea surface in dyn. cm. relative to 800 decibars during the north monsoon.

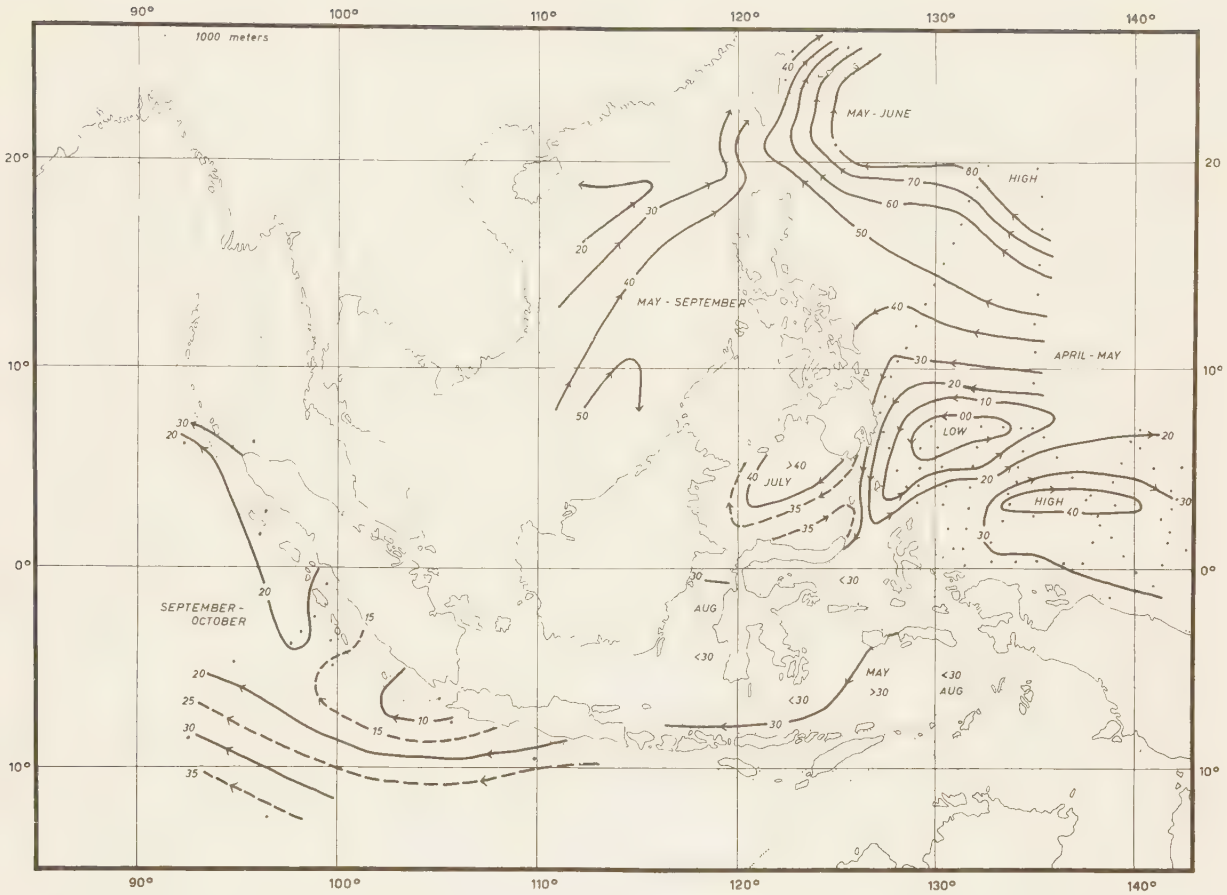

Plate 40. Dynamical topography of the sea surface in dyn. cm. relative to 800 decibars during the south monsoon.

Plate 41. Amplitude (cm) of the semidiurnal tide, $M_2 + S_2$. Dots indicate positions for which harmonic constants are computed.

Plate 42. Cotidal lines of the semidiurnal tide M_2 in lunar hours.

Plate 43. Amplitude (cm) of the diurnal tide, $K_1 + O_1$. Dots indicate positions for which harmon constants are computed.

Plate 44. Cotidal lines of the diurnal tide K_1 in hours.